IFERP®
connecting engineers... developing research

ICFE

ICFE-22

Virtual Conference

INTERNATIONAL CONFERENCE ON FUTURE OF ENGINEERING

22ND & 23RD SEPTEMBER 2022

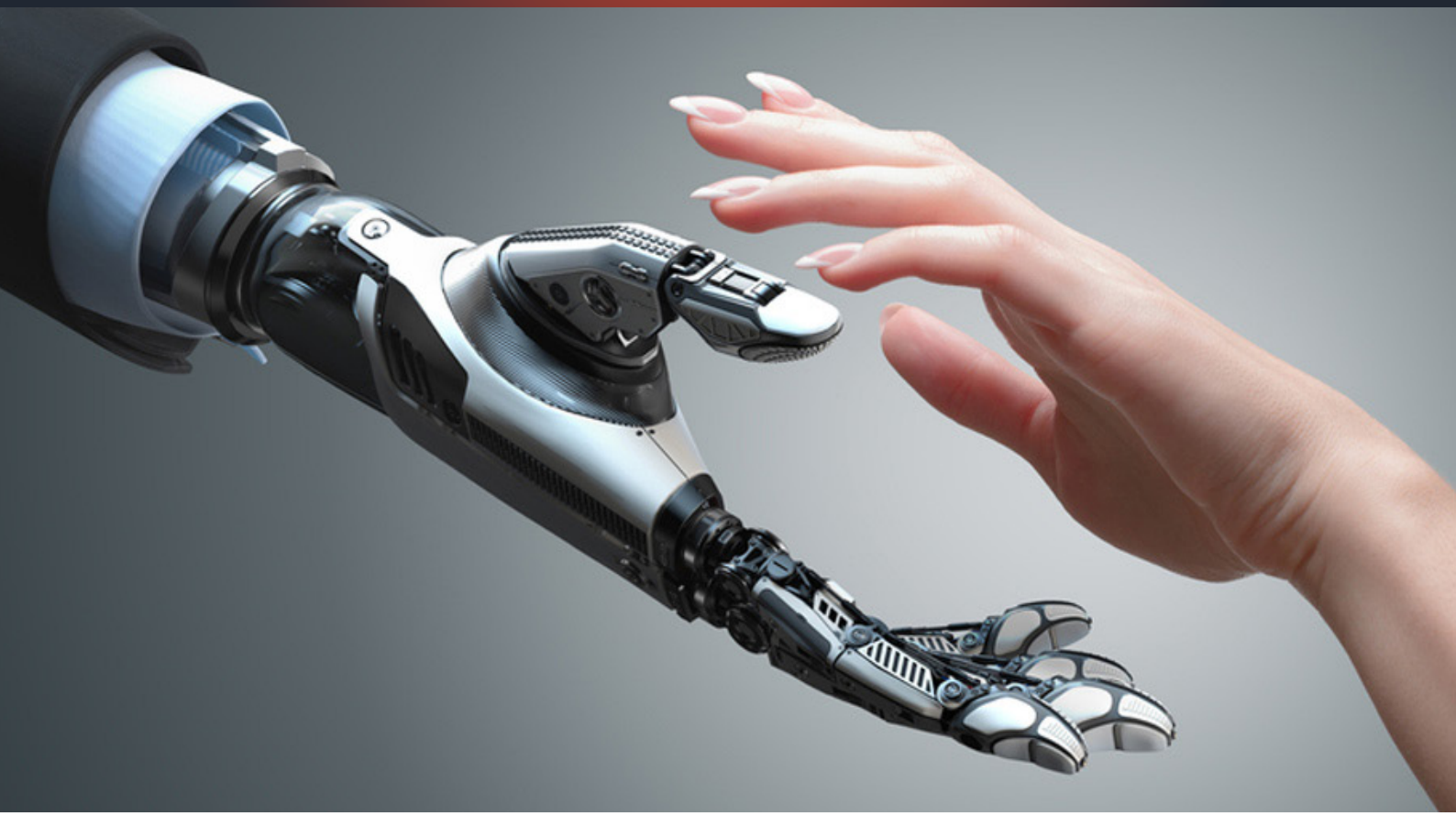

Organized by

Institute For Engineering Research and Publication (IFERP)
Philippines chapter

ISBN : 978-93-92105-22-7

IFERP®
connecting engineers... developing research

ICFE

1st International Conference on
Future of Engineering

Theme: Rapid Advancement in Future of Science, Engineering & Technologies

22nd & 23rd September, 2022 - Virtual Conference

Organized by

Institute For Engineering Research and Publication (IFERP)
Philippines Chapter

Publisher: IFERP Explore

Editorial

We cordially invite you to attend the 1st International Conference on Future of Engineering (ICFE-22) which will be held as Virtual Conference on 22nd-23rd September, 2022. The main objective of this conference is to provide a platform for researchers, students, academicians as well as industrial professionals from all over the world to present their research results and development activities in relevant fields of Engineering and Technology. This conference will provide opportunities for the delegates to exchange new ideas and experience face to face, to establish business or research relationship and to find global partners for future collaboration.

These proceedings collect the up-to-date, comprehensive and worldwide state-of-art knowledge on cutting edge development of academia as well as industries. All accepted papers were subjected to strict peer-reviewing by a panel of expert referees. The papers have been selected for these proceedings because of their quality and the relevance to the conference. We hope these proceedings will not only provide the readers a broad overview of the latest research results but also will provide the readers a valuable summary and reference in these fields.

The conference is supported by many universities, research institutes and colleges. Many professors played an important role in the successful holding of the conference, so we would like to take this opportunity to express our sincere gratitude and highest respects to them. They have worked very hard in reviewing papers and making valuable suggestions for the authors to improve their work. We also would like to express our gratitude to the external reviewers, for providing extra help in the review process, and to the authors for contributing their research result to the conference.

Since July 2022, the Organizing Committees have received more than 100 manuscript papers, and the papers cover all the aspects in Engineering and Technology. Finally, after review, about 59 papers were included to the proceedings of ICFE-22.

We would like to extend our appreciation to all participants in the conference for their great contribution to the success of ICFE-22. We would like to thank the keynote and individual speakers and all participating authors for their hard work and time. We also sincerely appreciate the work by the technical program committee and all reviewers, whose contributions made this conference possible. We would like to extend our thanks to all the referees for their constructive comments on all papers; especially, we would like to thank to organizing committee for their hard work.

Acknowledgement

Rudra Bhanu Satpathy
Founder & Chief Executive Officer (CEO)
Institute for Engineering Research and Publication (IFERP)

IFERP is hosting the 1st International Conference on Future of Engineering (ICFE-22) this year in month of September. The main objective of ICFE-22 is to grant the amazing opportunity to learn about groundbreaking developments in modern industry, talk through difficult workplace scenarios with peers who experience the same pain points, and experience enormous growth and development as a professional. There will be no shortage of continuous networking opportunities and informational sessions. The sessions serve as an excellent opportunity to soak up information from widely respected experts. Connecting with fellow professionals and sharing the success stories of your firm is an excellent way to build relations and become known as a thought leader.

I express my hearty gratitude to all my Colleagues, Staffs, Professors, Reviewers and Members of organizing committee for their hearty and dedicated support to make this conference successful. I am also thankful to all our delegates for their pain staking effort to make this conference successful.

Welcome Message

Mr. Junrey Garcia
Program Chairperson, Electrical Engineering Program,
Romblon State University, Philippines

Biography

A professional registered electrical engineer with 9+ years of professional experience engaged in the field of academe, research and building construction project implementations. Capable in both theoretical and technical engineering fields of practice. Knowledgeable in power system analysis and design, renewable power systems and electrical building construction management, his role is vital in attaining the goals and objectives of the company, maintaining professional practice with high ethical values and integrity.

Keynote Speaker

Mr. Manish Advani

TEDx Speaker, Start-up Advisor,
Founder & CEO, MIMO POTENTIO, Maharashtra, India

Biography

Manish Advani is an 8 times TEDx Speaker, Award Winning Story teller and a Business Leader who has 20 years of Corporate Experience spread across Change Management, Marketing, Purpose based Branding, Public Relations, Internal Communications, Corporate Communications, Risk Management, Business Development, IT Project Management and Development.

Manish has worked with some of the leading companies such as Microsoft Canada, Jaguar Land Rover, Mahindra SSG, Schindler, National Centre for Transportation, and Industrial Productivity - USA, on Managerial, Consulting or Leadership roles in different geographies such as India, Canada, Middle East and the United States of America.

Manish is expert in integrating Leadership & Employee Development with Internal Communications and Personal / Employer Branding.

Manish has featured in the Economic Times, The Hindu Business Line, Awesome TV's Show, NJIT's Highlander Show, Sustainability Next, Times of India, Bakstage's Podcast.

Manish assists individuals and Organizations in addressing mental obstacles or roadblocks, unleashing their potential, improving performance and in exceeding expectations of the stakeholders.

Speech

Title: SWOT to WOLF Analysis

Abstract: It's a well-known fact 9 out of 10 start-ups fail, why only start-ups even large corporates have similar story, 12% of the Fortune 500 companies in 1955 continued to exist in the year 2017, remaining 88% companies have either gone bankrupt, merged with or have been acquired by some other company, some of them still exist after falling from the list of top Fortune 500 companies. Most of the companies which are out of the list must have done SWOT (Strength, Weakness, Opportunity & Threats) analysis which is one of the most popular exercise amongst companies of all sizes, however many didn't realize their today's strengths could be their tomorrows weakness, to help individuals and organizations evolve in their journey they need to dive deeper in to WOLF (Worry, Obsession, Limitations and Fear) analysis, Every individual and Organization experiences different kind of WOLF in different stages of their Life, the one who knows how to Conquer the WOLF is going to be the one who will be able to sail through worst of storms.

Discussion Points/Outcomes:
- Have Deeper understanding of Problems
- Become better at taking decisions
- Create Conducive environment for Growth

Keynote Speaker

Prof. Mohamed Fayad
Full Professor, Entrepreneur, Innovator,
San Jose State University, San Francisco Bay Area

Biography

Dr. M.E. Fayad is a full professor of Computer Engineering at San Jose State University since 2002. Previously, he was J.D. Edwards's professor of Software Engineering in the Department of Computer Science & Engineering at the University of Nebraska, Lincoln, from 1999 to 2002. Between 1995 and 1999, he was an associate professor of Computer Science and a faculty of Computer Engineering at the University of Nevada. He has more than fifteen years of industrial experience in addition to ten years as a software architect in companies, such as McDonnell Douglas and Philips Research Laboratory. His reputation has grown by his achievements in the industry—he has been an IEEE distinguished speaker, an associate editor, editorial advisor, a columnist for The Communications of the ACM (his column is Thinking Objectively), a columnist for Al-Ahram Egyptians Newspaper (2 million subscribers), an editor-in-chief for IEEE Computer Society Press—Computer Science and Engineering Practice Press (1995–1997), a general chair of IEEE/Arab Computer Society International Conference on Computer Systems and Applications (AICCSA 2001), Beirut, Lebanon, June 26–29, 2001, and the founder and president of Arab Computer Society (ACS) from April 2004 to April 2007.

Keynote Speaker

Prof. I.C.Gupta
Professor Emeritus, Dean of Management and Tourism,
Devi Ahilya University, Indore, India

Biography

Qualifications:

Ph.D.(Services Marketing), MBA,(Marketing), M.A.(Economics), M.A.(English Literature), A.T.M. (Advanced Tourism Management), IITTM-WTO Spain.

International Teaching Edhec, Lille, France, Assumption International University, Thailand University of Mauritius, Mauritius GBS Royal University of Bhutan.

Research Conducted:

1. Research Council of Thailand Bangkok, “Positioning Thailand as Tourists”.
2. UNICEF & Government of M P India “Evaluating Distribution of Iodized Salt”.
3. Marketing Research for Ten Corporate Houses in India.
4. Participated in Mercer Research Competition Singapore “Factors Affecting Mobility of Migrants to Thailand”.
5. Research Project for Ministry of Tourism “Functioning of Tourism Police”.

Special Event

Dr. R. Priyadarshini
Assistant Professor, School of Computer Science & Engineering,
Vellore Institute of Science and Technology, Chennai, India

Biography

R. Priyadarshini is working as an Assistant Professor Senior Grade in the School of Computer Science Engineering, Vellore Institute of Technology, Chennai. She has a Post-Doctoral fellowship in Faculty of Computer Science Engineering in Lincoln University Malaysia. She has 15 years' experience in teaching computer science and Information Technology and 2 years' experience as Software engineer and others. She completed her PhD in Information Technology from UGC recognized B.S. Abdur Rahman Crescent Institute of Science and Technology and Completed M. Tech Information Technology in College of Engineering, Guindy, Anna University, Chennai. She has a national and international patent grant to her credit in IoT Cloud and Data Analytics. She also has six patents published in IoT Cloud, Data Analytics, Cloud Security and Network Security. She has published more than 40+ papers in reputed international conferences and journals. She has 5 book chapters and 1 Book to her credit. More recently, she has contributed to interdisciplinary research in block chain, medical health and IoT. Her work corresponds to designing frameworks for various real time problems in IoT, Modern Web, NLP, Big Data, Machine Learning, Cloud, Networks and Cyber Security. She is a consultant for web designing, development and digital content development. Being a passionate teacher & topper in all her academic records and also a continuous learner, she has 35+ certifications in her research areas to her credit from various reputed institutions like IBM, NPTEL, SWAYAM, CSC, JPA, Spoken Tutorials IIT Mumbai, Udemy, GVN etc. and she has been awarded as best researcher, one of the top reviewer by various national and international bodies. She contributes her interests in various international conferences and serves as a reviewer in IEEE, Elsevier, Springer, and Inderscience publishers. She is an active member of CSI since July 2007 and also member of ACM, IFERP etc. and being recognized for her extraordinary contribution towards voluntary skill developing activities in Rotaract Club, SofSkills Training, IIIT club (Crescent University), TADHCO (Skill development through State Govt.), AICTE SPDC (Skill development through Central Govt.,) and SPOC for Infosys Springboard (Skill development through Corporate). Her interests include transforming people's life through life coaching, rejuvenating people's mind-set, creating awareness about avoiding chemicals in food for health and beauty, Aspiring career coaching for school and college students and a current technology mentor who likes to give technical seminars on the research findings.

Her motto us Practice, Preach and Prosper…….

International Advisory Committee

Saswat Khatai
School of Mechanical Engineering,
KIIT Deemed to be University, India

Dr. R. Priyadarshini
School of Computer Science & Engineering
Vellore Institute of Science and Technology
Chennai, India

Dr. Uma Kamboj
Department of Physics
Lovely Professional University Punjab, India

Dr. Syed Ahmad Helmi Al Haddad
Faculty of Engineering
Universiti Teknologi Malaysia (UTM), Malaysia

Paquito G. Fernando Jr.
BS Computer Engineering
Mindoro State University-Bongabong Campus,
Philippines

Dr. Mohammad Israr
Maryam Abacha American University of Nigeria,
Nigeria

Dr. Alireza Heidari
Molecular Spectroscopy
California South University, USA

Hadi Erfani
Department of Chemical Engineering
Islamic Azad University, Iran

Dr. Ng Yin Hoe
Faculty of Engineering
Multimedia University, Malaysia

Dr. Tan Siok Yee
Faculty of Information Science And Technology,
Universiti Kebangsaan Malaysia, Malaysia

Dr. Agung Kristanto
Department of Industrial Engineering
Universitas Ahmad Dahlan, Indonesia

Faridah Yahya
Computer Engineering
UniKL MIIT, Kuala Lumpur, Malaysia

Ahmad Zuhairi Abdullah
School of Chemical Engineering
Universiti Sains Malaysia, Malaysia

Dr. Ashish Kumar
Department of Science and Technology
Government of Bihar, India

Dr. Zeyar Aung
Department of Electrical Engineering and
Computer Science, Khalifa University, UAE

Dr. Tamer Mansour
Agricultural Economic Department
National Research Centre undefined, Egypt

Shankar Moguthala
EEE, Siddhartha Institute of Engineering and
Technology, Ibrahimpatnam, Telangana, India

Dr Chetan J. Shingadiya
Associate Professor, Computer Science/IT
Engineering Department, RK University , India

G.B.Renuka
Computer Science and Engineering,
Madanapalle Institute of Technology and
Science Andra Pradesh, India

Dr. Lovely Jain
Mathematics, Amity University Noida,
Uttar Pradesh, India

National Advisory Committee

Shielilo R. Amihan
Social Sciences and Humanities, The University of Perpetual Help System Dalta - Calamba Campus, Philippines

Dr. Noelah Mae D. Borbon
International Hospitality Management
Lyceum of the Philippines University Batangas, Philippines

Dr. Emerson B. Cuzzamu
Internal Audit and Quality Assurance
Tarlac Agricultural University, Philippines

Junrey Garcia
Electrical Engineering Program
Romblon State University, Philippines

Allyzza Nichole V. Maranan
Industrial Engineering Department
University of Batangas Main Campus, Philippines

Jemuel S. Vidal
Arts, Science, and Teacher Education
Philippine Christian University, Philippines

Maricel Magpantay Lacbay
Environmental Management
Batangas State University Lipa, Philippines

Dr. Leah B. Laforteza
Educational Administration
Philippine Christian University, Philippines

Dr. Nathaniel Vincent Lubrica
Research and Services Office
University of the Cordilleras, Philippines

Dr. Renato Dan Pablo II
Information Technology
Angeles University Foundation, Philippines

Michael Generalo Albino
College of Communication and Information Technology, President Ramon Magsaysay, State University, Philippines

Scientific Review Committee

Dr. Ahmad Rasmi Albattat
(Convener)
Hospitality Management, Management and Science University, Malaysia

Dr. Balakrishnan. S
(Conference Co-Chair)
Computer Science and Business Systems, Sri Krishna College of Engg & Technology, Coimbatore, India

Selim S
(Review Committee Member)
Computer Engineering, Karatekin University, Turkey

Yulia M. Kom
(Patron)
Faculty of Industrial Technology, Petra Christian University undefined, Indonesia

Gihan Suresh Aluvihara
(Review Committee Member)
Department of Chemical and Process Engineering, University of Peradeniya, Sri Lanka

Donabel R. De Veas - Abuan
(Review Committee Member)
Computer Science Department, De La Salle University, Manila, Philippines

Dr. Ajay Roy
(Program Chair)
Electronics & Communication Engineering Lovely Professional University Jalandhar, India

Dr. K. Hemachandran
(Session Chair)
Department of AI and ML, Woxsen University Hyderabad, India

Dr. N. Rajendran
(Session Chair)
Information Technology, B.S. AbdurRahman Crescent Institute of Science & Technology, India

Dr. Bernandino P Malang
(Scientific Committee Member)
College of Information Technology and Engineering, Bulacan State University, Philippines

Dr P. Vamsi Krishna
(Session Chair)
Department of Mechanical Engineering, NIT Warangal, India

Dr. Ahmed A. Elngar
(Session Chair)
Computer Science Department, Beni-Suef University, Egypt

Dr. Animesh Kumar Sharma
(Scientific Committee Member)
Mathematics, Raipur Institute of Technology (RITEE), India

Index

Index

IFERP connecting engineers...developing research
1st International Conference on Future of Engineering 2022

Review of Blockchain Technology

Abhishek Guleria[1], Er. Himanshu[2]*

[1,2] Department of Mathematics, University Institute of Science, Chandigarh University, Gharuan, Mohali, Punjab, India
Email: [2]himanshu.e11818@cumail.in

Abstract:
"One of the greatest technologies of the twenty-first century is blockchain. In technical terminology, a blockchain is a collection of time-stamped records that contain an immutable record of data and are controlled by a network of independent computers". Cryptographic functions are used to secure and connect each of these recordings of data, known as blocks. The first actual use of blockchain is with bitcoin. Bitcoin is not the only application of blockchain technology, though. We will discuss the use of blockchain technology across many areas in this paper.

Keywords:
Blockchain technology; Decentralized Finance; Supply Chain

I. INTRODUCTION

"A distributed database of records, or public ledger, of all transactions or digital events, is what blockchain technology is". The most well-known application of this technology is the "decentralized peer-to-peer digital currency" known as Bitcoin [10]. Bitcoin is a type of electronic cash. Bitcoin is both digital money and a method of online payment. Satoshi Nakamoto, an anonymous person or entity, designed Bitcoin in 2009 (published on January 9, 2009) [1,3]. "The blockchain is a distributed ledger that keeps track of all bitcoin transactions. It continues to rise as miners upload new blocks every 10 minutes to track the latest transactions. Every full node (i.e., every computer connected to the bitcoin network via a client) has a copy of the blockchain that is automatically downloaded when a miner joins the bitcoin network" [3]. There is a vast number of applications of blockchain technology apart from bitcoin such as digital finance, food supply chain, and, smart contract. Blockchain has many advantages, including a distributed ledger, decentralization, information transparency, tamper-proof architecture, and openness. Blockchain's evolution has been slow. Blockchain is currently split into three versions based on its applications: 1.0, 2.0, and 3.0. The three generations of blockchain are discussed in greater detail in Appendix[1] [3,5,9].
"Blockchain technology, the underlying technology for distributed ledgers, offers a ground-breaking platform for a new decentralized and transparent transaction mechanism in industries and businesses. Governments and major companies have investigated how to adapt and improve this technology in a number of application areas, including supply chain networks, design, manufacturing, and finance" [5]. The application of blockchain technology and smart contracts to supply chain management is analysed critically. The four types of barriers to the use of blockchain technology that are now available are inter-organizational, intraorganizational, technical, and external obstacles. Real business and supply chain transformation are still in their early phases [4]. The advantages of implementing blockchain in the supply chain are clear, including decreased risks to food safety, increased supply chain efficiency, expedited collaboration, and decreased carbon footprint. However, advancements are also required to maximize supply chain management [2]. The health, quality of life, and safety of people are all directly or indirectly threatened by China's major food safety issue. Many nations and regions have created and implemented the traceability system as an efficient method of managing and controlling product quality and safety [9].
Blockchain technology enables the emergence of decentralized financial services in the financial sector. These services are frequently more inventive, decentralized, interoperable, limitless, and transparent [6]. "Based on the concept of the European Credit Transfer System (ECTS), the author proposes a global blockchain-based higher

education credit platform, named EduCTX". The platform on which the system is based, the distributed P2P network system, is the open-source Ark platform. It could eventually evolve into a university-led, simple, and popular credit-grading system for higher education [8].

II. LITERATURE SELECTION PROCESS

Multiple reports from previous reports are chosen to represent connected work and the assessment. The 11 most important reports for this literature review were hand-picked and thoroughly examined.

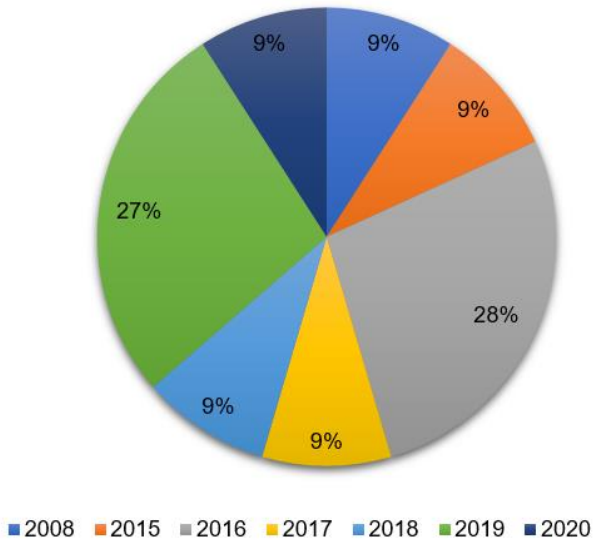

Fig 1; Paper bifurcation according to year

III. REVIEW OF BLOCKCHAIN TECHNOLOGY

The author in [1] represents a "purely peer-to-peer version of electronic cash that would allow online payments to be sent directly from one party to another without going through a financial institution". Satoshi Nakamoto, an anonymous person or entity, designed Bitcoin in 2009 (published on January 9, 2009) [2,4]. The technology behind bitcoin is blockchain.

According to the author of [6], Blockchain technology can bring about a new era of decentralized business models by lowering transaction costs, enlarging the scope of transactions, and enabling peer-to-peer transactions. "Decentralized finance has emerged as a result of this new paradigm, using blockchain technology to create an alternative financial system that is more decentralized, creative, interoperable, borderless, and transparent". Entrepreneurs and creators have been experimenting with decentralized business models that would not have been feasible without blockchain technology, despite the fact that a number of issues still exist. If successful, decentralized business models could revolutionize entrenched markets and usher in a new era of innovation and entrepreneurship.

The author of [8] is a representative of EduCTX, a global blockchain-based network for higher education credit. With the use of the blockchain, the suggested platform creates a highly reliable credit and grading system for higher education. "The EduCTX platform, which is built on the open-source Ark blockchain technology, was demonstrated by the author as a proof of concept. While HEIs profit from timely data regardless of a student's educational background, students benefit from a single, clear view of their completed courses." It is anticipated that such a system will ultimately develop into a uniform, straightforward, and widely used credit and grading system for higher education.

The adoption of blockchain in the food supply chain is represented by the author in [2]. The advantages of adopting blockchain technology in the supply chain are clear, including decreased risks to food safety, increased supply chain effectiveness, accelerated collaboration, and reduced environmental impact.

The author in [7] illustrates how decentralization of ITS(Intelligent Transport System) is possible with blockchain technology (Intelligent Transport system). "Blockchain can be used to build a secure, decentralized, and autonomous ITS environment that enables the better utilization of current ITS technology and resources, which is especially useful for crowdsourcing".

The author of [11] illustrates how blockchain technology is being used in the healthcare industry. "The management of electronic medical records, management of the medicine and pharmaceutical supply chain, biomedical research and teaching, remote patient monitoring, and health data analytics are just a few of the many applications for healthcare that blockchain can be used for".

Fig 2: Summary of major findings in blockchain technology in Tabular form

S.No.	Ref. No. & Year	Findings	Author
1.	[1] 2008	"Bitcoin: A peer-to-peer electronic cash system"	Satoshi Nakamoto
2.	[2] 2018	"The impact of blockchain on food supply chain"	Tan B, Yan J Chen S Liu X.
3.	[6] 2020	"Blockchain disruption and decentralized finance"	Chen Y Bellavitis C

4.	[7] 2016	“Blockchain-based intelligent transportation systems”	Yuan Y Wang FY
5.	[8] 2018	“EduCTX: A blockchain-based higher education credit platform”	Turkanović M Hölbl M Košič K Heričko M Kamišalić A
6.	[11] 2019	“Blockchain technology in healthcare”	Agbo CC Mahmoud QH Eklund JM.

IV. APPENDIX

There are Three Versions of Blockchain As depicted below:

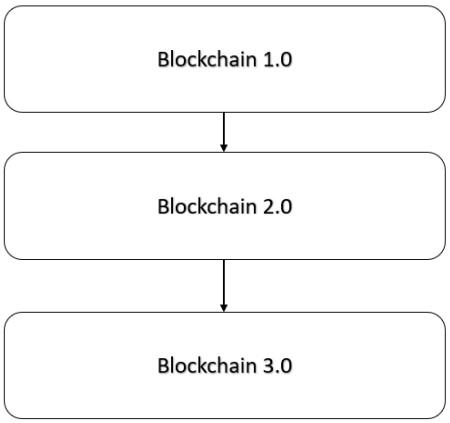

Fig 3: Different versions of Blockchain Technology

4.1 Blockchain 1.0(Cryptocurrency)

In 2005, Hall Finley introduced Blockchain Version 1.0, which is the first program based on Crypto money and contains DLT (Distributed Ledger Technology). This allows financial transactions to be carried out using Bitcoin and Blockchain technology (or DTL). This version is permissionless, thus any participant may conduct a legitimate Bitcoin transaction. Currency and Payments are the most common applications for this kind [3].

4.2 Blockchain 2.0 (Smart Contracts)

The inefficiency of bitcoin mining in version 1.0 and the network's insufficiency for scalability led to the introduction of the new version of the blockchain. Version 2.0 now has the problem fixed as a result. This iteration of the term "blockchain" will also contain "smart contracts," expanding it beyond only cryptocurrencies. Small Contracts, as a result, are miniature computers that live on blockchains. Free software programs on these tiny computers automatically monitor conditions including facilitation, verification, and compliance while lowering transaction costs. In Blockchain 2, Ethereum took the place of Bitcoin. Blockchain, 2.0 was able to efficiently process a high number of transactions on the public network as a result [3].

4.3 Blockchain 3.0 (DApps)

After version 2, a new version with DApps (decentralized applications) was made available. The fact that a DApp's interface can be written in any language and called the backend, and that the backend code operates on a decentralized point-to-point network, makes it comparable to a normal application. Network. It makes advantage of decentralized networks for communication and storage, like Ethereum Swarm. Available decentralized applications include BitMessage, BitTorrent, Tor, Popcorn, and others [3].

V. CONCLUSION

Due to this technology's tremendous appeal, we are already seeing its widespread implementation. This alone has the power to increase consumer confidence in these technological changes. Like any new technology, the origins of this one are not fully understood. In addition to improving tasks in existing sectors, “blockchain technology appears to have the ability to alter systems that keep track of the history of artefacts through a significantly improved, transparent ledger system”.

REFERENCES

[1] Nakamoto S. Bitcoin: A peer-to-peer electronic cash system. Decentralized Business Review. 2008 Oct 31:21260.

[2] Tan B, Yan J, Chen S, Liu X. The impact of blockchain on food supply chain: The case of walmart. InInternational Conference on Smart Blockchain 2018 Dec 10 (pp. 167-177). Springer, Cham.

[3] Swan M. Blockchain: Blueprint for a new economy. " O'Reilly Media, Inc."; 2015 Jan 24.

[4] Saberi S, Kouhizadeh M, Sarkis J, Shen L. Blockchain technology and its relationships to sustainable supply chain management. International Journal of Production Research. 2019 Apr 3;57(7):2117-35.

[5] Abeyratne SA, Monfared RP. Blockchain ready manufacturing supply chain using distributed ledger. International journal of research in engineering and technology. 2016 Sep 9;5(9):1-0.

[6] Chen Y, Bellavitis C. Blockchain disruption and decentralized finance: The rise of decentralized business models. Journal of Business Venturing Insights. 2020 Jun 1;13:e00151.

[7] Yuan Y, Wang FY. Towards blockchain-based intelligent transportation systems. In2016 IEEE 19th international conference on intelligent transportation systems (ITSC) 2016 Nov 1 (pp. 2663-2668). IEEE.
[8] Turkanović M, Hölbl M, Košič K, Heričko M, Kamišalić A. EduCTX: A blockchain-based higher education credit platform. IEEE access. 2018 Jan 5;6:5112-27.
[9] Tse D, Zhang B, Yang Y, Cheng C, Mu H. Blockchain application in food supply information security. In2017 IEEE international conference on industrial engineering and engineering management (IEEM) 2017 Dec 10 (pp. 1357-1361). IEEE.
[10] Crosby M, Pattanayak P, Verma S, Kalyanaraman V. Blockchain technology: Beyond bitcoin. Applied Innovation. 2016 Jun;2(6-10):71.
[11] Agbo CC, Mahmoud QH, Eklund JM. Blockchain technology in healthcare: a systematic review. InHealthcare 2019 Apr 4 (Vol. 7, No. 2, p. 56). MDPI.

IFERP connecting engineers...developing research
1st International Conference on Future of Engineering 2022

An Optimized Approach for Privacy Preserving of Big Data using GDTM and Random Number Generators with GNN

D.Kavitha[1], Dr.T.Adilakshmi[2], Dr.M.Chandra Mohan[3]

[1] PH. D Scholar, JNTUH, Kukatpally, Hyderabad, India
[2] Prof. & Head, Dept of CSE, Vasavi College of Engineering, Hyderabad, India
[3] Prof. of CSE & Director of Evaluation, JNTUH, Computer Science & Engineering, Hyderabad, India
Email: [1] kavithadasari.it2005@gmail.com

Abstract:
In this paper we propose a Privacy preserving mechanism of big data using GDTM along with Random Number generators. Given the rapid explosion of data being used across Enterprises, Individuals and Sensors, billions of data is being streamed and exchanged across the network. There is a high possibility of sensitive data being exchanged and stored, it's important to preserve sensitive data of Individuals and Enterprise data.
Most of the current techniques of privacy preserving in particular in the areas of data perturbation has been done on Static data. Given the dynamic nature of the applications and the huge data that is being generated it's important to evaluate the privacy preserving on big data without losing the accuracy.
Our research contribution is on Privacy preserving of big data using Geometric data transformation, random number generator and GNN techniques [5].
We would like to extend our research further on improving the accuracy of big data.

Keywords:
Privacy Preserving, Rotation, Translation and Scaling, GNN, Geometric Data perturbation, Random Number Generators

I. INTRODUCTION

Every day, vast amounts of data is being generated and collected by Enterprises, and devices(sensors) across the globe which might have details of customers, competitors etc. Numerous organizations and Enterprises analyses this data for crucial findings, decision makings and discoveries.
Data mining is predominantly used for extracting knowledge from huge amounts of data during this process there is a high probability to disclose sensitive information about individuals and organizations. Securing of sensitive data from unauthorized users when sharing information across the wire is of prime importance.
Privacy preserving of sensitive data has become a great concern, our research primarily addresses this concern by using Geometric data perturbation techniques, random number generators and GNN on big data.

Our Contribution can be summarized as follows:

1. For the first time we have applied the Geometric data perturbation (Rotation, Translation) with random number generators on the big data using GNN and observed high accuracy [3].
2. As a next step, to further improve the accuracy, we have added scaling perturbation technique to the above-mentioned methodology.

II. RELATED WORKS

Merve Kanmaz[14] proposed a methodology is based on Geometric data perturbation and generating of noise using random numbers. This method made use of Linear Congruential Generator for generation of the noise. This method has shown better results compared with existing data perturbation techniques. The research was conducted using 5 different data sets and evaluated using NB, J48 and DT and OneR. The methodology was evaluated again Attack Resistance using ICA and has shown promising results.

Aldeen, Y.A.A.S., Salleh, M. & Razzaque, M.A. proposed PPDM techniques based on distortion, associative classification, randomization, distribution, and k-anonymization. In this model sensitive data has been masked, transformed and retrieve the transformed outcome.

Chen, K., Liu, L. proposed Geometric Data Perturbation (GDP) method in this model which selectively preserves the task/model specific information in perturbation which has shown better privacy guarantee. GDP method was compared against well-known data-mining models and random projection perturbation and also evaluated against different level of attacks and proven. It has been proved GDP has provided better privacy guarantee and good accuracy as well.

F. Scarselli, M. Gori, A. C. Tsoi, M. Hagenbuchner and G. Monfardini, proposed on GNN. A learning algorithm to estimate model parameters was provided and demonstrated that the method is suitable also for large data sets. Based on the experimental results, solid results were observed.

III. DATASET

Dataset Details

Traffic Based IoT Sensor Big Data has been used. http://iot.ee.surrey.ac.uk:8080/datasets.html

Base Dataset Shape (3795475, 9)

The test data is split into the ratio of 75 (Training): 25 (Testing).

IV. PROPOSED METHODOLOGY

Geometric data perturbation (Rotation, Translation and Scaling) with random number generator (Noise) on big data using GNN. Below figure shows details of the proposed method.

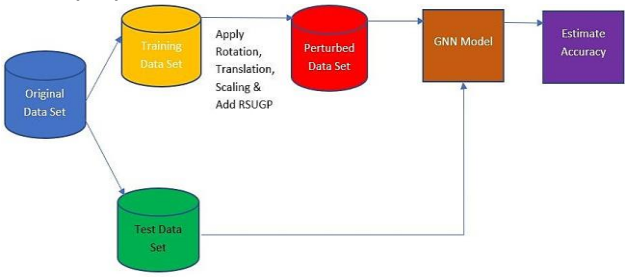

4.1 Geometric Perturbation

One of the widely used perturbation technique is Geometric Data Perturbation.

Data is rotated using a random angle, translated, scaled and finally noise is added to the data (calculated using random generators) based on below formula.

RX represents Rotation, T represents Translation, S represents Scaling of the original data in sequence,

∆-Adding of Noise to the data:

$$G(X) = RX + T + S + \Delta$$

4.2 Noise addition

Noise is generated using **Linear Congruence Generators**

Xi+1 = aXi + c (mod m)

'm','a' and 'c' represents the maximum value, standard deviation and average values in the data.

V. RESULTS AND DISCUSSION

5.1 Classification Accuracy

Classifier model performance has been evaluated using below formula.

$$\text{Classification Accuracy} = (T\,P + T\,N)/(P + N)$$

Confusion Matrix &Accuracy Comparison of GNN with and without Scaling

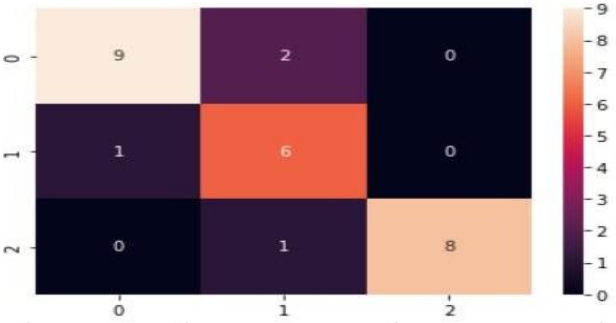

Model	GNN without Scaling [17]	GNN with Scaling
Test Accuracy values	0.9325	0.9419

5.2 Graph showing Accuracy vs Loss in GNN Training

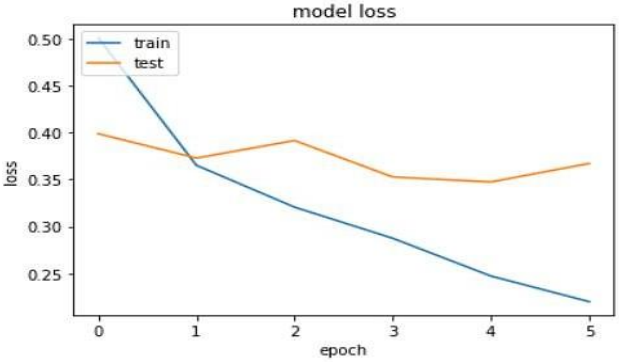

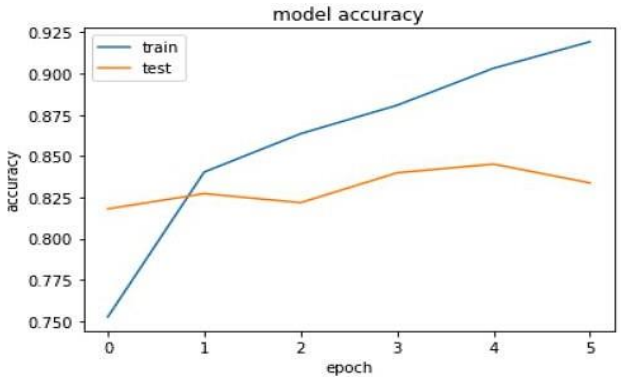

VI. CONCLUSION

As the volume of data increases particularly big data, it's important to preserve and retrieve the data correctly. With the proposed approach training and classification accuracy has increased by adding scaling transformation to Geometric data perturbation with random number generators using GNN [15]. Proposed method has proven to be a feasible approach for Privacy protecting of sensitive data and Classification Accuracy has increased from 93% to 94%.

REFERENCES

[1] Chen, K., Liu, L. Geometric data perturbation for privacy preserving outsourced data mining.

[2] Knowl Inf Syst 29, 657–695 (2011). https://doi.org/10.1007/s10115-010-0362-4

[3] Aldeen, Y.A.A.S., Salleh, M. & Razzaque, M.A. A comprehensive review on privacy preserving data mining. SpringerPlus 4, 694 (2015). https://doi.org/10.1186/s40064-015-1481-x

[4] [3]F. Scarselli, M. Gori, A. C. Tsoi, M. Hagenbuchner and G. Monfardini, "The Graph Neural Network Model," in IEEE Transactions on Neural Networks, vol. 20, no. 1, pp. 61-80, Jan. 2009, doi: 10.1109/TNN.2008.2005605.

[5] Merve Kanmaz1,∗ , Muhammed Ali Aydin2 and Ahmet —A New Geometric Data Perturbation Method for Data Anonymization Based on Random Number Generators‖ https://journals.riverpublishers.com/index.php/JWE/article/view/7983.

[6] D. Kavitha, Dr. T. Adilaxmi, Dr. M. Chandra Mohan. (2022). Efficient Privacy Preservation of Big Data Using Random Number Generators and Geometric Data Transformations. Mathematical Statistician and Engineering Applications, 71(3), 268 –. Retrieved from https://www.philstat.org.ph/index.php/MSEA/article/view/164

[7] https://www.sciencedirect.com/science/article/abs/pii/S0167739X17324391?via%3Dihub

IFERP®
connecting engineers...developing research
1st International Conference on Future of Engineering 2022

Spectrometry for Nitrogen and Phosphorous Macronutrients Detection in a Soil

Claze Therese de Vera[1], Roy D. Tipones[2], Juvy de Jesus[3], Juco R. Cantorne[4]

[1,2,3,4] University of Nueva Caceres, Philippines
Email: [1] claze.devera@unc.edu.ph, [2] roy.tipones@unc.edu.ph

Abstract:
Soil testing is a tool to diagnose the fertility status of the soil by determining the number of essential nutrients such as NPK macronutrients. To warrant a high yield of produce during harvest, plants should receive a balance of the proper nutrients it needs. The study developed a Soil Nutrient Tester (SNT) that uses the visible light spectrum and absorption principle to measure Nitrogen (N) and Phosphorous (P) in soil. This study aims to develop an inexpensive soil N-P nutrient tester and have an accuracy comparable to the spectrophotometer used in the laboratory. The SNT utilizes an RGB color sensor to detect the transmitted light passing through the sample solution. It used Arduino Uno Microcontroller as the brain of the device and an RGB LED as a light source that emits 450 nm and 700 nm wavelengths for Nitrogen and Phosphorus, respectively. The SNT identified the Nitrogen and Phosphorous level based on the soil test interpretation standard utilized by the Regional Soils Laboratory. The device results were compared and calibrated with the measurements of the Hitachi U-1800 Spectrophotometer to improve its accuracy and precision. A t-test revealed that the device's measurements have no significant difference from the concentration measurements of the reference device for a confidence level of 95%, proving that the device is competent in measuring N-P macronutrients accurately. The device was also able to reduce the time spent evaluating N-P nutrient content and the cost of the spectrophotometer. This device will allow farmers and home gardeners to regularly check their soil's N-P nutrient status to decide the proper amount of fertilizer to apply.

Keywords:
Absorption Principle, Nitrogen, Phosphorus, Soil Nutrient Tester

I. INTRODUCTION

Soil Testing is a tool to diagnose the fertility status of the soil. It determines the concentration of essential nutrients in a soil sample. If deficient, it allows the recommendation of the right kind of fertilizer or other soil ameliorants at the right amount and timing of application. Soil tests are essential in ensuring the health of your lawn or ploughland where vegetable crops or plants are cultivated. To warrant a high yield of produce during harvest, plants should receive a balance of the proper nutrients it needs.

These soil nutrients are the N-P-K macronutrients. These three nutrients are essential to the survival of every plant. Nitrogen (N) is vital to chlorophyll, allowing plants to carry out photosynthesis and it aids in the compounds that allow for energy storage and use. Phosphorus (P) promotes roots and growth. At the same time, Potassium (K), sometimes referred to as the “Quality Element,” is essential in regulating processes in the plant, such as osmosis and enzyme activities. Measuring and provisioning the amount of these three soil nutrients are vital for proper plant growth and adequate fertilization. It is impossible to tell just by looking at the soil if it receives enough nutrients. Thus, researchers and interested individuals find ways to test their soil regularly without consuming time and spending money on a local testing laboratory whenever they need soil testing.

Today, there are two methods to test N-P-K macronutrients available at the regional soil laboratory. The Soil Test Kit or STK shows how much Nitrogen, Phosphorous, and Potassium your soil holds through the color change it has undergone. Although cheap, test kits sometimes don't provide the most accurate results. The second method is having it tested using the UV-Visible Spectrophotometer. The result will give you a precise quantity of the N-P-K nutrients and make it a better choice than the former on choosing a fertilizer, but testing is expensive. In search of a cheaper solution, many researchers have tried to develop NPK detection devices from various methods, including optical, electrochemical, acoustic, electromagnetic, and mechanical sensors. Among these methods, the optical detection method was recently identified to

have a higher potential for real-time detection because of its extreme sensitivity and fast response. There are various reasons why farmers are not having their soil tested despite its benefits. The first is the high testing fee, 750php for the three major nutrients. Some even choose a cheaper STK (Php 100.00) that will give a rather vague result but is better than not having their soil tested at all. Another major factor limiting farmers in performing soil tests is time and distance. Soil analysis processing time is long because tests are conducted by batch to maximize chemical solutions used in soil sample preparation. Also, chemical analysts would then have to draft the test results and interpret them manually before giving fertilizer recommendations. These tests are conducted only in regional soil labs; thus, they must travel far, which adds to the farming costs, which most farmers do not have.

A. Statement of the Problem

This study aims to create a soil nutrient tester using LED as its optical transmitter based on the absorption principle that will give a real-time detection of the content of each nutrient in a sample of soil. Specifically, this aims to answer the following questions:

1. Is there a significant difference between the measurements of the quartz cuvette being utilized at the Department of Agriculture Region V Soils Laboratory and the glass cuvette used by the proponents?
2. What are the best light wavelengths to produce accurate results?
3. Are the device measurements accurate and precise compared to the concentration measurements of the Regional Soils Laboratory?
4. Will the device reduce the time spent evaluating the amount of Nitrogen and Phosphorus nutrients in a soil sample?
5. Is the device a cheaper method of testing Nitrogen and Phosphorus nutrients?

B. Scope and Limitations

This study is limited to designing, developing, and evaluating a soil nutrient tester for Nitrogen (N) and Phosphorus (P) macronutrients in soil. The resulting output will be the content of each nutrient in the sampled soil through ranges set at HIGH, MEDIUM, and LOW parameters, which apply for both Nitrogen and Phosphorus. The results were compared using the Hitachi U-1800 Spectrophotometer at the Department of Agriculture Region V Soils Laboratory.

C. Significance of the Study

Soil Testing is a tool to diagnose the fertility status of the soil. It determines the concentration of essential nutrients in a soil sample. If deficient, it allows the recommendation of the right kind of fertilizer or other soil ameliorants at the right amount and timing of application. Soil tests are essential in ensuring the health of your lawn or ploughland where vegetable crops or plants are cultivated. To warrant a high yield of produce during harvest, plants should receive a balance of the proper nutrients it needs. This study is significant to the following recipients:

Farmers and home gardeners. The device will allow them to check their soil's health status regularly. The device is cheaper than the Hitachi U-1800 Spectrophotometer used at the Regional Soils Laboratory and will help farmers save the money they will spend every time they go and request a soil test. The device will also reduce their time evaluating nitrogen and Phosphorus nutrients in a soil sample.

Department of Agriculture. This device can provide a cheaper alternative to the currently used Spectrophotometer.

Future Researchers. This research can provide new insights into spectroscopy in measuring nutrients in a soil sample.

II. METHODOLOGY

This study employs a qualitative descriptive research design to explore, describe, and understand the broad collective challenges of soil testing and create an innovative solution to address the challenges. This approach will gather descriptive quantitative items of the sample's nutrient content and compare the result to the commercially procured soil testing equipment the Regional Soil Laboratory is currently using. Elements of the real-time data capture will also be used to test the reliability, accuracy of the device, and speed in displaying test results. This approach is used to understand the research problem and give an elegant solution through experimentation and analysis. It aims to describe the characteristic of the sample and assess both the performance and costing. Use of qualitative description permits. The data vital to this research will be gathered by experimentation in the Regional Soil Laboratory.

A. Conceptual Framework

Figure 2: Conceptual Framework

 ISBN: 978-93-92105-22-7

Fig. 2 illustrates the conceptual framework of the Soil N-P Nutrient Detector. The first step is calibrating the device using the cuvette with distilled water. After calibration, the second step is to put the soil solution's cuvette. The device will then test the sample, and the Arduino Microcontroller processes the resulting absorption level and calculates the test result. The LCD will then display the qualitative characteristics of the soil sample with ranges of Low, Medium, and High. These results can now be a basis for choosing a suitable crop fertilizer.

B. Design Discussion

Figure 3: Block Diagram

Fig. 3 illustrates the process and interconnection of the components of the device. First, incident light flashes at the soil solution, and an absorption process occurs. The sensor will then read the transmitted radiation that passed through the solution. Afterward, the microcontroller will read the output from the sensor and process it for further computation of the concentration of a nutrient on the sample. Finally, the LCD shows the soil nutrient levels.

C. Program Flow Chart

The program flow of the device is illustrated in Fig. 4. The program starts with the calibration – a cuvette filled with water is inserted in the sample compartment – and after the LED flashes a different wavelength of light, the LCD will display a notification that the calibration has been completed and will now start the testing process. The LCD will display directions for the user's convenience. The testing process will begin with Nitrogen; the LCD will ask the user to insert the desired soil sample solution and press the mode button that commands the program to continue to the next test. When done, the program will test the Phosphorus content of the same soil sample. After testing, the microcontroller will perform algebraic operations to compute the nutrient concentration in the soil sample. The result displayed in the LCD is based on the proponent's set range for each parameter.

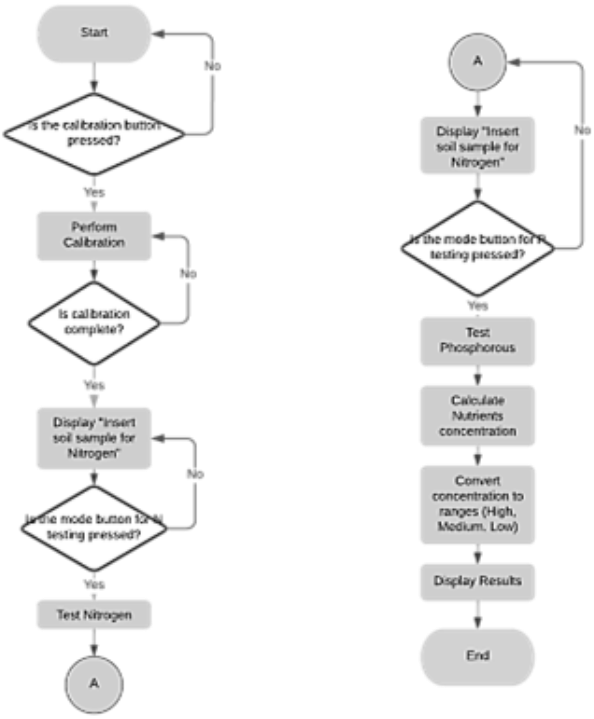

Figure 4: Program Flowchart

D. Device Model Design

The designed model of the device is composed of a few parts. The said parts are LCD (Liquid Crystal Display), Push Buttons, Switch, Sample Compartment, Sensor, LED (Light Emitting Diode), Cuvette, and a charging input. The designed device is shown in Fig. 5. The figure shows the developed model from various viewing angles. It also shows the position of the different parts of the designed model.

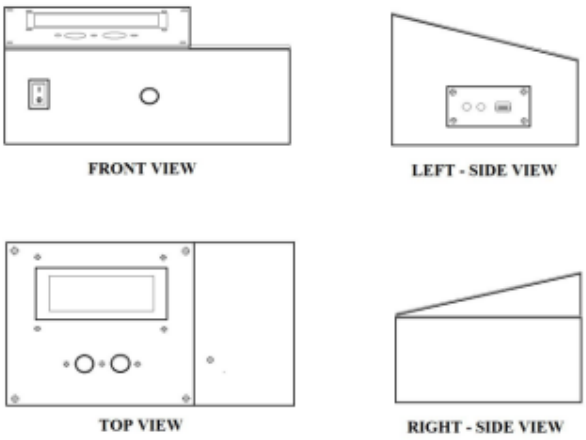

Figure 5: Device Design

E. Schematic Design

This section discusses the schematic design of the device. This includes the component used, its function, and how the specific element for the device was chosen. The schematic diagram in Fig. 6 shows the different components used in the devices and how they are connected for proper circuit operation.

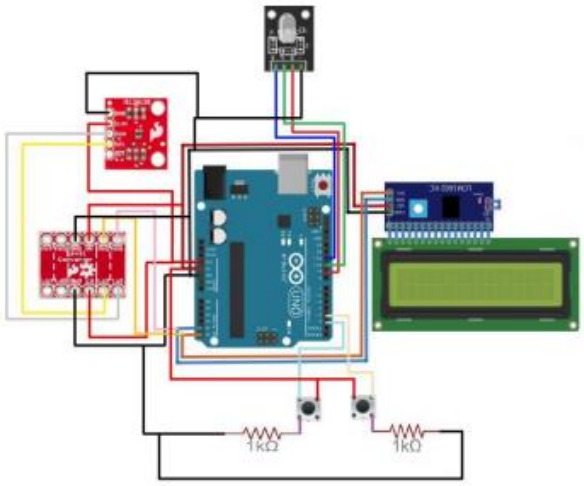

Figure 6: Schematic Circuit Diagram

A single pole single throw (SPST) switch is the main switch connected to the power source, a rechargeable lithium battery. It enables the user to switch the device on and off. The ISL 29125 RGB Sensor is used to read the color absorption. It measures the light intensity passed through the soil sample and converts it to electrical signals. The sensor has an on-chip ADC converting electrical signals to digital counts. The ISL 29125 is chosen for its high sensitivity and accurate RGB spectral response. The sensor is also easy to interface to the microcontroller. This sensor runs on 3.3V logic, requiring a bidirectional logic level converter that steps down the 5V power from the microcontroller. The level converter is easy to use. The board needs to be powered from the two voltage sources (high and low voltage) that the system is operating, in this case, 5V and 3.3V.

For the microcontroller, Arduino Uno is used. The microcontroller will act as the brain of the device. It processes the acquired data from the sensor and performs algebraic operations. The proponents chose this microcontroller because it provides enough RAM (Random Access Memory) and ROM (Read Only Memory) for the proper operation of the device. The RAM is the one that provides the smooth flow of functions of the microcontroller, and the ROM is responsible for the storage of the main program on the microcontroller. Arduino Uno is also chosen because the device only utilizes a few components.

The device uses a 20 x 4 LCD (liquid crystal display) to show the Nitrogen and Phosphorus nutrient content in each soil sample. The user will view if the soil has a Low, Medium, or High range of the nutrient being tested. Initially, the LCD shows various instructions that shall be followed by the user for proper testing procedures when using the device. The LCD will then display what button should be pressed and what sample shall be placed inside the sample compartment. After following the instructions shown in the LCD, it will now display the content of each nutrient on a soil sample in its specified ranges.

An RGB LED module is utilized as the light source of this device. This LED plays a vital role because the illuminated light is the basis for the absorption in the sample. The instrument used a diffused common cathode LED, and the wavelength of the light was varied in the program using HEX codes. The RGB LED is located inside the sample compartment and placed directly parallel to the cuvette and sensor.

F. Determining the Concentration Equations

The Soil Nutrient Tester device contains one (1) RGB color sensor that detects the transmitted light that passed through the sample. The ISL 29125 RGB color sensor has three photodiode arrays that convert light transmitted into the current readings. The current output is converted to a digital count by an on-chip Analog-to-Digital Converter (ADC) at the light-to-signal processor. The ADC converter resolution is selectable from 12 to 16 bits with a full-scale ADC code of 65535 counts. The proponents used the ADC count value that was read by the sensor. It is integrated into the Beer–Lambert's Equation as the baseline, which indicates the value for when the light passed through an optically transparent solution (i.e., water), and the current reading, which specifies the amount of absorption that took place when the light passed through a soil solution. The equations are as follows:

For Nitrogen,

$$A_N = \log_{10}\left(\frac{baseline}{currentReading}\right) \quad (3)$$

For Phosphorus,

$$A_P = \log_{10}\left(\frac{baseline}{currentReading}\right) \quad (4)$$

Now that we have a result for the absorption that took place for each nutrient, the microcontroller will continue to determine each nutrient's concentration on the soil sample. The proponents used the calibration standard shown in Tables 1 and 2 used during the initial tests conducted at the Regional Soils Laboratory to obtain equations for the concentration of each nutrient.

Table 1: Calibration Standards for Phosphorus

Standard No.	Vol. of 50 mg/L Stock solution (mL)	Final Volume (mL)	Concentration of working std. (mg/L P)	Equivalent concentration in soil (mg/L P)
1	1	250	0.2	4
2	1	100	0.5	10
3	2	100	1.0	20
4	4	100	2.0	40
5	6	100	3.0	60
6	8	100	4.0	80

Table 2: Calibration Standards for Nitrogen

Standard No.	Mass of O.C. (mg)	Sucrose Solution (mL)	H_2O (mL)	$K_2Cr_2O_7$ (mL)	H_2SO_4 (mL)	H_2O (mL)
1	0	0.00	2.00	2	5	18
2	1	0.25	1.75	2	5	18
3	2	0.50	1.50	2	5	18
4	3	0.75	1.25	2	5	18
5	4	1.00	1.00	2	5	18
6	5	1.25	0.75	2	5	18
7	6	1.50	0.50	2	5	18
8	7	1.75	0.25	2	5	18
9	8	2.00	0.00	2	5	18

Fig. 7 shows the relationship of the concentration and absorbance generated from the calibration standard for the Nitrogen Test set up at the Soils Laboratory.

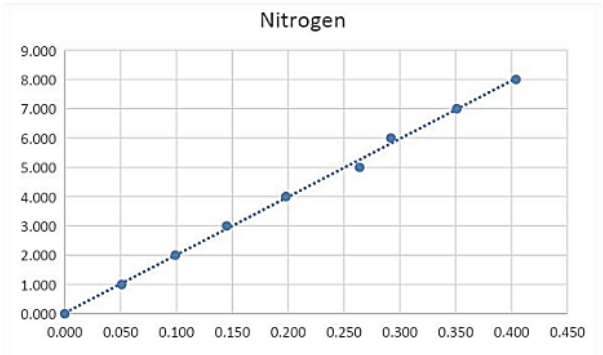

Fig. 7: Calibration Standard for Nitrogen Result

To generate an equation from the graph, the linear best fit function in excel was utilized. The regression line can be considered an acceptable estimation of the actual relationship between concentration and absorbance.

$$absorbanceN = 19.822 concentrationN + 0.0044 \quad (5)$$

It is notable to mention that the R-squared indicated after generating the regression equation represents the proportion of the variance for the concentration explained by the absorption shown in the regression model. The output is considered good when the R-squared is not lesser than 0.995; wherein, 1 is the most desirable proportion. A low R-squared value, in this research, accounts for an improper setup of the chemicals prepared for testing and will lead to a not very accurate measurement of the concentration.

From this equation, the formula for the Nitrogen concentration can be derived

$$concentrationN = 0.05044899606497830693 absorbanceN - 0.0013520330945141862 \quad (6)$$

The generated equation for Nitrogen concentration was used to determine the Organic Carbon. The result will then be integrated and processed to determine Nitrogen's Percent Organic Matter (%OM) content.

$$OC = \frac{concentrationN}{0.5 \times 1000} \times 100$$
$$OM = OC \times 1.72$$
$$N = OM \times 0.05 \quad (7)$$

Where,
OC = Organic Carbon
OM = Organic Matter
N = % OM of Nitrogen

Sequentially solving for the indicated equations will provide the %OM content of Nitrogen which can now be translated to the following Soil Test Characteristic based on the Regional Soils Laboratory Standard Operating Procedure (SOP):

$High$: $\%OM \geq 4.5\%$
$Medium$: $\%OM$ *is between* $2.1 - 4.5\%$
Low: $\%OM \leq 2.0\%$

Similar procedures were conducted to determine the concentration of Phosphorus. Fig. 8 shows the relationship between the concentration measured and absorbance generated from the calibration standard for the Phosphorus Test that was set up at the Soils Laboratory.

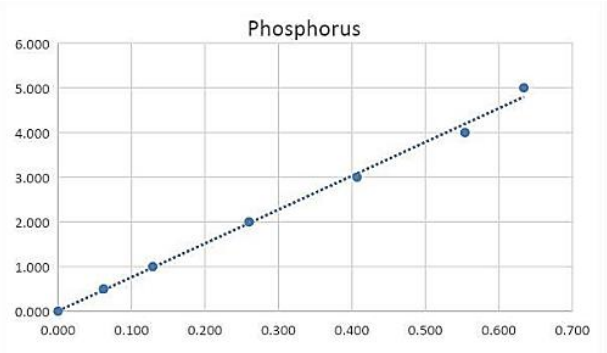

Fig. 8: Calibration Standard for Phosphorous Result

The regression equation generated from the linear best fit function gives the acceptable estimation of the actual relationship between concentration and absorbance for Phosphorus.

$$absorbanceP = 7.5608 concentrationP + 0.0044 \quad (8)$$

The equation for the concentration of Phosphorus is derived from the regression equation.

$$concentrationP = 0.13226113638768394298 absorbanceP - 0.00581949000105808909 \quad (9)$$

The Phosphorus concentration equation is multiplied by a factor of 20 to find the Parts per Million (PPM) equivalent. The result is then translated to the Soil Test Characteristic for Phosphorus based on the Soil Lab Standard operating procedures.

$High$: $PPM \geq 20$
$Medium$: PPM *is between* $10 - 20$
Low: $PPM \leq 10$

III. DATA GATHERING

To determine the reliability of the proponent's device, several tests were conducted at the Regional Soils Laboratory, a branch of the Department of Agriculture (DA), in Del Rosario, Naga City. Tests were conducted by comparing results with the reference device, Hitachi U-1800 Spectrophotometer, and the researcher's device. The samples used were taken from different places in Camarines Sur, such as San Juan Pagao, Bombon (sample 1), Paolbo, Calabanga (sample 2), and Carolina, Naga City (sample 3).

A. Soil Procurement

1. Prepare the following tools: bucket, shovel, bolo, and a pouch or sack
2. Divide the perimeter of the land according to
   a. Soil color
   b. Texture
   c. Amount of Fertilizer
3. Every soil sample is taken from a 5-hectare perimeter, divided according to the type of crop planted, kind of soil, and topography needs a (1) kilo of the composite sample. Get a soil sample after the harvesting season or before putting a fertilizer. Don't get a soil sample in the same place the fertilizer was embedded or where crops are planted.
4. Using the shovel, dig in the soil a 20 cm deep V-shaped sample, 2 cm thick and 5 cm wide. Place it in the bucket, then repeat the process until ten samples are taken. Gently blend and grind the samples.
5. Lay the composite sample in a sack, then air-dry. Make sure not to mix the soil samples and that no dirt will be included.
6. When dried, crash it again until fine, then divide it into four (4) parts. Take the 2nd and 4th portion, then throw the 1st and 3rd. Repeat four (4) times until it weighs a half kilo. Afterward, store it in a pouch.

B. Preparation of Soil Solution for the Device

Materials:

1. Measuring cups
2. Container (e.g., plastic bottle)
3. Distilled water
4. Soil

Instructions:

1. Measure two teaspoons of soil and put them in the container.
2. Measure a ¼ cup of water and put it in the container with the soil.
3. Mix the soil and the water for 1 to 2 minutes.
4. Wait for 3 to 5 minutes for the undissolved soil to rest at the bottom of the container. 5. Slowly transfer the soil solution to the cuvette and avoid the undissolved soil transferred to minimize the error.

IV. RESULTS AND DISCUSSION

A. Comparison of Quartz and Glass Cuvette

The device utilizes a glass cuvette as it is cheaper than the quartz cuvette used at the Department of Agriculture Region V Soils Laboratory. This test will determine whether there is a significant difference in absorbance between the two cuvettes. Using the calibration standards made by the chemist at the soil's laboratory, glass and quartz cuvettes were tested in the reference device.

Table 3 shows the test results when comparing a glass cuvette with a quartz cuvette using calibration standards for phosphorus.

Table 3: Comparison of Quartz and Glass Cuvette using Calibration Standard for Phosphorus

Standard No.	Quartz Cuvette		Glass Cuvette	
	ABS	CONC	ABS	CONC
1	0.000	0.000	0.000	0.000
2	0.061	0.500	0.077	0.500
3	0.143	1.000	0.144	1.000
4	0.266	2.000	0.278	2.000
5	0.411	3.000	0.416	3.000
6	0.543	4.000	0.554	4.000
7	0.640	5.000	0.652	5.000
	p-value =	0.9516	α =	0.05

To identify whether there is a significant difference between the two cuvettes in terms of absorbance in Phosphorus, a t-test was conducted. The statistical test revealed that the p-value, 0.9516, is greater than the level of significance, 0.05; thus, we fail to reject the null hypothesis. This means that there is no significant difference between the absorbance of the two cuvettes. This suggests that using a glass cuvette will not affect the results of the device for Phosphorus. Table 4 shows the test results when comparing a glass cuvette with a quartz cuvette using calibration standards for nitrogen.

Table 4: Comparison of Quartz and Glass Cuvette using Calibration Standard for Nitrogen

Standard No.	Quartz Cuvette		Glass Cuvette	
	ABS	CONC	ABS	CONC
1	0.000	0.000	0.000	0.000
2	0.051	0.500	0.060	0.500
3	0.099	1.000	0.118	1.000
4	0.145	2.000	0.173	2.000
5	0.198	3.000	0.229	3.000
6	0.264	4.000	0.288	4.000
7	0.292	5.000	0.367	5.000
8	0.351	6.000	0.411	6.000
9	0.404	7.000	0.455	7.000
	p-value =	0.6449	α =	0.05

To identify whether there is a significant difference between the two cuvettes in terms of absorbance for Nitrogen, a t-test was conducted. The statistical test revealed that the p-value, 0.6449, is greater than the level of significance, 0.05; thus, we fail to reject the null hypothesis. This means that there is no significant difference between the absorbance of the two cuvettes. This suggests that using a glass cuvette will not affect the results of the device for Nitrogen.

B. Test of Wavelength

This test is conducted to identify the best wavelength to be used when measuring Nitrogen and Phosphorus. The results are compared to the results of the reference device. The reference device utilizes the wavelength 627 nm for N and 882 nm for P. Initially, the wavelength of the proposed device was set to these wavelengths, and the samples were tested. The results show that the average percent error is above the designated 5% tolerance of the device's design, as shown in Table 5.

The percent error is calculated using the formula:

$$\%error = \frac{Output_{reference} - Output_{proposed}}{Output_{reference}} \times 100 \quad (10)$$

Table 5: Initial Test for Wavelength (N = 627 nm and P = 882nm)

	Nitrogen			Phosphorus		
	Reference Device	Proposed Device	Percent Error	Reference Device	Proposed Device	Percent Error
1	3.14	3.58	14.01%	23.82	39.61	66.29%
2	0.41	0.29	29.27%	22.02	39.61	79.88%
3	3.71	3.41	8.09%	24.42	39.61	62.20%
		Ave =	**17.12%**		Ave =	**69.46%**

Several wavelengths were tested to determine the wavelength that will produce the best results, and the percent error was calculated. Based on the results, the wavelengths that had the least error are 450 nm for nitrogen and 700 nm for phosphorus. This is parallel to the study results by Yusof et al.

C. Test for Accuracy

To test the accuracy of the proposed device, its reading is compared to a reference device specifically, Hitachi U-1800 UV/VIS Spectrophotometer, the instrument used in the Regional Soil Lab. The percent error is used to determine if the proposed device is accurate or within the tolerance.

For Nitrogen, the test results revealed that for three samples, the device is 96.97% accurate. Table 6 summarizes the results of the accuracy test for Nitrogen.

Table 6: Accuracy Test: Nitrogen

Sample	Reference Device	Proposed Device	Percent Error (%)
1	3.14	3.252	3.57
2	0.41	0.421	2.68
3	3.71	3.605	2.83
		Average	3.03%

p-value = 0.93248 *α=0.05*

To identify whether the measurements are within the acceptable standard measurements, a paired t-test is conducted. The statistical test revealed that the p-value, 0.93248, is greater than the level of significance, 0.05; thus, we fail to reject the null hypothesis. This means that there is no significant difference between the measurements of the two devices for Nitrogen.

The same test was conducted for Phosphorous. The test results revealed that for three samples, the device is 98.98%. Table 7 summarizes the results of the accuracy test for Phosphorus.

Table 7 Accuracy Test: Phosphorus

Sample	Reference Device	Proposed Device	Percent Error (%)
1	23.82	22.87	3.99
2	22.02	22.87	3.86
3	24.42	24.124	1.21
		Average	3.02%

p-value = 0.825295; α=0.05

The statistical test revealed that the p-value, 0.825295, is greater than the level of significance, 0.05; thus, we fail to reject the null hypothesis. This means that there is no significant difference between the measurements of the two devices for Phosphorous.

These two results show that the device measurements are highly accurate and reliable, with an accuracy rate of 97% for Nitrogen and Phosphorus.

D. Test for Precision

A precision test was conducted to determine whether the device could be trusted and reliably reproduce accurate results time after time. The three samples are measured for ten trials, and the standard deviation is calculated. Table 8 summarizes the results.

Table 8: Precision Test

Trial No.	Sample 1		Sample 2		Sample 3	
	N	P	N	P	N	P
1	3.31	22.87	0.43	22.87	3.63	22
2	3.27	22.87	0.43	22.87	3.56	24.96
3	3.27	22.87	0.42	22.87	3.54	24.96
4	3.2	22.87	0.42	22.87	3.61	24.96
5	3.27	22.87	0.42	22.87	3.57	22.87
6	3.24	22.87	0.42	22.87	3.59	22.87
7	3.26	22.87	0.42	22.87	3.67	24.96
8	3.23	22.87	0.42	22.87	3.64	24.96
9	3.25	22.87	0.42	22.87	3.59	22.87
10	3.22	22.87	0.41	22.87	3.65	24.96
Standard Deviation	0.031198	0	0.005676	0	0.04223	1.217767

The results revealed slight variation among the results for all three samples, as seen in the small values of the standard deviation. The results indicate that the proposed device is precise in giving its measurements.

E. Latency Test

The Latency Test compares the speed of the proposed device to the reference device to determine which is faster in giving the result. Table 9 shows the time it takes to determine the nutrient levels, starting from when the cuvettes were placed inside the sample compartment of each device to the result being translated to its quantitative equivalent. Through a Stopwatch, the proponents could determine the speed for each test conducted in a minute-second.

Table 9: Latency Test

Trial	Reference device (minute: second)	Proposed Device (minute: second)
1	3:49	1:35
2	4:13	1:28
3	4:05	1:34
4	3:56	1:29
Average	4:00	1:31

The latency test reveals that the device successfully reduced the nutrient testing time. The proposed device is 2.63 times faster than the reference device in measuring the nutrient concentrations.

F. Cost Comparison

Table 10 shows the cost comparison between the reference device and the proponent's device. The cost for the reference device refers to its market price, and the cost of the proponent's instrument is the total expenses of the proponents in constructing the device. This reveals that the proposed device is 100 times cheaper than the device available in the market.

Table 10: Cost Comparison

Device	Cost
Hitachi U – 1800 Spectrophotometer	P 398,660.00
Proposed Device	P 4,324.00

REFERENCES

[1] Dor, E. (2013). Soil Spectroscopy: Principle and Applications. Brno, Czech Republic: European Facility for Airborne Research.

[2] Gillaspy, R. (n.d.). What is Soil? - Definition, Structure & Types. Retrieved from Study.Com.

[3] Kulkarni, Y., Warhade, D. K., & Bahekar, D. S. (2014, May). Primary Nutrients Determination in the Soil Using UV Spectroscopy. International Journal of Emerging Engineering Research and Technology, Volume 2 (Issue 2), 198-204.

[4] Laboratory, R. S. (n.d.). Standards Operating Procedures.

[5] Lines-Kelly, R. (1992, October). Plant nutrients in the soil. Soil Sense.

[6] Mallarino, A. (2005). Encyclopedia of Soils in the Environment.

[7] Masrie, M., Rosman, M. S., Sam, R., & Janin, Z. (2017). Detection of Nitrogen, Phosphorus, and Potassium (NPK) nutrients of soil using Optical Transducer. 1-4.

[8] Nocita, M., Stevens, A., Wesemael, B. v., Aitkenhead, M. J., & al., e. (2015). Soil Spectroscopy: An Alternative to Wet Chemistry for Soil Monitoring. Advances in Agronomy.

[9] Owen, T. (2000). Fundamentals of UV-Visible Spectroscopy. Germany: Agilent Technologies. Soil Organic Matter. (2008). Agronomy Fact Sheet Series, p. Fact Sheet 41.

[10] Viscarra, R., & McBratney, A. (2008). Diffuse Reflectance Spectroscopy as a Tool for Digital Soil Mapping.

[11] Wetterlind, J., Stenberg, B., & Rossel, R. A. (2013). Soil analysis using visible and near-infrared spectroscopy. Methods in molecular biology, 95-107.

[12] Yusof, K. b., Isaak, S. b., Ngajikin, N. H., & Che, N. b. (2016). LED-Based Spectroscopy. Buletin Optik, 2-3.

IFERP connecting engineers...developing research
1st International Conference on Future of Engineering 2022

Review of Advanced Battery Management System Algorithm for Li-ion Batteries' Module in Electric Vehicles

Himanshu Maithani[1], Dr S.K. Goel[2]

[1] PhD Scholar, [2] Professor
Email: [1] mhimanshu2910ee@gmail.com, [2] drgoelsk@yahoo.com

Abstract:
Batteries are crucial in switching towards renewables, especially solar and wind. Efficient and reliable energy storage technologies motivate people to relinquish traditional generators that use fossil fuels, coal etc. which are non-eco-friendly and cause so many greenhouse gas emissions. Efficient batteries like Li-ion batteries (LIBs) also suffer from memory effects, thermal instability at a higher temperature, and ageing due to over-charging and undercharging conditions. It is also impossible to operate all cells in the same module with the same charging and discharging rate. Also, monitoring the temperature of all the cells is crucial to work within the rated range to avoid the possibility of thermal runaway. Battery Management System (BMS) technology, along with the data acquisition system, is like a doctor that continuously monitors the state of charge (SoC), state of health (SOH), state of function (SOF), etc. of every cell by measuring quantities like current, voltage, temperature, impedance, etc. of the cells in real-time for performing charge balancing, thermal management, and protection against over-charging and under-charging by implementing efficient algorithms to perform state estimation with the highest accuracy which contains very minimum noise or errors. Conventional passive charge balancing is easy and inexpensive but inefficient. This paper discusses some advanced SOC estimation algorithms for BMS like Data-driven (Support Vector Machine) SVM Kernel, (Radial Basis Function) RBF Neural Network, Backpropagation Neural Network (BPNN), Deep Neural Network (DNN), modal-based (recursive Bayesian estimation) filtering algorithms like Kalman filter (KF), Unscented Kalman filter (UKF), Extended Kalman filter (EKF), Particle filter (PF), etc., Sliding Mode Observer (SMO), Fuzzy logic, and Electrochemical impedance spectroscopy (EIS) to monitor performance and implement the control strategy to obtain efficient and reliable battery performance with enhanced cycle life.

Keywords:
Algorithm, ANN, Battery Management System, Electric Vehicle, SOC estimation, SOH estimation

I. INTRODUCTION

Climate change and global warming have become major issues because of unnecessary and plenty of greenhouse gas emissions to the environment that adversely impact the environment or cause environmental degradation. Excessive use of fuel-based sources (coal, crude oil, and natural gas) and gasoline-powered engines significantly contribute to greenhouse gas emissions. Among all the sectors automotive sector contributes a significant role in polluting the environment because the increase in the number of vehicles on the road daily causes increased gasoline consumption proportionally. The issue of climate change influenced many researchers to think of alternative ways of acquiring energy from clean sources like solar, wind, hydro, etc., to fulfil the needs by avoiding dependencies on fossil fuels. Automobile Industries Tesla, Hyundai, Mercedes-Benz, TATA, TOYOTA, etc., started switching towards Electric vehicles like Hybrid EVs (HEVs), Plug-in HEVs (PHEVs), Battery EVs (BEV), and Fuel-cell EVs (FCEVs) from traditional gasoline or diesel-powered engines. However, batteries have been a significant issue because they are temperature sensitive and suffer ageing due to improper charging-discharging rates and sometimes overcharging. After rigorous advancements in energy storage technologies, more specifically Lithium-ion based electric batteries that have very high volumetric energy density (W-hr/l), very high gravimetric energy density (W-hr/Kg), high specific power (W/Kg), high shelf life, low self-discharge rate, and high cycle life makes it the first choice of EVs and other also suffers from thermal instability due to inevitable reactive nature of the lithium metal that may cause thermal

runaway when operating in high temperature. So, the temperature is a critical factor that significantly impacts the performance of lithium-ion-based chemistries in batteries. Also, overcharging and discharging of lithium-ion batteries and the formation of SEI layer in the anode surface can affect the cycle life and may cause the ageing of the batteries. In electric vehicles, it is crucial to monitor the batteries' operating temperature and their charging and discharging processes, which is possible using efficient and reliable monitoring technology called Battery Management System (BMS). The transportation and electricity production sectors account for more than 50% of total greenhouse gas emissions as both rely on fossil fuels as the energy source. Promising solutions include the electrification of the transportation industry and the decarbonisation of electrical grids. However, the mass adoption of electric vehicles and renewable energy remains low due to the high adoption cost attributed to the Li-ion batteries4. A significant challenge in Li-ion batteries research is the state of charge (SOC) estimation which signifies the amount of electric charge left in a Li-ion battery cell5. Accurate SOC estimation allows the Li-ion battery cells to be used to their maximum potential before disposal, resulting in tremendous cost savings in the manufacturing and adoption costs [2]. Accurate state of charge SOC estimation of lithium- ion (Li-ion) batteries is crucial in prolonging cell lifespan and ensuring its safe operation for electric vehicle applications [2]. As the core of BMS, SOC estimation dramatically affects electric vehicle safety, dynamics and economy. If an accurate SOC can be obtained, the SOC range can be used for batteries could be extended [12] by implementing an efficient algorithm which helps in estimating less erroneous and reliable state estimation of battery, i.e., SoC and SoH. There are many BMS algorithms in the literature. Still, the conventional and most widely used is the Coulomb Counting (CC) or Current integration method, which is a direct SOC method because of its simplicity and does not require a complete battery model to estimate the SoC and SoH but is prone to cumulative error accumulation during the integration of charging or discharging current using the algorithm and not reliable applications like EVs, micro-grid, Grid-tied Solar PVs, etc. applications which may lead to overall performance degradation of the whole battery module. The model-based and data-driven approaches are the two most common approaches used in SOC estimation. The most advanced algorithms, such as EKF and UKF, are model-based state estimation algorithms which are efficient based on state estimation. The data-driven-based SOC estimation algorithms like Artificial Neural Network (ANN), Support Vector Machine (SVM), Radial Basis Function (RBF NN), Deep NN etc., are very efficient and reliable but require lots of training data.

II. BATTERY MANAGEMENT SYSTEM

A. Introduction to Battery Management System

SOC is a crucial parameter for BMS and energy management. Batteries must be monitored and managed to maintain the vehicle's safety, efficiency, and reliability [1]. The BMS is responsible for safe operation, performance, and battery life under diverse charge-discharge and environmental conditions, which monitors cell voltage and temperature, estimates SOC and SOH, limits power input and output for thermal and overcharge protection, controls the charging profile, balances the state-of-charge of individual cells, and isolates the battery pack from the load when necessary [4]. CC state estimation method is relatively straightforward and non-expensive to implement. The CC method is the most used for SOC estimation, is relatively easy to implement, requires relatively low computational resources, and calculates battery SoC by accumulating the battery current over time. Since it applies open-loop control, the estimation error will be integrated with time. The open- circuit voltage method is one of the alternatives, requiring batteries to be static for a while after use. Thus, these methods cannot achieve real-time observation under dynamic working conditions. In contrast, Machine learning approaches require large amounts of training data to establish the relationship between inputs and outputs, resulting in a computational burden [11]. In the CC method, the remaining capacity of the battery is determined by accumulating the charge transferred in and out of the Li-ion cell, and the SOC is estimated by using,

$$SOC(t) = SOC(t_0) + \frac{1}{C_n}\int_{t_o}^{t} \eta\, I(t)\, dt$$

Where, SOC(t) is the initial SOC, Cn is the nominal capacity, η is the coulombic efficiency, and I(t) is the battery current [3]. The accuracy and efficiency are no significant concerns.

Still, the applications like Solar PV, WECS, and EVs demand safe and reliable batteries and efficient and reliable battery monitoring systems to ensure the safe operation of all the batteries connected to the system. Since lithium-ion batteries are very prevalent in such applications, they require proper thermal management and monitoring to ensure all batteries should operate in a safe operating area (SOA). By integrating the current over the sampling units, the

CC method estimates the equivalent electric charge. However, the small error will accumulate in the long term due to its open-loop nature and lack of error correction ability, leading to significant inaccuracy. However, more efficient and reliable algorithms are published by the researchers who provide very accurate and insignificantly low erroneous estimates of the battery SOH and SOH because they are dependent on the complete battery model and non-linear state estimators like UKF, etc. and ANN data-driven based algorithms which are used to train the neural network with the massive amount of data so that the system can predict the output with high precision like Deep Neural Network, SVM, RNF NN etc. A Li-ion battery cell can be considered a nonlinear system with unknown internal state parameters, and only the external input and output can be measured. The SOC of Li-ion batteries is one of the most critical internal metrics that indicates the current remaining capacity of batteries in use. Therefore, it is difficult to observe after batteries are manufactured. Many studies and algorithms have been proposed for battery SoC estimation, from the non-model-based methods like the CC method and the OCV-SOC method and machine learning approaches like ANN-based algorithms, fuzzy logic-based, and SVR, RBF etc. to model-based methods and filtering algorithms like KF, EKF, UKF, Particle filter, and sliding mode observer (SMO) [11].

B. Working of BMS in traction battery of EVs powertrain

Fundamentally EVs powertrain contains a Traction battery system, On-board Battery charger unit, DC-DC power converter system, various sensors, Electronic Control Unit (ECU), DC-AC power converter system, Variable frequency drive (VFD), Fuel Cell stacks if it is FCEV, Supercapacitor, etc. Still, most of the vehicle cost is due to the whole battery system over the chassis because of many Li-ion cells in the system that contains precious metals like Nickel, Manganese, Cobalt, Aluminum, etc. and because of the battery monitoring control circuitry or BMS which are connected to every module of the Li-ion cells that requires sensors, Thermal Management Unit (TMU), active balancing circuitry, etc. So, the efficiency, cost, and reliability of the whole vehicle depend on the type of batteries like NMC, NCA, LFP, etc., and their safety is crucial. So, a compelling state estimation algorithm is necessary for BMS to control the cell balancing and rate of charge/discharge cycle and protect against overvoltage and deep discharge for efficient vehicle performance.

III. REVIEW OF ADVANCED STATE OF CHARGE (SOC) ESTIMATION ALGORITHMS

A. Direct SOC Estimation Method

Accurate estimation of a battery's state of charge (SOC) is critical for battery safe, efficient and reliable management. There are two primary approaches to estimating the SOC of a
battery are voltage-based approach and the current-based approach. The voltage-based process serves as a table lookup method in which the measured voltage across the battery terminals matches its corresponding SOC in the OCV-SOC characterisation curve. Such a voltage-based approach requires the battery to be "rested" when the voltage measurement is taken - to reduce the effect of hysteresis and relaxation effects on the measured voltage. The current-based approach is also known as the Coulomb counting method. Coulomb counting is the most straightforward approach to estimating the SOC of the battery. Assuming the knowledge of the initial SOC, the Coulomb counting method computes the effective change in Coulombs in/out of the battery based on the measured current and time to compute the updated SOC. The critical advantage of the Coulomb counting approach is that it does not require any prior characterisation, such as the OCV-SOC characterisation in the voltage-based SOC estimation method. However, the Coulomb counting method can result in SOC estimation error due to the following factors initial SOC, current measurement error, present integration error, uncertainty in the knowledge of the battery capacity, and timing oscillator error [3]. Since the algorithms perform the integration over the charging and discharging current values without considering the temperature conditions and calibration of the initial values, the chances of error accumulation are entirely possible. Consequently, the measured values deviate from the actual values, which makes the algorithm less reliable and inefficient for the applications like EVs, microgrid Solar PV applications, etc. The coulomb counting method is the most accurate technique for short-term estimation. However, a small error will accumulate in the long term due to its open- loop nature and lack of error correction ability, leading to significant inaccuracy [5].

B. Model-based SOC estimation method

Indirect SOC estimation methods are modern based approaches to estimate the state of charge of the batteries like Li-ion-based batteries, which are very common in applications efficiently because, in the indirect method, the algorithm can access the approximated equivalent circuit model of the battery

and use linear and non-linear controllers like Kalman filter, EKF, UKF, Particle fitter, etc., which are recursive Bayesian based filters for accurate state estimation and prediction [4]. The model-based approach leverages an in-depth understanding of domain knowledge such as the internal chemical reaction in the cell, electrical properties of the components used to model them and complex mathematical equations to estimate the SOC. Prominent model-based techniques include the Sliding Mode Observer, Luenberger Observer, Kalman filters, Electrochemical Model, Equivalent Circuit Model, and Electrochemical Impedance Model. While the model-based approach can result in reliable and accurate models, it requires extensive domain knowledge, rigorous feature engineering, and a relatively long development time. Apart from that, the model- based approach also does not scale well across battery cells' different chemistry. As a result, cell chemistry alterations require the model's re-development. Additionally, the model- based approach does not account for cell anomalies, such as manufacturing inconsistencies, unpredictable operating conditions, cell degradation, etc. Systems in the real world contain very high non-linearities and disturbances, so the algorithm based on UKF and particle filter can precisely estimate the SOC in real-time. The KF algorithm reduces the uncertainty value of SOC and SOH. This is because the algorithm of KF includes recursive equations, which are evaluated repeatedly during system operation [6]. SOC is a crucial parameter for battery and vehicle energy management. Conventional SOC estimation methods for lithium-ion batteries for vehicles are straightforward. They lack appropriate battery modelling and are susceptible to voltage and current signals sampling noise. To improve the accuracy of SOC estimation, the extended Kalman filter algorithm needs a linear approximation of the system equation. The UKF algorithm was used to reduce the influence of sampling noise and an improved algorithm with a better filtering effect and SOC estimation accuracy. The UKF algorithm is a filtering algorithm for nonlinear systems, which is fundamentally different from the EKF algorithm. It does not need to linearise the system equation. Also, the UKF estimation filtering algorithm's mathematical modelling is explained using the PNGV battery model [8]. Model-based methods allow battery models to self-correct and tackle unexpected disturbances through closed-loop observers. The Kalman filter-related methods like UKF and the EKF are commonly used to conduct the battery SOC estimation. Kalman filter-based estimation methods assume that the system noises and the covariance of measurements have to be known. However, parameters initialised using static battery models may conflict with various actual applications. Moreover, these methods are less robust due to model uncertainty and system disturbance. A sliding mode observer was used, which shows robust control properties against modelling errors and uncertainties. Model-based estimation methods require a precise battery model to depict internal battery parameters. The model accuracy strongly influences the SoC estimation accuracy. [11]. Kalman filter and other observer-based approaches have also been used to estimate the SOC. An EKF based on several non-linear state space models has been reported to estimate the SOC of HEV Li-ion batteries. The performances of these filters depend on the modal accuracy and simplicity. For example, EKF cannot achieve good estimation performance on highly non-linear systems, and KF requires the system noise to be gaussian. PF can be utilised to do SOC estimation for non-linear Li-ion batteries' models with complex forms in a condition of non- gaussian distributed system noise. KF-based methods are widely used to do Li-ion battery SOC estimation. The EKF is utilised to make SOC estimation and model parameter identification online. However, such methods are dependent on the model's simplicity and accuracy. For example, EKF can't achieve good estimation performance on a highly nonlinear system. On the other hand, KF requires the system noise to be Gaussian [14]. PF is a probability-based estimator with high accuracy. PF uses a set of weighted particles sampled by the Monte Carlo method to approximate the posterior distribution of the system without any explicit assumption about the form of the distribution. PF is suitable for state estimation for the complex model with strong nonlinearity. Therefore, PF can be utilised to do SOC estimation for a nonlinear LIB model with complex form in non-Gaussian distributed system noise [14]. PF is a probability-based estimator with high accuracy and is a credited alternative for dealing with non-linear/non-Gaussian models. PF approximates the posterior distribution by a set of weighted particles sampled by Monte-Carlo methods [15].

C. Data-driven or ANN-based state of charge estimation methods

The data-driven method is another indirect state estimation algorithm that relies on a large amount of training data to estimate the SOC efficiently. Since the algorithm gives requires large training vectors (feature vectors), which may result in high

computational complexity and sometimes cause overfitting of the data. Using efficient neural network-based algorithms like SVM, RBF NN, Deep Neural Network, etc., gives a very accurate and reliable estimation. To estimate the SOC of a high-capacity lithium iron manganese phosphate (LiFeMnPO4) battery cell from an experimental dataset using the SVM method is discussed in [13], which is a learning machine based on statistical learning theory. SVM for regression (SVR) is used as an automated learning tool with a different focus to successfully predict the SOC of a high- capacity lithium iron manganese phosphate (LiFeMnPO4) battery cell as a function of cell voltage, cell current, and cell temperature. SVMs are a set of related supervised learning methods used for classification and regression that can universally approximate any multivariate function to any level of accuracy. SVMs were initially developed to solve classification problems. They were later generalised to solve regression problems using an SVR method. The SVM goal is to find a functional form that can correctly predict new cases not tackled before. This can be achieved by training the SVM model on a sample set called a training set, which involves sequential optimisation of an error function. Many regression problems cannot be linearly regressed in the space of the inputs. However, they might be regressed in a higher dimensional feature space given a suitable mapping (the kernel trick). Different kernel functions are described, such as RBF kernel, polynomial kernel, etc. The RBF is by far the most popular choice of kernel types used in SVMs. A kernel must be chosen to use an SVM to solve a regression problem for data that is not linearly separable. Then, the relevant parameters that can be expected to map the nonlinearly separable data into a linearly separable feature space must be selected. This paper checks each combination of hyperparameter choices using cross-validation, and the parameters with the best cross-validation accuracy are chosen [13]. [20] presents a robust sliding mode observer (RSMO) for the SOC estimation of a lithium-polymer battery (LiPB) in electric vehicles (EVs). A radial basis function (RBF) neural network (NN) is employed to learn an upper bound of system uncertainty adaptively. [20] A robust sliding mode observer (RSMO) has been developed to estimate the SOC for a LiPB in EVs. This methodology integrates the RSMO with the online parameter identification for a battery equivalent circuit model (BECM) by applying the forgetting factor recursive least square (FFRLS) algorithm and the learning capability of an RBF neural network for the approximation of the upper bound of the system uncertainty. This integration allows the RSMO to start with the appropriate initial switching gain and then adjust the switching gain adaptively to ensure the convergence of the SOC estimation errors.

D. Sliding mode observer SOC estimation method

A sliding mode algorithm is adopted to estimate the SOC of a battery. The dynamic battery model and related SOC estimation methods establish an adaptive battery model. A sliding mode observer for SOC estimation with some advantages like eliminating systemic error of battery model effectively, online analysis of parameters, no need for accurate initial parameters, transmission errors are avoided by independent parameter observer, simple mathematical operation, etc. SMO method is constructed to eliminate the error of the battery model and reduce the noise of measurement based on battery parameters identified online to consider the variation of internal battery characteristics under variable environments [18]. In the presence of a non-linear system, modelling errors, and uncertainties, SMO has been applied as a reliable and robust tool for SOC estimation, which adapts to the battery's non-linearity [19]. By the established second-order equivalent circuit model and parameter identification of Lithium-Ion battery, aiming to improve the estimation accuracy of lithium battery SOC, an improved sliding mode observer for SOC estimation of lithium battery is proposed in [20].

E. Electrochemical Impedance Spectroscopy SOC estimation method

Impedance spectroscopy is one of the most promising methods for characterising the ageing effects of portable secondary batteries online because it provides information about different ageing mechanisms. However, the method requires a fast impedance measurement process, an accurate model applicable with several batteries and a robust method for model parameter estimation. The advantage of impedance spectroscopy (IS) for characterising ageing effects is that a significant amount of information can provide more insight into ageing mechanisms. Impedance spectroscopy allows impedance determination for a frequency range impedance spectroscopy enables the estimation of the impedance for a frequency range. Because of the large amount of information available from impedance experiments and the relative short measurement time, IS remains the most promising non- destructive method. For the estimation of the parameters, a meta-heuristic evolutionary strategy is employed for global optimisation along with

Levenberg–Marquardt heuristic algorithm since the algorithm has stochastic and can find the global minima effectively [21]. EIS thoroughly explains reaction kinetics and transport mechanisms in LIBs and provides a promising nondestructive tool for the state of charge (SOC) estimation [22]. The internal impedance of a battery is an important characteristic that directly affects its operating voltage, rate capability and efficiency and can also affect its practical capacity. EIS is a powerful and widely used non-invasive test method for characterising LIBs. As a non- destructive technique, EIS can be used at various points throughout a battery's lifetime as a diagnostic or prognostic tool for quality assurance for the state estimation, including SOC estimation, SOH estimation, SOF estimation, monitoring of internal temperature, and characterisation for second-life applications [23].

IV. COMPARATIVE ANALYSIS

Estimation accuracy is greatly improved because of a vast amount of training data sets to train the neural network to generate the modal, efficiently predicting the battery's state.

TABLE I Comparative analysis of the state estimation algorithms

ALGORITHMS	BASED ON	CHARACTERISTICS
OCV-SOC method	Voltage and current-based approaches or direct methods	Very less accurate and not preferred for the applications
CC Method		Less accurate because very prone to errors and disregards important parameters like temperature, battery impedance, etc.
Kalman Filter	Recursive Bayesian estimation- based filtering algorithm	Accurate only for linear models and gaussian-based systems.
EKF		Accurate for linear/non-linear systems and system noise to be gaussian
UKF		Accurate for linear and highly non-linear systems
Particle Filter		Very accurate for linear/highly non-linear models, but the system noise is non-necessary be gaussian.
SMO	Filtering algorithm	A robust filtering algorithm for SOC estimation
SVM Kernel	Data-driven & Supervised learning algorithms	A supervised learning algorithm requires a significant amount of training data related to different parameters (features) of the battery called feature vectors to train the neural network, which eventually develops a classification and regression model to predict the battery's state accurately.
RBF NN		
DNN		
Fuzzy logic	Fuzzy rules	Good accuracy and flexibility
EIS	Impedance spectroscopy of the LIBs	Very accurate and robust SOC estimation method based on the impedance spectroscopy of the battery by analysing the whole electrochemistry to gain insight into the ageing mechanism.

Of charge in a data-driven approach. After developing a mathematical model of the battery from the approximate equivalent that should effectively represent the real Li-ion battery modal can be used to estimate the SOC accurately by employing a modal-based estimator called the Kalman filter, which is efficient for a linear model. The precision of SOC estimation relies on the accuracy of the battery model, and static battery models are generally adopted in

Implementation includes Rint, RC, Thevenin, PNGV, and nonlinear equivalent circuit model. However, static battery models initialised in the laboratory cannot adapt to the actual variable using the environment Though many robust SOC observers have been built to reduce the negative impacts, such as sliding mode observer, proportional integral observer, and extended Kalman filter observer [12]. Also, UKF and Particle filtering methods are very efficient and reliable.

V. CONCLUSION

Efficient and reliable BMS algorithms are required for accurate and error-free state estimation of batteries. Advanced algorithms like data-driven or ANN-based and model-based like the Extended Kalman filter for SOC and SOH estimation exhibit accurate results compared to their traditional counterparts, i.e., the Coulomb Counting algorithm. Since model-based state estimation considers the complete battery model and all the associated parameters, EV performance improves because of the battery efficiency, reliability, and performance enhanced by a reliable battery monitoring system.

Advancements in the Lithium-ion battery chemistry like LTO, LFP, etc., also contributed to the module's overall performance because they are more thermally

stable and don't react to any damage. Consequently, advanced BMS state estimation algorithms ensure cells should operate in SOA defined by the manufacturer.

REFERENCES

[1] B. Balakumar, A. Mostafa, P. Krishna, "Battery Management Systems-Challenges and Some Solutions," DOI: 10.3390/en13112825

[2] M.A. Hannan, et al., "Deep learning approach towards an accurate state of charge estimation for lithium-ion batteries using self-supervised transformer model," Article number: 19541 (2021), https://doi.org/10.1038/s41598-021-98915-8

[3] M. Kiarash, A. R. Sheikh, B. Balakumar, "Performance Analysis of Coulomb Counting Approach for State of Charge Estimation," 2019 IEEE Electrical Power and Energy Conference (EPEC), 16-18 October 2019, Montreal, QC, Electronic ISBN:978-1-7281-3406-2, Print on Demand (PoD) ISSN: 2381-2842, DOI: 10.1109/EPEC47565.2019.9074781

[4] https://in.mathworks.com/solutions/power-electronics- control/battery-management-system.html

[5] K.C. Ndeche, S.O. Ezeonu, "Implementation of Coulomb Counting Method for Estimating the State of Charge of Lithium-Ion Battery," DOI: 10.9734/PSIJ/2021/v25i330244

[6] L. Qiang, L. Ranyang, J. Kaifan, D. Wei, "Kalman Filter and Its Application," 2015 8th International Conference on Intelligent Networks and Intelligent Systems (ICINIS), Tianjin, China, 01-03 November 2015, ISBN:978-1-4673-8222-9, DOI: 10.1109/ICINIS.2015.35

[7] L. Chao, H. Yitong, G. Qi, W. Lixin, S. Yankong, "State-of- Charge Estimation of Lithium-ion Batteries Based Deep Neural Network," 2020 Global Reliability and Health Management (PHM Shanghai) 16-18 October 20204, Electronic ISBN: 978- 1-7281-5946-1, DOI: 10.1109/PHM- Shanghai49105.2020.9280940.

[8] A.T. Paris, M.N. Ramadan, F. Ghufron, et al., "State of Charge (SOC) and State of Health (SOH) estimation on lithium polymer battery via Kalman filter," 2016 2nd International Conference on Science and Technology Computer (ICST), 27- 28 October 2016, Electronic ISBN: 978-1-5090-4357-6, Print ISBN: 978-1-5090-4356-9, DOI: 10.1109/ICSTC.2016.7877354.

[9] W. Weida, W. Xiantao, X. Changle, W. Chao, Z. Yulong, "Unscented Kalman Filter-Based Battery SOC Estimation and Peak Power Prediction Method for Power Distribution of Hybrid Electric Vehicles," date of publication June 29, 2018, DOI: 10.1109/ACCESS.2018.2850743

[10] N. Nassim, B. Loic, J. Samir, "A Review of Battery State of Health Estimation Methods: Hybrid Electric Vehicle Challenges," Published: 16 October 2020, DOI: 10.3390/wevj11040066

[11] T. Carlo, O. Simona, "State of Charge Estimation Using Extended Kalman Filters for Battery Management System," 2014 IEEE International Electric Vehicle Conference (IEVC), Date of conference: 17-19 December 2014, Florence, Italy, Electronic ISBN:978-1-4799-6075-0, DOI: 10.1109/IEVC.2014.7056126

[12] Z. Li, P. Zhang, Z. Wang, Q. Song, Y. Rong, "State of charge estimation for Li-ion battery based on extended Kalman filter", The 8th International Conference on Applied Energy –ICAE2016, DOI: 10.1016/j.egypro.2017.03.806

[13] C. A. A. Juan, J. G. N. Paulino, B. V. Cecilio, A. V. V. Jose. "Support Vector Machines Used to Estimate the Battery State of Charge," December 2013, IEEE Transactions on Power Electronics 28 (12): 5919-5926, DOI: 10.1109/TPEL.2013.2243918

[14] J. Du, Y. Wang, C. Wen, "Li-ion battery SOC estimation using particle filter based on an equivalent circuit model," 2013 10th IEEE International Conference on Control and Automation (ICCA), 12-14 June 2013, Hangzhou, China Electronic ISBN:978-1-4673-4708-2, Electronic ISSN: 1948-3457, DOI: 10.1109/ICCA.2013.6565047

[15] Z. Taimoor, X. Guoqing, L. Weimin, Z. Lei, X. Kun, "Performance analysis of particle filter for SOC estimation of LiFeP04 battery pack for electric vehicles," 2014 IEEE International Conference on Information and Automation (ICIA), 28-30 July 2014, Hailar, China, Electronic ISBN:978- 1-4799-4100-1, DOI: 10.1109/ICInfA.2014.6932806

[16] C. Mengying et al., "Sliding Mode Observer for State-of- Charge Estimation Using Hysteresis-Based Li-ion Battery Model," Published: 5 April 2022, Energies 2022, 15(7), 2658; https://doi.org/10.3390/en15072658

[17] N. Bo, X. Jun, C. Binggang, W, Bin, X. Guangcan, "A Sliding Mode Observer SOC Estimation Method Based on Parameter Adaptive Battery Model," DOI: 10.1016/j.egypro.2016.06.08

[18] X. Binyu, Z. Huajun, D. Xiangtian, T. Jinrui, "State of Charge Estimation based on Sliding Mode Observer for Vanadium Redox Flow battery," 2017 IEEE Power & Energy Society General Meeting, 16-20 July 2017, Chicago, IL, USA Electronic ISBN:978-1-5386-2212-4, Electronic ISSN: 1944- 9933, DOI: 10.1109/PESGM.2017.8274042.

[19] H. Bouchareb, K. Saqli, N.K. M'sirdi, M. Oudghiri Bentaie, A, Naamane, "Sliding Mode Observer Design for Battery State of Charge estimation," 2020 5th International Conference on Renewable Energies for Developing Countries (REDEC), 29- 30 June 2020, Marrakech, Morocco, Electronic ISBN:978-1- 7281-5595-1, Electronic ISSN: 2644-1837, 10.1109/REDEC49234.2020.9163592

[20] C. Xiaopeng, et al. "Robust Adaptive Sliding-Mode Observer Using RBF Neural Network for Lithium-Ion Battery State of Charge Estimation in Electric Vehicles," IEEE Transactions on Vehicular Technology (Volume: 65, Issue: 4, April 2016), pp. 1936 – 1947, 19 May 2015, Electronic ISSN: 1939-9359, Funding agency: Project of Electric Vehicle

Control Systems and Power Management (Grant Number: C2-801), DOI: 10.1109/TVT.2015.2427659

[21] K.W. Qian, J.H. Yi, N.S. Jia, S.H. Xiao, F.M. Zi, "State of Charge-Dependent Polynomial Equivalent Circuit Modeling for Electrochemical Impedance Spectroscopy of Lithium-Ion Batteries," IEEE Transactions on Power Electronics (Volume: 33, Issue: 10, October 2018), pp. 8449 – 8460, 06 December 2017, Electronic ISSN: 1941-0107, DOI: 10.1109/TPEL.2017.2780184

[22] T. Uwe, K. Olfa, R.T. Hans, "Characterizing ageing effects of lithium-ion batteries by impedance spectroscopy." University of the Bundeswehr Munich Institute for Measurement and Automation, 85579 Neubiberg, Germany, DOI: 10.1016/j.electacta.2005.02.148

[23] M.Nina et al., "Application of electrochemical impedance spectroscopy to commercial Li-ion cells: A review,", https://doi.org/10.1016/j.jpowsour.2020.228742

[24] J. Du, Z. Liu, Y. Wang, C. Wen, "A fuzzy logic-based model for Li-ion battery with SOC and temperature effect," 11th IEEE International Conference on Control & Automation (ICCA), 18-20 June 2014, Taichung, Taiwan, Electronic ISBN:978-1- 4799-2837-8, Electronic ISSN: 1948-3457, DOI: 10.1109/ICCA.2014.6871117.

IFERP connecting engineers...developing research
1st International Conference on Future of Engineering 2022

BIM Gauge: Design and Development of a Web-Based Building Information Modeling Implementation Maturity Assessment Tool for Construction Projects in the Philippines

Lemuel Lumbera[1], Mico Cruzado[2]

[1,2] Technological Institute of the Philippines, Philippines
Email: [1] lemuel.lmbr@gmail.com, [2] mcruzado.ce@tip.edu.ph

Abstract:
The purpose of this research was to apply the established BIM Gauge Framework to the creation of a web-based BIM Maturity Assessment Tool for use in the Philippines' BIM sector. This instrument will assess the present state of BIM implementation inside a business and help determine the best way to enhance it to fit its needs. This study analyzed and compared the characteristics, benefits, frameworks, and methods of various existing BIM evaluation systems, as well as surveyed the relevant literature. The study concluded that the AEC sector has acknowledged a variety of BIM evaluation models which are crucial in implementing diverse BIM-based projects based on their features and purposes. These models were used to generate the BIM Gauge framework which consists of six main components that will measure the maturity of an organization in different areas. The study identified that the various parts of the BIM Gauge Framework are useful for assessing how BIM-based projects must and should be executed. As a result, respondents seemed to be satisfied with the use and result of BIM gauge as a tool for assessing the maturity of their BIM implementation.

Keywords:
BIM, BIM Gauge, BIM Maturity Assessment Tool, BIM Maturity Models

I. INTRODUCTION

Building Information Modeling (BIM) is an effective approach and powerful tool for building development and an emerging technique in the construction industry. The model is described as a digital representation of the functional and physical characteristics of a facility, containing all the building elements and the information associated with the elements [1]. It utilizes digital modelling software in the effective design, building, and management of projects. BIM allows the sharing and integration of multidisciplinary knowledge covering engineering and architecture, that benefits life cycle building optimization. It is characterized by intelligent and data-intensive features, a process which is computer-based for the visualization and simulation of a facility, having advantages of information extraction and analysis. The BIM technology provides visual-aid simulation and real-time data in order to facilitate exchange of knowledge and reduce construction rework and design alteration of a project [2]. Implementation of BIM has the life cycle benefits of planning optimization, dynamic onsite construction management, site selection, improvement in collaborative design efficiency, and innovative property management [3].

As the construction industry underwent a paradigm shift from a mere building design to the management of the building throughout its life cycle, a far more sophisticated information system which is digital based was developed, known as Building Information Modelling (BIM). A single visualization building model can be developed using the BIM, which is capable for use throughout the project life cycle. The model provides reliable foundation for decision making and a platform for automated analysis to assist design, planning, construction, maintenance, and operation activities. It has the capability of satisfying different criteria in the provision of comfortable and high-quality buildings while complying with building regulations, minimizing costs to clients, optimizing energy costs, confirming internationally accepted energy performance levels, and reducing environmental impacts [1].

Although extensive research has been carried out on the implementation of BIM in the construction industry, limited research has been conducted on the integration of BIM in project management in the construction industry in the development of assessment tool for measuring the effectiveness of BIM along with different success factors in the overall project performance. Current BIM studies focus on awareness of its adoption, policies, and implementation such as the studies of [4, 5, 6]. The present research study will fill this gap, providing a proposed assessment tool in the evaluation of success in managing projects in the construction industry, focusing on BIM complementary component. Thus, the present study will be focused on developing a BIM Maturity Assessment Tool, which will evaluate the organization's current condition in BIM implementation through a BIM maturity framework.

II. METHODS

The study will utilize a qualitative and quantitative approach to create a BIM Gauge Framework for the development of the Web-Based BIM Assessment tool. The developed web-based assessment tool can be used by industry experts, BIM Managers, BIM users, and stakeholders to assess their BIM Implementation. The development of the assessment tool will be divided into three phases.

Phase 1: Existing BIM Maturity Models

Phase 1 of the study covers the assessment of existing BIM maturity models: it is necessary to apply a selection principle to determine the tools to be evaluated. The selected tools should be:

- Well-recognized by the industry
- Developed by reputable research studies
- With detailed information and available literature

Phase 2: Development of BIM Gauge Framework

Phase 2 of the study will identify the BIM Gauge framework to be used on the proposed web-based BIM Assessment tool.

Through the study of different maturity models and their frameworks, the researcher will generate a main component of measures and each main component will consist of it's a sub-fundamental component of measures. Each component will have an objective that will help to measure the maturity of BIM Implementation across the organization. The generated components will form the BIM Gauge framework that will be used as the backbone for the development of the BIM assessment tool.

Phase 3: Development and Validation of BIM Maturity Assessment Tool

All the gathered data is used to develop a web-based BIM assessment tool. A Waterfall development methodology will be used to develop the tool inside a firebase database. The web-based assessment tool will evaluate the organization's BIM Capability and BIM Competency.

A validation will be then conducted to know the effectiveness of the developed web-based BIM assessment tools. The user's ratings, views, experiences, opinions, and suggestion will be recorded to help further improve the developed tool.

III. RESULTS

This section provides an introduction of the selected evaluation tools that have been used to assess the planning and design phases, performance, and the sustainability of BIM-based projects, which serves as a foundation for comprehensive comparisons.

3.1. BIM Evaluation Tools

Table 1. Comparison of Different BIM Maturity Assessment Models

Tool / Models	Purpose	Categories / Process Area	Maturity Level Attributes
BIM CAREM	Establish an appropriate BIM Capability assessment model for AEC/FM projects	Process, Technology, Organizations, human aspect, BIM Standard	Incomplete BIM Performed BIM Integrated BIM Optimized BIM
NBIMS BIM CMM	Provides tabular and dynamic BIM ratings for project outcomes and operational processes.	Data richness, life cycle view, roles or disciplines, change management, business process, timelines / response, delivery method, graphical information, spatial capability, and interoperability / IFC.	Not Certified Minimum BIM Certified Silver Gold Platinum

BIM Proficiency Matrix	Ranks companies' BIM Service quality for use in selecting subcontractors	Physical accuracy, integrated project delivery methodology, calculation mentality, location awareness, content creation, contribution data, as-built modelling, and FM data richness	Working towards BIM Certified BIM Silver Gold Ideal
BIM Maturity Matrix	Analyzes the BIM knowledge, skills, and abilities of team members, as well as the organization's capacity, maturity, and project results.	BIM capability stages, BIM maturity levels, BIM competency sets, organizational scale and granularity level.	Ad-hoc Defined Managed Integrated Optimized
BIM QuickScan	Details the company's BIM prowess and flaws	Organization and management, mentality and culture, information structure and information flow, tools and applications.	Ranging 0-5
VDC Scorecard	Compares the project's results to those of similar initiatives in the same field.	Planning (objective, standard, and preparation), Adoption (organization and process), Technology (maturity, coverage, and integration), and Performance (quantitative and qualitative)	Conventional Practice Typical Practice Advanced Practice Best Practice Innovative Process
Organizational BIM Assessment Profile	Identifies the level of development of the company's BIM planning elements.	BIM strategy, BIM uses, Process, Information, Infrastructure, and Personnel	Non-Existent Initial Managed Defined Quantitatively Managed Optimizing
VICO BIM scorecard	Quantifies the efficacy of targeted BIM applications, including as coordination and cost prediction within the organizations.	Portfolio / Project management, cost planning, schedule planning, production control, coordination, and design team engagement	No capability Low capability Satisfactory Capability High capability
Multifunctional BIM Maturity Matrix	Analyzes the level of BIM development present in individual projects, business with many ongoing projects, and the sector as a whole.	Technology, process, and protocol.	Stage 0 Stage 1 Stage 2 Stage 3

The table 1 above shows the variations of different BIM Capability and Maturity Assessment tools that have been used in AEC/FM on their BIM-based projects. For the purposes of comparison, nine models were identified and considered as the basis, leading to the output of the present study. These nine models were as follows: BIM CAREM, NBIMS BIM CMM, BIM Proficiency Matrix, BIM Maturity Matrix, BIM QuickScan, VDC Scorecard, Organizational BIM Assessment Profile, VICO BIM Scorecard, and Multifunctional BIM Maturity Matrix.

3.2. Development of BIM Gauge Framework

After a thorough review of each maturity framework and models, the researcher come up and generate six main fundamental components and fourteen sub-fundamental components. The sub-fundamental component is based on the criteria of the grouped assessment questions.

Table 2. Main Fundamental Component

Main Fundamental Component
BIM Usage and Information Flow
Infrastructure (Tools and Applications)
Organization and Management
Strategy (Collaboration and Working Strategy)
Personnel (Mentality and Culture)
Information Exchange and Data Structure

Table 3. Sub-fundamental Component

Sub-Fundamental Component	
BIM Usage and Information Flow	Coordination Information Flow
Infrastructure (Tools and Applications)	System IT Security
Organization and Management	Organizational Requirements Management Awareness and Motivation
Strategy (Collaboration and Working Strategy)	BIM Use Working Practice
Personnel (Mentality and Culture)	Roles and Responsibilities Qualification and Training Knowledge Management
Information Exchange and Data Structure	Information Exchange Data Structure

Table 3 to 7 below shows the description of the generated assessment questions on each main component of measures. There will be different sub-components measuring BIM maturity in different areas.

Table 4. Assessment Criteria under BIM Usage and Information Flow

Sub-fundamental Components	BIM Uses
Visualization	Increasing the use of BIM in design communication in order to make it more efficient and cut down on any mistakes that may occur.
4D BIM	Enabling the use of BIM for construction sequencing in order to establish a phase-wise construction simulation for a project by synchronizing 3D geometry, building data, and the scheduling of materials
5D BIM	Performing material procurement may be done considerably more quickly, easily, and efficiently with the help of doing quantity take-offs based on BIM models; and this also saves time.
Sub-fundamental Components	Information flow
Information requirements	Defining the level of information that is required in each phase of a project in order to efficiently and clearly define and specify the content of Building Information Modeling (BIM).
Interoperability	Increasing the integration and efficiency of Open BIM across the industry will make it simpler for design and construction experts to share information with one another.
Collaborative process	Defining process maps for working on BIM models in order to gain an understanding of the overall BIM process, identifying the sharing of information that will be exchanged between two parties, and clearly articulating the various processes that need to be carried out for the identified BIM uses are all necessary steps.
Common Data Environment (CDE)	Doing an analysis of how the Common Data Environment can be used to improve the sharing of information that supports the building information modeling (BIM) delivery of the project.

Table 5. Assessment Criteria under Strategy (Collaboration and Working Strategy)

Sub-fundamental Components	Coordination
Virtual Design Review	Integrating building information modeling (BIM) technology into all construction and architectural projects as the primary means to drive change and help with execution.

3D Coordination and Drawings	Taking into consideration how the model will be used during the design and construction phases, as well as how it will immediately link to the generation of documentation like drawings.
Discipline Model Reviews	Determining whether or not the relevant checks and validations have been carried out in order to guarantee that the sharing of information is carried out in an appropriate manner.
Sub-fundamental Components	Working practice
Strategic	Ensuring the uninterrupted flow of information, requirements, and requirements as well as efficient discourse among external partners by figuring out the primary design workflow in order to improve productivity, accuracy, and coordination.
Quality Check	Performing quality checks on BIM models to ensure that they are consistent and conform to the BIM standards that are being utilized for the project.

Table 6. Assessment Criteria under Infrastructure (Tools and Applications)

Sub-fundamental Components	System
Software and hardware	Making sure that everything runs smoothly through the availability of hardware needed to run BIM software and through the use of computer programs to deliver BIM in an effective and efficient way.
Physical spaces	Creating a space within the business that is both physically and functionally equipped to facilitate the delivery of BIM services.
Sub-fundamental Components	IT Security
Data back-up and security	Taking into account data security with the goals of preventing data breaches, lowering the risk of data exposure, and making sure that regulations are met during the process of putting BIM into place in the Philippines.
Knowledge infrastructure	Managing of network systems for the gathering, storing, and dissemination of information both within and between organizations by means of shared platforms.

Table 7. Assessment Criteria under Organization and Management

Sub-fundamental Components	Organizational Requirements
BIM Execution Plan	Utilizing a BIM Execution Plan (BEP) to codify how information will be managed and provided in accordance with the requirements of the customer with reference to the implementation of the project.
BIM Contractual Obligations	Making it possible for the project team to reach an agreement and sign on to contractual duties, which will reduce the number of procedural and contractual issues.
Sub-fundamental Components	Management
BIM Vision	Creating and achieving the organization's vision, which describes what the organization wants to be in the long run, and using BIM technology to learn more about where the building and construction industry is going.
Management support	Increasing the level of support for BIM planning is essential to guarantee the successful implementation of BIM across the construction industry.
BIM Champion and Planning Committee	Putting together a BIM Planning Committee that will be responsible for developing the organization's BIM project strategy and putting together a BIM implementation plan.
Sub-fundamental Components	Awareness and Motivation

General Plans	Developing a strategy for the use of building information modeling (BIM) helps an organization make sure it is ready to use a new process or technology with the resources it has planned for.
BIM dissemination	Increasing motivation and maintaining constant awareness with regard to the adoption of BIM among the firm's key actors by promoting a leader, a motivator, or a follower inside the company.

Table 8. Assessment Criteria under Information Exchange and Data Structure

Sub-fundamental Components	Information exchange
Document/Model Referencing, Version Control, and Status	Assessing how effective the BIM model referencing, version control, and status features that have been implemented to manage code revisions are working.
Open Standards deliverables	Providing assistance to the project team in the form of organizing electronic submittals that have been approved during design and construction and providing a consolidated electronic operation manual with minimal effort by verifying deliverables according to open standard specifications such as IFC and Cobie.
Sub-fundamental Components	Data Structure
Model Element Classification	Organizing and defining the functional parts of a building using a categorization system to ensure a uniform structure that will allow people, software, and robots to communicate and use building information in an accurate and efficient way.
Level of Geometry (LoG) and Level of Information (LoI)	Providing data and information throughout the different stages of a BIM-based project by describing the level of geometric detail to which a model element is to be developed and the level of information (LoI) content that a model element is to have. This will help structural engineers, technicians, and other professionals understand their responsibilities in terms of data and information.

Table 9. Assessment Criteria under Personnel (Mentality and Culture)

Sub-fundamental Components	Qualifications and Trainings
Training and Experiences	Implementing a fast-track BIM training programme for in-service professionals and management staff to understand BIM from a management perspective rather than a technical perspective. Providing sufficient training options featuring a variety of technical modules, such as BIM management and R&D at various levels. Sample courses could include a BIM CPD course, BIM certificate course, BIM diploma course, etc. by training institutes
Sub-fundamental Components	Knowledge Management
Collaboration and channels	Integrating infrastructure project management and infrastructure asset management to ensure that all the members of a project team are knowledgeable enough about BIM-based project and technology.
Feedback	Establishing a mechanism for staff to provide feedback on the information structure and BIM products
Platforms	Investing on the use of a Common Data Environment (CDE) platform and offering cross training and rotational schemes to encourage mutual understanding between different teams on the use of BIM.

Moreover, Figure 1 below shows the total number of assessment questions for each sub-fundamental component. BIM gauge has a total of forty-five assessment questions which are distributed on the six main components. BIM Usage and Information flow has a total of 9 assessment question which 3 of it is BIM Use and 6 questions is under Information flow. Strategy (Collaboration and Working Strategy) has a total of 8 assessment questions which equally divided to Coordination and Working Practice sub-component. Infrastructure (Tools and Applications) contains a total of 6 assessment question which both system and IT security have 3 questions. Organization and Management component has a total of 9 assessment questions which 2 of them is under organizational requirements, 4 questions are under management and 3 questions are under awareness and motivations. Information Exchange and Data structure component has 5 assessment questions which 2 of them is under Information exchange and 3 is under data structure. Lastly, Personnel (Mentality and Culture) component has a total of 8 assessment questions which 3 is under roles and responsibilities, 2 for qualification and training and 3 is under knowledge management.

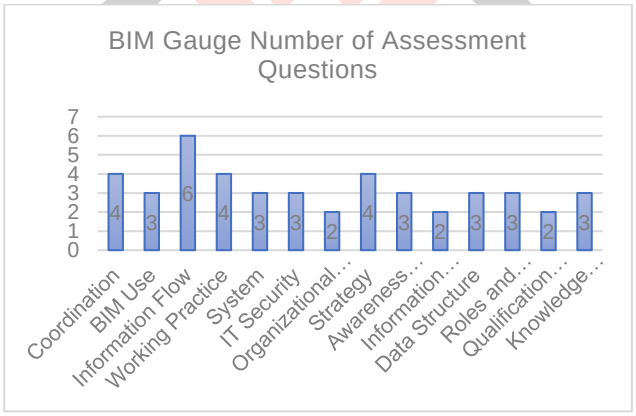

Figure 1. BIM Gauge Number of Assessment Question on main fundamental components

Figure 2 below shows the developed BIM Gauge Framework that consist of the six main components: BIM Usage & Information Flow, Infrastructure (Tools and Applications), Organization & Management, Strategy (Collaboration and Working Strategy), Information Exchange & Data Structure, Personnel (Mentality and Culture). Each main component has its own sub-fundamental components to measure the maturity on different aspects of implementation. BIM Usage & Information Flow component will assess the BIM Usage and Information Flow. Strategy (Collaboration and Working Strategy) will evaluate the organization's coordination and their working practices. Infrastructure (Tools and Applications) component will evaluate the technological system and IT security. Organization & Management will assess organization's requirements, management, and their awareness and motivations. Information Exchange & Data Structure will evaluate how the organization applies any BIM standards or protocol with regards to Information exchange and data structure. Finally, Personnel (Mentality and Culture) will assess how the management implements innovation with the implementation of BIM, the roles and responsibilities, qualification, and training of the people for BIM-based projects and how they do their knowledge management.

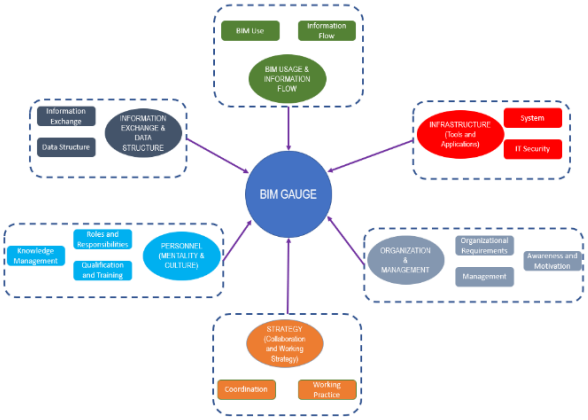

Figure 2. BIM Gauge Framework

3.3. Development of Web-based BIM Assessment Tool

After grouping all assessment questions into 6 main component and 14 sub-fundamental components, a web-based application is developed using a firebase database in an angular framework and waterfall development methodology. The development has 5 phases namely, Phase 1: Requirement gathering, Phase 2: Design, Phase 3: Development, Phase 4: Testing, and Phase 5: Deployment. The web-based application has a user interface wherein the user will first input some of his general information before proceeding with the assessment questions. After the self-assessment, a dashboard will show the result of their assessment and will also show an appropriate recommendation if some of its sub-fundamental component doesn't meet the required grade of 60% or above. Figure 3 below shows the landing page of the developed web-based BIM assessment tool.

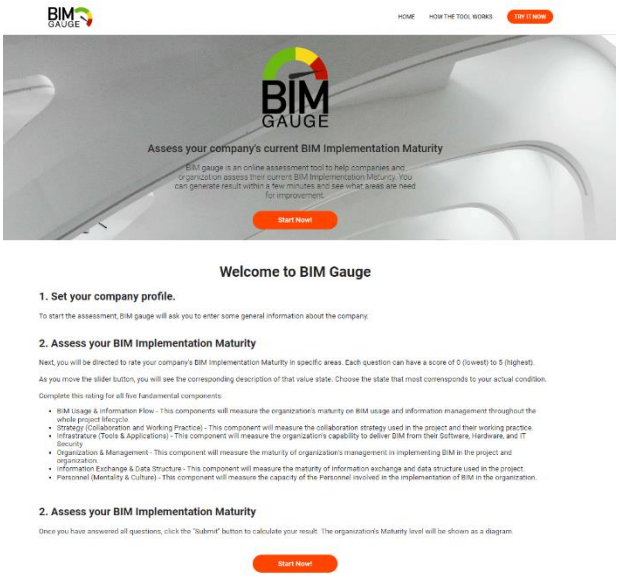

Figure 3. BIM Gauge web-based BIM Assessment tool landing page. *http://www.bimgauge.com*

3.4. Overall BIM Gauge Effectiveness

Table 10 showed the frequency and percentage distribution of the selected respondents in connection to the level of difficulty from the last time of using BIM gauge. The results showed that most of the respondents answered none with 18 respondents or equivalent to 62.1% while only one respondent or equivalent to 3.4% answered that it's hard to use the tool.

Table 10. Frequency and Percentage Distribution of the Respondents in Terms of Level of Difficulty from the Last Time of Using BIM Gauge

Category	Frequency	Percentage
It's hard to use the tool	1	3.4
User interface design is not friendly	3	10.3
Too many assessment questions	7	24.1
None	18	62.1
TOTAL	29	100.0%

On the other hand, with regards to the respondents' perception of agreeing with the result of BIM gauge, it can be seen that most of them answered Yes with 24 respondents or equivalent to 82.8% as compared to those who answered Somehow which garnered five respondents or equivalent to 17.2% of the total number of respondents included in the study (see table 5).

Table 11. Frequency and Percentage Distribution of the Respondents in Terms of their Perception of the Agreeing with the Result of BIM Gauge

Category	Frequency	Percentage
Somehow	5	17.2
Yes	24	82.8
TOTAL	29	100.0%

With regards to Table 12, in terms of the respondents' perception if the recommendation provided by the tool are considered to be relevant in helping the organization to improve their BIM implementation, it can be seen that majority of the respondents answered Yes with 25 respondents or equivalent to 86.2% while only about four respondents or 13.8% answered Somehow.

Table 12. Frequency and Percentage Distribution of the Respondents in Terms of their Perception if Recommendation Provided by the Tool are Relevant to Help the Organization to Improve their BIM Implementation

Category	Frequency	Percentage
Somehow	4	13.8
Yes	25	86.2
TOTAL	29	100.0%

Further, with regards to the distribution of the respondents in terms of their experience of the ease of using the BIM gauge, it can be noted that most of them answered Somewhat Easy with 17 respondents or 58.6% as compared to those who answered Extremely Easy with only four respondents or equivalent to 13.8% of the total number of respondents, as indicated in table 38.

Table 13. Frequency and Percentage Distribution of the Respondents in Terms of their Experience of Ease in Using the BIM Gauge

Category	Frequency	Percentage
Extremely Easy	4	13.8
Extremely Difficult	8	27.6
Somewhat Easy	17	58.6
TOTAL	29	100.0%

As for the respondents' perception in terms of finding out the result of the BIM gauge, it can be seen that most of them answered Very Reliable with the highest number of respondents of 18 respondents or about 62.1% as compared to those who answered Somewhat Unreliable with only one respondent or about 3.4% of the total number of respondents included in the present research.

Table 14. Frequency and Percentage Distribution of the Respondents in Terms of their Perception of Finding Out the Result of BIM Gauge

Category	Frequency	Percentage
Somewhat Reliable	10	34.5
Somewhat Unreliable	1	3.4
Very Reliable	18	62.1
TOTAL	29	100.0%

On the other hand, based from the findings presented in Table 15, in connection with the frequency and percentage distribution of the respondents in terms of their perception of using the BIM gauge again, majority of the respondents answered Yes with 27 respondents or about 93.1% as compared to those who answered Maybe with only two respondents or about 6.9%.

Table 15. Frequency and Percentage Distribution of the Respondents in Terms of their Perception of Using the BIM Gauge Again

Category	Frequency	Percentage
Maybe	2	6.9
Yes	27	93.1
TOTAL	29	100.0%

As for the findings presented in Table 16, in connection with the respondents' perception of how the BIM maturity assessment tool will be considered to be helpful in the construction industry to assess and improve their BIM implementation, it can be seen that most of the selected respondents of the study answered Yes with 28 respondents or equivalent to 96.6% as compared to those who answered Maybe with only one respondent or equivalent to 3.4% of the total number of respondents.

Table 16. Frequency and Percentage Distribution of the Respondents in Terms of their Perception of how the BIM Maturity Assessment Tool will be Helpful in the Construction Industry to Assess and Improve their BIM Implementation

Category	Frequency	Percentage
Maybe	1	3.4
Yes	28	96.6
TOTAL	29	100.0%

3.5. BIM Gauge as a Tool

The following tables presented the weighted of the responses provided by the selected respondents with regards to assessing BIM gauge as a tool.

Table 17. Weighted Mean of the Rate of Satisfaction on BIM Gauge Usage

Indicator	Mean	Verbal Interpretation
Easily Accessible	4.31	Very Satisfied
Ease of Use	4.14	Somewhat Satisfied
Browser Compatibility	4.28	Somewhat Satisfied
Security	4.14	Somewhat Satisfied
Look and feel	4.14	Somewhat Satisfied
Overall Reliability	4.24	Somewhat Satisfied
Overall Tool Performance	4.24	Somewhat Satisfied
Composite Mean	4.21	Somewhat Satisfied

In terms of the weighted mean of the rate of satisfaction generated on BIM gauge usage, it can be seen that the indicator "Easily Accessible" had obtained the highest mean of 4.31 and was verbally interpreted as Very Satisfied. On the other hand, the indicators "Ease of Use"; "Security" and "Look and feel" gained the lowest mean of 4.14 respectively and was verbally interpreted as Somewhat Satisfied. The overall weighted mean for the rate of satisfaction generated on BIM gauge usage was 4.21 and was interpreted as Somewhat Satisfied.

IV. SUMMARY OF FINDINGS

This chapter discusses a brief narrative regarding the study. It includes important information that was found in the study. It presents generalization and answers to the problems and objectives stated at the beginning of the study. Furthermore, it includes suggestions or proposed solutions for the problems encountered during the study.

4.1. BIM Assessment models and its questions, frameworks, and mechanisms

1. Number and Quantifications of Questions / Measurements

a. VDC Scorecard - has 96 questions, indicating the challenging and resource-intensive to use the technology and to which highlight the importance of BIM maturity in the context of the organization and its processes

b. Owner's BIM CAT – has 66 questions, demonstrating the challenging and resource-intensive to use these technology

c. Characterization Framework – has 56 questions, showing how difficult and time-consuming it is to implement the technology. In the context of the organization and the procedures it uses, this

model emphasizing the significance of BIM maturity.

d. NBIMS CMM - has 20 questions, demonstrating its simplicity
e. BIMCS - has 20 questions, also signifying its simplicity which emphasized technical features of BIM.
f. IU BIM Proficiency Index - has 32 questions, medium difficulty
g. BIM MM (Level 2) - has 36 questions, medium difficulty which features a more uniform question distribution
h. BIM Quick Scan - has 44 questions, medium difficulty
i. BIM Assessment Profile - has 30 questions, medium difficulty

2. BIM Capability and Maturity Assessment Models

a. BIM-CAREM - It creates a suitable BIM capacity assessment model for AEC/FM projects focusing on the process, technology, organization, human elements, and standards across four maturity level attributes.
b. NBIMS BIM CMM - It prioritizes tabular and dynamic BIM ratings for project results and operational procedures. It has six features and three levels of maturity: data richness, life cycle view, roles or disciplines, change management, business process, timeliness/response, delivery method, graphical information, spatial capability, interoperability/IFC, and six identified attributes in its maturity level.
c. BIM Proficiency Matrix - It is useful when choosing contractors. Based on the five maturity level attributes, it was also able to integrate to reach physical correctness, integrated project delivery methodology, calculating mindset, location awareness, content creation, contribution data, as-built modeling, and FM data richness.
d. BIM Maturity Matrix - It evaluates the entire organization's BIM expertise, maturity, and project outcomes.
e. BIM QuickScan - It reveals the ins and outs of the firm's BIM capabilities and weaknesses. This is more focused on the organization and management, mentality and culture, information flow, tools, and applications in a BIM-based projects.
f. VDC Scorecard - It compares a project's progress to that of others in its field. Due to its three classification levels of metrics in four areas—planning, adoption, technology, and performance—it provides comprehensive coverage of BIM.
g. Organizational BIM Assessment Profile - It provides understanding on how far along in their BIM planning stages an organization. This framework is perfect for improving the BIM strategy, BIM applications, processes, data, and resources of your business.
h. VICO BIM Scorecard - It is used for measuring the ROI of specific BIM usages, such as project management and budget forecasting which focused on the portfolio and project management, budgeting, allocating time and resources, monitoring and coordinating production, and getting the design team involved.
i. Multifunctional BIM Maturity Matrix - It evaluates the degree to which BIM has progressed in specific projects, companies with multiple active projects, and the industry as a whole which offers moderate adaptability.

4.2. Development of BIM Gauge Framework

1. BIM Gauge Framework components

a. BIM Usage and Information Flow – measure the organization's maturity on BIM usage and information management throughout the whole project lifecycle.
b. Strategy (Collaboration and Working Strategy) - measure the collaboration strategy used in the project and their working practice.
c. Infrastructure (Tools and Applications) - measure the organization's capability to deliver BIM from their Software, Hardware, and IT Security
d. Organization & Management - measure the maturity of organization's management in implementing BIM in the project and organization.
e. Information Exchange & Data Structure - measure the maturity of information exchange and data structure used in the project.
f. Personnel - assess how the management implements innovation with the implementation of BIM, the roles and responsibilities, qualification, and training of the people for BIM-based projects and how they do their knowledge management.

4.3. Development of Web-Based BIM Assessment Tool

It is developed using a firebase database in an angular framework and waterfall development methodology.

The development has 5 phases namely:

- Phase 1: Requirement gathering
- Phase 2: Design
- Phase 3: Development
- Phase 4: Testing, and
- Phase 5: Deployment

4.4. BIM Gauge Experience

1. In terms of their time spent in BIM gauge website, majority of them had been spending between 5-8 minutes in the BIM gauge website with 10 respondents or about 34.5%.
2. In connection to the level of difficulty from the last time of using BIM gauge and showed that most of the respondents answered none with 18 respondents or equivalent to 62.1%.
3. In terms of the important main fundamental components measured by the tool, the most important main fundamental component is the process with 24 respondents or equivalent to 82.8%.
4. In terms of their perception of the need to consider the assessment questions under the Process component (BIM Usage & Information Flow) to measure BIM maturity satisfactory, most of the respondents answered Somewhat Satisfied with 13 respondents or equivalent to 46.4%.
5. In terms of the respondents' perception of the need to consider the assessment questions under Technology component (Tools & Applications) to measure BIM maturity satisfactory, most of the respondents answered Very Satisfied with 13 respondents or about 44.8%.
6. In terms of the respondents' perception of the need to consider the assessment questions under Organization component (Organizations & Management) to measure BIM maturity satisfactory, most of the respondents answered Very Satisfied with 13 respondents or equivalent to 44.8%.
7. In terms of the respondents' perception of the need to consider the assessment questions under Standard component (Information Exchange & Data Structure) to measure BIM maturity satisfactory, most of the respondents answered Somewhat Satisfied with 13 respondents or about 44.8%.
8. In terms of the respondents' perception of the need to consider the assessment questions under People component (Mentality & Culture) to measure BIM maturity satisfactory, most of the respondents answered Very Satisfied with 14 respondents or equivalent to 48.3%.
9. In terms of the distribution of the respondents in terms of their perception of the important sub-fundamental components measures under Process (BIM Usage & Information Flow), it can be seen that most of the selected respondents answered Information Flow with 20 respondents or about 69%.
10. With regards to the important sub-fundamental components measures under Technology (Tools & Applications), the respondents answered that the sub-component of System is the more significant for them with 28 respondents or about 96.6%.
11. In terms of the respondents' perceptions of the important sub-fundamental components measured under Organization (Organizations & Management), it can be noted that most of the respondents answered Strategy with 22 respondents or equivalent to 75.9%.
12. The respondents' perception of the important sub-fundamental component of Standard (Information Exchange & Data Structure), it can be seen that Data Structure was considered by the respondents as the most important sub-fundamental component of Standard component with 24 respondents or equivalent to 82.8%.
13. The respondents' perception of the important sub-fundamental component of People (Mentality & Culture), it can be seen that People and Responsibilities was considered by the respondents as the most important sub-fundamental component of People component with 22 respondents or equivalent to 75.9%.
14. With regards to the respondents' perception of agreeing with the result of BIM gauge, it can be seen that most of them answered Yes with 24 respondents or equivalent to 82.8%.
15. In terms of the respondents' perception if the recommendation provided by the tool are considered to be relevant in helping the organization to improve their BIM implementation, it can be seen that majority of the respondents answered Yes with 25 respondents or equivalent to 86.2%.
16. With regards to the distribution of the respondents in terms of their experience of the ease of using the BIM gauge, it can be noted that most of them answered Somewhat Easy with 17 respondents or 58.6%.
17. As for the respondents' perception in terms of finding out the result of the BIM gauge, it can be seen that most of them answered Very Reliable with the highest number of respondents of 18 respondents or about 62.1%.
18. In connection with the frequency and percentage distribution of the respondents in terms of their perception of using the BIM gauge again, majority of the respondents answered Yes with 27 respondents or about 93.1%.

19. In connection with the respondents' perception of how the BIM maturity assessment tool will be considered to be helpful in the construction industry to assess and improve their BIM implementation, it can be seen that most of the selected respondents of the study answered Yes with 28 respondents or equivalent to 96.6%.
20. Some respondents shared those certain improvements that should be concentrated more on providing further or more elaborate explanation or description under each item; changing the way that answers are selected for convenience; being more specific on questions or adding more assessment questions; and should be able to generate statistical and graphical results for better understanding. It was also added that it should be modified to be used as a mobile device app for convenience and improved access; more streamlining and appropriate alignment of questions with regards to BIM implementation and gauging; as well as the need to improve choices; and finally, its overall interface for improved and better use and performance.

4.5. BIM Gauge as a Tool

In terms of the weighted mean of the rate of satisfaction generated on BIM gauge usage, it can be seen that the indicator "Easily Accessible" had obtained the highest mean of 4.31 and was verbally interpreted as Very Satisfied.

V. CONCLUSIONS

Based on the findings of the study, the following conclusions were drawn:

1. The AEC/FM sector has acknowledged a variety of BIM evaluation tools. Among these assessment methods are the BIM-GBI Assessment Method model, which produced and maintained standardized information on buildings' green rating system certification; the BIM Use Assessment (BUA) Tool, which was designed for the application levels of BIM use in the planning and design phases; and the BIM Performance Assessment Tools, which were more focused on competency and capability/maturity assessment. It was concluded that different BIM evaluation tools are crucial in implementing diverse BIM-based projects based on their features and purposes, as evidenced by the findings.
2. The findings revealed a wide range of questions and quantifications of measurements across a wide range of identified models, including the VDC Scorecard, Owner's BIM CAT, Characterization Framework, NBIMS CMM, BIMCS, IU BIM Proficiency Index, BIM MM (Level 2), BIM Quick Scan, and BIM Assessment Profile. Measuring features on six frameworks (BIM Usage and Information flow, Infrastructure, Organization and management, Strategy, Personnel, and Data Structure and Information Exchange) were used to provide a critical evaluation of these models. BIM-CAREM, NBIMS BIM CMM, BIM Proficiency Matrix, BIM Maturity Matrix, BIM QuickScan, VDC Scorecard, Organizational BIM Assessment Profile, VICO BIM Scorecard, and Multifunctional BIM Maturity Matrix were included for comparison analysis in the current study. These outcomes demonstrate that these models have been leveraged by the AEC/FM industry and organizations to successfully implement their BIM-based projects. So, the study's results show that these BIM models can be used over and over again to do BIM-based projects the way they were meant to be done.
3. BIM Gauge framework development has uncovered a variety of assessment questions in each tool. Thus, there were 9 types of questions and measures for organization and management, 5 types of questions and measures for the standard which focused on information exchange and data structure, and 8 types of questions and measures for people, specifically on mentality and culture. Importantly, the BIM Gauge Framework has highlighted areas where distinct metrics have been placed, including Strategy, Infrastructure, Organization & Management, Information Exchange & Data Structure, and Personnel. It follows that the various parts of the BIM Gauge Framework are useful for assessing how BIM-based projects must and should be executed and evaluating their efficacy based on the areas/aspects as indicated.
4. It can be concluded that the development of the Web-Based BIM Assessment Tool took into account five (5) factors, which are as follows: Phase 1 is for gathering requirements, Phase 2 is for design, Phase 3 is for development, Phase 4 is for testing, and Phase 5 is for deployment. As a result, if the five phases are carried out correctly, the BIM Gauge tool may be effectively implemented as a web-based BIM assessment tool to monitor the overall effectiveness of BIM-based project execution utilizing this designed tool.
5. It can be concluded that based from the findings of the study, the demographic profile of the respondents can be considered to be strong or

sufficient enough in order to make their use or application of BIM as part of their company or industry's construction process well-integrated and also can help to enhance their skills with its improved usage.

6. As such, it can also be concluded that the majority of the respondents had a good and productive experience of using BIM gauge although there are still some improvements in its features that the respondents wanted to emphasize but are also acceptable since they consider such factors as a hindrance in their effective use of the BIM gauge tool.
7. Overall, the respondents seemed to be satisfied with the use and experience of BIM gauge as a tool for assessing the maturity of their BIM implementation.

REFERENCES

[1] Kumanayake, R. & Bandara, R. (2012). Building information modelling (BIM): How it improves building performance, ResearchGate, 1-14.

[2] Jin, R., Zhong, B., Ma, L., Hashemi, A., Ding, L. (2019). Integrating BIM with building performance analysis in project life-cycle, Automated Construction, 106(10286).

[3] Wong, J. & Zhou, J. (2015). Enhancing environmental sustainability over building life cycles through green BIM: A review, Automated Construction, 57, 156–165.

[4] Enegbuma, W. & Ali, K. (2011). A preliminary study on building information modeling (BIM) implementation in Malaysia, Proceedings of 2011 3rd International Post Graduate Conference in Engineering, 1, 399-407, The Hong Kong Polytechnic University.

[5] Enegbuma, W., Aliagha, G., Ali, K., Badiru, Y. (2016). Confirmatory strategic information technology implementation for building information modelling adoption model, Journal of Construction in Developing Countries, 21(2), 113–129, https://dx.doi.org/10.21315/jcdc2016.21.2.6.

[6] Latiffi, A., Mohd, S., Brahim, J. (2015). Application of building information modeling (BIM) in the Malaysian construction industry: A story of the first government project, Applied Mechanics and Materials, 773(774), 943-948, Trans Technology Publications, Ltd., www.scientific.net/AMM.773 774.943, Switzerland.

IFERP connecting engineers...developing research
1st International Conference on Future of Engineering 2022

Video Game RPG-Idle Base "Tapel Saga"

Naftali[1], Novida Nur Miftakhul Arif[2], Jurike V. Moniaga[3]

[1] Binus School Of Computer Science, Bina Nusantara, Jakarta, Indonesia
[2] Binus Design Communication Visual, Bina Nusantara, Malang, Indonesia
[3] Binus Computer Science, Bina Nusantara, Jakarta, Indonesia
Email: [1]naftali@binus.ac.id, [2]novida.nur@binus.ac.id, [3]jurike@binus.edu

Abstract:
Tapel Saga is a mobile game that mixing RPG (A role-playing game (RPG) is a genre of video game where the gamer controls a fictional character (or characters) that undertakes a quest in an imaginary world). Idle game(An idle game is a game that progresses with no interaction from the player.) and Visual novel (Visual novel (VNs) video games are text-based adventure games that combine interactive fiction and traditional anime or manga art styles to give the gamer the experience of reading a novel in a visual format). To create engaging experiences though the unique gameplay. With The Fundamental Game Design to forged Tapel Saga, that concept was implemented on some variant mode: main story, endless run and boss rush.

Keywords:
Video Game, Visual Novel Game, RPG Game

I. INTRODUCTION

Recent technological advances are so rapid, especially in the computer field. Computer graphics can be used to simulate most areas of life. Human life, history, culture and even imagination can be viewed as a game.[1] Interest in video game addiction has stimulated a group of parents and some researchers have linked video games to problematic behavior and lack of social skills in children, academic integration and dysfunction. [2]. First what is video game. Video game is interactive digital entertainment that you can play via computer, game console, smartphone or tablet. Everyone can enjoy video game these days based on the genre they play there's a ton video game genre such as:

1. Role-Playing (RPG, ARPG)

RPG or role-playing game is a genre of video games where the gamer controls a fictional character that undertakes a quest in an imaginary world so basically we play as someone else story, plot to achive they goal most of rpg focused on the combat aspect rather than the narrative ones and in this game " Taple Saga" is action RPG where the main character fight bunch of monster. There's a lot of RPG game out there such as: //
A. Masketeers
B. Final Fantasy
C Persona Series

2. Action-Adventure

An Action-adventure game can be defined as a game with a mix of elements from an action game and an adventure game especially crucial elements like puzzles. Action require many of the same physical skills as action games, but also offer a storyline we pretend to be someone else we follow their story to achieve their goal example of action-adventure game: Legend of Zelda, Tomb Raider, etc.

3. Visual Novel

A visual novel is a video game genre that tells an interactive story primarily through text. They usually feature static character models and locations, and while they might have some animated cutscenes, these are typically short (if present at all).

4. Idle

Idle Games or its called Incremental Games re video games whose gameplay consists of the player performing simple actions (such as clicking on the screen) repeatedly to gain currency. This can be used to obtain items or abilities that increase the rate at which currency accrues."
In " Tapel Saga" we use C# Programming language so what is C#?
The C # language is universal and object-oriented Programming language. It was designed and developed by Microsoft and .NET platforms. there are many Various software developed in C # language

and .NET Platforms for desktop applications, web applications, offices, etc. Applications, websites, games, mobile applications, etc .[3]

II. METHODOLOGY

Game engines are complex and versatile tools for creating games, Multimedia content. They provide an environment for efficient development and Sometimes without knowledge of scripting.

The game engine

It covers different areas of the game development process, including: Rendering, Physics, audio, animation, artificial intelligence, user creation interface.[4]

In tapel saga we used Unity Engine to build the game. Unity is a game engine powerful cross-platform IDE for developers.

As well as a game engine, Unity is an IDE. IDE stands for “Integrated Development Environment,” which describes an interface that gives you access to all the tools you need for development in one place. The Unity software has a visual editor that allows creators to simply drag and drop elements into scenes and then manipulate their properties. And next is game design, Game Design is for amusement, education, fitness, or experimental objectives is the practice of using design and aesthetics. Gamification is the process of applying game design's aspects and tenets to other kinds of interactions. In another study, Game art style and story complexity designed to assist players. Reduce three cognitive biases to professionally designed video,Same purpose.[5]

So in order to making this game we combine much aspect in game with using unity game engine and extension. First we think how the game will work and how to play it. We choose RPG, Idle, Action, and Visual Novel as Core Genre. We get inspiration from Masketeers game its an Idle game but we mix it with some different feature and also different story and character. There is some step for making this game we used Fundamental Game Design as the main guide but we selected the suitable aspects [6]:

-Game Concept

its simplest form, is the easy-to-understand vision you have for your game. It’s also a way for you to sell your game idea.

- Game World’s

A place of imagination and is usually placed in an alternate fictional universe and its aim is to immerse the player and make them feel as if they are in control of this game world

- Creative and Expressive play

Expressive character help player feel how the story turns in.

- Character Development

Best character development make player connect with the main characters itself how he choose to act how the ending will be

- Storytelling

Storytelling are arranged to increase player interest.

- Creating the User Experience

User experience here is important because we want players to feel into the game not just the story also the ui mechanism easy to access, easy to learn so player can enjoy the game

- Gameplay and Core Mechanics

Determine how the game will be played and what are the mechanic core.

- Game Balancing

Its to make player didn’t get a difficult situation while playing the game or make them feel too easy when playing

- General Principles of Level Design

Level Design is the phase of game development that deals with creating the stages of the game.

III. RESULT AND DISCUSSION

The concept of gameplay itself is RPG, Idle, Visual Novel Game . Idle games are a recent trend in gaming in which the game is left running with little player interaction[7] .We used bubble in order to gain health attack point , and special skill. Sometimes Idle games live around digital games and are automated application. This new genre of games is rarely or totally unnecessary No interaction with player [8] according to Rakimahwati (2020) the application of this type of Idle game that will lead the

Gamer who actively seeks information to enrich knowledge while playing.[9]. The game also mixed with some RPG genre The game genre of narrative-focused alternative action is one that is highly emphasized with its narrative, alternative ways of interacting, and dialogue. Additionally, it features a reward mechanism for players.[10] RPG Game design is a complex process that involves many uncertainties. Just like the games themselves, it is an exciting and challenging activity.[11]

Not just video game mechanism but also there’s a story in there in “ Tapel Saga” Video games are developed day by day using several methods and understandings, to do a game review and make it better. Metrics comes in here, To create the perfect case for related software and games, the perfect video game is not a game which game has the best story, or the best gameplay, nor the best graphic, it all depends on Integration and echo of each component.[12] The game itself also have a cultural part such as keris, topeng, etc. Some history games

claim to be informative and educational, but others may be less than informative or even misleading.[13]. Next about battle mechanism there’s a lot aspect in battle:

1. Skills

There’s 2 skill in battle first is damage in damage skill bar must be filled in order to use it. First large damage area and the second one is attack speed that’s a common thing that rpg game have skill [14]

2. Bubble Mechanism

Bubble mechanism is a buff to the character either its to fill skill bar, give hp, or attack power. Just like idle game bubble can effect the main character to gain anything [15]

3. Gacha

In Gacha games we can obtain some monster to help destroy the enemy Gacha is a system in which players pay either in-game currency or real money to obtain an item from a pool of other items.[16]

4. Items

Item in shop help you gain more damage and speed in order to get money/ currency in game that play the game and buy item through shop. Not just for damage but item can used it for skin exclusive skin so the player didn’t border and have a variant item. [17]

5. Currency

We can get currency in-game through the battle either its story, boss rush, endless rush currency also can buy item through shop, upgrade item, level up the character. But there’s no microtransaction. Microtransactions allow players to purchase additional game content or premium items[18]. Everything gain in game.

Here some feature in the game:

1. Main Story

(Image 1.1: Main Story Mission)

2. Endless Rush

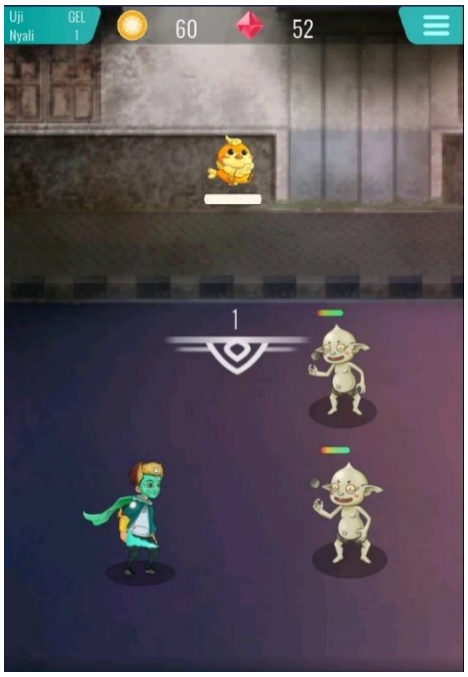

(Image 1.2 : Endless Rush)

3. Boss Rush

In main story we use visual novel as a story where a boy name “ Inu “ gain some superpowers. Visual novels is a game in which there are multimedia elements such as text, images, sound, and video, as well as giving players the opportunity to choose from a wide variety of in-game options [19]. Games that featuring the storyline brings the players interact in the game is a game type visual novels.[20] there are 2 Chapter in the game itself.

Second is Endless Dummy

Just like endless-run concept but what is endless run concept? Combinatorial approaches allow you to create gameplay using endless run concepts,

creating a combinatorial approach that merges multiple concepts. Equipped with an infinite game format.[21] each 5 round get a currency that we can buy in the shop. Just like Clicker game These are games where you can click on numbers and see them increase.

Finally, many of these games allow you to set what you want to click effectively. to you [22] but the difference that every round the enemy gets harder and harder more damage and more health.

Last one is Boss Rush in boss rush the main goal is defeat boss but its not going to be easy one unlike other boss in story this one is very special they got more health point, damage, and speed.

IV. CONCLUSION

With systematic game development, the development team was successfully combined several genres & gameplay elements. The RPG, idle & visual are work properly & supports each others. During the development with limited resources and time, the development team was challenged with so many problems. After published on May 2021, the development team still worked so hard to fixes bugs and errors. However Tapel Saga needs a lot of improvement and far from perfect, but the development team has created a unique gameplay that has a lot of potential for further development.

REFERENCES

[1] Game RPG “ The Royal Sword” Berbasis Desktop Dengan Menggunakan Metode Finite State Machine (FSM)Fadel Marzian, Mukti Qamal (2017)

[2] Video Game Addiction: The Push To Pathologize Video Games Anthony M. Bean 1 Rune K. L. Nielsen Antonius J. Van Rooij Christopher J. Ferguson [2017]

[3] Interactive and Virtual / Mixed Reality Applications for Mechatronics Education Developed in Unity Engine Erik Kucera Oto Haffner Roman Leskovsky (2018)

[4] Antonín Šmíd Comparison of Unity and Unreal Engine (2017)

[5] Educational Game Design: An Empirical Study of the Effects of Narrative Chaima Jemmali, Sara Bunian, Andrea Mambretti, Magy Seif El-Nasr

[6] Adams. Ernest, Fundamentals of Game Design, third edition (New Riders, San Francisco, 2014), pp.180-204.

[7] Mechanics or Mechanisms: defining differences in analog games to support game design Micael Sousa[2021]

[8] Perfecting A Video Game with Game Metrics Junaidi* 1 , Andy Julianto2 , Nizirwan Anwar3 , Safrizal4 , Harco Leslie Hendric Spits Warnars5 , Kiyota Hashimoto(2018)

[9] Story versus history: the contentious creation of the historical videogame Versailles 1685 Edwige Lelièvre [2019]

[10] Perancangan Game RPG “ Mari Mengenal Provinsi Di Indonesia” Menggunakan UnityRahmat Kurniawan 1 , Setiawan Assegaff 2 , Eni Rohaini (2020)

[11] Interpassivity and the Joy of Delegated Play in Idle Games Sonia Fizek (2018)

[12] How do players experience a gacha game depending on their perspective as a starting or a veteran player? A case study of Genshin Impact Dominykas Jecius, Alexander Frestadius (2022)

[13] More Than Just Skins(s) In The Game : How One Digital Video Game Item Is Being Used For Unregulated Gambling Purposes Online John Vrooman Haskell (2017)

[14] Video Game Monetization (e.g., ‘Loot Boxes’): a Blueprint for Practical Social Responsibility Measures Daniel L. King1 & Paul H. Delfabbro1 (2018)

[15] Pengembangan Visual Novel Game Mata Pelajaran Ilmu Pengetahuan SoSial di Sekolah Menengah Pertama. Adrie Satrio, Abdul Gafur (2017)

[16] Perncangan Desain Karakter Senjata Tradisional Untuk Game Visual Novel Berbasis PowerPoint Eliana Wulandari1 , Hendro Aryanto2 (2021)

[17] Mobile Game Design for Learning Chemical Bonds with Endless Run Approach Muhammad Hafis, Ahmad Afif Supianto (2018)

[18] Wait Wait… Don’t Play Me: The Clicker Game Genre and Conguring Everyday Temporalities Oscar Moralde (2019)

[19] Playing to Wait: A Taxonomy of Idle Games Sultan A. Alharthi,1 Olaa Alsaedi,1 Zachary O. Toups,1 Theresa Jean Tanenbaum,2 Jessica Hammer3 [2018]

[20] “It Started as a Joke”: On the Design of Idle Games Katta Spiel, Sultan A. Alharthi, Andrew Jian-Lan Cen , Jessica Hammer , Lennart E. Nacke , Z O. Toups and Theresa Jean Tanenbaum(2019)

[21] Developing of Interactive Game Based on Role Play Game to Improve the Reading Abilities Rakimahwati Rakimahwati, Desmawati Roza

[22] An RPG Game Design for English Learning using ADDIE Methods Tony Wibowo1 , Felnando2 [2022]

IFERP connecting engineers...developing research
1st International Conference on Future of Engineering 2022

QR Code Detector and Follower with Kalman Filter

Pranesh Kumar[1], Dr. Arti Khaparde[2]

[1] M.Tech, Department of Electronics and Communication Engineering, Dr. Vishwanath Karad MIT World Peace University, Pune, Maharashtra, India
[2] Professor, Department of Electronics and Communication Engineering, Dr. Vishwanath Karad MIT World Peace University, Pune, Maharashtra, India
Email: [1]1032200103@mitwpu.edu.in, [2]arti.khaparde@mitwpu.edu.in

Abstract:
For any robot, animal, or social animal to learn, understand, and respond appropriately, visual perception is the most critical capacity. This paper presents an example of computer vision-based research written in the Python programming language which employs libraries like OpenCV and NumPy. To navigate a robot on its own USB 2.0 high-definition camera mounted on robot captures the video stream in the operating area. Identification and decoding of QR code from the visible environment of camera using the image processing and QR code detection algorithm. Tracking of QR code is done using the Kalman filter. The robot will function according to the decision taken by program logic developed in minicomputer depending on data input from the camera.

Keywords:
Raspberry Pi 4, Kalman Filter, QR code

I. INTRODUCTION

The demand for a technical solution has grown as a result of human exposure to hazardous work environments and the current COVID-19 outbreak. Small efforts can be made to mitigate this risk. 'Computer Vision' is a term that refers to a computer's ability to extract, classify, and create a model in order to function effectively.

Robots are multipurpose programmed, versatile manipulators designed to direct material, parts, tools, or specialized devices through numerous predefined directions in order to do a number of tasks. Robot vision is the cyber-physical augmentation of computer vision on a robot or machine to complete a task.

Some work related to autonomous navigation has been done previously. Unlike another computer vision-based autonomous navigation techniques, to ease the process of way-finding use of simple geometric shapes of a specific color and area calculation has been involved in this paper. This concept will navigate the robot more effectively. It will transform and advance more research based on driverless vehicle technology.

OpenCV is a computer vision framework that is used to process digital images in order to control the robot more intelligently.

II. LITERATURE SURVEY

In this paper[1], the authors proposed a system for finding location of the soccer playing robot in a soccer play field in steady condition using EKF. In this Article[2], the authors discussed about SLAM with KF and EKF for mobile robot.

In this paper[3], the recent developments in the Kalman filter for robotic visual perception are discussed in this study. Localization, estimate, exploration, navigation, tracking, mapping, modelling and other applications are typical contributions. Readers can get a general sense of the status of the art by looking at representative works. A variety of strategies for resolving visual acquisition issues are examined. More than 20 different types of approaches based on Kalman filters, EKFs, and UKFs are discussed.

In paper [4], This work presents an adaptive robust EKF based on a discontinuous Lyapunov-based controller to increase the tracking accuracy of robotic manipulators with temporal variation disturbances. In paper [5], During estimating, any structural breaks have no effect on the KF. Because it is a recursive approach, it makes use of the whole history of a series and has the advantage of estimating the stochastic path of the coefficients rather than the deterministic one. The Gauss-Markov theorem improves the KF's ability to answer various statistical

inference tasks. In this approach, the KF stands out because it predicts condition of system even without particular system nature unknown the past, present and future. In paper [6], The Unscented Kalman filter is used in this paper to create a visual tracking system. The encoder, inertial sensors, and active beacon data are all integrated into the planned system. The UKF is a sensor fusion algorithm viz., used for location and attitude of a mobile robot. Two separate UKF models (one intended for slip and the other for no-slip case) and a slip detector, the suggested system effectively reduces sensor position errors. By comparing the data from the accelerometer and encoder, the slip detector detects the slip state and chooses either UKF model as the system's output. In paper [7], A Multi remodeled UKF estimator for skid-steered mobile robots navigation in offroad environments is presented in this research. A slip-aware kinematic model for a four-wheeled SSMR is developed based on the ICR model. The introduced remodeled UKF estimator is created by combining previous advances with the UKF process. GNSS, IMU, and Encoder data are combined to determine the location, attitude, velocity, and wheel slippage of mobile apparatus DUBHE. In paper [8], The information offered by measurement innovation technique in intermittent measurements when a mobile robot is examining its surroundings has been proven in this research. Even when data is lacking, the robot can still estimate its location, its mistakes are statistically bounded if and only if the initial state covariance, process, and measurement noises are minimal enough viz the robot finds logical confidence in its environment surroundings. In this paper[9] author states that wireless network deployment requires location tags to be successful. To achieve accurate label positioning, four base station tags are suggested. This work addresses the challenge of eliminating NLOS environments first, followed by the clock synchronisation approach. The NLOS-K approach is efficient and robust in both indoor and outdoor contexts, according to the findings of the experiments. Existing estimate approaches based on Kalman filter based on NLOS or alone, on the other hand, cannot be employed indoors, and their outdoor performance is significantly poorer than that of this research. In this paper[10], the SoC of a Lithium-ion battery was estimated using two variants of the Kalman filter: EKF and UKF. It has been demonstrated that when battery is discharged at a steady current, UKF performs better in the majority of the simulation. UKF fared significantly better in the second simulation test, which involved alternating charging and draining of a battery using a steady current and loud process.

III. HARDWARE AND SOFTWARE IMPLEMENTATION

A. Hardware Description

Computer vision approaches assist us in comprehending additional visual data, particularly in the domain of contour and counting geometric edges. The frame captured by camera acts as input for the minicomputer's algorithm by the help of computer vision technique. The algorithm helps robot to take decision whether to move or not. Computer vision is the study of how machines, and robots can see. It's a form of artificial intelligence that gathers data or information from images or video, then performs operations on them in order to determine properties. It makes use of to do tasks using image processing algorithms. Images are used throughout the computer vision process. Image acquisition, processing, analyze, and extraction. This information, which is derived from visual sources, the content is converted into a detailed description. Information compiled in a multi-dimensional format that can be linked to arrays with several dimensions. OpenCV is the library used in python to define the computer vision.

Kalman Filter

Kalman filtering is an algorithm that gives estimates of some unknown variables given the measurements observed over time. Kalman filters are demonstrating its usefulness in various applications. Kalman filters have relatively simple form and need small computational power.

Table 1 : Index of notation

Notation	Description
xk	Current time state
xk-1	Previous time state
A	State transition matrix
P	Covariance matrix of Process
Q	Covariance matrix of Process noise
B	Control input matrix
u	Control input
R	Covariance matrix for measurement
H	Mapping matrix
KG	Kalman gain
k	Time instant
z	Measurement

Predict:

$$x_k = A.x_{k-1} + B.u \quad (1)$$

$$P_k = A.P_{k-1}.A^T + Q \quad (2)$$

Update:

$$KG = \frac{P_k.H^T}{H.P_k.H^T + R} \quad (3)$$

$$x_{k'} = x_k + KG.(z - H.x_k) \quad (4)$$

$$P_k = (I - KG.H).P_k \quad (5)$$

Equations(1) and (2) define the predicted state and covariance matrixth of process with use of matrix A,B,Q and u.
Equations(3) and (4) define the Kalman gain and estimated state with the help of process covariance, mapping matrix and measurement.
Equation(5) define the process covariance matrix to be used for computing next state.

B. Hardware implementation setup

In the block diagram USB camera is connected to Raspberry Pi 4B board. The L298D H-bridge i.e., motor controller is connected to Raspberry Pi using jumper wires to various GPIOs, battery operated dc motors are connected to the two output ports. The onboard power supply is designed using the Lithium ion batteries and the dc-dc converter to provide power supply to the Raspberry Pi board as well as to the motor controller. This completes our system as described in Fig.1 , above mentioned components are mounted on robot chassis viz 5cm above from ground level.

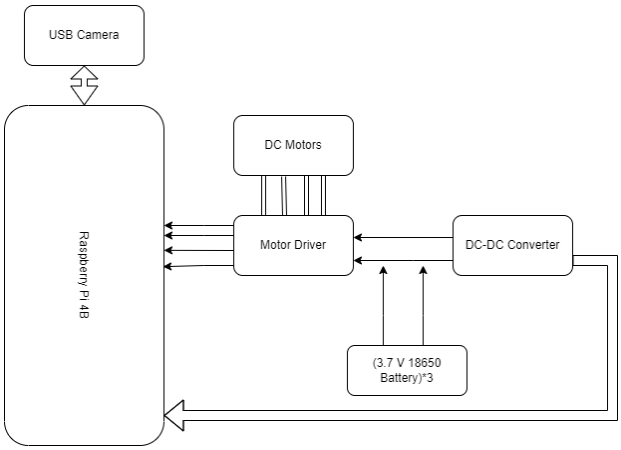

Fig.1 Hardware block diagram implementation setup

Fig.2 Side view of robot

Fig.2 describes the actual robot apparatus used in the implementation of the project.

C. Flow chart of software implementation

Capture the frame using camera and provide as input to algorithm in which search for the QR code inside the environment and the four edges of QR code then decode message of QR code and simultaneously tracking the QR code if it is displaced from previous frame, find its edges and find its centre using any two coordinates of edges of QR code and draw a red circle using Kalman filter update function otherwise keep previous update. The robot will move forward only if the QR code detected in the frame is having decoded message as 'Target' if it is the case then the robot will move forward towards it till its in the vicinity of the camera as described in Fig.3,4.

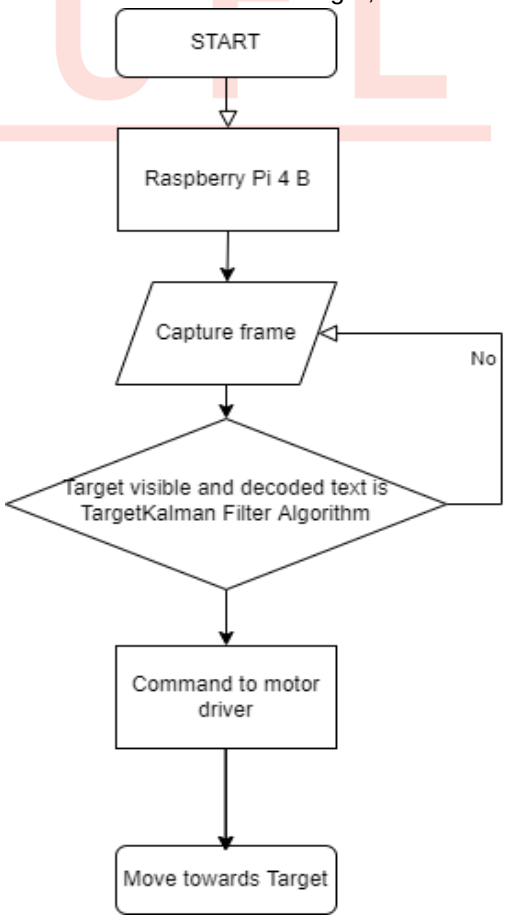

Fig.3: Flowchart of software implementation for target tracking trough Kalman filtering algorithm.

Fig.3 defines all the possible states which are involved in the code flow of project. It depicts the transition from one function to another during execution of code.

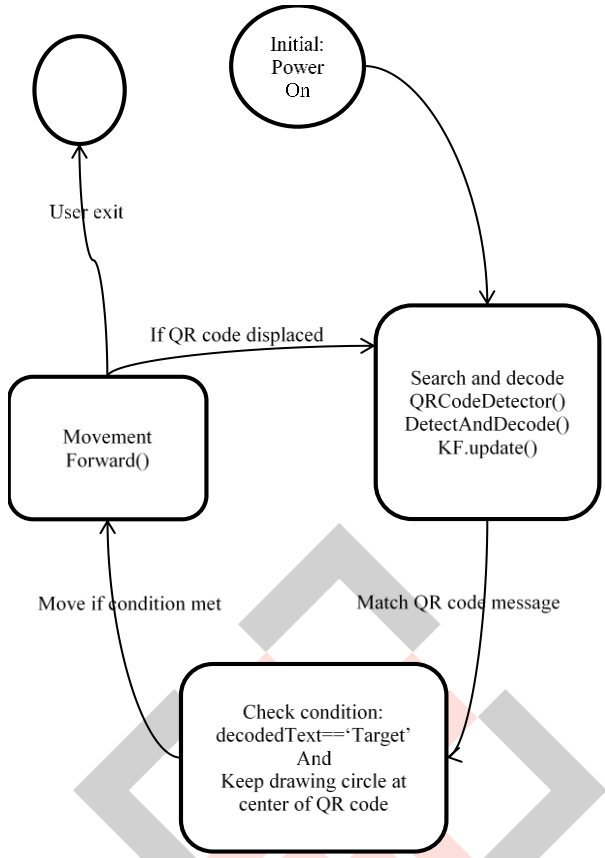

Fig.4: State Diagram of entire software implementation

IV. TEST RESULTS OF EXPERIMENT

The QR code is feed to the program using USB camera and given as input to the QR code decode function, which results the decoded message of QR code. If the QR code is displaced from previous place the four coordinates of the QR code is updated by giving input to the Kalman filter update function which continuously monitors any change in it. Then the decoded message of QR code is checked with the required message to move the robot, if the decoded message matches to it then the robot move towards it.

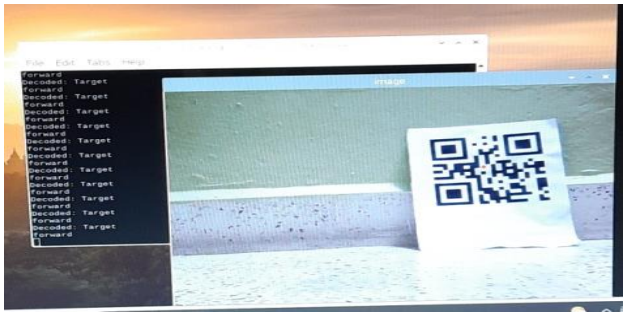

Fig.5 Decoding the input QR code and command to motor

The Fig.5 describes the required QR code been placed infront of camera and the algorithm decodes the message and command to motor to move towards it.

Fig.6 Testing with different QR code

The Fig.6 describes the system is been tested with input as QR code.It decodes QR code message but it is not as required message so robot does not move towards it.

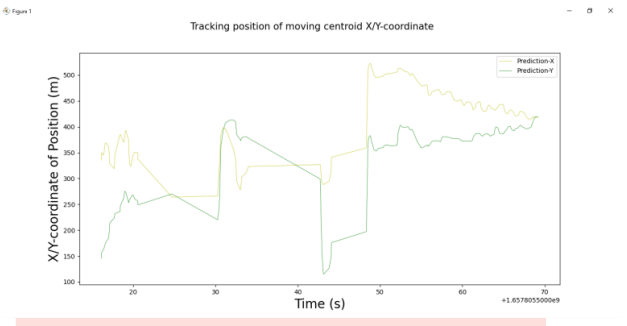

Fig.7:Simulation result with Kalman filter

The Fig.7 describes the x-coordinate and y-coordinate of the centroid of identified QR code while simulation.

V. CONCLUSION

Computer vision is a burgeoning technology that will transform the industry and looks to be more promising for human safety and accuracy.

The following are the assumptions for successful implementation of this project. The movement of the robot will be only straight forward. There is no obstruction or object in the environment of camera. The camera is stationary. The robot will move forward only if the decoded QR code is ‘Target’ as captured from camera otherwise stationary. The OpenCV tool helps in capturing video and sends it as input for the mobility of robot.

Acknowledgment

I would like to take opportunity to thank Head of department, Mentor for the throughout encouragement towards project which helped in success of it. i would also thank my PArent for their

moral and financial support During Entire phase of the project.

REFERENCES

[1] Claudio Urrea, Rayko Agramonte “Kalman Filter: Historical Overview and Review of Its Use in Robotics 60 Years after Its Creation” Hindawi Journal of Sensors Volume 2021, Article ID 9674015, 21 pages https://doi.org/10.1155/2021/9674015

[2] Inam Ullah , Xin Su , Xuewu Zhang , and Dongmin Choi “Simultaneous Localization and Mapping Based on Kalman Filter and Extended Kalman Filter” Hindawi Wireless Communications and Mobile Computing Volume 2020, Article ID 2138643, 12 pages https://doi.org/10.1155/2020/2138643

[3] F. Liu, X. Li, S. Yuan and W. Lan, "Slip-Aware Motion Estimation for Off-Road Mobile Robots via Multi-Innovation Unscented Kalman Filter," in IEEE Access, vol. 8, pp. 43482-43496, 2020, doi: 10.1109/ACCESS.2020.2977889.

[4] A. R. Ghiasi, A. A. Ghavifekr, Y. S. Hagh and H. SeyedGholami, "Designing adaptive robust extended Kalman filter based on Lyapunov-based controller for robotics manipulators," 2015 6th International Conference on Modeling, Simulation, and Applied Optimization (ICMSAO), 2015, pp. 1-6, doi: 10.1109/ICMSAO.2015.7152248.

[5] Hamzah Ahmad & Toru Namerikawa “Extended Kalman filter-based mobile robot localization with intermittent measurements” a (2013) Extended Kalman filter-based mobile robot localization with intermittent measurements, Systems Science & Control Engineering: An Open Access Journal, 1:1, 113-126, DOI: 10.1080/21642583.2013.864249

[6] S. Y. Chen “Kalman Filter for Robot Vision: A Survey” IEEE TRANSACTIONS ON INDUSTRIAL ELECTRONICS, VOL. 59, NO. 11, NOVEMBER 2012

[7] M. M. Shaikh et al., "Mobile robot vision tracking system using Unscented Kalman Filter," 2011 IEEE/SICE International Symposium on System Integration (SII), 2011, pp. 1214-1219, doi: 10.1109/SII.2011.6147622.

[8] Rick Midclleton, Michaela Freestoll and Leonie McNeill “APPLICATION OF THE EXTENDED KALMAN FILTER TO ROBOT SOCCER LOCALISATION AND WORLD MODELLING.”, Copyright © IFAC Mechatronic Systems,Sydney, Australia. 2004

[9] Zhanjun Hao, Beibei Li1, Xiaochao Dang “An Improved Kalman Filter Positioning Method in NLOS Environment”

[10] Ivan Jokić, Žarko Zečević, and Božo Krstajić, “State-of-Charge Estimation of Lithium-ion Batteries using Extended Kalman filter and Unscented Kalman filter” 2018 23rd International Scientific-Professional Conference on Information Technology (IT)

IFERP® connecting engineers...developing research
1st International Conference on Future of Engineering 2022

Experimental and Mathematical Performance Analysis of a Corrugated Plate Heat Exchanger using CuO Nano Fluids

Sachin Kumar[1], Dr Ajeet Kumar Rai[2]

[1,2] Department of Mechanical Engineering, VIAET, SHUATS Prayagraj UP, India
E-mail: [1]sachinkumar5181@gmail.com, [2]ajeet.rai@shiats.edu.in

Abstract:
In experimental analysis and investigated study to carried out to the heat transfer rate and their characteristic exergy loss effectiveness and friction factor of water based CuO nanofluid as a coolant in corrugated plate type heat exchanger. The analysis has been carried out for a 1-1 pass heat exchanger under parallel and counter flow situations, with different weight concentration CuO nanofluid. The effect of nanofluid (CuO in water .5, 1. in volume concentration and 70gm in weight %) and water as coolants as on heat transfer and those required properties of the nano fluids wear measured. The required pump power increased with increased in nanofluid weight concentration for better heat transfer rate in effectiveness in lower consumption of power or LMTD reduced in lower rate of 0.5 - 1LPM. The average heat transfer rate coefficient has been found to reduce by 45-60% when the angle of inclination of corrugation angle of inclination plate of heat exchanger is 45°.

Keywords:
mass flow rate, enhanced heat flow, Reynolds number, Nusselt number, PHE

Nomenclature
A = total heat transfer area, (m^2);
c_p = specific heat, (J kg^{-1} K^{-1})
h = convective heat transfer coefficient, (Wm^{-2} K^{-1}),
L = plate length, (mm),
N number of corrugated plates,
Nu = Nusselt number,
P = pressure,
Pr = Prandtl number,
Q = heat transfer rate, (W),
Re = Reynolds number,
t = corrugation pitch, mm,
U = overall heat transfer coefficient, (Wm^{-2} K^{-1}),
V= volume flow rate, (L min^{-1})
W = plant width, (mm),
E = exergy loss (W),
m = mass flow rate,
A = area of cross section,
i = inlet, P= pressure,
F = friction factor,
L=length (m),
R = capacity ratio,
Q = heat transfer rate (W).

I. INTRODUCTION

A heat exchanger is the device used to exchange the thermal heat energy between two or more different fluids, in this mechanism of a heat transfer are one of the most important engineering tools to save the energy in different applications, such as chemical and food industries mechanical automotive radiator etc. This design requirement is to saving energy and reduced to cost effectiveness, in globalised to enhance better performance rate. Nanofluids are mainly used as working fluids in heat transfer equipment, such as heat exchangers. As pointed out by Kumar et al. [1], any debate about heat transfer and heat exchangers may not be able to draw correct and logical understandings and conclusions without referring to nanofluids, and vice versa. Heat exchangers can be indexed as indirect contact type and direct contact type. Tubular heat exchangers are efficient process equipment that produce significantly improved heat transfer with high fluid flow rates. Plate heat exchangers are usually arranged of a stack of thin corrugated metal plates, with apertures at the corners to supply channels for two fluid systems, allowing heat transfer between the two fluid media. Nowadays, nanofluids have been widely used in solar energy systems, heat exchangers, automobile radiators, electronic chips, etc. However, especially in a solar energy system, nanofluids have a great potential [2], some practical limitations and enormous challenges [3]. Michael and Iniyan [4] improved the

thermal performance of photovoltaic thermal collectors using CuO-water nanofluids. They found that the thermal efficiency increased up to 45.76% for a CuO-water nanofluid with 0.05% volume fraction, compared to water at a mass flow rate of 0.01 kg/s. Chen et al. [5] analyzed the entropy generation and exergy destruction of a graphene nanoplatelets nanofluid in a ribbed triple-tube heat exchanger (RTTHX). It was observed that the total exergy destruction of the whole RTTHX was reduced when the nanoparticle mass fraction increased. Kumar and Chandrasekar [6] analyzed heat transfer characteristics of double helically coiled tube heat exchangers with MWCNT- water nanofluids based on a comparison of the Dean Number. It was found that for a 0.6 vol.% nanofluid, the Nusselt number and pressure drop increased by 30% and 10% at a dean number of 2000, respectively. Radka et al. [7] investigated convective heat transfer characteristics of helical copper tube heat ex- changers under a constant wall temperature condition. They found that the average Nusselt number increased by 18.6% for 0.25 vol.% ZnO nanofluid. Bianco et al. [8] numerically investigated the heat transfer performance of an asymmetric heated channel filled with Al2O3 -water nanofluid. The increase of the Nusselt number was 15% for the 6% Al2O3 water nanofluid at a Reynolds number of 1000. Huang et al. [9] investigated thermal performance of Al2O3 and Al2O3−MWCNT hybrid nanofluids in a chevron plate heat exchanger. They proposed a correlation to predict all the experimental data within an error band of ±10%. Bhattad et al. [10] pointed out that increasing the volume ratio of MWCNT nanoparticles in an Al2O3 −MWCNT hybrid nanofluid was beneficial for the performance improvement of the plate heat exchangers. This Is very important role of industrial application and widely used to significant increase their thermal conductivity and eventually their heat transfer coefficient. their where efficient cooling is a strong need to reduced cost, and energy consumption and environmental impact of the system.

II. ABOUT COPPER OXIDE (CUO) NANO PARTICLE

COPPER OXIDE	Description
Purity	99.9%
Average Particle Size	30-50nm
SSA	60-80m^2/g
Molecular Weight	79.549 g/mol
Molecular Formula	CuO
Melting Point	1326°C
Bulk Density	2.7g/cm^3
CAS NO.	1317-38^{-1}
Physical Form	Powder
Morphology	Spherical
Colour	Black

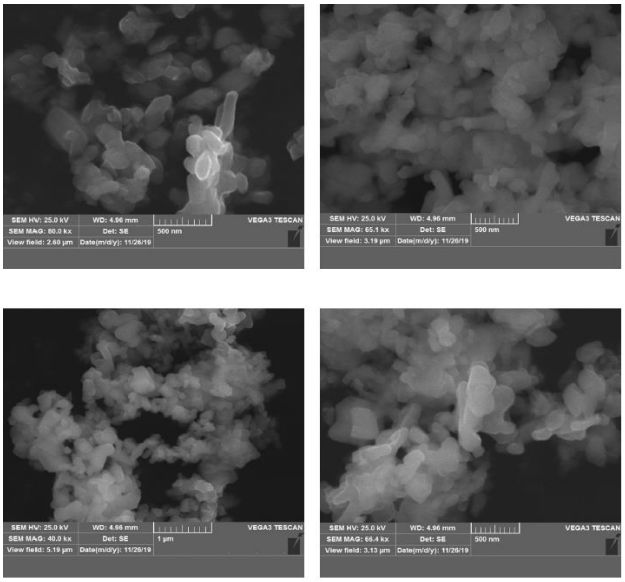

Fig. 1. Scanning electron microscope (SEM) images CuO Nano Particle

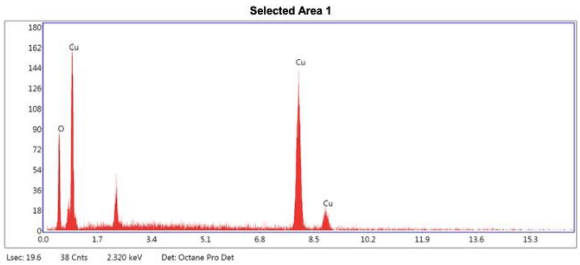

eZAF Smart Quant Results

Element	Weight %	Atomic %
O K	23.36	54.77
CuK	76.64	45.23

Fig. 2. eZAF smart Quant Results CuO nano particle

III. THERMOPHYSICAL PROPERTIES OF COPPER OXIDE (CUO) WATER FLUID

wt. in gm	Ψv	Cp(J/Kg-K)	μ (mPa. s)	ρ(kg/m3)	K(W/m.K)	Re	Pr	Nu
water	Nil	4180	0.789	995.7	0.615	29543.6	5362.634	8446.829268
70	0.0259	3950	0.9503447	1044	0.69	25717.65	5440.379	7528.695652
140	0.0518	3960	1.0165766	1045	0.698	24065.12	5767.398	7442.406877
210	0.0777	3970	1.0894555	1046	0.699	22476.78	6187.608	7431.759657
280	0.1036	3980	1.169864	1047	0.6998	20951.89	6653.414	7423.26379
350	0.1295	3990	1.2588329	1049	0.7	19508.3	7175.347	7421.142857

IV. EXPERIMENTAL SETUP

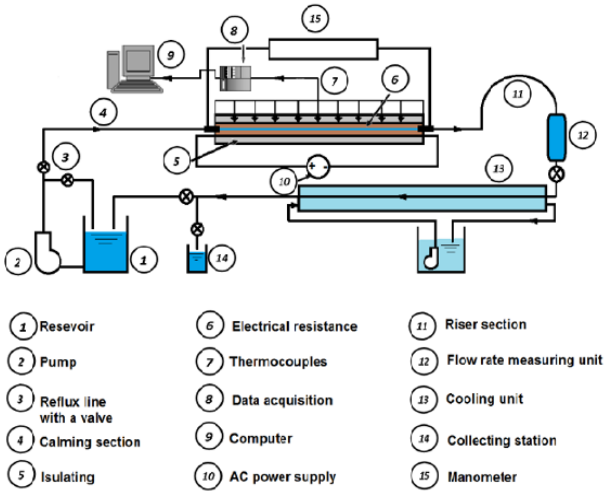

Fig .3 Schamatic view of the Exprimantal set up

The picture of experimental set up are fabricated in 22-gauge GI SHEET. In this experiment the two different cases are applicable in the form of arrangement of set up parallel flow and counter flow of the experiment includes the water loop of the measurement system comprises a water tank are containing heater and flow rate are measure thermally insulated material like wood dust and hot fluid are flow in central channel and cold fluid are flow in upper and lower channel. This Is very important role of industrial application and widely used to significant increase their thermal conductivity and eventually their heat transfer coefficient. their where efficient cooling is a strong need to reduced cost, and energy consumption and environmental impact of the system. Specifications of the experimental setup. Set up Length 100 cm, set up Width 10 cm, the gap between corrugated plates 5 cm and angle of the plate is 45°, the plate material is GI of 22 gauges.

V. EXPERIMENTAL PROCEDURE

Experimental procedure Hot and cold water are two different cases in inlet and outlet temperature of water provided in the different channel first in inlet hot water temperature and outlet. The Cold-water loop compromise a water tank is considerable 40˚ to 70˚C inlet temperature of hot water in parallel and counter flow arrangement. varying at 0.50 to 1 LPM and 0.50 to1 LPM. The flow rate is measure by noting done in time for fixed and different volume of the fluid. In the hot and cold channel loop in a measurement system, thermocouple device is used for temperature measurement flow through the central corrugated channel to maintain the channel surfaces at approximately constant temperature the hot water loop comprises in a water tank, and heater and water tank with pump. In the whole system are thermally insulated with wood dust particle, and water flow are in measure LPM unit base.

VI. NUMERICAL METHODOLOGY

Eqs. (1) and (2), respectively. Qave represents the average heat power of the hot fluid and the cold fluid and is calculated by Eq. (3)

$Q_h = m\ h\ C\ p_h.\ (T_{h,\ in} - T_{h,\ out})$ ..... (1)

$Q_c = m_c\ C_p,\ c\ (T_{c,\ out} - T_{c,\ in})$ ..... (2)

$Q_{ave} = (Q_h + Q_c) / 2$ ..... (3)

The overall heat transfer coefficient (U) can be calculated by eqn (4)

$U = Q_{ave} / A \cdot LMTD$ ..... (4)

where *A* represents the total heat transfer area (0.369 m^2). LMTD represents the logarithmic mean temperature difference, and it is calculated by in this eqn… (5)

$$LMTD = \theta m = \frac{\theta_2 - \theta_1}{\ln \frac{\theta_2}{\theta^1}} \quad \text{.....} \quad (5)$$

The heat transfer coefficient of the nanofluid (h n_f) can be calculated using Eq. (6):

$$\frac{1}{U} = \frac{1}{\bar{h}n_f} + \frac{\delta}{\lambda} + \frac{1}{h\omega} \quad \text{.....} \quad (6)$$

Where, δ and λ represent the width and thermal conductivity of the corrugated plate, respectively. *h w* is the convective heat transfer coefficient of the water. In this work, the heat transfer performance of the hot water was obtained by using the following equation

$$Nu = 1.\ 615\ [\ (f.\ Re / 64)\ Re.Pr.\ D / L]^{1/3}$$

Where, Nu, Re, and Pr are Nusselt number, Reynolds number and Prandtl number, respectively. f is related to the flow characteristics and structure of the corrugated plate. D is the equivalent diameter, i.e., the plate depth for this work. The Reynolds number

(Re) and Prandtl number (Pr) can be calculated by the following equations.

$$Re = \rho u D / \mu$$

$$P r = \mu c_p / k$$

velocity (v), viscosity (μ) and thermal conductivity (k). The Nusselt number of the hot water can be calculated as follows:

$$Nu = hD / k$$

In this paper, density and specific heat of the nanofluid are calculated as suggested in
Refs. [15, 16]:

$\rho nf = (1 - \phi)\ \rho w + \phi \rho p$

$(\rho cp)\ nf = (1 - \phi)\ (\rho cp)\ w + \phi\ (\rho cp)\ p$

VII. RESULTS AND DISCUSSION

In this experiment the effectiveness of heat exchanger is calculated by 1-1 passes through the corrugated plate heat exchanger by using nanofluids.

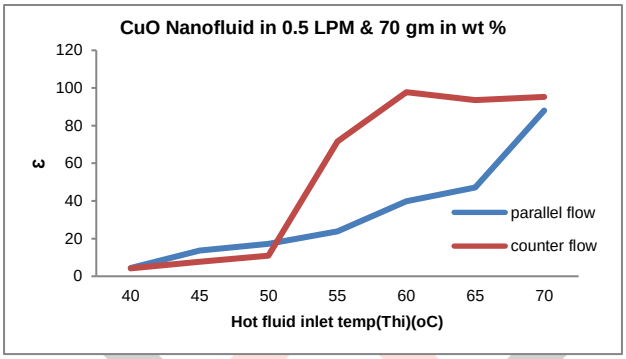

Fig :4 Variation of hot fluid inlet temperature at fixed mass flow rate at 70gm CuO

In above figure fixed mass flow rate at different inlet hot fluid temperature observed that the effectiveness of heat exchanger is increased 25% in counter flow arrangement with minimum loss of energy.

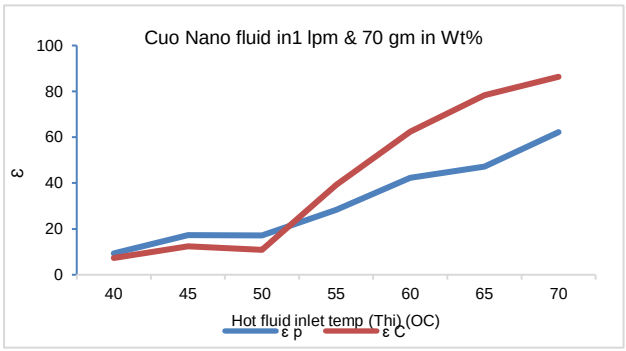

Fig :5 Variation of hot fluid inlet temperature at fixed mass flow rate at 70gm CuO.

In the above figure the variation of a graph between hot fluid inlet temperature the effectiveness will be increased in 32 % maximum temperature in 60^0 c in parallel and counter flow arrangement.

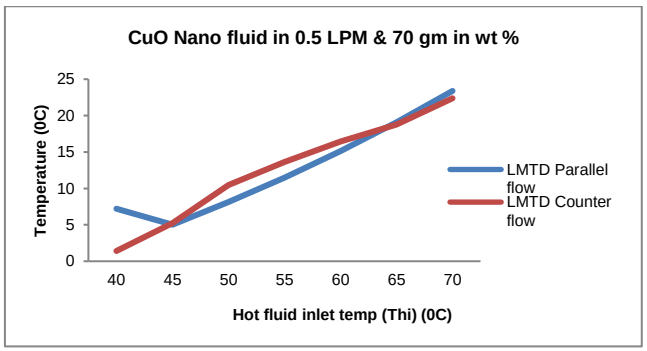

Fig :6 Temperature V/s Hot fluid inlet temperature at fixed mass flow rate at 70gm CuO.

In above figure temperature will be maximum in parallel flow arrangement with comparison to counter flow arrangement.

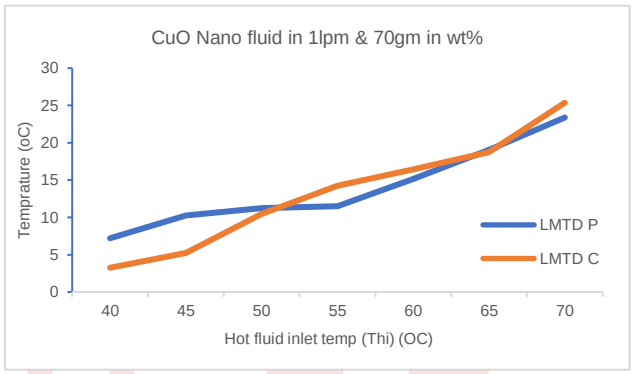

Fig :7 Temperature v/s Hot fluid inlet temperature at fixed mass flow rate 1lpm at 70gm CuO.

In above figure temperature will be maximum in parallel flow arrangement with comparison to counter flow arrangement with minimum loss of energy in 23 % and pressure drop is in maximum in counter flow then in parallel.

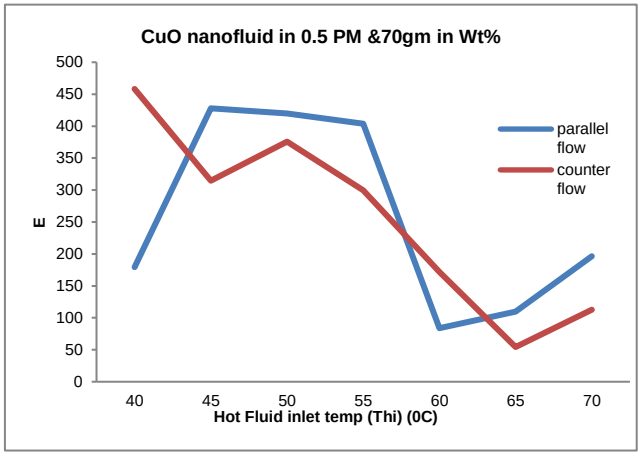

Fig :8 Exergy v/s Hot fluid inlet temperature at fixed mass flow rate.5 lpm at 70gm CuO.

In above figure is observed that the exergy losses in maximum 45^oc and minimum loss 60^0c.in parallel flow arrangement with compression to counter flow.

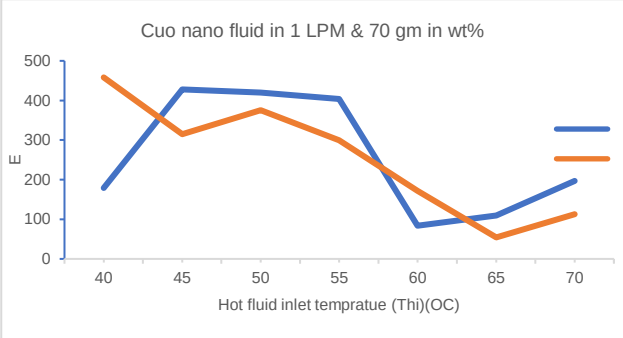

Fig :9 Exergy v/s Hot fluid inlet temperature at fixed mass flow rate in 1 lpm at 70gm CuO.

In above figure is observed that the exergy losses in maximum 42^{o}c and minimum loss 60^{0}c.in parallel flow arrangement with compression to counter flow in fixed in 1lpm in mass flow rate, and weight concentration.

VIII. CONCLUSION

In this study, in order to increase the performance of a plate heat exchanger by using CuO nano particle in different mass flow rate (0.5 to 1 lpm) and different weight concentration.

In thermo physical properties will be more effective in CuO nano fluid with compression to base fluid, the performance of plate heat exchanger at different input heat load was measured in counter flow and parallel flow arrangement. Exergy analysis was performed to find its behaviour in parallel and counter flow arrangement and losses is 17.5% in parallel flow then in counter flow arrangement. Effectiveness is more effective in counter flow arrangement like 58%. In effect of temperature Thi from 40^{o}c to 70^{0}c is more significant on Th_2 when plane cold water is used, as volume % of CuO nano particle in weight basis 70 gm. The initial temperature of hot fluid becomes less or no significant. Exergy analysis was performed to find its behaviour in parallel and counter flow arrangement, exergy loss was found 9.6% more in parallel flow then in counter flow arrangement.

REFERENCES

[1] **V. Kumar, A.K. Tiwari, S.K. Ghosh**, Application of nanofluids in plate heat exchanger: a review, Energy Convers Manage. 105 (2015) 1017–1036.

[2] **A. Wahab, A. Hassan, M.A. Qassim, H.M. Ali, H. Babar, M.U. Sajid**, Solar energy systems potential of nanofluids, J. Mol. Liq. (2019) 289.

[3] **T.R. Shah, H.M. Ali**, Applications of hybrid nanofluids in solar energy, practical limitations and challenges: a critical review, Sol. Energy 183 (2019) 173–203.

[4] **J.J. Michael, S. Iniyan**, Performance analysis of a copper sheet laminated photo- voltaic thermal collector using copper oxide-water nanofluid, Sol. Energy 119 (2015) 439–451.

[5] **N. Mazaheri, M. Bahiraei, H. Abdi Chaghakaboodi, H. Moayedi**, analysing performance of a ribbed triple-tube heat exchanger operated with graphene nanoplatelets nanofluid based on entropy generation and exergy destruction, Int. Commun. Heat Mass Transf. 107 (2019) 55–67.

[6] **P.C. Mukesh Kumar, M. Chandrasekar,** CFD analysis on heat and flow characteristics of double helically coiled tube heat exchanger handling MWCNT/water nanofluids, Heliyon 5 (2019) e02030.

[7] **R.N. Radkar, B.A. Bhanvase, D.P. Barai, S.H. Sonawane**, intensified convective heat transfer using ZnO nanofluids in heat exchanger with helical coiled geometry at constant wall temperature, Mater. Sci. Energy Technol. 2 (2019) 161–170.

[8] **V. Bianco, F. Scarpa, L.A. Tagliafico**, Numerical analysis of the Al 2 O3-water nanofluid forced laminar convection in an asymmetric heated channel for ap-plication in flat plate PV/T collector, Renew. Energy 116 (2018) 9–21.

[9] **D. Huang, Z. Wu, B. Sunden**, Effects of hybrid nanofluid mixture in plate heat exchangers, Exp. Therm. Fluid Sci. 72 (2016) 190–196.

[10] **A. Bhattad, J. Sarkar, P. Ghosh**, Experimentation on effect of particle ratio on hydrothermal performance of plate heat exchanger using hybrid nanofluid, Appl. Therm. Eng. 162 (2019) 11430.

[11] **Kumar Ashish, Dr. Rai Ajeet Kumar, sachan Vivek (2014).** "Experimental Study of heat transfer in a corrugated plate heat exchanger". Department of Mechanical Engineering, SSET, SHIATS-DU, Allahabad (U.P) INDIA-211007. IAEME vol. 5, Issue 9, September (2014), pp. 286-292.

[12] **K.Y. Leong, R. Saidur (2011),** "Modelling of shell and tube heat recovery exchanger operated with nanofluid based coolants" International Journal of Heat and Mass Transfer.

[13] **Lin Chien-Nan, Jang Jiin-Yuh**, **(2002),** "conjugate Heat Transfer and Fluid Flow Analysis in Fin-Tube Heat Exchangers with Wave-Type Vortex Generators", Journal of Enhanced Heat Transfer, Vol.9, PP.123-136."

[14] **L. B. Wang, S. D. Gao and Y. G. Mei, (2002), "**Local and Average Characteristics of Heat / Mass Transfer Over Flat Tube Bank Fin with Four Vortex Generators Per Tube", Transactions of the ASME, Journal of Heat Transfer, Vol.124, pp.546-552.

[15] **B.C. Pak, Y.I. Cho,** Hydrodynamic and heat transfer study of dispersed flu- ids with submicron metallic oxide particles, Exp. Heat Transf. 11 (1998) 151–170.

[16] **Y.M. Xuan, W. Roetzel,** Conceptions for heat transfer correlation of nanofluids, Int. J. Heat Mass Transf. 43 (2000) 3701–3707.

IFERP connecting engineers...developing research
1st International Conference on Future of Engineering 2022

A Deep Transfer Learning-Based Approach to Detect Skin Disease

Md Shariar Kabir[1], Md. Ahasanul Kobir Opy[2], Md Sefatullah[3], Md Parvez Mosaraf[4], Jakia Khanom[5], Kazi Shiam Hossain[6]

[1,2,3,4,5,6] Dallas International University, Texas, USA
E-mail: [1]shariar15-2414@diu.edu.bd, [2]ahasanul15-2427@diu.edu.bd, [3]sefatullah15-2103@diu.edu.bd, [4]parvez15-2348@diu.edu.bd, [5]jakia15-2552@diu.edu.bd, [6]shiam15-2100@diu.edu.bd

Abstract:
Human body can have many types of disease. Some of those is internal & some of those is external. Here, we talk about external disease. Which is generally attacks the skin. Then it is called skin disease. According to who the skin disease rate in Bangladesh reached 1131 or 16% [1]. It is usually caused by seasonal changes, pollution, dirty environment, allergy and lack of skin care. Other diseases can also be caused for this disease. Our research is about all kinds of skin diseases. First, we have collected images of various skin diseases. Then we classified it using transfer learning-based algorithm. Transfer learning is currently a very popular system that is now used in almost every automation technology in the world. Our main objective is to make people aware of their skin diseases very easily. We have used some transfer learning-based algorithm to classify the skin disease. Some algorithm showed us a very good performance. But among all we have adopt MobileNetV2 and its performance. Which is 99%. We have planned to make an android app by using our adopt model where anyone can check their skin disease & confirm about their disease classification.

Keywords:
skin, transfer-learning, classification, prediction, deep-learning

I. INTRODUCTION

If we want to divide the disease in the human body into two parts, then one will be internal disease and the other will be external disease. Internal disease is what we cannot see. They are inside the body. And external disease is what we see, because they are outside the body on the skin. Some of the common skin diseases are: Acne, Atopic, Shingles, Hives, sunburn, Diaper Rash etc. The first mistake we make when we have this type of disease is that we don't understand what category it actually falls under. Then the mistake we make is that we do not pay attention to the disease. What happens after that is that the disease takes a very complicated form. The main reason for this is that we do not understand what disease we actually have. Because not all of us are experienced in this matter. And we don't always have a doctor around us. That's why we ignore small things. And later on, it takes a much more complex shape. In this paper, we our target was to classify all type of skin disease. We have collected skin disease image from reputed valid website. Which is approved by health organization. At first, we have chosen 5 types of common skin disease. Then we have collected the images of these skin disease image from some reputed websites. After collecting all the images, we labeled it. Then we have made 5 classes. After that we pre-processed the dataset. Then we have trained the dataset by using some transfer learning algorithm. After using some algorithm, we have got the best accuracy. Which is 99%. MobileNetV2 have done this.

II. RELATED WORK

Authors [1] have proposed a model that able to detect the skin disease. They have four types of class in their dataset. Eczema, Melanoma, Psoriasis, Healthy skin. They resized the image of the dataset & made the same length in height as well as width. At first, they preprocessed the image then feature

Authors [2] have collected the dataset where seven types of screen disease exist such as Mollusca, Systemic Disease, Seborrheic Keratosis, Nevus, Bullous, Actinic Keratosis, Acne and Rosacea. They have proposed a web application where anyone can able to upload their image then detect their own skin is affected or not. They have used four deep learning algorithm CNN, RESNET152V2, INCEPTION V3, ALEXNET & got the best accuracy 99% from CNN.

Authors [3] have collected data from publicly accessible dermatology repositories. They have used 80% of dataset for training and 20% of dataset for testing. This dataset has seven types of class. They have used MobileNet algorithm & got accuracy 93.6%. After that they have built a mobile application by using deep learning model. Where user can upload their image and detect their disease.

Authors [4] proposed a method and developed a computer view detection system for segmentation and recognizing skin disease. They have predicted the class both manually and automatically. They used Support Vector Machine for detecting malignant and benign tumors and the other classes are detected by manually.

Authors [5] have applied support vector machine & CNN to classify the image. They have collected dataset from Beni-Suef University Hospital, Cairo University Hospital etc. They have total 3000 data. They got the best accuracy from Support Vector Machine.

Authors [6] They have collected data from google. After collecting the dataset, they have classified this by using machine learning algorithm. They have used OpenCV for process the dataset. For implementation they have used Keras Model of Python.

Authors [7] have collected data from google. After that they have used CNN for classification the image. Their training accuracy was 91.74 % and Value accuracy was 87.33 %. They have proposed CNN for it research model.

Authors [8] They have collected data from google. They have total 9 class of image. They used deep learning to classify the image. After using some algorithm, they have adopted MobileNet V2 for their proposed model. But they also tried CNN but got less accuracy as compare to MobileNet V2.

Authors [9] Have collected dataset from Kaggle. The dataset contains total of forty thousand images. They have used total

3 machine learning algorithm. Such as, Support Vector Machine, K-Nearest Neighbor, Ensemble Bagged Tree Algorithm. And also used deep learning algorithm. Such as, VGG16, GoogleNet, ResNet50. After that they have got their best accuracy by using Bagged Tree Ensemble of a machine learning model.

Authors [10] have used CNN to classify the image. After that they also add Keras Sequential API for adding one layer at a time. After that they have got their best accuracy by using CNN. Their accuracy is 93.28 %.

III. METHODOLOGY

In our research, we have tried so many algorithms. But for better performance we have adopt MobileNetV2 algorithm.

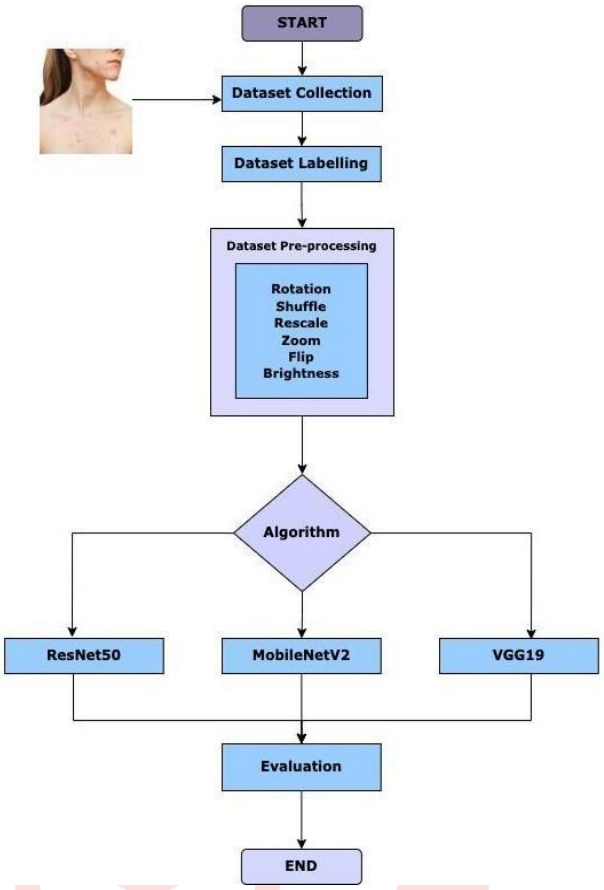

Fig.1 Methodology

Fig.1 shows us the methodology of our process. At first, we have collected data from reputed websites. Then we have labeled the data. After labeling we did some pre-process our dataset because of it was not so much clean. We have done some technique. Such as, Rotation, Shuffle, Rescale, Zoom, Flip, Brightness. Then tried some algorithms. Between some algorithm MobileNetV2 have done the best performance.

IV. DATASET DESCRIPTION

To complete our study, we gathered our dataset from some reputed. We use this data for training our model, validating and testing process. The dataset contains a total number of 772 images about various skin diseases. In our dataset there are five classes such as Acne, Hair Loss, Nail Fungus, Normal and Skin Allergy. Fig shows us the sample of five different types of skin.

Fig 2. Sample of five different states of skin

The dataset is a total of 772 images with five various classes. Acne consists of 108 images, Hair loss contains 126 images, Nail Fungus contains 172 images, Skin Allergy contains 161 images and Normal class contains 205 images. Table shows the total number of simple tests used to train the model and test.

Table 1. Dataset

Classes	Total Data	Training Sample	Testing Sample
Acne	108	82	26
Hair Loss	126	95	31
Nail Fungus	172	140	32
Skin Allergy	161	128	33
Normal	205	156	49
Total	772	601	171

V. ALGORITHM DESCRIPTION

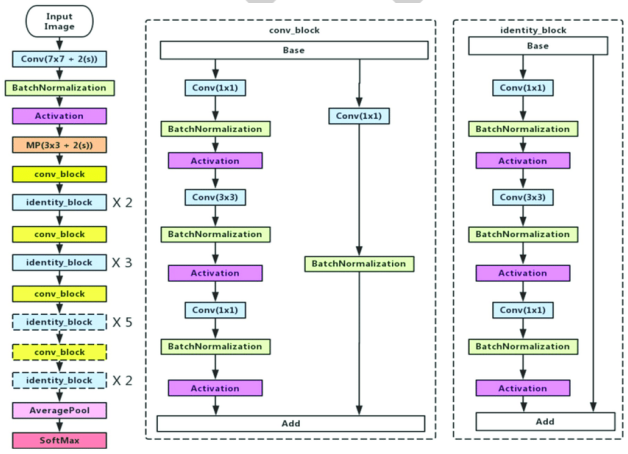

Fig.3 Architecture of ResNet50 Algorithm

In our paper, we used ResNet-50 model. It's known as a convolutional neural network (CNN) and it consists of 50 layers [12]. It is a pretrained model that was trained on over a million photos from their ImageNet database. Almost all ResNet models included double or triple layers skips with non-linearities and batch normalization. It's called ResNet50 because it can work with 50 neural network layers.

Evaluation of ResNet-50 model:

$$H_l = ReLU(b_l * f_l(H_{l-1}) + id(H_{l-1})).$$

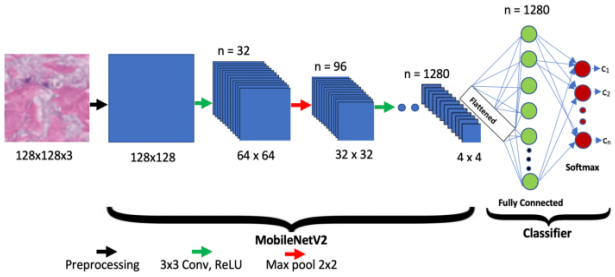

Fig.4 Architecture of MobileNetV2 Algorithm

MobileNetv2 is also a convolutional neural network, and it consists of 53 layers [11]. This algorithm aims to perform better on a mobile device. It has also pretrained network that can classify images into 1000 object classification. It is known as a powerful feature extractor that can recognize and segment objects. It is an open source model and these mobile-first computer vision models were created for TensorFlow and are optimized for accuracy.

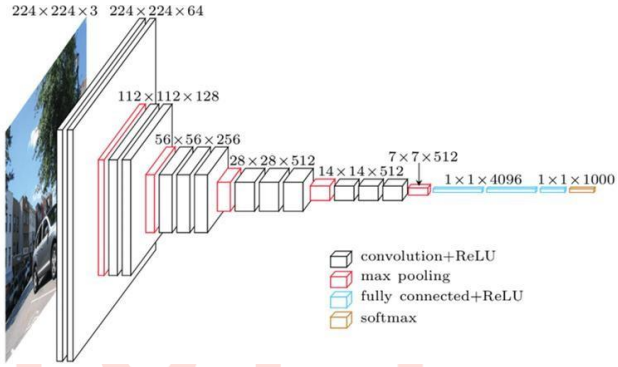

Fig.4 Architecture of VGG19

We already know that VGG19 is one of the common convolutional neural network that has 19 layers [13]. A pre - trained model variant of the network built over than a million images from the ImageNet database can be loaded. The pretrained network can categorize images into 1000 different object classes. The primary goal of the VGG network was to achieve the ILSVRC matching challenge.

VI. FEATURE EXTRACTION

In our research, the MobileNetV2 algorithm has been used to classify all kinds of features of the dataset. MobileNetV2 have two types of blocks in this algorithm. First block is residual block. Which has 1 stride. Second block have 2 strides. Which is used for downsizing. All blocks have 3 different kinds of layer. The first layer is 1 * 1 convolution with ReLU6. The second layer is depthwise convolution. And the last layer is also 1 * 1 convolution but it has no linearity. In our implementation the ReLU6 function helps us to introduce all the hidden layers. The size of the target model was (224,224). The MobileNetV2 did some

fewer losses. Which is 0.009%. But the VGG19 & the ResNet50 did more losses than MobileNetV2. Which are accordingly 0.14% & 0.03%.

Input	Operator	t	c	n	s
$224^2 \times 3$	conv2d	-	32	1	2
$112^2 \times 32$	bottleneck	1	16	1	1
$112^2 \times 16$	bottleneck	6	24	2	2
$56^2 \times 24$	bottleneck	6	32	3	2
$28^2 \times 32$	bottleneck	6	64	4	2
$14^2 \times 64$	bottleneck	6	96	3	1
$14^2 \times 96$	bottleneck	6	160	3	2
$7^2 \times 160$	bottleneck	6	320	1	1
$7^2 \times 320$	conv2d 1x1	-	1280	1	1
$7^2 \times 1280$	avgpool 7x7	-	-	1	-
$1 \times 1 \times 1280$	conv2d 1x1	-	k	-	

Fig.5 Structure of MobileNetV2

VII. RESULT AND DISCUSSION

In this paper, we have used 3 models to detect skin disease. In these 3 models we have got our best accuracy by using MobileNetV2 algorithm. Which is 99%. We have also tried another algorithm but got less accuracy. We have got least accuracy by using VGG19 algorithm. Which is 87%. ResNet50 also gave us good accuracy which is 97%.

Table.2 Performance

Model Name	Accuracy	Lost Function
VGG19	87%	0.14
ResNet50	97%	0.03
MobileNetV2	99%	0.009

VIII. ERROR ANALYSIS

Fig.6 Training Loss & Validation Accuracy

Fig No-6 shows the training loss and accuracy estimate. The following figure tells us that, The MobileNetV2 algorithm training loss and accuracy with the graph chart. On the figure the blue line stands for training accuracy and the orange line is for training loss accuracy. On the other hand, the orange line is for train loss.

Precision:

Precision is the number of accurate class predictions that are truly positive class predictions. Basically, Precision is one evaluation of a machine learning model's efficiency and it can measure the accuracy of a positive prediction provided by the algorithm. The equation of precision is –

$$\text{Precision} = \frac{TP}{TP + FP}$$

Recall:

The recall is derived as the proportion of Positive cases that had been actually identified as Positive to that same total number of samples. Recall can find out the actual positive values.The equation of recall given below-

$$\text{Recall} = \frac{TP}{TP + FN}$$

F1 score:

The harmonic mean of accuracy and recall is used to get the F1 score. In mathematical meaning f1 score is found by the average ratio of precision and recall values. The equation that can derived the f1 score is-

$$\text{F1 score} = 2 * \frac{Precision * Recall}{Precision + Recall}$$

Table.3 Precision, Recall, F1 Score

Classes	Acne	Hairloss	Nail Fungus	Normal	Skin Allergy
Precision	0.96	1.00	1.00	1.00	1.00
Recall	1.00	1.00	1.00	1.00	0.97
F1 Score	0.98	1.00	1.00	1.00	0.98

IX. CONCLUSION

Our research was about skin disease. We have found many interesting results in this study. Many people in Bangladesh, who do not know about this disease. They do not give importance to it. They just ignore it. As a result, it takes on huge terrifying forms. Our aim was to make every person of Bangladesh aware of this disease. That's why we started this research. At first, we have selected some common skin disease. After that we have collected the images of skin disease from internet. Then we did some pre-processing & tried to classify. We have used transfer learning-based algorithm to classify this. After tried some of algorithm we have found that MobileNetV2 performs better. Then we have adopted this algorithm. Our accuracy is 99%. Which is very amazing result. Because our dataset was very mess. After getting the result we have made a model.

In future, we will make an android app. By using our app anyone can detect their skin disease very easily & free. After detecting the disease, they will also able to know about this disease. Because we will also provide all kind of information about every skin disease in our mobile app. We think it will be very helpful for everyone.

REFERENCES

[1] N. S. A. ALEnezi, "A Method Of Skin Disease Detection Using Image Processing And," ScienceDirect, p. 92, 2019.

[2] D. V. M. N. N. S. ,. B. T. Swapna1, "Detection and Classification of Skin diseases," The International journal of analytical and experimental modal analysis, vol. 13, no. 8, pp. 1096-1101, 2021.

[3] C. P. J. W. A. J. A. J. S. C. M. Jessica Velasco1, "A Smartphone-Based Skin Disease Classification Using MobileNet CNN," International Journal of Advanced Trends in Computer Science and Engineering, vol. 8, no. 5, pp. 2632-2637, 2019.

[4] 1. X. G. a. Y. W. Xin Xiong, "Modeling of Human Skin by the Use of Deep Learning," Hindaw, vol. 2021, p. 11, 2021.

[5] R. K. 2. A. H. 3. P. C. 4. Ahmed A. Elngar 1, "Intelligent System for Skin Disease Prediction using Machine," Journal of Physics: Conference Series, vol. 9, no. 13, 2021.

[6] 2. M. 3. S. 4. V. A. Srushti, "Skin Disease Detection Using Deep Learning," International Journal for Research Trends and Innovation, vol. 5, no. 8, pp. 12-16, 2020.

[7] V. P. M. S. S. S. K. Sruthi Chintalapudi1, "SKIN DISEASE DETECTION USING DEEP LEARNING," International Research Journal of Engineering and Technology (IRJET), vol. 8, no. 4, pp. 3152-3158, 2021.

[8] H. M. 2. ,. S. S. 3. ,. A. M. A. 4. ,. Pravin R. Kshirsagar 1, "Deep Learning Approaches for Prognosis of Automated," MDPI, pp. 2-16, 2022.

[9] P. S. K. B. P. A. B. D. S. P. Payal Bose, "Skin Disease Detection: Machine Learning vs Deep Learning," Preprints, vol. 13, no. 9, 2021.

[10] P. S. Y. O. N. P. D. S. B. Kritika Sujay Rao, "Skin Disease Detection using Machine Learning," International Journal of Engineering Research & Technology (IJER, vol. 9, no. 3, pp. 64-68, 2020.

[11] "ResearchGate," [Online]. Available: https://www.researchgate.net/figure/The-proposed-MobileN etV2-network-architecture_fig1_350152088.

[12] "ResearchGate," [Online]. Available: https://www.researchgate.net/figure/Left-ResNet50-architect ure-Blocks-with-dotted-line-represents-modules-that-might- be_fig3_331364877.

[13] "ResearchGate," [Online]. Available: https://www.researchgate.net/figure/Details-of-the-19-layers -of-VGG19-network-21-used-for-feature-extraction_fig3_33 4388209.

IFERP connecting engineers...developing research
1st International Conference on Future of Engineering 2022

Height of Highway Embankment for Tolerable Residual Settlement of Loose Cohesionless Subsoil Overlain by Stronger Soil

Sharifullah Ahmed P.Eng

[1] Ph. D. Scholar (Geotechnical), Department of Civil Engineering, Bangladesh University of Engineering and Technology (BUET), Dhaka, Bangladesh & Sr. Geotechnical Engineer, Soil Investigation Division, Bangladesh Highway Research Laboratory (BRRL), Mirpur, Dhaka, Bangladesh

Abstract:
Residual settlement of cohesionless or non-plastic soil of different strength underlying highway embankment overlain by stronger soil layer is studied. A parametric study is carried out for different heights of embankment and different ESAL factors. The sum of elastic settlements of cohesionless subsoil due to axle induced stress and due to self-weight of pavement layers is termed as the residual settlement. The values of residual settlement (S_r) for different heights of road embankment (H_e) are obtained and presented as design charts for different SPT Value (N_{60}) and different ESAL factors. For rigid pavement and flexible pavement in approach to bridge or culvert, the tolerable limit of residual settlement is 0.100m. Tolerables limit is taken as 0.200m for flexible pavement in general sections of highway except approach to bridge or culvert. A simplified guideline is developed for design of highway embankment underlain by very loose to loose cohesionless subsoil overlain by stronger soil layer for limiting value of the residual settlement. In the current research study range of ESAL factor is 1-10 and range of SPT value (N_{60}) is 1-10. That is found that, ground improvement is not required if the overlying stronger layer is minimum 1.5m for general road section of flexible pavement except bridge or culvert approach. For rigid pavement or flexible pavement in bridge or culvert approach thickness of stronger layer to be 4.0m to avoid ground improvement. A guideline is prepared including tables and charts to obtain minimum allowable height of highway embankment to limit the residual settlement with in mentioned tolerable limit. Allowable values of the embankment height including pavement layers (H_e) are obtained corresponding to tolerable or limiting level of the residual settlement of loose subsoil for different values of SPT (N_{60}), thickness of stronger layer (d) and ESAL factor. The developed guideline is issued to be used in assessment of the necessity of ground improvement in case of cohesionless subsoil underlying highway embankment overlain by stronger subsoil layer to ensure limiting level of residual settlement. The ground improvement is only to be required if the residual settlement of subsoil is more than tolerable limit.

Keywords:
Axle Pressure, Equivalent Single Axle Load (ESAL), Ground Improvement, Highway Embankment, Tolerable Residual Settlement

I. INTRODUCTION

Construction of Highway Embankment in Bangladesh may be proceeded over loose cohesionless natural subsoil overlain by stronger soil layer. Often ground improvement is provided to strengthen the loose cohesionless subsoil underlying the highway embankment. However, the ground improvement not to be mandatory when the residual settlement of subsoil is not more than tolerable limit. This research study is done to prepare a guideline to identify the necessity of ground improvement for proposed highway embankment underlain by very loose to loose cohesionless soil considering limiting residual settlement.

II. AXLE LOAD ON SUBSOIL

The stress on pavement of highway embankment is axle load of transport vehicle. And the stresses on subsoil underlying the embankment is both of the transferred portion of axle load and self-weight of the embankment including pavement.

According to [1], in national highways in the Bangladesh, the value of the *ESAL factor* for dual tyre single axle is found larger than 30. Considering this over loading and the future enlargement possibility of acceptable *ESAL* limit, the *ESAL factor*

up to 10 are considered for calculation of elastic settlement of loose subsoil in current study.

Actual Axle Load (kN), W_a = (*ESAL Factor*).W_r (1)

Where, *ESAL* is the Equivalent Standard Axle Load and W_r is Standard axle load (80kN) for dual tyre single axle.

III. DISTRIBUTION OF AXLE LOAD

As per 2 vertical to 1 horizontal spreading of stress [2], a particular wheel load reduced to a larger area at lower depth. The reduced stress at a specific depth z,

$$\sigma_z = \frac{\sigma_0 BL}{(B+z)(L+z)} \quad (2)$$

The current study the concentrated load on pavement, $\sigma_0 BL = (W_a/2)BL = W_a/2$ (3)

Considering interface or overlap of pressure from two wheel in an axle [3],

$$\sigma_z = \frac{W_a}{(B+H_e)(L+H_e)} \quad (4)$$

where, W_a is axle load, B is width of tyre to pavement contact area, L is length of tyre to pavement contact area and H_e is total height of embankment above natural ground level including pavement layers.

In this case according to Equation (4) pressure on loose granular subsoil overlain by below strong soil of thickness d due to pressure from two wheel in an axle,

$$\sigma_z = \frac{W_a}{(B+H_e+d)(L+H_e+d)} \quad (5)$$

Where, d is the thickness of stronger soil overlying loose granular soil.

The contact tyre area of dual tyre single axle for HS 20-44 Truck is a single rectangle having width, B= 510mm and length, L= 250mm [4][5] are used in calculation of axle stress in current study.

IV. IV. SETTLEMENT OF LOOSE SUBSOIL

As suggested by Bowles [6], Elastic Settlement of loose granular soil due to Axle Load (for $B + H_e > 1.22\text{m}$),

$$S_e\,(\text{m}) = \frac{0.002\sigma_z}{N_{60}F_d}\left[\frac{(B+H_e+d)}{(B+H_e+d)+0.3}\right]^2 \quad (6)$$

F_d =1+0.33(D_f+d)/(B+H_e+d) (7)

where, H_e is the height of highway embankment including embankment fill and thickness of pavement layers, σ_z is reduced axle pressure on subsoil , d is the depth of stronger soil overlying loose subsoil, N_{60} is SPT value at immediate top layer just below the embankment, B+H_e is width of distributed wheel load at subsoil level and D_f is the depth of foundation below existing ground level=0.

Similarly, Elastic Settlement of granular soil due to self-weight of pavement layers for $B + H_e - H_p + d > 1.22\text{m}$,

$$S_e\,(\text{m}) = \frac{0.002H_p\gamma_e}{N_{60}F_d}\left[\frac{(B_t+H_e-H_p+d)}{(B_t+H_e-H_p+d)+0.3}\right]^2 \quad (8)$$

and F_d =1+0.33D_f/(B_t+H_e−H_p + d)=1 (9)

Where, H_p is thickness of pavement layers, γ_e is average unit weight of pavement layers(kN/m^3).

V. RESIDUAL SETTLEMENT

Residual Settlement is the portion of total settlement which to be occurred after construction of road pavement overlying embankment fill.

The Residual Settlement, S_r=S_{e1} +S_{e2} (10)

Where, S_{e1} is the Elastic Settlement of loose subsoil below embankment due to reduced axle pressure (σ_z) obtained from Equation (6) and S_{e2} is Elastic Settlement of loose subsoil below embankment due to self-weight of pavement layers ($H_p\gamma_e$) obtained from Equation (8).

As per [7] for rigid pavement and flexible pavement at approach to bridge or culvert the tolerable limit of residual settlement is 0.100m and the tolerable limit of residual settlement is taken as 0.200mm for flexible pavement in general road sections except bridge or culvert approach.

VI. ANALYSIS RESULT

A. Residual Settlement Charts

As per [8] the range of width of carriage way of road in Bangladesh is 3.0m to 22.0m. Then the range of corresponding crest width to be 5.0m to 30.0m. For 4 Lane highways and expressways the range of crest width is 30m-40m. In this study, the range of crest width is used 5m to 50m.

The range of embankment height including thickness of pavement layers is 1m to 12m and the side slope of is 1V:2H are used in current analysis. Thickness of pavement layers (H_p) is taken 1.5m for analysis of residual settlement.

As observed through current study, the change of Residual Settlement (S_r) with change of B_t between 5m to 50m is not insignificant. Among small differences the Highest value of S_r is found for the highest value of B_t=50m. For this consideration, the residual settlement charts are prepared for B_t=50m.

However, the variation of S_r with N_{60} is significant. Considering this variation, separate residual

settlement chart is prepared for SPT values N_{60}=1, 2 and 3. Value of average bulk unit weight of pavement layers (γ_{ep}) is 19.5kN/m^3 considered in all cases of analysis.

Residual settlement, S_r (m) for different values of N_{60} and d are obtained from calculations and are presented graphically in Figure 1.0 to Figure 14.0 for different values of Embankment Height (H_e) and *ESAL* factor.

Residual settlement is depends on transfer of stresses to loose granular subsoil. For more height of highway embankment and more thickness of stronger layer the reduction of stresses at loose subsoil is more. For more reduction of stresses, the residual settlement is also reduced.

Hence, basic finding of current analysis is – in residual settlement charts presented in Figure 1.0 to Figure 14.0, this is observed that, the residual settlement (S_r) is decreases with increase of embankment height (H_e) and stronger layer thickness (d). For a particular value of N_{60} the residual settlement value (S_r) may be obtained from corresponding chart among those Figures for different values of Embankment height (H_e), stronger layer thickness (d), N_{60} and *ESAL* factor for B_t=50m. Same value may be used for B_t less than 50m.

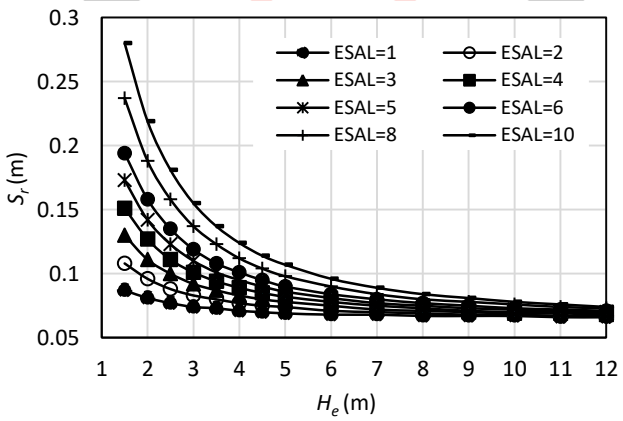

Figure 1.0: H_e Vs S_r for for N_{60}=1, d=0.45m

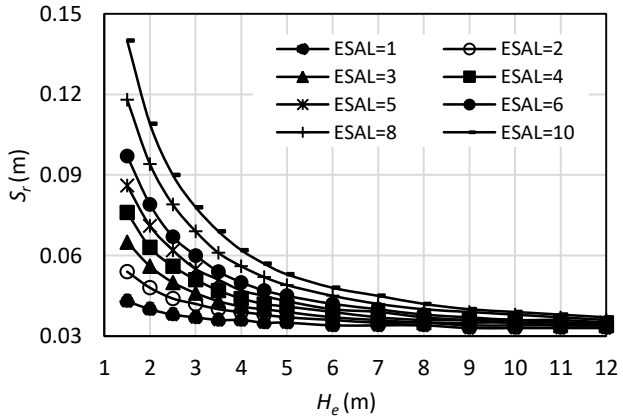

Figure 2.0: H_e Vs S_r for for N_{60}=2, d=0.45m

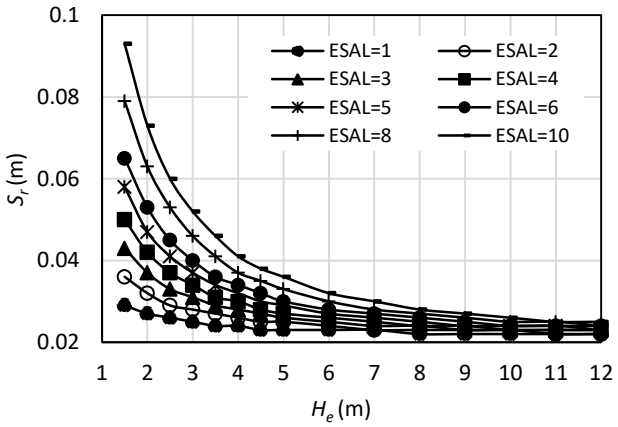

Figure 3.0: H_e Vs S_r for for N_{60}=3, d=0.45m

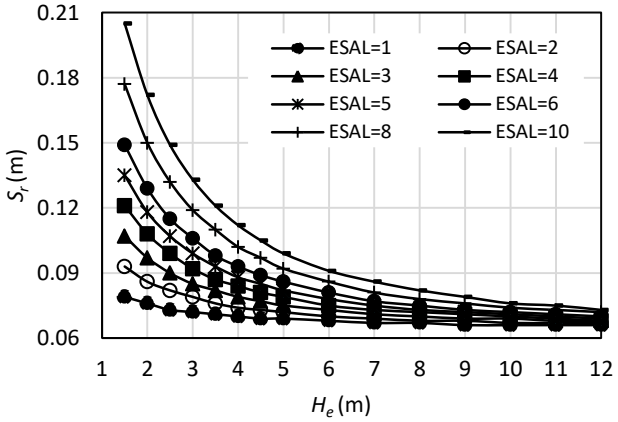

Figure 4.0: H_e Vs S_r for for N_{60}=1, d=1.0m

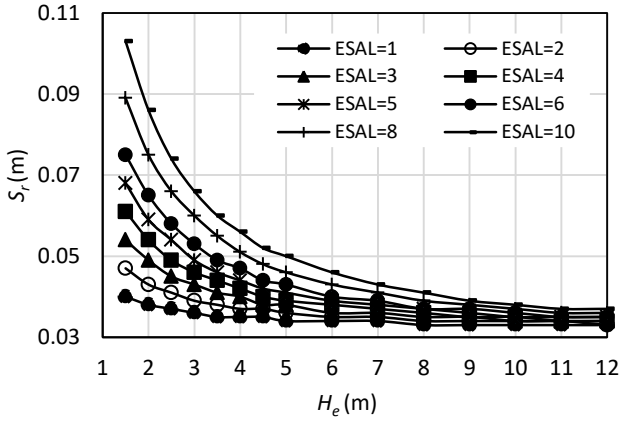

Figure 5.0: H_e Vs S_r for for N_{60}=2, d=1.0m

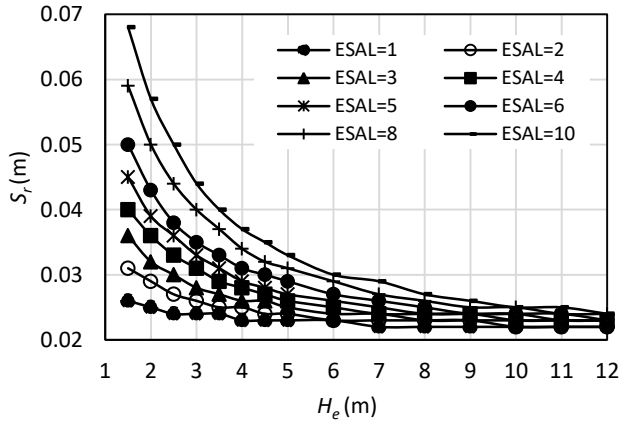

Figure 6.0: H_e Vs S_r for for N_{60}=3, d=1.0m

 ISBN: 978-93-92105-22-7

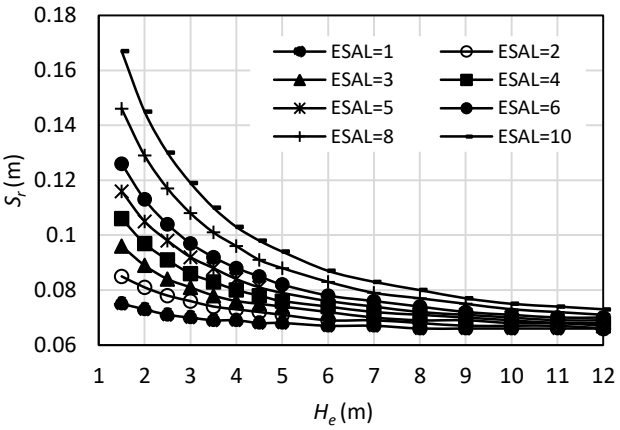

Figure 7.0: H_e Vs S_r for for N_{60}=1, d=1.5m

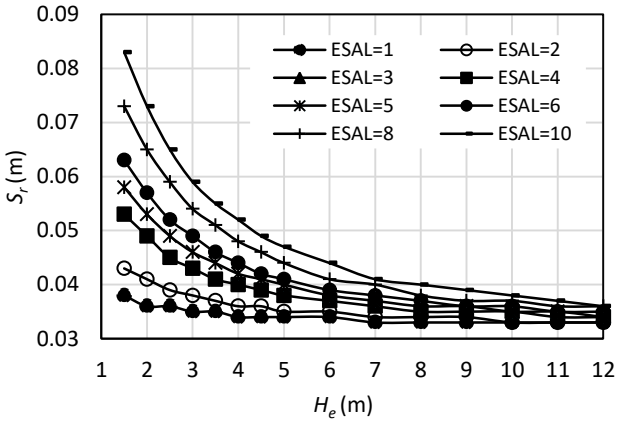

Figure 8.0: H_e Vs S_r for for N_{60}=2, d=1.5m

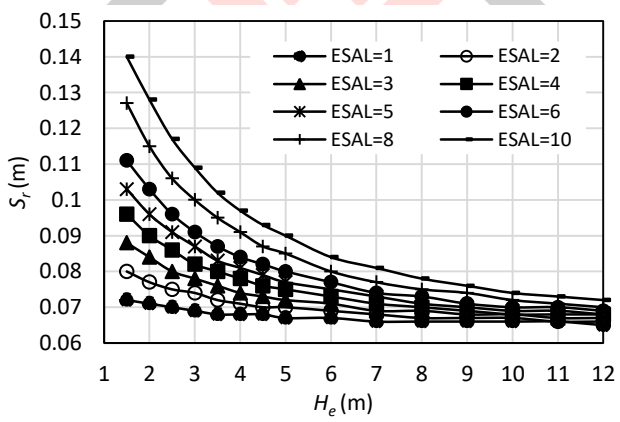

Figure 9.0: H_e Vs S_r for for N_{60}=1, d=2.0m

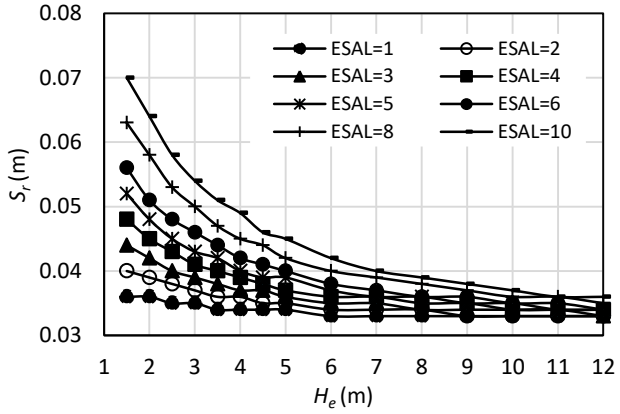

Figure 10.0: H_e Vs S_r for for N_{60}=2, d=2.0m

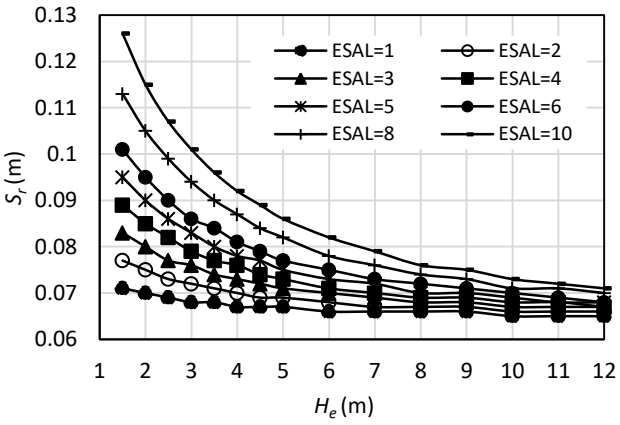

Figure 11.0: H_e Vs S_r for for N_{60}=1, d=2.5m

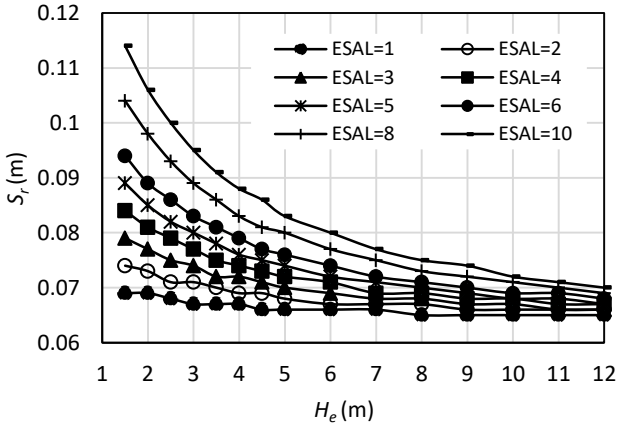

Figure 12.0: H_e Vs S_r for for N_{60}=1, d=3.0m

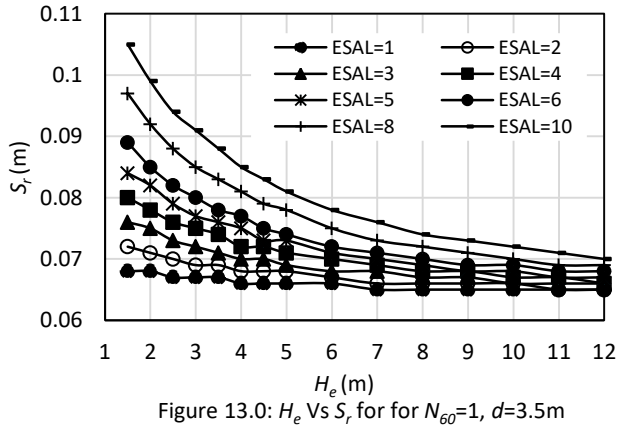

Figure 13.0: H_e Vs S_r for for N_{60}=1, d=3.5m

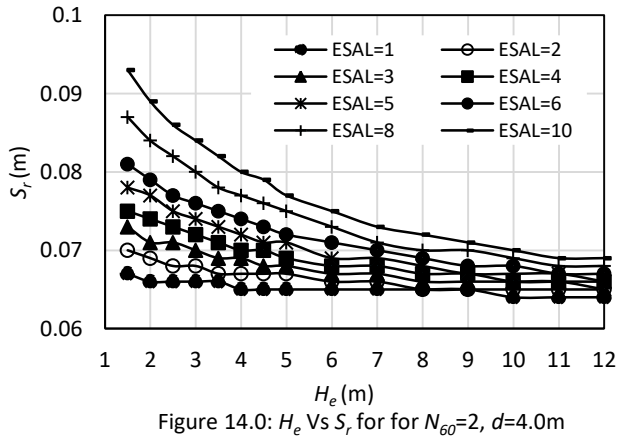

Figure 14.0: H_e Vs S_r for for N_{60}=2, d=4.0m

 ISBN: 978-93-92105-22-7

B. Guideline for Tolerable S_r

Minimum allowable values of embankment height to satisfy residual settlement S_r≤0.100m and S_r≤0.200m are obtained from residual settlement charts presented in Figure 1.0 to 14.0 and are tabulated in Table 1 to Table 4 for B_t=50m. For particular values of N_{60} , d and $ESAL$ factor the minimum value of H_e not to be less than the tabulated value of H_e in Table 1, 2, 3 and 4 to limit the residual settlement at 0.100m and 0.200m. These tables may be used for crest width of highway embankment≤50m. The same guideline is represented as Design Charts in Figure 8.0 and Figure 9.0.

Minimum allowable value of embankment height to satisfy residual settlement, S_r≤0.100m is termed as $H_{e,0.1}$ and minimum allowable value of embankment height to satisfy residual settlement, S_r≤0.200m is termed as $H_{e,0.2}$.Values of $H_{e,0.1}$ and $H_{e,0.2}$ for rigid pavement or flexible pavement at bridge approach and flexible pavement in general road sections are presented in Figure 15.0 to Figure 18.0 successively for various values of SPT (N_{60}).

The empirical relationship for minimum allowable height of Highway Embankment overlying loose subsoil to satisfy S_r≤0.100m or S_r≤0.200m is obtained from 2 order polynomial trend line of Figure 15.0 to Figure 18.0. This empirical relationship is expressed by equation (11) –

$$H_{e,0.1} \text{ or } H_{e,0.2} = a(ESAL)^2 + b(ESAL) + c \qquad (11)$$

In equation (11) the coefficients a, b & c are to be used as presented in Table 5.

Table 1 Minimum allowable height of embankment to satisfy S_r≤0.100m for rigid pavement and flexible pavement in bridge approach underlain by loose granular soil at 0.45m-1.0m below ground surface (d=0.45m to 1.0m) for $ESAL$ factor=1-10 and B_t=50m is termed as $H_{e,0.1}$

SPT	Minimum allowable height of embankment to satisfy S_r≤0.100m for B_t=50m is termed as $H_{e,0.1}$							
	ESAL =1	*ESAL* =2	*ESAL* =3	*ESAL* =4	*ESAL* =5	*ESAL* =6	*ESAL* =8	*ESAL* =10
N_{60}=1 (d=0.45m)	0.5	1.4	2.2	2.9	3.48	4	4.83	5.64
N_{60}=2 (d=0.45m)	0.01	0.01	0.01	0.1	0.5	1	1.82	2.3
N_{60}≥3 (d=0.45m)	No ground Improvement Required							
N_{60}=1 (d=1.0m)	0.3	1	1.7	2.3	2.85	3.38	4.2	4.92
N_{60}=2 (d=1.0m)	0.01	0.01	0.01	0.01	0.05	0.33	1	1.52
N_{60}≥3 (d=1.0m)	No ground Improvement Required							

Table 2 Minimum allowable height of embankment to satisfy S_r≤0.200m for flexible pavement in general road section except bridge/culvert approach underlain by loose granular soil at 0.45m-1.0m below ground surface (d=0.45m to 1.0m) for $ESAL$ factor=1-10 and B_t=50m is termed as $H_{e,0.2}$

SPT	Minimum allowable height of embankment to satisfy S_r≤0.200m for B_t=50m is termed as $H_{e,0.2}$							
	ESAL =1	*ESAL* =2	*ESAL* =3	*ESAL* =4	*ESAL* =5	*ESAL* =6	*ESAL* =8	*ESAL* =10
N_{60}=1 (d=0.45m)	0.01	0.01	0.1	0.5	1	1.4	1.88	2.16
N_{60}≥2 (d=0.45m)	No ground Improvement Required							
N_{60}=1 (d=1.0m)	0.01	0.01	0.01	0.01	0.1	0.5	1.1	1.54
N_{60}≥2 (d≥1.0m)	No ground Improvement Required							

Table 3 Minimum allowable height of embankment to satisfy S_r≤0.100m for rigid pavement and flexible pavement in bridge approach underlain by loose granular soil at 1.5m-2.0m below ground surface (d=1.5m to 2.0m) for $ESAL$ factor=1-10 and B_t=50m is termed as $H_{e,0.1.}$

SPT	Minimum allowable height of embankment to satisfy $S_r \leq 0.100$m for B_t=50m is termed as $H_{e,0.1}$							
	ESAL =1	*ESAL* =2	*ESAL* =3	*ESAL* =4	*ESAL* =5	*ESAL* =6	*ESAL* =8	*ESAL* =10
N_{60}=1 (*d*=1.5m)	0.5	1	1.4	1.83	2.36	2.79	3.6	4.3
N_{60}=2 (*d*=1.5m)	0.01	0.01	0.01	0.5	1	1.4	1.83	2.24
$N_{60}\geq 3$ (*d*=1.5m)	No ground Improvement Required							
N_{60}=1 (*d*=2.0m)	0.01	0.5	1	1.4	1.71	2.21	3	3.7
$N_{60}\geq 2$ (*d*=2.0m)	No ground Improvement Required							
d≥2.0m	No ground Improvement Required							

Using this equation the minimum allowable height of Highway Embankment to be obtained for a particular *ESAL* factor and SPT value N_{60}.

If the height of proposed Highway Embankment is less than $H_{e,0.1}$ in case of rigid pavement and flexible pavement in approach to bridge or culvert then Ground Improvement shall be required.

Similarly, if the height of proposed Highway Embankment is less than $H_{e,0.2}$ in case of flexible pavement in general road sections except bridge or culvert then Ground Improvement shall be required.

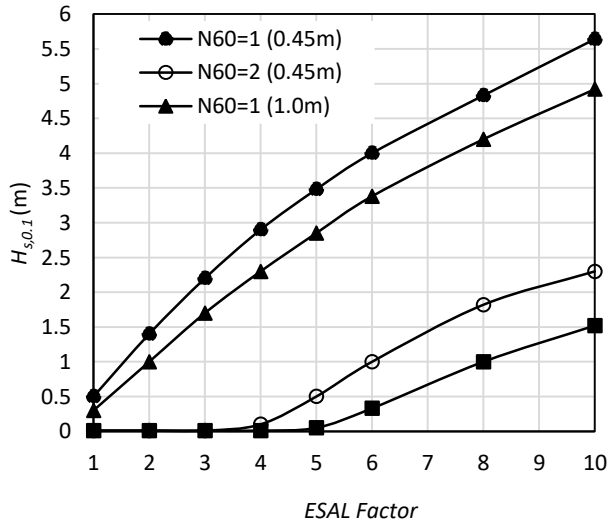

Figure 15.0: $H_{s,0.1}$ Vs *ESAL Factor* for *d*=0.45-1.0m

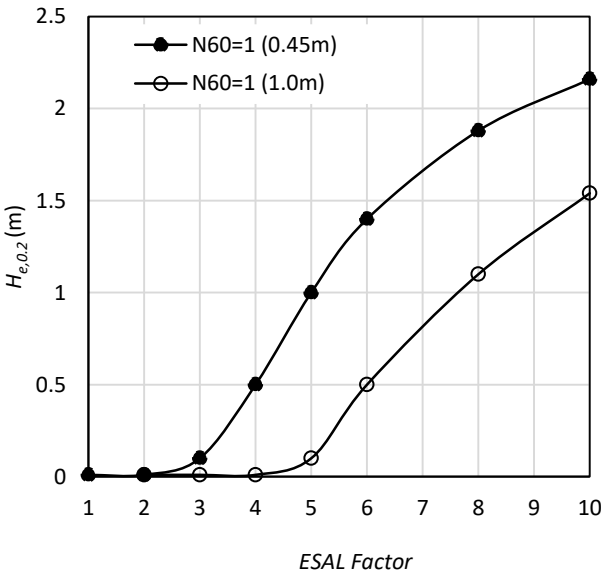

Figure 16.0: $H_{s,0.2}$ Vs *ESAL Factor* for *d*=0.45-1.0m

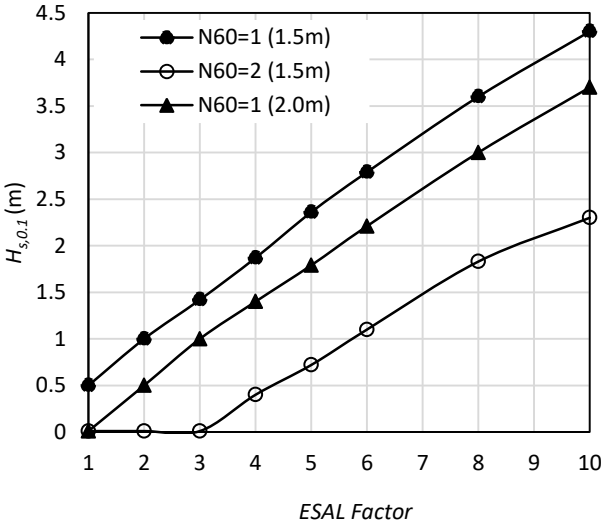

Figure 17.0: $H_{e,0.1}$ Vs *ESAL Factor* for *d*=1.5-2.0m

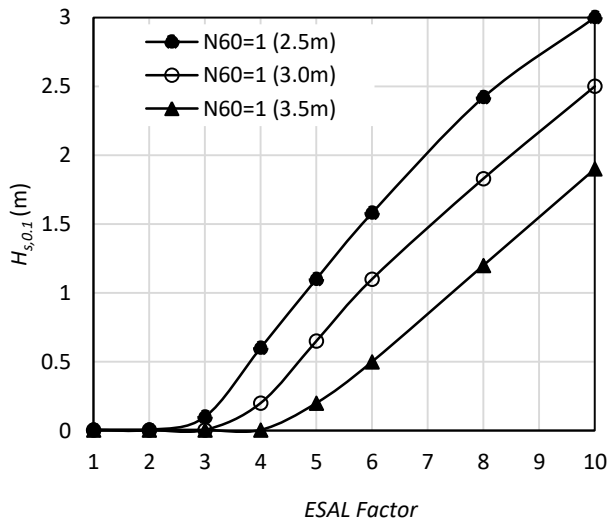

Figure 18.0: $H_{e,0.1}$ Vs *ESAL Factor* for *d*=2.5-3.5m

Table 4 Minimum allowable height of embankment to satisfy $S_r \leq 0.200$m for rigid pavement and flexible pavement in bridge approach underlain by loose granular soil at 1.5m-2.0m below ground surface (*d*=1.5m to 2.0m) for *ESAL* factor=1-10 and B_t=50m is termed as $H_{e,0.2}$

SPT≥1	Minimum height of embankment to satisfy $S_r \leq 0.200$m for B_t=50m is termed as $H_{e,0.2}$
	ESAL =1 to10
d≥1.5m	No ground Improvement Required

Table 5 Value of coefficients a, b & c

S_r	H_e	Ranges of parameter		*a*	*b*	c	Minimum R^2
≤0.100m	$H_{e,0.1}$	*d*=0.45	N_{60}=1	-0.03	0.879	-0.189	0.998
			N_{60}=2	-0.038	0.945	-3.26	
			N_{60}≥3	Ground. Imp. Not Required			
		d=1.0m	N_{60}=1	-0.025	0.787	-0.455	0.999
			N_{60}=2	-0.018	0.597	-2.58	
			N_{60}≥3	Ground. Imp. Not Required			
		d=1.5m	N_{60}=1	-0.034	0.931	-0.339	0.997
			N_{60}=2	-0.025	0.731	-2.463	
			N_{60}≥3	Ground. Imp. Not Required			
		d=2.0m	N_{60}=1	-0.025	0.789	-0.462	0.998
			N_{60}=2	-0.008	0.42	-1.868	
			N_{60}≥3	Ground. Imp. Not Required			
		d=2.5m	N_{60}=1	-0.02	0.687	-1.801	0.999
			N_{60}≥2	Ground. Imp. Not Required			
		d=3.0m	N_{60}=1	-0.014	0.582	-1.897	0.999
			N_{60}≥2	Ground. Imp. Not Required			
		d=3.5m	N_{60}=1	-0.004	0.27	-1.28	0.999
			N_{60}≥2	Ground. Imp. Not Required			
		d≥4.0m	Ground. Imp. Not Required				
≤0.200m	$H_{e,0.2}$	*d*=0.45	N_{60}=1	-0.039	0.817	-2.127	0.998
			N_{60}≥2	Gr. Imp. Not Required			
		d=1.0m	N_{60}=1	-0.023	0.643	-2.515	0.999
			N_{60}≥2	Gr. Imp. Not Required			
		d=1.5m	N_{60}=1	-0.033	0.729	-1.823	0.997
			N_{60}≥2	Gr. Imp. Not Required			
		d=2.0m	N_{60}=1	-0.001	0.289	-1.197	0.986
			N_{60}≥2	Gr. Imp. Not Required			
		d≥2.5m	Ground. Imp. Not Required				

VII. CONCLUSION

The sum of Elastic Settlement due to the stress induced by reduced axle pressure and due to self-weight of pavement layers those to be occurred after construction is considered as the Residual Settlement of loose subsoil underlying the highway embankment overlain by stronger soil layer. The variation of Residual Settlement with change of crest width is not significant and considering this fact, the residual settlement charts and guideline for tolerable

Residual Settlement were prepared for 50m crest width. Those charts and guideline prepared for the range of SPT value (N_{60}) and *ESAL* Factor of 1-10. Same value of Residual Settlement may be used for embankment crest width less than 50m. In all cases at least 1.5m height of embankment (H_e) is to be considered.

In case of stronger layer thickness, *d*=0.45m-2.0m for N_{60} greater than 2, no Ground Improvement to be necessary if *ESAL* factor is not more than 10 for rigid pavement and flexible pavement in bridge or culvert approach. If N_{60} is 2 or less the prepared guideline to be used to identify the necessity of Ground Improvement to keep residual settlement within tolerable limit if *d*=0.45m-3.5m for rigid pavement and flexible pavement in bridge or culvert approach. For stronger layer thickness, *d*=2.5m-3.5m the same guideline to be used for N_{60} greater than 1 instead of 2. On the other hand, if *d* is 4.0m or greater and if *ESAL* factor is not more than 10 no ground improvement to be necessary for rigid pavement and flexible pavement in bridge or culvert approach even for N_{60} =1.

In case of stronger layer thickness, *d*=0.45m-2.0m for N_{60} greater than 1, no Ground Improvement to be necessary if *ESAL* factor is not more than 10 for flexible pavement except bridge or culvert approach. If *d* is 2.5m or greater and *ESAL* factor is not more than 10 no ground improvement to be necessary even for N_{60} = 1 in general road sections. If N_{60} is 1 the prepared guideline to be used to identify the necessity of Ground Improvement to keep residual settlement within tolerable limit if *d*=0.45m-2.0m for flexible pavement except bridge or culvert approach.

A guideline for satisfying tolerable limit of residual settlement is prepared in the forms of tables, figures and empirical equations for different value of stronger layer thickness (*d*), SPT (N_{60}) and *ESAL* factor. In design or assessment of highway embankment the ground improvement to be required if the height of embankment (H_e) is less than $H_{e,0.1}$ in case of rigid pavement and flexible pavement in approach to bridge or culvert or less than $H_{e,0.2}$ for flexible pavement in general road sections except bridge or culvert approach.

ACKNOWLEDGEMENT

The author acknowledged the support of the authority and RHD personal of Bangladesh Road Research Laboratory (BRRL), Mirpur, Dhaka, Bangladesh.

REFERENCES

[1] Road Master Plan (2009), Roads and Highways Division (RHD), Bangladesh, Ch. 3.

[2] Holtz, R. D., and Kovacs, W. D. (1981), “An Introduction to Geotechnical Engineering, Prentice-Hall, Inc, Eaglewood Cliffs, New Jersey.

[3] Ahmed, S. (2022), “The Influence Depth of a Highway Embankment”, International Research Journal of Engineering and Technology (IRJET), Volume 9, Issue 8.

[4] FHWA-IF-12-027 (2012), “Manual For Design, Construction, and Maintenance of Orthotropic Steel Deck Bridges”, US Department of Transportation, Federal Highway Administration, P. 76.

[5] AASHTO (2016), “HL-93 Vehicular Live Loading, Truck, Tandem and Design Lane Load”.

[6] Bowles J. E. (1977), "Foundation Analysis and Design. 5th ed.", New York: McGraw-Hill.

[7] Ahmed, S. (2022), “Depth of Soft Cohesive Soil Underlying Highway Embankment for Limiting Residual Settlement”, International Journal of Science and Research (IJSR), Volume 11, Issue 8.

[8] Geometric Design Standards Manual (2005), Roads and Highways Division (RHD), Bangladesh, P. 116.

IFERP connecting engineers...developing research
1st International Conference on Future of Engineering 2022

The Significance of IoT and Blockchain Integration for Businesses

Tejaswini Ojha[1], Tripur S Josh[2], Prashant Hemrajani[3*]

[1,2,3] Department of Computer and Communication Engineering, Manipal University Jaipur, Jaipur, India
Email: [1] tejaswini.209303043@muj.manipal.edu, [2] tripur.209303042@muj.manipal.edu,
[3] prashant.hemrajani@jaipur.manipal.edu

Abstract:
Rapid technological advancement encourages the development of innovative solutions. Industries around the globe are preparing for transformation. As the number of connected devices and the value of the digital economy rise, the challenge of maximizing system efficiency intensifies. In a centralized system, privacy and transparency, as well as productivity and scalability, are only a few characteristics that conflict with one another. The demand for efficient workflow in businesses is driving the integration of diverse technology. Blockchain and the Internet of Things (IoT) will play a vital role in increasing industrial productivity. Blockchain enhances security by decentralization, and IoT improves inter-connectivity through sensors and the internet. Both technologies can overcome the existing obstacles so businesses can effortlessly implement these technologies. This fusion of anonymity and inter-connectivity pushes the industries operating over primitive architecture to switch towards a modern approach. The proposed research presented an architectural solution to data management and security problems. The design incorporates Blockchain technology's immutability, authenticity, traceability, and decentralization trademarks. The design's flexibility helps lower the risk of a privacy invasion. This integration will result in enhancing the security of the data and the efficiency of the system.

Keywords:
Blockchain, IoT, Decentralization, Smart Contracts, Distributed Systems, Business, Business Management, security, industrial application

I. INTRODUCTION

The commercial sector is rapidly growing to its maximum potential. New technology is integrated daily to make fast-paced industrial work more effective. IoT, machine learning, cloud computing, and other technologies have contributed to the industry 4.0 revolution. Technology benefits all the working sectors by reducing operating hours and making them more advanced. Technological innovations are often used as enablers for commercial, financial, and communicable change and are accessible while ensuring the security of confidential data.

IoT is one of the technologies that has facilitated the industrial industry the most. By altering how devices connect and the people who use those technologies, the Internet of Things has ensured that workplaces are more productive. IoT [1]has recently expanded into various industries, increasing digital communication and cooperation. The Internet of Things is upgrading industrial operations by providing more accurate and sensible insight into the flow of commodities and services.

However, security concerns have always made storing data created by the Internet of Things (IoT) devices difficult. Developing an ideal secure sharing technique in the IoT is quite challenging. Many problems exist, one of which is a data connection. The security challenge arising from IoT data sharing has become a critical and challenging issue in data security as IoT devices will access the user data as part of the information exchange process. This problem can be solved by Blockchain technology.

With the popularisation of blockchain technology in 2008 [2], a new era dawned. It began with bitcoin as the foundational technology, but it is now expanding its wings across a wide range of industries, including banking, security, networking, enterprises, healthcare, etc, as shown in figure 1. Several thriving businesses are investing in and experimenting with blockchain technology. The immutability and timestamped nature of blockchain transactions is ensured via distributed ledgers. Blockchain technology allows parties to monitor and execute

agreements amongst themselves using Smart Contracts. Its benefit is that it can complete a transaction without the involvement of a third party. The issue with third parties is that they may be hacked, exploited, or mishandled, resulting in malpractice.

The data is kept in an immutable ledger that network members can only access with authorization. The blockchain is used to create immutable ledgers and transaction records that aren't modifiable, erasable, or damageable, and it is also referred to as distributed ledger technology (DLT). The decentralized and autonomous characteristics of blockchain make it appropriate for the foundation of company security solutions. Merkle tree algorithms are used in the blockchain method to accomplish this. Combining blockchain and IoT will change and fulfill business process management demands (BPM), which focuses on creating, implementing, supervising, and improving business processes[3].

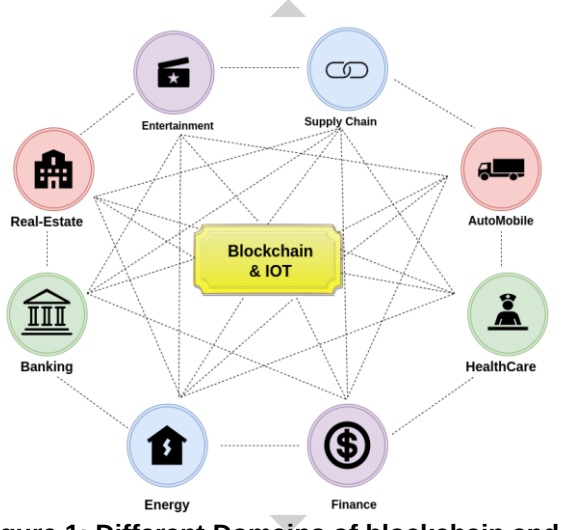

Figure 1: Different Domains of blockchain and internet of things applications

II. RELATED WORK

A business model is needed to run any sector systematically. It has acquired momentum in the last decades of the 20th century, making it a relatively new concept in the market[4]. And with time, the practical approach and its effect are gaining more attention from the researchers, which resulted in much more developed, functional, and different ideas of the business models that are put into practice. Traditional businesses have no unique definition of business models[5]. The four principles that a business model is made of, according to[6], are Infrastructure Management, Product Innovation, Customer Relationship, and Financial Aspects. With all this research in perspective, the rise of advancement in technology is also updating the traditional business models to E-business models. These technologies have different use cases in various fields of business. Internet of Things has taken a larger space in the cooperative world than any other technology, and it is now a feature of its own. In the early 1980s, the concept of IoT was introduced, which established communication between devices through the internet, which led to numerous innovating inventions and notions like Smart Cities[7], E-Health [8] , and many others. The centralized nature of these IoT-based applications raises one shared concern: security and privacy. The solution is to make the centralized system decentralized, which can be achieved by blockchain technology. Blockchain technology provides a decentralized approach by storing data in distributed public ledgers in a chain of blocks linked through a hash code[9]. Table I shows that different research publications on blockchain linked to business process management and the Internet of Things (IoT) have been analyzed in this study. The common challenges, techniques, domains, and gaols regarding the integration of blockchain and IoT models are shown.

Table 1: The summarized review of the blockchain and IoT ecosystem.

Ref. No.	Challenge	Technique	Domain	Goal
[3]	Risk is associated with centralized data and the risk of leaving traces.	Used blockchain for securing data and introduced Proof of interoperability.	Health	Propose a methodology for safely and efficiently exchanging medical data across a network.
[10]	Financial remodeling risk	Integrated Delphi technique and blockchain	Financial	Improving blockchain technology in finance

[11]	SupplyChain Management and Big data Analytics	Delphi Technique	SupplyChain	From a corporate and supply chain perspective, highlights potential and challenges connected to big data analytics while illustrating the development of the shift from a digital business environment
[12]	Problems with scalability: revamping the blockchain's data model	Blockchain verification is divided into two stages: standardization and testing.	Transport	Blockchain architecture and key characteristics were included in their comprehensive survey.
[1]	Scalability and Performance Assessment, Integration of Database Design into Data Model Layer	BlockBench	Financial Banks	BlockBench examines aggregate and component-by-component performance in terms of throughput, latency, scalability, and fault-tolerance.
[13]	Distribution and logistical networks using blockchain technology.	Financial, non-financial spheres, and blockchain	Industries	Explored the possibility of using Kouvola Innovation's blockchain-based application.
[7]	Analyzing the performance of a semantically augmented blockchain	Logistic, Financial analysis, and blockchain	Smart Cities	Semantic blockchain improvement in multiple domains is optimized.

Prior research has highlighted the advantages, limits, effectiveness, and challenges of adopting blockchain technology in various IoT devices.

The study, as mentioned above, illustrates the early stages of IoT and blockchain concepts, which may be developed into more efficient and practical techniques. However, these innovations cannot eradicate the conventional business process. They are merely the progression of standard Internet of Things models. Integration offers enhanced security by creating brand-new models through IoT and blockchain.

III. BLOCKCHAIN TECHNOLOGY

The term "blockchain" refers to a series of interconnected blocks representing a collection of data or records. When Stuart Haber and Scott Stornetta pioneered the notion of digital time-stamping in 1991, they laid the groundwork for blockchain. The paper proposed the idea of the digital time-stamping of the documents computationally. It combats the problem of digital file mutability by making it impossible for users to back-date or forward-date documents.

After 20 years, Satoshi Nakamoto reinstituted the earlier discussed concept of time-stamping and hashing in 2008. He integrated it with the consensus protocol "Proof of Work" to construct a completely new system. Here, each block has its ledger system. The network establishes a connection using metadata and the preceding block's hash. It represented a chain hence, named "Blockchain," demonstrated in figure 2. In the financial ecosystem, Satoshi introduced this concept to solve the issues of double-spending and third-party dependability. Many blockchains have since emerged with a similar concept and consensus mechanisms. Ethereum, Solana, Polkadot, and others. By inventing the notion of "Smart Contract," they helped broaden the scope of blockchain's applicability. Smart Contracts have ushered in a new era of blockchain and decentralized innovation. Still, cannot restrict to the premise that the blockchain only acts as a ledger system. With that in mind, new innovative decentralized applications in blockchain are possible.

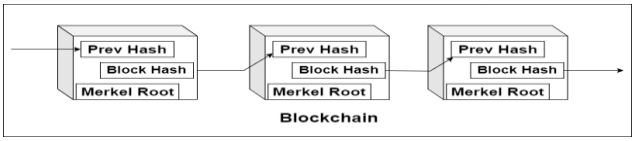

Figure 2**: connectivity between blocks in blockchain system**

Blockchain technology has emerged in many ways over the past couple of years, based on its architecture and configuration. It could be constructed and accessed in different ways. And this can be broadly summarized into three major parts as shown in figure 3:
Permissioned, Permissionless, and Hybrid Blockchains.

i) Permissionless Blockchain:
Permissionless blockchains provide open access to all without any restrictions. It is also known as a "pseudo-anonymous" chain as no central administration is there to modify protocols, update ledgers, or engage in other core activities. The ability to read, write and audit ongoing operations are unrestricted. Anyone can create a "node" and participate in the network. The network is self-governing, which gives it ultimate decentralization as anybody can see the ledger and check the accuracy of transactions that maintain the network's consistency and transparency. The decision-making process takes into account the participation of each member. It works on incentivization, encouraging new users to join and existing users to keep the ecosystem agile. The entire system operates in a democratic and decentralized atmosphere. Despite many benefits, the system does have some drawbacks. The one that stands out the most is the enormous power consumption. Because it is an open blockchain, many users will be performing several transactions simultaneously. Increasing transaction rate will increase the load on the system, and as a result, power consumption will be high. It also lacks anonymity and privacy since anyone can access it. It tends to compromise network security and tamper with network participants' identities. Because of the chain's openness, it attracts rogue individuals who try to tamper with the network's operations and engage in nefarious actions such as hacking, token theft, network clogging, and more. Another limitation is byzantine fault tolerance (the famous 51% attack). Public blockchains are currently the only type of blockchain categorized under the permissionless blockchain. The transaction may be seen and verified by anybody. The algorithms of public blockchains are scalable. Ethereum, Bitcoin, and many others are examples of public blockchains.

ii) **Permissioned Blockchain:**
Permissioned blockchains aren't open to all. Here, not everyone is eligible to join. Those who pass the verification process are eligible to be one. Users are obligated to follow the assigned instructions and complete them. The governing authority controls reading, writing, and auditing activities and provides special permissions to specific users. Technically, not everyone is capable of running a full node. The governing body decides over it, portraying it as partially decentralized. The operator has the right to override, edit, or delete the necessary entries on the blockchain. Everyone is also not accorded equal rights as the consensus protocol for mining and public access to the ledger records is restricted. It's also more susceptible to cyber-attacks. It does, however, have an efficient system in place to reduce transaction delays and increase throughput. It is a mixed bag of public and private chains. It acts as a secured database operating in a closed environment. All the characteristics of a permissioned blockchain lead to transactional finality and desirable transactional qualities.
Permissioned blockchains consist of two categories: private and consortium blockchains. These are also known as Managed blockchains. In private blockchains, there is only one governing node. While in a consortium blockchain, there is a group controlling it rather than one entity. The consortium provides a more decentralized ecosystem. It applies to the node whose ownership may be selected ahead of time and typically has business-to-business relationships. When compared to private, it has a better level of security. However, there may be some difficulties in getting it set up. Its possibilities include inter-party cooperation, logistical problems, and potential antitrust risks. CargoSmart launched the Global Shipping Business Network Consortium, an example of a consortium blockchain.
Hybrid Blockchain: The hybrid blockchain is managed and governed by a single or a group of organizations. The organization can decide the accessibility of the system by defining its jurisdictions. Central institutions, in accordance with their requirements, can modify these policies. They are a blend of permissioned and permissionless blockchains. The hybrid is modifiable (can be modified) according to the architecture. Hybrid blockchain content can be public or private and can be considered Partially Decentralized like Hyperledger.

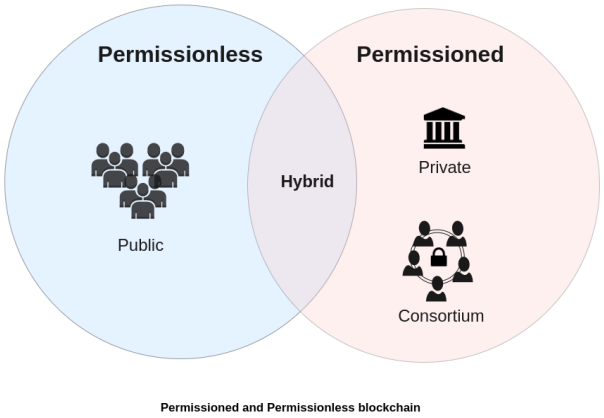

Figure 3: Types of Blockchain

Blockchain is a new technology, especially in the corporate sector. Blockchain technology is famous for its reliably secure nature. Blockchain is entirely implemented over a decentralized network to eliminate the governance of a central authority. Due to this reason blockchain is now gaining more attention which is leading to more secure and innovative applications. The true essence of blockchain is yet to be discovered. There could be considerably more blockchain applications apart from just a ledger system for transactions. For instance, 'Smart Contracts' deployment, designing DAAPs (Decentralized Applications), DAOs (Decentralized Autonomous Organizations), and DeFi (Decentralized Finance), among others. These all are becoming apparent towards the shift of the advanced internet and contributing to the rise of 'Web 3.0'. Blockchain technology is part of the web3 revolution which is impacting many research areas among scientists. In the starting era of blockchain researchers mainly focused on the financial sectors but with time blockchain came to know as more than just a finance tech. Presently, various innovations and notions are coming up in different fields for example the gaming sector, supply chain sector, and health sector. The core mechanism is every block is connected to the next block with a hash code which increases its security. A block is a storing space containing the timestamp, nonce, and transaction history. The first-ever block in the blockchain that has no parent block is called the genesis block. Blockchain works on the concept of decentralization [9].

IV. IOT IMPLEMENTATION IN BUSINESS

Internet of Things (IoT) has redesigned the concept of machine-to-machine interaction[10]. Human-to-machine communication is changing quite fast around the globe. The "Internet of Things" allows smart interconnection between everyday appliances. IoT enables control of these appliances remotely as shown in Figure 4.

A vast range of devices and services make up the ecosystem of IoT. Storage capacity, system uptime, and connectivity range are all problems that the massive network faces. Network protocols deal with such challenges. These protocols are effective for long-range as well as short-range. The IoT sector employs an expansive range of protocols, including cellular, BLE, RFID, Z-wave, 6LoWPAN, and many others[3].

The Internet of Things evolved into the industrial internet, allowing industries to reach new heights in the realm of technology[14]. Healthcare, finance, transportation and logistics, manufacturing, and other enterprises have quickly adapted to the Industrial Internet.

Emerging technologies, such as blockchain, can be combined with IoT to move the business world forward. It has the potential to increase the number of applications for many industries.

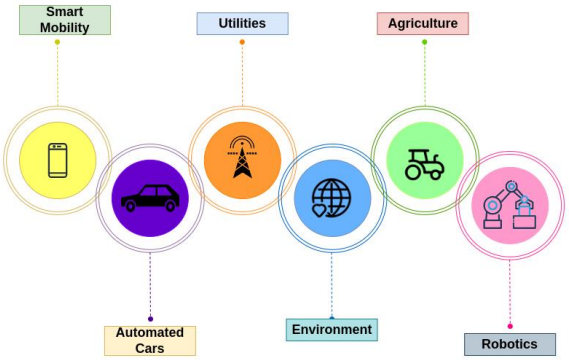

Figure 4: Connectivity of IoT devices

V. INTEGRATION OF IOT AND BLOCKCHAIN

It is also of utility for Internet-of-things (IoT) to solve their open problems, such as security [15]. The blockchain method collects all data from the IoT node and forms the data book for the private agreement mechanism. The IoT source data is reliable and the data is stored by a centralized network system. In IoT sensors devices, infrared sensors, and other IoT devices are used to store, transmit, and compute the frequency of sensors

The blockchain methodology has capabilities of reducing redundancy and improving the efficiency of IoT devices. The IoT data is necessary to categorize, combine data expression and allocate storage operations[9]. Smart systems for industrial automation, e-health, logistics, etc., aim at providing efficient solutions for business processes by leveraging the benefits of the Internet of Things (IoT).

The merger of IoT and Blockchain technology will change the world of business[16]. The IoT deals with innovating device-to-device communication, and blockchain enhances privacy, security, and decentralization. They can mutually handle all sorts of limitations and responsibilities[4]. An immutable ledger approach will minimize overhead at the local IoT edge level. While at the higher level, decentralization increases security. The distributed trust technique links the devices. The linkage enables the exchange, request, save, and transaction of data or information. The retrieved data gets encrypted and divided into blocks. The connected ecosystem of those blocks results in a blockchain. The encrypted data related to transactions is employed as a shared key for all sorts of incoming and outgoing transactions. The permission to access various IoT resources present over the blockchain is available globally[2](Figure 5).

Combining various IoT sensors to the same blockchain node facilitates network scalability[5]. The ongoing stream of real-time data from a specific device is monitored. Thus, the coupling of the two technologies enriches the business framework. The major examples of integration of IoT and blockchain are listed below in table 2.

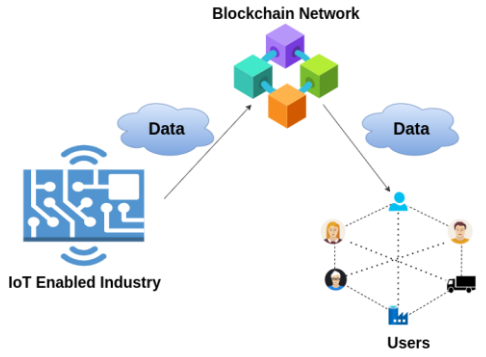

Figure 5: Integration of blockchain and IoT increases the security of data

Table.2. List of companies using the integration of IoT and Blockchain

VI. METHODOLOGY

A secured key pair of private and public keys assigned to the IoT devices can connect them to the blockchain. For generating the key pair of the blockchain like Bitcoin, Ethereum, and more prefer "Elliptic Curve Cryptography." [22] The Elliptic Curve Cryptography assists in creating digital signatures. The most commonly used one is "Secp256k1". The mathematics for generating one is as follows.

General equation for Secp256k1 elliptic curve:

$$y^2 = x^3 + (ax + b) \quad (1)$$

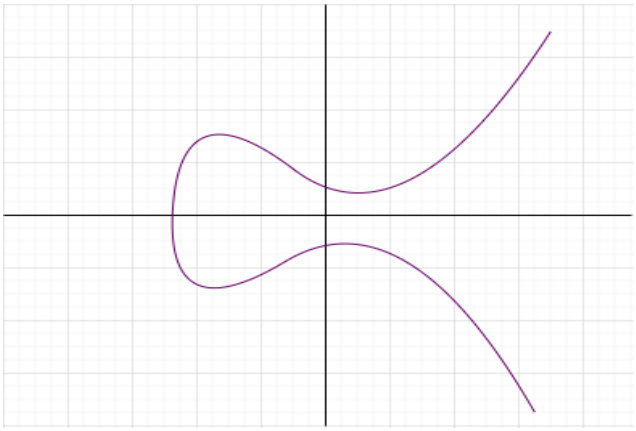

Figure 5: GENERAL SECP256k1 elliptic curve graph (1)

To perform public key cryptography, the elliptic curve Secp256k1 is used. Users may produce a public key from their own private key by multiplying their private key by the Generator Point, a specific point on the secp256k1 curve, a = 0 and b = 7 generates the expression $y^2 = x^3 + 7$ (2) for secp256k1. Secp256k1 is symmetric across the x-axis because the y component of the equation is squared, and for any value of x, there are two values of y, one odd and the other even. Public keys may now be uniquely recognised using just their x- and y-coordinate parities, resulting in considerable data use savings on the blockchain.

The employed form of Secp256k1 curve:

$$y^2 = x^3 + 7 \quad (2)$$

Prime Modulo: EEEEEEEE EEEEEEEE EEEEEEEE EEEEEEEE EEEEEEEE EEEEEEEE EEEEEEEF FFFFFC2F = : $2^{256} - 2^{32}$- 29 - 28 - 27 - 26 - 24 - 1

Base Point: 04 79AB669E F8CCBCAB 53B16297 CF708A07 029BEACB 2DCE24D8 59C3725B 16E91298 483BAD77 26B2C465 5DA4ABAC 0E1107C7 FD17C339 A6855217 9C21C08F FB02C4B8 (4)

Order of Base Point: EEEEEEEE EEEEEEEE EEEEEEEE EEEEEEEE BADEACE6 AC39A03B AEC25E8C D0289141 (5)

Elliptic curve cryptography relies on the fact that, given a base point (4) and order of a base (5), a hash value may be effectively calculated.

Bitcoin could be taken as an example here to understand it more precisely [20, 21].

In the algorithm Elliptic Curve Digital Signature, the private key is generated randomly between 1 and the order (2^{256}). The scalar multiplication of the private key and the base point results in a public key.

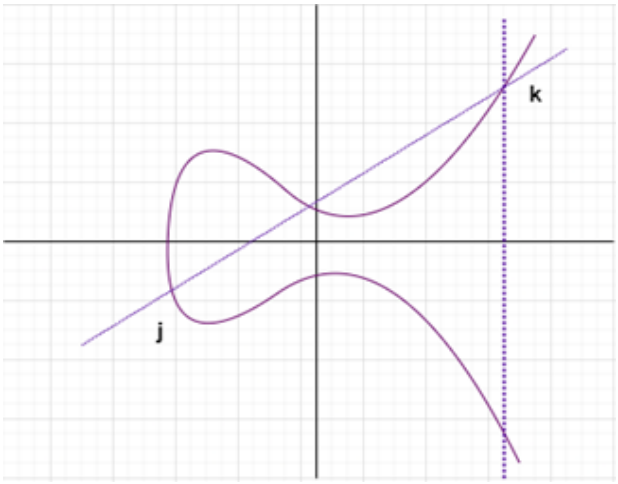

Figure 6: The graph represents the above equation

For simplification, we can also use a single point on the graph and perform similar mathematics.

VII. EXPERIMENT STUDY

The study's goal is to comprehend the uses of IoT and blockchain technologies in business operations. Chronicled integrates blockchain and Internet of Things (IoT) devices to provide an end-to-end chain solution. It allows all stakeholders involved in the process will be completely aware of the provenance and any issues that may develop. The primary objective of this research is to enhance the security of data provided by IoT devices during monitoring and tracking applications.

1) Condition Monitoring in Industries

Condition monitoring (CM) combines sensor data with temperature, humidity, and other factors to anticipate machine health and safety. Remote monitoring of machine and plant settings is made easier using CM. It also provides a warning in the event of a change in health status, allowing prompt action. The goal of Industry 4.0 is to increase operational efficiency via automation. In CM, the data is recorded through efficient IoT sensors. The data is then secured via Blockchain, which encrypts and distributes information in a decentralized manner throughout the network. In case of a change, an alert is sent through sensors and circulated over the Blockchain.

The proposed Algorithm for sensor monitoring is shown in Table 3. It depicts the architecture's initial tier. Sensors communicate with actuators, Zigbee, and Bluetooth devices at the primary layer. Low-power radio-based devices were utilized to keep the architecture light. Sensors, among other things, calibrate resistance, temperature, and humidity. Sensors are also used to control the machine's dynamic and static movements.

TABLE 3. THE PROPOSED IOT ALGORITHM IN CM

1. Variables declaration
2. MQ calibration initiated
3. If val==0 val -> determined value
4. for (initial value< calibrated_Sample_time)

Val += MQResistanceCalculation(analogRead(mq-pin))

return " Sample_time_interval"

5. if (val < calibaration_Sample_time) && (val< Ro_Clean_Air_Factor)

return "val"

6. End function

Table 4 represents the proposed Blockchain Algorithm. It allows for the autonomous execution of code. The agreement gives the users access to the information received through sensors. Contracts are signed between the user and the owner, giving the user access. The solution allows us to store the acquired data in a distributed manner using the InterPlanetary File System (IPFS).

TABLE 4. THE PROPOSED BLOCKCHAIN ALGORITHM IN CM

1. Contract Monitoring
2. Constructor Declaration
3. Create modifiers- member& user
4. if user is true

return "user address"

else

return "Restricted to users"

5. Create struct - userData, list pointer
6. Mapping of user address
7. Is User

if(user.length == 0)

return "false"

else

return " monitored data received from sensors"

8. end function

2) Cold Chain Transport Tracking

In the supply chain, fresh produce and other perishable goods are destroyed or wasted due to poor temperature management. The term "cold chain" refers to a temperature-controlled transportation system. The cold chain encompasses everything from clever cold storage to delivery to the customer. Cooled food and pharmaceutical goods are transported to clients at low temperatures. Sensors are used to keep track of the cargo's temperature and other information. The encrypted data is then

delivered through IPFS, a distributed blockchain storage system.

Table 5 shows the intended cold chain algorithm. The shifting temperature might degrade the quality of the items. Consequently, it will affect the health and safety of the consumer. The cold chain reports real-time dynamic evaluation. At the same time, it will transmit an alarm, resulting in a prompt diagnosis of the problem and rapid, less invasive troubleshooting.

TABLE 5. THE PROPOSED IOT ALGORITHM IN COLD CHAIN TRACKING

1. Initiated application interface
2. Variables declared: temperature & humidity
3. Address mapped of user & transporter
4. if published event and data is true
5. if location data is true

return “OK and provide details”
else
return “Failed”
If void temperature (data> NULL)
Store temperature details
return “temperature read successfully”
else
return “NO data available to read”

6. End function

Table 6 displays the Blockchain Algorithm suggested for cold chain monitoring. Data dispersed over a decentralized network can be used for remote monitoring and enhanced maintenance. Data tampering can be prevented, leading to better and safer product delivery.

TABLE 6. THE PROPOSED BLOCKCHAIN ALGORITHM IN COLD CHAIN TRACKING

1. Contract Tracking
2. Constructor Declaration
3. Create Struct: pname, description, manufacturing,initialized
4. Uers address mapped using uuid
5. Create events: Track Create & Reject Create
6. if trackstore is initialized

return “msg sender”
else
return “Trac with this uuid already exists”
if (walletStore uuid = true)
return “uuid, manufacture”
else
return “Track”

7. End function

VIII. CONCLUSION

The paper discussed combining IoT with Blockchain, revolutionizing the corporate world. Blockchain is an innovation that is rapidly becoming a requirement across all sectors and boosting the database security of the platform. Similarly, IoT enables effective device communication. Combining blockchain technology with the Internet of Things has the potential to advance the business world. Integrating blockchain and intelligent machines can improve the efficiency and profitability of all associated organizations. This paper demonstrates the integration of several blockchain smart contract algorithms with IoT machines. This resulted in increasing present technology's authenticity, anonymity, and scalability. Further study is necessary to analyze IoT and blockchain technologies' possibilities thoroughly.

REFERENCES

[1] A. Pal, C. K. Tiwari, and N. Haldar, “Blockchain for business management: Applications, challenges and potentials,” *Journal of High Technology Management Research*, vol. 32, no. 2, Nov. 2021, doi: 10.1016/j.hitech.2021.100414.

[2] S. Nakamoto, “Bitcoin: A Peer-to-Peer Electronic Cash System.” [Online]. Available: www.bitcoin.org

[3] D. Mohey, E.-D. M. Hussein, M. Hamed, N. Taha, and E. M. Khalifa, “A Blockchain Technology Evolution between Business Process Management (BPM) and Internet-of-Things (IoT),” 2018. [Online]. Available: www.ijacsa.thesai.org

[4] Y. Zhang and J. Wen, “The IoT electric business model: Using blockchain technology for the internet of things,” *Peer-to-Peer Networking and Applications*, vol. 10, no. 4, pp. 983–994, Jul. 2017, doi: 10.1007/s12083-016-0456-1.

[5] R. Amit and H. E. Aldrich, “Value drivers of e-commerce business models Historical analysis and organizational evolution View project Ecological succession & small businesses in inner cities View project,” 2000. [Online]. Available: https://www.researchgate.net/publication/228556588

[6] A. Osterwalder and Y. Pigneur, “An eBusiness Model Ontology for Modeling eBusiness,” 2002. [Online]. Available: http://aisel.aisnet.org/bled2002/2

[7] A. H. Alavi, P. Jiao, W. G. Buttlar, and N. Lajnef, “Internet of Things-enabled smart cities: State-of-the-art and future trends,” *Measurement: Journal of the International Measurement Confederation*, vol. 129, pp. 589–606, Dec. 2018, doi: 10.1016/j.measurement.2018.07.067.

[8] F. Z. Fagroud, H. Toumi, E. H. ben Lahmar, M. A. Talhaoui, K. Achtaich, and S. el Filali, “Impact of IoT devices in E-Health: A Review on IoT in the context of COVID-19 and its variants,” in *Procedia Computer Science*, 2021, vol. 191, pp. 343–348. doi: 10.1016/j.procs.2021.07.046.

[9] S. Ramamoorthi, B. Muthu Kumar, M. Mohamed Sithik, T. Thinesh Kumar, J. Ragaventhiran, and M. Islabudeen, “Enhanced security in IOT environment using Blockchain: A survey,” *Materials Today: Proceedings*, Apr. 2021, doi: 10.1016/j.matpr.2021.03.346.

[10] W. Viriyasitavat and D. Hoonsopon, “Blockchain characteristics and consensus in modern business processes,” *J Ind Inf Integr*, vol. 13, pp. 32–39, Mar. 2019, doi: 10.1016/j.jii.2018.07.004.

[11] D. Mohey, E.-D. M. Hussein, M. Hamed, N. Taha, and E. M. Khalifa, “A Blockchain Technology Evolution between Business Process Management (BPM) and Internet-of-Things (IoT),” 2018. [Online]. Available: www.ijacsa.thesai.org

[12] T. Ali Syed, A. Alzahrani, S. Jan, M. S. Siddiqui, A. Nadeem, and T. Alghamdi, “A Comparative Analysis of Blockchain Architecture and its Applications: Problems and Recommendations,” *IEEE Access*, vol. 7, pp. 176838–176869, 2019, doi: 10.1109/ACCESS.2019.2957660.

[13] W. Viriyasitavat, L. da Xu, Z. Bi, and V. Pungpapong, “Blockchain and Internet of Things for Modern Business Process in Digital Economy - The State of the Art,” *IEEE Transactions on Computational Social Systems*, vol. 6, no. 6, pp. 1420–1432, Dec. 2019, doi: 10.1109/TCSS.2019.2919325.

[14] W. Liang and N. Ji, “Privacy challenges of IoT-based blockchain: a systematic review,” *Cluster Computing*, vol. 25, no. 3, pp. 2203–2221, Jun. 2022, doi: 10.1007/s10586-021-03260-0.

[15] T. Ali Syed, A. Alzahrani, S. Jan, M. S. Siddiqui, A. Nadeem, and T. Alghamdi, “A Comparative Analysis of Blockchain Architecture and its Applications: Problems and Recommendations,” *IEEE Access*, vol. 7, pp. 176838–176869, 2019, doi: 10.1109/ACCESS.2019.2957660.

[16] V. J. Morkunas, J. Paschen, and E. Boon, “How blockchain technologies impact your business model,” *Business Horizons*, vol. 62, no. 3, pp. 295–306, May 2019, doi: 10.1016/j.bushor.2019.01.009.

[17] “Helium – Introducing The People’s Network.” https://www.helium.com/ (accessed Aug. 12, 2022).

[18] “Chronicled.” https://www.chronicled.com/ (accessed Aug. 12, 2022).

[19] “filament.com” https://filament.com/ (accessed Aug. 12, 2022).

[20] “HYPR: True Passwordless Multi-Factor Authentication (MFA).” https://www.hypr.com/ (accessed Aug. 12, 2022).

[21] “GridPlus.” https://gridplus.io/ (accessed Aug. 12, 2022).

[22] A. K. Yadav, “Significance of Elliptic Curve Cryptography in Blockchain IoT with Comparative Analysis of RSA Algorithm,” in *Proceedings - IEEE 2021 International Conference on Computing, Communication, and Intelligent Systems, ICCCIS 2021*, Feb. 2021, pp. 256–262. doi: 10.1109/ICCCIS51004.2021.9397166.

IFERP connecting engineers...developing research
1st International Conference on Future of Engineering 2022

Impact of the Electric Boats in Distribution Network Load Modeling

Eder A. Molina-Viloria[1*], John E. Candelo-Becerra[2], Miguel Garnica[3]

[1] Science and Technology Corporation for the Development of Naval, Maritime and River Industry, Cra. 2 11 Naval Base (Cotecmar), Pl. de San Pedro Claver #4-34, Cartagena de Indias, Province of Cartagena, Bolívar, Colombia
[2] Department of Electric and Automatic Energy, National University of Colombia, Medellin Campus
[3] Naval Communication, Control and Design Research Group, "Almirante Padilla" Naval Cadet School, Cartagena; de Indias, D. T. y C. (Bolívar), Colombia
Email: [1]edermolinav@hotmail.com, [2]jecandelob@unal.edu.co, [3]miguel.garnica@armada.mil.co.

Abstract:
Rapid technological advancement encourages the development of innovative solutions. Industries around the globe are preparing for transformation. As the number of connected devices and the value of the digital economy rise, the challenge of maximizing system efficiency intensifies. In a centralized system, privacy and transparency, as well as productivity and scalability, are only a few characteristics that conflict with one another. The demand for efficient workflow in businesses is driving the integration of diverse technology. Blockchain and the Internet of Things (IoT) will play a vital role in increasing industrial productivity. Blockchain enhances security by decentralization, and IoT improves inter-connectivity through sensors and the internet. Both technologies can overcome the existing obstacles so businesses can effortlessly implement these technologies. This fusion of anonymity and inter-connectivity pushes the industries operating over primitive architecture to switch towards a modern approach. The proposed research presented an architectural solution to data management and security problems. The design incorporates Blockchain technology's immutability, authenticity, traceability, and decentralization trademarks. The design's flexibility helps lower the risk of a privacy invasion. This integration will result in enhancing the security of the data and the efficiency of the system.

Keywords:
Blockchain, IoT, Decentralization, Smart Contracts, Distributed Systems, Business, Business Management, security, industrial application

I. INTRODUCTION

What is important in the power electric system planning and the operation are related with the stability. Hence the importance of load modeling that allows electric systems an optimal operation. The load modeling is the process to obtain a mathematical representation of the load connected to a bus [1]. Also, it is used composite static ZIP load modeling and third-order asynchronous machine as load model structure, and the particle swarm optimization algorithm (PSO) is used in the parameters identifications of the model structure through measurements [2]. Various parameters have been developed about this topic, in [3] is presented the impact of the different types of load modeling in a distribution red, using as power supply the wind energy. In [4], is proposed a combination of the static ZIP load modeling and an asynchronous generator for the load modeling considering distributed sources; this focusing shows satisfying results in the representation of loads with low and high levels of distributed sources penetration. In [5] is studied the impact of the wind power generation, it can be described by widespread load model compound by asynchronous machine in parallel with static load.

One of the most important aspects that affect the voltage stability studies of a power system are related with how is modeled the load. This article summarizes the state of art of the representation of the power system loads for the dynamic performance with analytic purposes. It includes the discussion about the importance of the load modeling, important considerations to different load types and different types of analysis [6].

This bibliography about the load modeling articles complements the paper that it is been analyzed and organize standardized load models. The listed

projects are classified in function of the applications about the discussed load modeling [7][8].

This article analyzes some of the factors that makes the load modeling to stabilize the voltage a challenge and brings information about key aspects that have to take into account at the time of doing practical studies [9].

In [10] is proposed a structure of integral load modeling that considered the distributed photovoltaic power generation. On this basis is proposed a method of aggregation equivalence of the integrated load modeling parameters that simulate with precision features of the integrated load of the distribution red with photovoltaic power generation.

In this paper [11], the principles and the load modeling methods are described briefly. Pointing to the problems of new energies access at large scale to the re, the existing load modeling methods are introduced. The non-resolved issues in this field and the future investigation figure.

In [12] this article, a new structure of load modeling taking in account there release features of multiple levels of low voltage. In the proposed model, low three levels strain the characteristic release parameters are introduced in the model of existing synthesis load (ESL) for simulate the release liberation features of low voltage of the load during the perturbation.

In this paper [13] is presented a revision and a comparation of the 2 existing methodologic most used to the load modeling, namely, the focusing based on measurements and based on components. Also are proposed a general critical and updated description of the opportunities and the challenges of load modeling with networks and emerging components.

In this paper [14], the two types od load modeling are derived by a composition high load engine, and its performance Is compared and analyzed through case studies considering both the voltage and the dependence of the load model frequency.

This investigation is presented a load model to electric boats connected to an autonomous micro grind, this paper has been organized in three more sections as follows: section 2 presents the methodologic and the designs for the ROV construction, section 3 present the results of this investigation and at last section 4, are presented the conclusions and future projects.

1. Model structure

The load model can be classified in static and dynamic load models. A static load model is a mathematical representation of the active and reactive power connected to a bus in any moment like a function of voltage measured at the same time. Also, a dynamic load model offers a representation that depends on the measured strain in previous moments, and that can also depend on the real measure.

In this paper, it was chosen and adapted a system of dynamic energy. Like is shown in the Fig. 1 that consist on an induction engine, static load. The models of each part are described below.

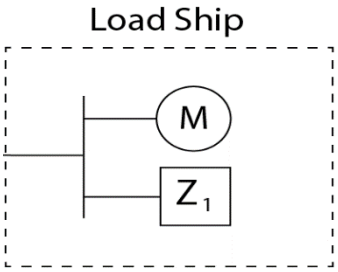

Fig. 1

The mathematical model that we have chosen for the electric boat is an induction engine since the engine that propels the boat is electrical added to a resistive load that comes to represent the rest of the electrical load of the boat as are the illumination systems, navigation systems, etc.

For the mathematical model of the induction engine is adopted the three steps model under the synchronous coordinate system, presented in [15]

$$\frac{de'_x}{dt} = s(1+\omega_B)e'_y - \frac{1}{T'_0}\left\{e'_x + \frac{x_s - x'}{r_1{}^2 - (\omega x')^2}\left[r_1\left(u_y - \omega e'_y\right) - \omega x'\left(u_x - \omega e'_x\right)\right]\right\} \quad (1)$$

$$\frac{de'_y}{dt} = s(1+\omega_B)e'_x - \frac{1}{T'_0}\left\{e'_y - \frac{x_s - x'}{r^2{}_1 + (\omega x')^2}\left[r_1\left(u_x - \omega e'_x\right) + \omega x'\left(u_y - \omega e'_y\right)\right]\right\} \quad (2)$$

$$\frac{ds}{dt} = \frac{P_m}{T_J} - \frac{(r_1 e'_y + \omega x' e'_x)(u_y - \omega e'_y) + (r_1 e'_x - \omega x' e'_y)(u_x - \omega e'_x)}{T_J\left[r_1{}^2 + (\omega x')^2\right]} \quad (3)$$

$$T_m = T_0[A(1-s)^2 + B(1-s) + C] \quad (4)$$

To obtaining the resistive load model of the illumination and navigation systems, we were supported on the following formula of the law of ohm and the law of watt for obtain it.

Clearing I_n of the ohm's law are obtained (5) and (6) equations.

$$\frac{V_n}{X} = I_n \quad (5)$$

$$I = \frac{V}{X} \quad (6)$$

Clearing X from (5) and (6) , and then equating X it is obtained the following equation.

$$X = \frac{V}{I} = \frac{V_n}{I_n} \quad (7)$$

Clearing I from (7) it is obtained the following equation.

$$I = I_n * \frac{V}{V_n} \quad (8)$$

Using Watt's law and replacing it in the equation (8), it is obtained the following equation.

$$S = S_n * \frac{(V)^2}{(V_n)^2} \quad (9)$$

In the following equation it is obtained Z by equating the current values, similar as the previous equation.

$$Z = Z_n * \frac{V}{V_n} \quad (10)$$

Then, to obtain the equation (11) it is implemented the watt's law again

$$S = I^2 * Z \quad (11)$$

Replacing (10) in (11) it is obtained the following equation.

$$S = I_n^2 * Z_n * \frac{V}{V_n} \quad (12)$$

Regrouping the terms and by using watt's law $S_n = I_n{}^2 Z_n$ it is obtained the following equation.

$$S = S_n * \frac{V}{V_n} \quad (13)$$

$$S = S_n \quad (14)$$

From the equations (9), (12) and (13) it is possible to represent the compound load model or better known as the polynomial ZIP model [16] (constant impedance, constant current and power), which express the active and reactive power in function of the electric strain which it is subjected the charge like is shown in (14) and (15).

$$P = [a_{p0} + a_{p1} * \frac{V}{V_n} + a_{p2} * \frac{(V)^2}{(V_n)^2}] \quad (15)$$

$$Q = [a_{q0} + a_{q1} * \frac{V}{V_n} + a_{q2} * \frac{(V)^2}{(V_n)^2}] \quad (16)$$

II. SIMULATION SYSTEM

The distribution network load included the electric boat can be described through an induction engine in parallel with a static load. The system is made up of two load types. A residential load that is modeled like a ZIP load, and for an electric engine with a moderate consumption. Next, using the Matlab software Simulink it is analyzed the behave of this charge model interacting in a microgrid, with different types of loads domiciliary and industrials, as shown in Figure 2.

Results.

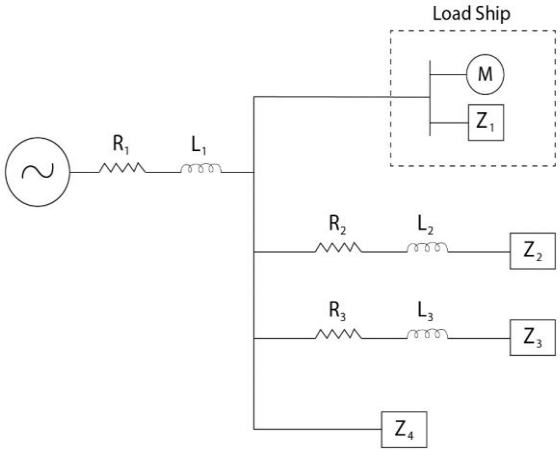

Fig2. Microgrid schematic

This electric microgrid will be operating with 3 residual and industrial loads during a 60 seconds period time and a fourth load, the one that it is been mathematically modeled, will enter in a 12 seconds period. Next, it is presented the graphics obtained by the simulations in Matlab software Simulink.

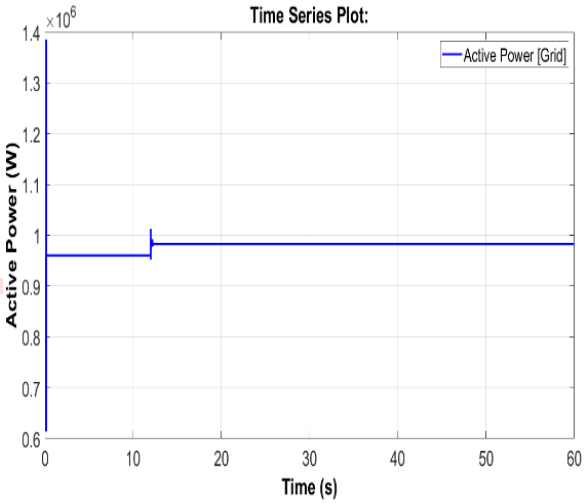

Fig. 3(a)

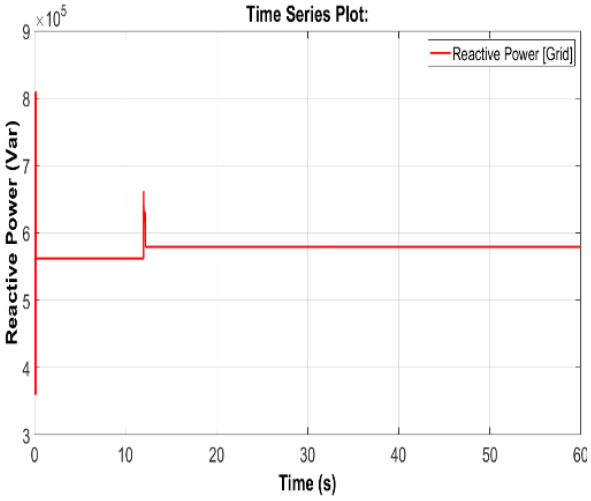

Fig. 3(b)

Figure 3(a) is the active power consumed by the microgrid, figure 3(b) is the reactive power consumed by the microgrid.

In figure 3(a) and figure 3 (b), it can be observed the active power consumed by all the electric loads that conform the microgrid, also it can be noticed an increase of the active power consumption and the power with the electric boat connection in time equals 12 seconds. Also it is appreciated the active power regulation is more efficient than the reactive power regulation.

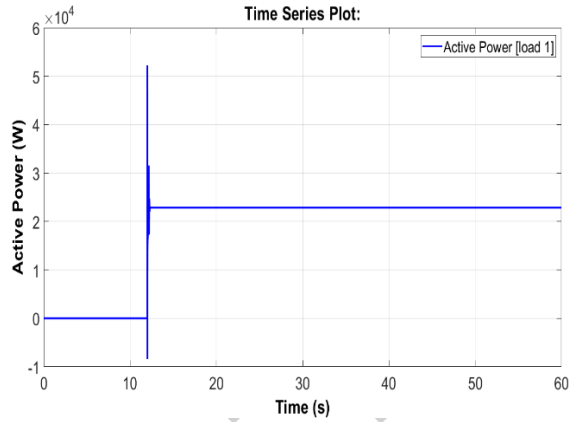

Fig. 4(a)

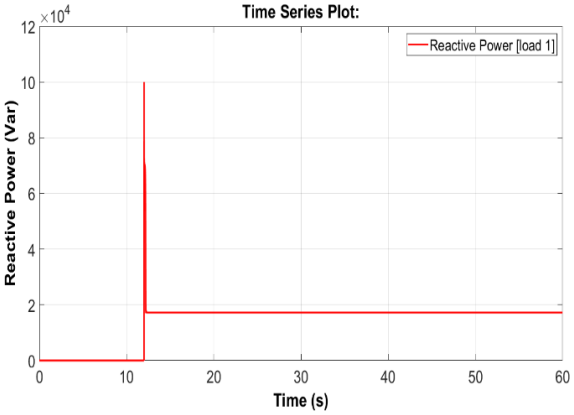

Fig. 4(b)

Figure 4(a) is the active power consumed by the electric boat model, figure 4(b) is the reactive power consumed by the electric boat model.

In the previous figures can be appreciated that the electric boat, during the first 12 seconds it not consume neither active and reactive power, as a consequence of not been connected with the microgrid, however in time equals 12 it is connected to the microgrid and automatically the changes are notable, which creates an increase in the microgrid until the las second of the simulation.

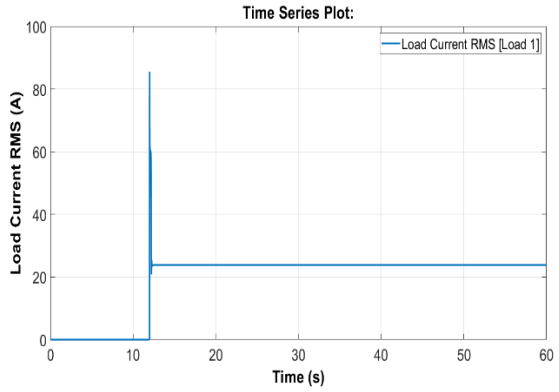

Fig. 5(a)

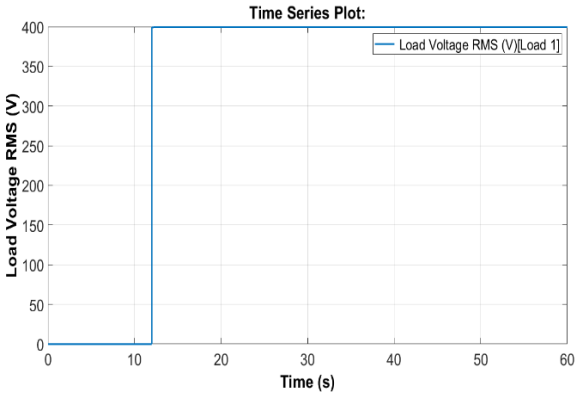

Fig. 5(b)

Figure 5(a) and 5(b) is represented the electric current and voltage in RMS that the mathematical model of the electric boat consumes.

In figure 5(a) can be observed the peak current with the electric boat connection since much electric motors have a starter current, which is usually four times the rated current consumption. In figure 5(b) can be observed the RMS voltage in 400 volts after 12 seconds as a result of the connection of the electric boat to the microgrid in that period

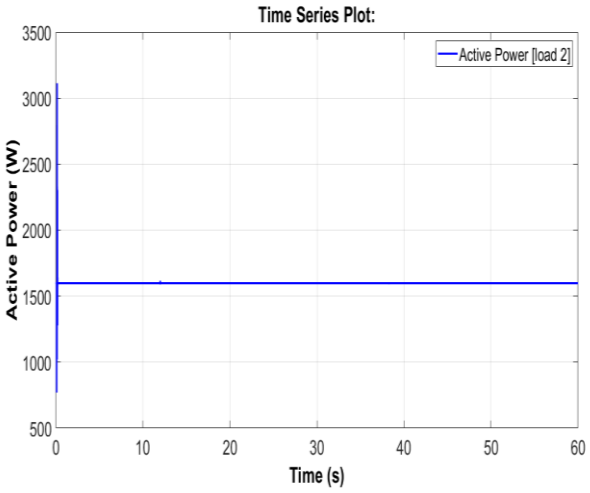

Fig. 6(a)

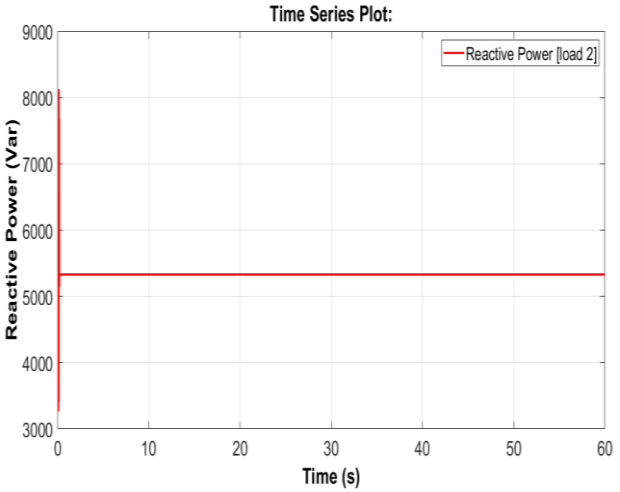

Fig. 6(b)

In the figure 6(a) can be observed the active power of the second electric load (20 Ω+ j 0.05) of the microgrid scheme in figure 2, which is constant during all the simulation, the same situation occurs in figure 6(b) with the reactive power which is constant during all the simulation too.

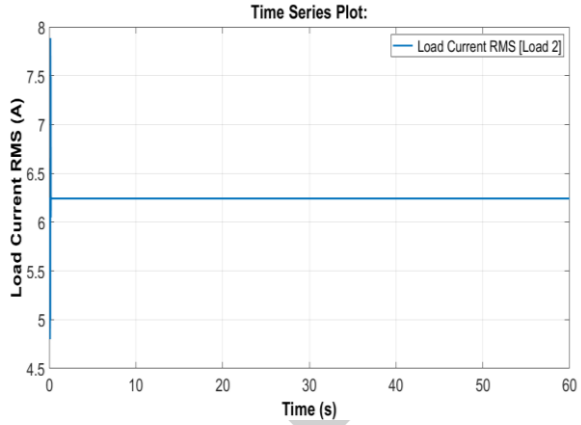

Fig. 7(a)

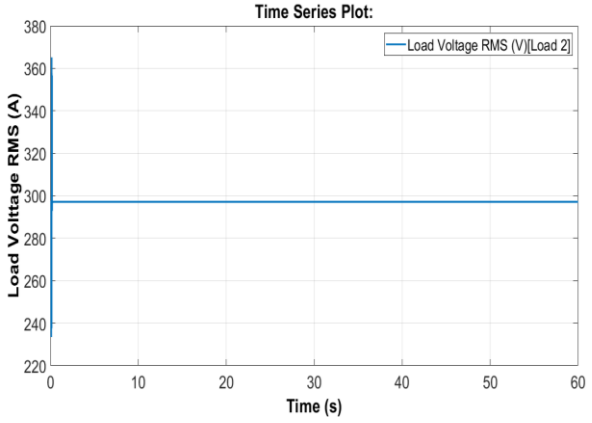

Fig. 7(b)

In figure 7(a) can be observed the RMS current that consumes the second electric load of the microgrid schematic, in which is observed constant consumption during the simulation, The same goes with the RMS load voltage which is represented in figure 8(b) and it is observed that is constant during 60 minutes of the simulation. Neither the current or the voltage of this load is affected by the electric boat connection, which is represented by a mathematical model.

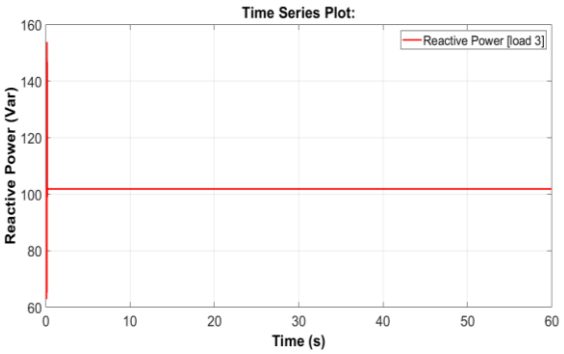

Fig. 8(a)

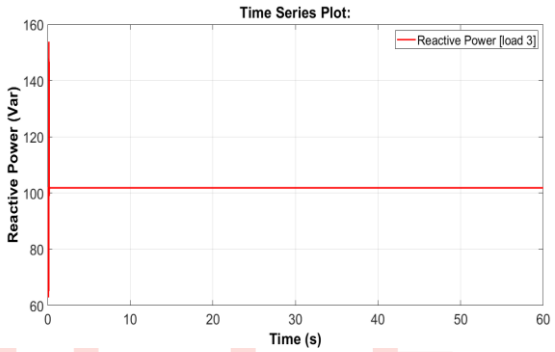

Fig. 8(b)

In The figure 8(a) it can be observed the active power of the third electric load that fully residential 500 ohms, which is represented in the microgrid scheme, which is constant during all the simulation, same situation occurs in figure 8(b) with the relative power which is constant during all the simulation.

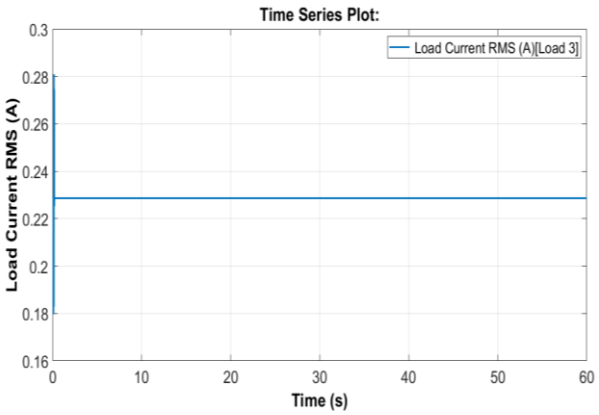

Fig. 9(a)

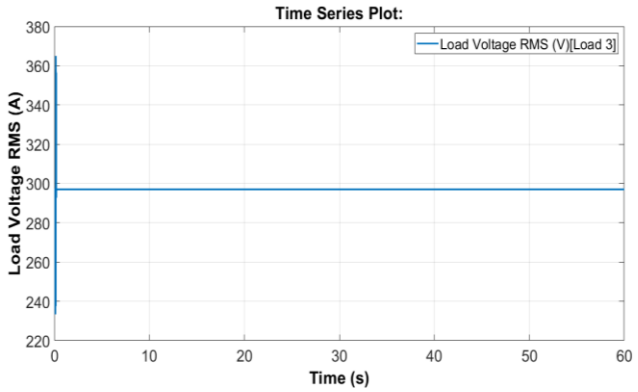

Fig. 9(b)

In the figure 9(a) it can be observed the RMS current that consume the third electric load of the microgrid scheme, which is totally residential in which can be observed a constant consumption throughout the simulation, the same happens with the RMS voltage of the load which is represented in the figure 9(b) is noted that both measures are constant during the first 60 seconds of the simulation. Neither current nor voltage is affected of this residential electric load with the connection of the electric boat, that is represented for a mathematical model.

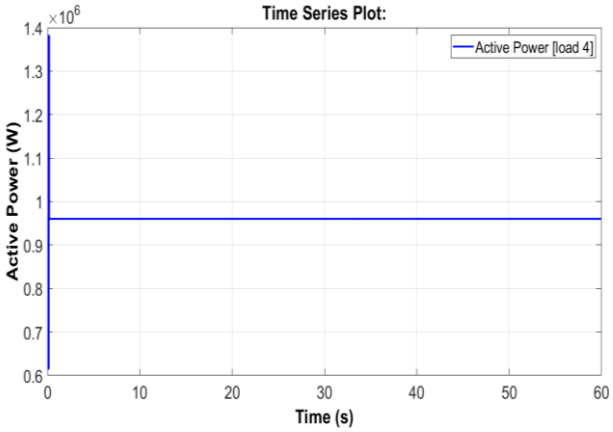

Fig. 10(a)

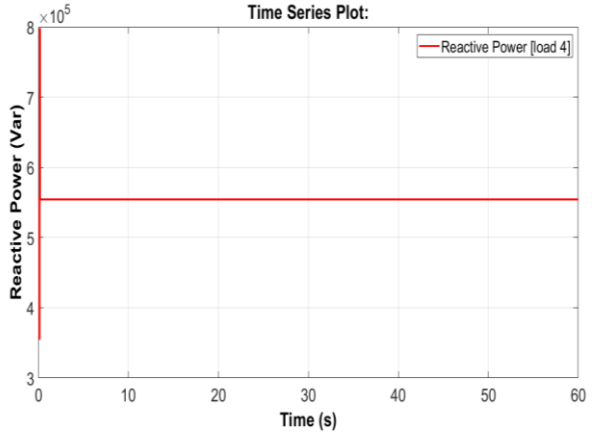

Fig. 10(b)

In the figure 10(a) it can be observed the active power of the fourth electric load of the microgrid scheme of the figure 2, which is constant during all the simulation, the same goes in the figure 10(b) with the reactive power, which is constant during all the simulation. As consequence of being a constant electric load during all the simulation.

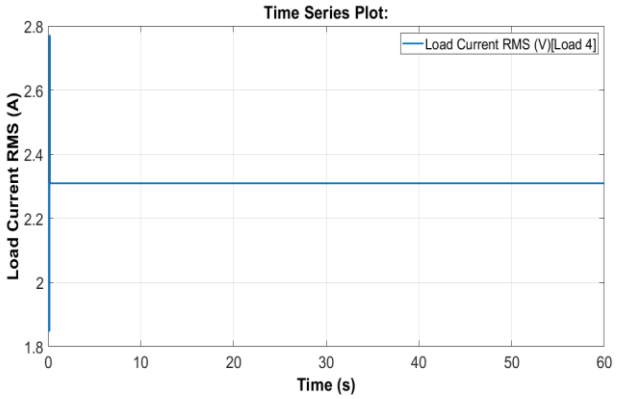

Fig. 11(a)

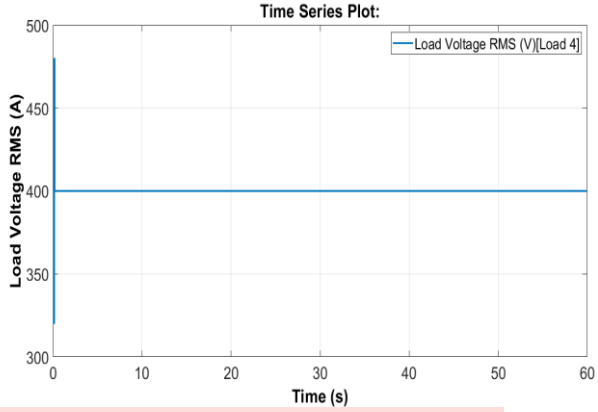

Fig. 11(b)

In the figure 11(a) can be observed the RMS current that consume the fourth electric load that is of 100 ohms, that is represented in the microgrid scheme of the figure 2, in which can be observed a constant consume during all the simulation, the same happens with the RMS voltage of the load that is represented in the figure 11(b) and can be observed that is constant during the 60 seconds of the simulation. Neither current nor voltage is affected of this load with the connection of the electric boat.

III. CONCLUSIONS

This paper was able to develop a mathematical model for an electric boat and analyze the impact that produce in a distribution network with local residential load, the boat acts as an electric load during a time period. It was able to achieve to establish this model based in existing models of electric loads pretty similar that interact on electric networks, in this article we worked in one.

A paper in the future would be good to implement this type of model that interact with the electric boat B2G or bidirectionals which acts as an electric load during a time period and in other like electric generators, since this type of loads are the future of the electric networks, and in which the coastal cities will deal in a near future. Also implementing this type of networks including well distributed generators can make a solar farm or a wind farm.

REFERENCES

[1] Kundur, Power system stability and control. New York: McGrawHill, 1993

[2] L. Rodríguez-García, S. Pérez-Londoño and J. Mora-Flórez “A Methodology for Composite Load Modeling in Power Systems Considering Distributed Generation”.

[3] N. K. Roy, M. J. Hossain and H. R. Pota, “Effects of load modeling in power distribution system with distributed wind generation,” in Proc. 2011 21st Australasian Universities Power Engineering Conf., pp.1-6.

[4] J. Wang, R.-M. He and J. Ma, “Load Modeling Considering Distributed Generation,” in Proc. 2007 IEEE Laussane Power Tech Conf., pp.1072- 1077.

[5] J. Qian, X. Li, J. Hui, “Impact of wind generation on load modeling of distribution network,” in Proc. 2009 Intl. Conf. Sustainable Power Generation and Supply, pp.1-5.

[6] IEEE Task Force on Load Representation for Dynamic Performance, “Load representation for dynamic performance analysis of power systems,” IEEE Trans. Power Systems, vol. 8, no. 2, pp. 472 – 482, may 1993.

[7] IEEE Task Force on Load Representation for Dynamic Performance, “Standard load models for power flow and dynamic performance simulation,” IEEE Trans. Power Systems, vol. 10, no. 3, pp. 1302 –1313, aug 1995.

[8] IEEE Task Force on Load Representation for Dynamic Performance, “Bibliography on load models for power flow and dynamic performance simulation”. IEEE Trans. Power Systems, vol. 10, no. 1, pp. 523-538, Feb. 1995

[9] K. Morison, H. Hamadani, and Lei Wang, “Load Modeling for Voltage Stability Studies,” in Proc. 2006 IEEE PES Power Systems Conf. and Expo., pp.564-568.

[10] “Research on Load Modeling Considering Distributed Photovoltaic Generation”,October 30-November 1, 2020. Wuhan, China.

[11] “ Summary of Load Modeling Methods Considering Distributed Generation”, Energy Internet and Energy System Integration November 8-10, 2019. Changsha, China

[12] “Power Load Modeling Considering Load Lowvoltage Releasing Characteristics”,

[13] “IEEE Draft Guide for Load Modeling and Simulations for Power Systems ”

[14] “Composite Load Model and Transfer Function Based Load Model for High Motor Composition Load”

[15] Xinran Li, Renmu He, Wen Zhou, and Lingli Zhang, "The generalized induction motor model and its description ability to synthetic loads of electric power system," Automation of Electric Power Systems, vol. 23, no. 9, pp. 23-27, May. 1999.

[16] Taskforce, "Load representation for dynamic performance analysis [of power systems]," IEEE Transactions on Power Systems, vol. 8, pp. 472-482,1993.

IFERP connecting engineers...developing research
1st International Conference on Future of Engineering 2022

The Effect of Rear Wing Height on ground Vehicle Aerodynamics

Essam M. Metwalley[1]*, Mahmoud Ibrahim Youssef[2], Mahmoud Atef[3]

[1] Department of Automotive and Tractors Engineering, Faculty of Engineering, Helwan University, Mataria, Cairo, Egypt
E-mail: [1] emmorsy@hotmail.com, [2]mahmoudyusuf.1989@gmail.com, [3]mahmoudatef_1978@yahoo.com*

Abstract:
Aerodynamic characteristics play an important role on stability and fuel economics of a vehicle. Rear wing is a tool used inverted role on the rear end of vehicle model for generating negative lift and improving aerodynamic performance. Aerodynamic loads and flow characteristics for a vehicle, when the rear wing is placed, are been developed by computational model. The purpose of this paper is focusing the effect of the rear wing height that is investigated in four different positions. The relative angle of attack of the rear wing is equal in all configurations. Hence, the differences in the results are due to the influence of the rear wing position. ANSYS Fluent CFD are performed. An optimal vehicle downforce-to-drag ratio and drag-to-downforce ratio are obtained for the rear wing placed.

Keywords:
Aerodynamic loads, rear wing, CFD, downforce, drag

ABBREVIATIONS & ACRONYMS:

CFD: Computational Fluid Dynamics
b: The distance from the trunk to the wing leading edge,
h: Distance from the trunk to the roof of the vehicle
F_D: Drag Force
F_L: Lift Force
C_d: Drag coefficient
C_l: Lift coefficient
ρ: Density of air
A: Frontal area
V: Vehicle forward speed

I. INTRODUCTION

Nowadays, vehicle industry is the quickest growing industry with taking care of the cost of a vehicle, its performance and service (Bhagat, et al., 2014). The developing trend for vehicles with mid-range weight to allow better efficiency for fuel, reduction of emissions like CO2 and consumption of energy (Anyasodor, et al., 2017). Lightweight engineering is used to optimize weight; a 10% reduction in vehicle weight can result in an 8% to 10% increase in fuel efficiency. (Anyasodor, et al., 2017) (Makhmale, et al., 2016). Well design of a vehicle provides a reduction in the total weight and fuel consumption. In addition, the vehicle can travel at higher speed with better stability and road holding (Tsai, et al., 2009).

One of the important elements for a vehicle is its aerodynamics, which effects on its efficiency and performance by variation of drag force at high speed (Corno, 2015) (Shende, 2007). To get the data for improving the aerodynamics of vehicles, many researches and experiments have been carried out.
The drag force is produced by way of relative motion between air and vehicle with about 60% of total drag at the rear end. A wing is tool which is locate in sedan-based vehicle model at rear end for improving aerodynamic performance. Wing means the “ruin adverse air motion throughout a car body in movement” it is whenever effect on aerodynamic overall performance. Wing installed on the front end of the car is known as Air Dams whereas the wing on the rear end is called rear wing (Kumar, et al., 2013) (S. M Rakibul Hassan, et al., 2014) (Fereydoon Diba, et al., 2014).
ANSYS Fluent was used to build a virtual prototype and the performance of proposed and existing designs was simulated. The model is simplified by removing wheels and rear-view mirrors and the bottom portion of the car was assumed to be a flat surface (2011).
Two positive pressure areas can be found: one is at the front of the vehicle body, and the other is between the hood and the windshield. At the same time, high negative pressure areas can be found at the front and

rear end of the roof and a small area at the front end of the hood. It is believed that positive pressure at the bottom and negative pressure at top will make the rear portion of the car to lift up from the ground and reduce the pressure between the wheels and ground, which causes loss of steering on the front axle and loss of traction on the rear axle. Pitching moment is usually negative i.e. the nose down, and this makes the rear axle lift off the ground, which further reduces the available traction (Yash Oza, et al., 2017).

Rear wing is a tool used inverted role on the rear end of vehicle model for generating negative lift and improving aerodynamic performance. Wing is very effective for producing proper amount of down force is very important for improving aerodynamic overall performance. As the Bernoulli's effect states, the downward force is provided with the inverted wings aerodynamics. The generated downward force results in the growth in vertical pressure of the tire on ground (X, 2006) (salehi, et al., 2017).

With inverted wing configuration downward pressure distribution can be changed and result, plays a big role in crucial impact due to distribution and affects the driver's protection and handling of race vehicles. In a passively operating aerodynamic device, the wings configurations are decided on according to the type of circuit, race vehicle dynamic behavior, tire houses and the climate situation. The performance of wing depends on its height. Different heights will result in different drag and lift coefficient. The higher the wing height on the vehicle, the more effective the wing will be reducing the lift force but the drag coefficient will be increased. The active inverted wings potential has been tested in various applications of vehicle for increasing the experience for comfort, control of the pitch movement, improving the vehicle management, and enhancing its brake. The lift forces were managed by means of changing the perspective of attack angles momentarily and decided to mount the wing on the vehicle frame. Important factors like lift and drag should be considered while designing a vehicle (X, 2006) (Ramesh, 2014).

This paper presents a numerical analysis of the value of drag coefficient and lift coefficient at different wing heights and different speed by using ANSYS Fluent software. From the analysis results of drag force was calculated to determine the most effective height of wing to reduce drag force. This study was conducted to determine the most suitable height of wing with the most reduction of drag coefficient for the generic model.

II. METHODOLOGY:

A studied vehicle from thesis of Cakir is used in the analysis. The dimensions of studied vehicle are shown in figure 1. Small details of the vehicle geometry, as tires and mirrors, are not modeled. While modeling those details increases complexity of CFD computational domain. As they are not considered to influence the results and therefore the time necessary to perform the CFD computations (Cakir, 2012).

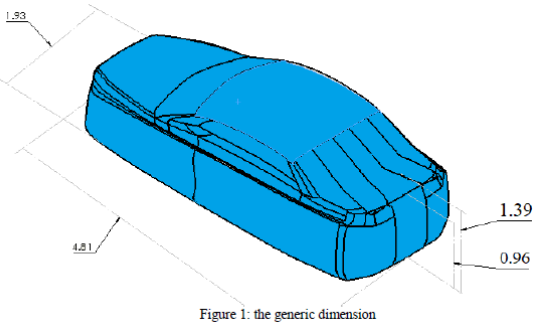

Figure 1: the generic dimension

The purpose of this paper is focusing on the effect of the rear wing mounting height on aerodynamic forces. In five different CFD computational models are created. One model without the rear wing and four models for various wing mounting heights. Figure 2 shows the studied vehicle together with different positions of the rear wing and show the variation of different heights of the rear wing (A. Buljac, 2015). Only one rear wing is considered at the time in each simulation.

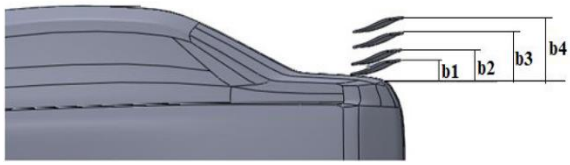

Figure 2: the generic model with four different mounting heights of the rear wing

Five 3D CAD models of the vehicle using Solidworks software are performed using CFD techniques. Computational 3D model is developed in Ansys Fluent 16.0 software. Figure 4 shows the 3D model (Akshay Parab, et al., 2014).

Figure 3: the 3D model by using SOLID WORK program

III. CFD:

CFD is the branch of fluid dynamics providing a cost-effective means of simulating real flows by the numerical solution of the governing equations (Abdelnaser, et al., 2018). It uses numerical methods and algorithms to solve problems that involve fluid flow. defined CFD as a set of numerical methods applied to obtain approximate solution of problems of fluid dynamics and heat transfer (V. Naveen Kumar, et al., 2013) (P. Ramasekhar Reddy, et al., 2017). CFD tool has three main components that is used to handle the object from the start point till analyzing the results. These components can be summarized a follow:

A. Pre-Processing:

This involves creating the geometry, computational domain and meshing. Meshing is to discretizing the computational domain into small control volumes, which are known as cells. The solution accuracy is a function of the number of generating cells in the computational domain.

B. The Solver:

This is the main part in the CFD simulation, where the flow governing equations will be discretized and solved.

C. Post-processing:

This is the final step in the CFD simulation process, which deals with extracting the important flow parameters such as velocity, density, pressure and forces. The simulation results will be compared to the experimental data and other numerical simulations. (Senan Thabet, et al., 2018)

Advantages of using CFD (Akhilesh Singh Tomar, et al., 2019)

1) Low cost
2) High number of iterations
3) Less time consuming
4) Real time simulations
5) Less error
6) Can examine various locations of vehicle

IV. MODELLING & VALIDATIONS:

By using ANSYS Fluent software, the vehicle (with and without wing) 3D CAD models are orientation according to geometry in the virtual wind tunnel with relevant dimensions as in table 1 and figure 4 (Lanfrit, 2005) (Cakir, 2012).

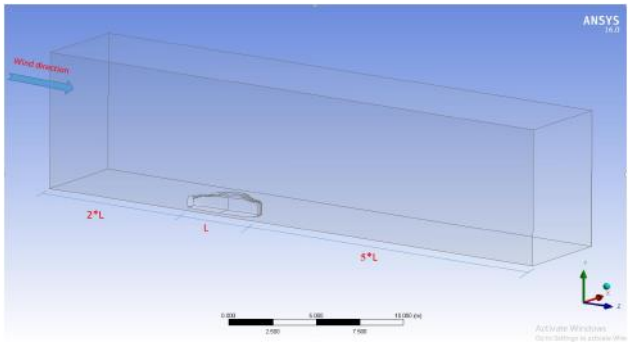

Figure 4: virtual wind tunnel dimensions

Table 1: virtual wind tunnel dimensions by using ANSYS Fluent Geometry Position

Position	Car front	Car rear	Car side	Car top
Dimensions (m)	2L= 9.62	5L= 24.05	L= 4.81	2L= 9.62

All 6 surfaces of the virtual wind tunnel (air-box) are named so the numerical solver of ANSYS Fluent could recognize them and apply the appropriate boundary conditions automatically. (figure 5)

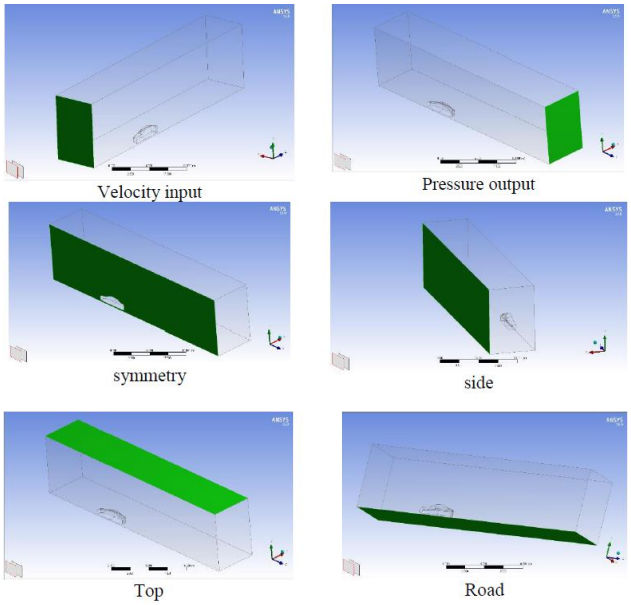

Figure 5 All 6 surfaces of the virtual wind tunnel

Next setup of CFD is ANSYS Fluent Meshing has generated the meshes with the sizing parameters (Cakir, 2012). Table 3 presents the mesh parameters and figure 6 shows the mesh property.

Table 2: mesh sizing properties

Global mesh sizing setting	
Use Adv. Size Fun.	On Proximity and Curvature
Relevance center	coarse
Curvature Normal Angle	12
Minimum Size	17.823 mm
Maximum Size	500 mm
Growth Rate	1.2 (20%)
Inflation	
Use Automatic Inflation	Program Controlled
Inflation Option	First Aspect Ratio

 ISBN: 978-93-92105-22-7

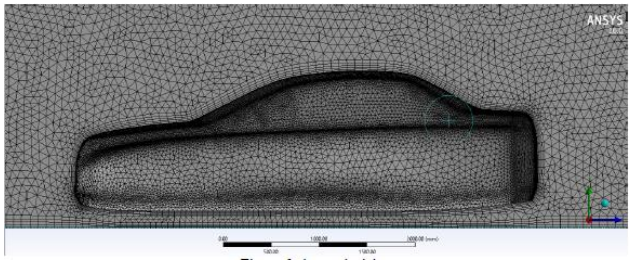

Figure 6: the mesh sizing

Once the virtual car-box was generated. Its mesh sizing was limited to 80mm with the "body sizing" functionality in the software. The new mesh became very detailed and ready to run in the solver (ANSYS, 2017) (Cakir, 2012). The relevant dimensions of the virtual car- box are given in the table 3. Figure 7 shows the virtual car-box orientation.

Table 3: virtual vehicle-box relevant dimensions Position

Position	Car front	Car rear	Car side	Car top
dimensions	L= 4.81	1.5L= 7.215	0.5L= 3.6075	1.5L= 7.215

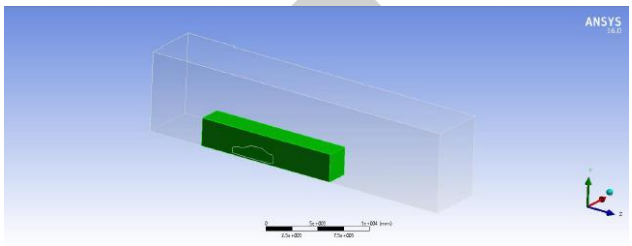

Figure 7: virtual vehicle-box orientation

The final meshing is presented in figure 8.

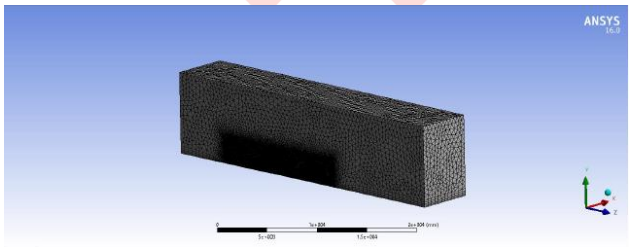

Figure 8: the final mesh

The final step is ANSYS Fluent Setup. The solver settings and boundary conditions for all cases are shown in the Table 4 (ANSYS, 2017) (Cakir, 2012).

Table 4: the solver setting Boundary Conditions Velocity Inlet Magnitude and Direction (m/s)

Boundary Conditions					
Velocity Inlet	Magnitude and Direction (m/s)	30.6	36.1	41.7	42.7
	Magnitude and Direction (km/h)	110	130	150	170
	Turbulence Specification Method	Intensity and Viscosity Ratio			
	Turbulence Intensity	1.00%			
Outlet pressure	Gauge Pressure Magnitude	0 Pascal			
	Gauge Pressure Direction	Normal to Boundary			
	Backflow Turbulence Intensity	10%			
Fluid properties	Fluid type	Air			
	Density	$\rho = 1.175\ kg/m^3$			
	Kinematic viscosity	$\nu = 1.8247 \times 10^{-5}\ kg/m.s$			
Viscous model	Turbulent model	k-ε (2-eqn)			
	k-ε Model	Realizable			
	Near-wall Treatment	Non-Equilibrium Wall Functions			
Pressure-Velocity Coupling					
Solver	Scheme	Coupled			
	Gradients	Least Squares Cell Based			
	Iteration	First Order Upwind for the first 100 iterations, Second Order Upwind until converged			
	Flow Courant Number	50			
Under-Relaxation Factors	Tur. Viscosity	0.8 for the first 100 iterations, then 0.95			

V. SIMULATION RESULTS:

- For the car only:

The primary results for the car model without wing was tested with four speeds. Table 6 shows the computer analysis of drag and lift coefficients and drag and lift forces at corresponding speed for the car model.

Table 5: results of the car only Speed

Speed V m/s	$Speed^2\ V^2$ (m^2/s^2)	Drag coefficient C_d	Drag Force	Lift coefficient C_l	Lift Force
30.6	936.36	0.24414	169.1198	-0.23327	-161.5899
36.1	1303.21	0.24825	239.3405	-0.22993	-221.678
41.7	1738.89	0.24497	315.1357	-0.22501	-289.4586
47.2	2227.84	0.24297	400.4509	-0.22228	-366.3507
average		**0.2451**		**-0.227623**	

- For the car model with four different heights of wing:

The same analysis was done with the same process and speed. Table 7 shows the drag coefficient and drag force obtained for each height of wing. Table 8 shows the lift coefficient and the lift force for each height of wings.

1) Drag force

Table 6: results of four different heights of a wing (drag coefficient and forces)

Speed V m/s	$Speed^2\ V^2$ (m^2/s^2)	The different heights of b, mm							
		b1= 76		b2= 170		b3= 273		b4= 371	
		C_d	D	C_d	D	C_d	D	C_d	D
30.6	936.36	0.222	153.6	0.1998	138.4	0.1867	129.3	0.18078	125.2
36.1	1303.21	0.222	213.7	0.1993	192.1	0.1864	179.7	0.1809	174.4
41.7	1738.89	0.221	284.7	0.1982	255	0.1867	240.1	0.18051	232.2
47.2	2227.84	0.222	365.9	0.1978	326.1	0.1864	307.1	0.18016	296.9
Average		**0.222**		**0.1988**		**0.1865**		**0.1805**	

(1) Lift Force:

Table 7: results of four different heights of a wing (lift coefficients and forces)

Speed V m/s	$Speed^2\ V^2$ (m^2/s^2)	The different heights of b, mm							
		b1= 76		b2= 170		b3= 273		b4= 371	
		C_l	L	C_l	L	C_l	L	C_l	L
30.6	936.36	-0.3225	223.4	-0.3377	233.9	-0.3183	220.5	-0.2948	204.2
36.1	1303.21	-0.3229	311.3	-0.3402	328	-0.3147	303.4	-0.2938	283.2
41.7	1738.89	-0.3265	420.1	-0.3449	443.7	-0.3153	405.6	-0.2938	377.8
47.2	2227.84	-0.3274	539.6	-0.3454	569.3	-0.3157	520.3	-0.2940	484.6
Average		**0.3248**		**0.3421**		**0.3160**		**0.2941**	

By comparing velocity magnitude (choosing the highest speed of 42.7 m/s) of with/without wing situations, (figure 9) it is seen that the recirculation zone behind the rear end of vehicle is different in all cases.

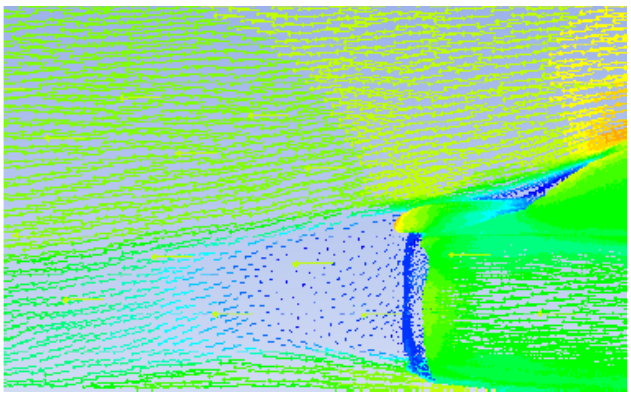

Car only

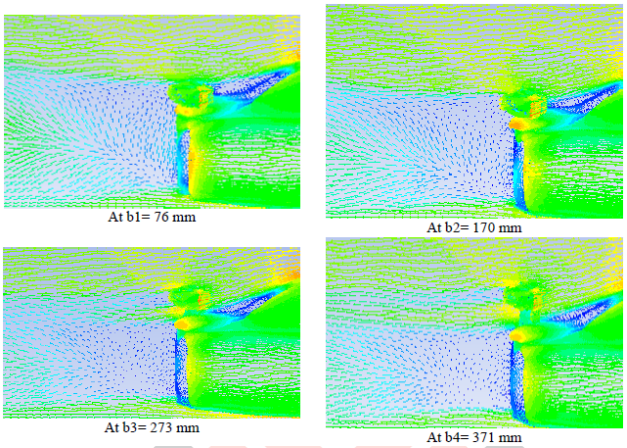

Figure 9: the velocity magnitude for all cases at 47.2 m/s

Based on the primary results, two graphs are plotted. Figure 9 is plotted according to the relation between drag force and $Speed^2$ in all cases. The drag force is directly proportional to the squared speed. This indicates that when speed was increased, the drag force also increased. Therefore, the results detected using five component balances for drag force was accepted.

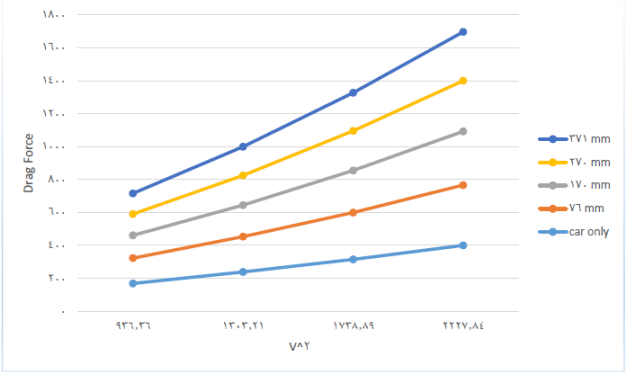

Figure 10: graphs of drag force vs. squared speed for all tests

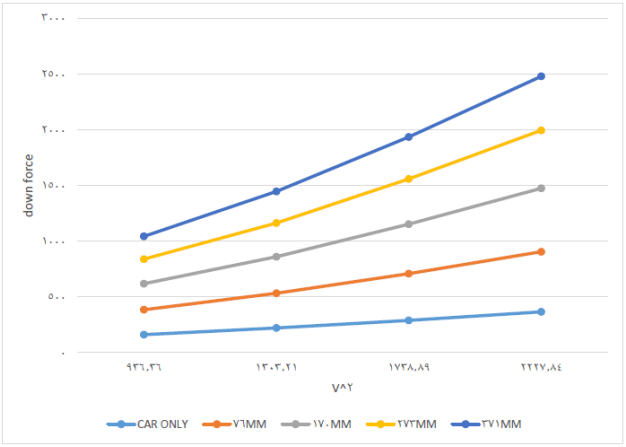

Figure 10: downforce force vs. $speed^2$ for all tests

In order to determine an optimal rear wing height with respect to drag and down force combined, the downforce-to-drag ratio and drag-to-downforce ratio are determined, figure 12,13. The optimal configuration is considered to be the one with large downforce along with the lowest possible drag force.

Table 8: downforce-to-drag ratio.

Speed V m/s	Car only	76mm	170mm	273mm	371mm
30.6	0.955	1.454	1.691	1.705	1.631
36.1	0.926	1.456	1.707	1.688	1.624
41.7	0.918	1.475	1.739	1.689	1.627
47.2	0.915	1.474	1.746	1.694	1.632

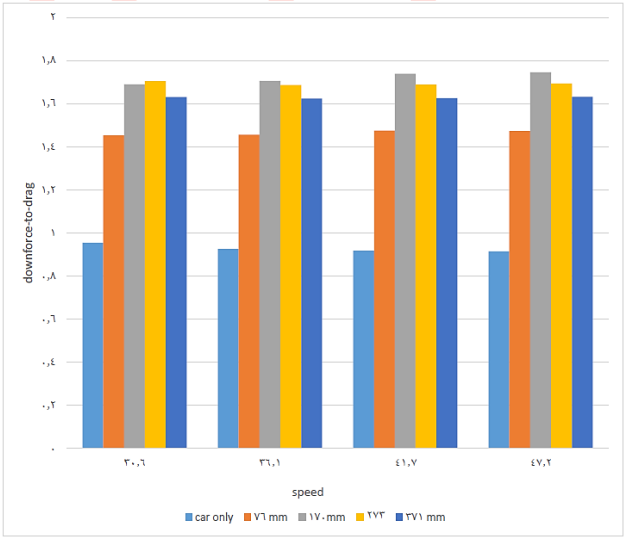

Figure 11: graph of downforce-to-drag ratio vs. speed for all tests

Table 9 drag-to-downforce ratio

Speed V m/s	Car only	76mm	170mm	273mm	371mm
30.6	1.046598828	0.687555953	0.591705857	0.586394558	0.613124388
36.1	1.079676377	0.686476068	0.585670732	0.592287409	0.615819209
41.7	1.088707332	0.677695787	0.574712644	0.591962525	0.614610905
47.2	1.093080756	0.678094885	0.572808712	0.590236402	0.612670243

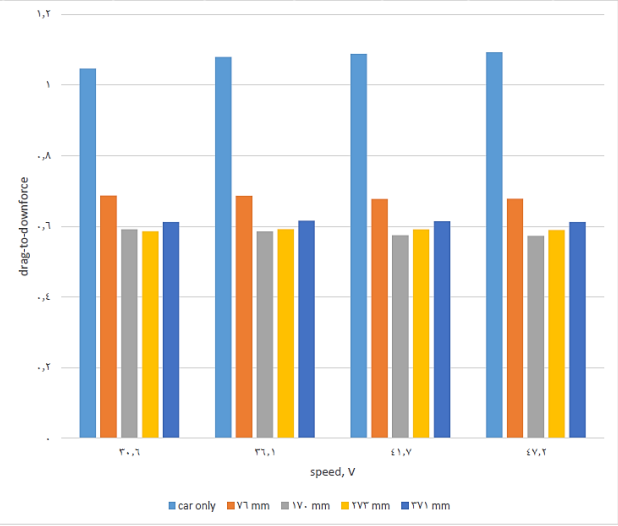

Figure 12 drag-to-downforce ratio vs. speed

According to figure 11 and figure 12, the car without a rear spoiler has a minimum value in figure 13 according to downforce-to-drag ratio and maximum values in figure 14 according to drag-to-downforce ratio. Otherwise, a car with a rear spoiler mount at 170 mm height has a maximum value in figure 13 according to downforce-to-drag ratio and minimum values at figure 14 according to drag-to-downforce ratio.

VI. CONCLUSIONS

The k-epsilon (2 eqn) model with realizable and non-equilibrium wall function is used to computationally study the impact of the height at which the rear wing is mounted on the aerodynamics of the vehicle. For the model with four different wing heights. ANSYS CFD Fluent has been used for every analyses. In all studied designs, the rear wing's ideal wind incidence angle is fixed in relation to the streamlines. In order to determine the height that provides the best position in terms of downforce-to-drag ratio and drag-to-downforce ratio, the results were compared with the model without a wing. The upper surface of the car trunk, at a height of 170mm, is found to be the ideal location for the rear wing. Maximum vehicle downforce-to-drag ratio of 1.746 is achieved at this position.

REFERENCES

[1] Automobile Bodies by Advance Material with Light Weight [Journal] / auth. Makhmale S. Asaram [et al.] // International Research Journal of Engineering and Technology. - 2016.

[2] A Review Analysis and Optimization of Car Bonnet [Journal] / auth. Bhagat R. Y. and A. P. More // International Journal of Innovative Research & Development. - 2014. - pp. 52-55.

[3] Aerodynamic Analysis of a Car Model Using Fluent-Ansys 14.5 [Journal] / auth. Akshay Parab [et al.] // International Journal on Recent Technologies in Mechanical and Electrical Engineering. - 2014. - 2349-7947 : Vol. 1. - pp. 7-13.

[4] aerodynamic Analysis of an Active Rear Split Spoiler for Improving Lateral Stability of High-Speed Vehicles [Journal] / auth. Ayyagari D. T. and He. Y. // International Journal of Vehicle Systems Modelling and Testing. - 2017. - Vol. 12. - pp. 217-239.

[5] An Experimental Investigation to Control the Flow Emerging from a Wide Angle Diffuser [Journal] / auth. Shende M. D. // IOSR Journal of Engineering. - 2007. - pp. 27-32.

[6] ANSYS Fluent 12.0 Theory Guide, [Online]. - July 26, 2011. - http://www.cadfamily.com/downinfo/285585.html.

[7] ANSYS FLUENT Theory Guide [Book] / auth. ANSYS Inc.. - U S A : ansys.com, 2017.

[8] Automobile Aerodynamics Influenced by Airfoil-shaped Rear Wing [Book] / auth. A. Buljac I. Korade, S. Krizmanic and H. Kozmar. - croatia : international journal of automotive technology, 2015.

[9] Automobile Aerodynamics Influences by Airfoil-Shaped Rear Wing [Journal] / auth. Andrija Buljac and Hrvoje Kozmar // International Journal of Automotive Technology. - 2016. - Vol. 17. - pp. 377-385.

[10] Best Practice Guidlines For Handling Automotive External Aerodynamics with Fluent [Journal] / auth. Lanfrit Marco // Fluent Deutschland GmbH. - 2005.

[11] CFD Analysis on Aerodynamic Effects on a Passenger Car [Journal] / auth. P. Ramasekhar Reddy and R. Lokanadham. - [s.l.] : International Research Journal of Engineering and Technology, 2017. - 09 : Vol. 4.

[12] CFD Analysis on the Aerodynamic Effects of Spoiler at Different Angle on Car Body [Journal] / auth. Akhilesh Singh Tomar [et al.]. - [s.l.] : International Journal of Innovative Technology and Exploring Engineering, 2019. - 7 : Vol. 8.

[13] CFD Simulation of the Air Flow Around a Car Model (Ahmed Body) [Journal] / auth. Senan Thabet and Thabit H. Thabit. - [s.l.] : International Journal of Scientific and Research Publications, 2018. - 7 : Vol. 8.

[14] CFD Study on Aerodynamic Effects of a Rear Wing/Spoiler on a Passenger Vehicle [Book] / auth. Cakir Mustafa. - [s.l.] : Mechanical Engineering Master Theses, 2012.

[15] CFD study on Aerodynamic Effects of a Rear Wing/Spoiler on Passenger Vehicle [Book] / auth. Cakir Mustafa. - 2012.

[16] Computational Fluid Dynamics Modelling of an Aerodynamic Rear Spoiler on Cars [Journal] / auth. Abdelnaser S. [et al.]. - [s.l.] : Nigerian Journal of Technology, 2018. - Vol. 37.

[17] Comutational Aero-Acustic Analysis of a Passenger Car With a Rear Spoiler [Journal] / auth. Tsai Chein-Hsiung [et al.] // Applied Mathematical Modelling. - 2009. - 3661-3673 : Vol. 11. - pp. 3661-3676.

[18] Design and Analysis the effect of rear spoiler and diffuser on Aerodynamic Forces using CFD
[19] [Journal] / auth. Ramesh K. // International Journal For Research in Engineering Science and Technology. - 2014. - Vol. 1. - pp. 29-34.
[20] Effect of Rear Spoiler and Diffuser Angle on Aerodynamic Characteristics of a Sedan [Journal] / auth. Md. Saifur Rahman and Khushbu Yadav // International Journal of Research in Engineering. - 2018. - 2250-0588 : Vol. 8. - pp. 105-117.
[21] Effects of Spoiler on Aerodynamic Analysis for Proton Persona by Experimental [Journal] / auth. N. Q. A. Aziz M. N. Musa. - 2015.
[22] Enhancement of Aerodynamic Characteristics in Automobiles [Conference] / auth. Kumar K. Sathish and C. S. Rajamanicham. - [s.l.] : International Conference on Energy Efficient Technologies for Sustainability, 2013.
[23] Experimental Study of Open-Wheel Race-Car Front Wings [Journal] / auth. Jaisinski W. and Selig, M. // SAE paper 983042. - 1998.
[24] Ground Effect of Aerodynamics of Race Cars [Journal] / auth. X J. Zhang // App. Mech Rev.. - [s.l.] : App. Mech Rev, 2006. - pp. 33-49.
[25] Handling and Safety Enhancement of Race Cars Using Active Aerodynamic Systems [Journal] / auth. Fereydoon Diba, Ahmed Barari and Ebrahim Esmailzadeh. - [s.l.] : International Journal of Vehicle Mechanics and Mobility, 2014. - Vol. 52.
[26] Industerial Based Volume Manufacturing of Light Weight Aluminium Alloy Panel Components with High Strength and Complex-Shape for Car Body and Chasis Structures [Conference] / auth. Anyasodor G. and C. koroschetz. - [s.l.] : Journal of Physics, 2017.
[27] Investigation of Drag and Lift Forces Over the Profile of Car with Rear Spoiler Using CFD [Journal] / auth. V. Naveen Kumar [et al.]. - [s.l.] : International Journal of Science and Research, 2013. - 9 : Vol. 4.
[28] Model of Car Wing Active Control in Order to Increase Stability of the Car on Corners of Roads [Conference] / auth. salehi M., M. A. Khanesar and F. Farivar. - [s.l.] : International Conference on Automatic Control and Dynamic Optimaization Techniques, 2017.
[29] Numerical Study on Aerodynamic Drag Reduction of Racing Cars [Conference] / auth. S. M Rakibul Hassan [et al.] // 10th International Conference on Mechanical Engineering. - [s.l.] : science Direct, 2014. - pp. 308-313.
[30] Performance Assessment of Active Aerodynamic Surfaces for Comfort and Handling Optimization in Sport Cars [Journal] / auth. Corno S. Matteo // Transactions on Control System Technology. - 2015. - Vol. 1.
[31] Race Car Aerodynamics [Book] / auth. Katz J.. - [s.l.] : Robert Bently, Inc., 1996.
[32] Review on Vehicle's Aerodynamic Drag Reduction [Journal] / auth. Yash Oza [et al.] // International Journal for Science Research & development. - 2017. - pp. 481-486.
[33] To Design Active Spoiler of High Speed Car to Swell Stability by Using CFD-Aerodynamics Analysis [Journal] / auth. Rajyagura Pranav // International Research Journal of Engineering and Technology. - 2017. - Vol. 4. - pp. 1678-1684.

IFERP®
connecting engineers...developing research
1st International Conference on Future of Engineering 2022

Effect of the Inlet-Outlet Key Slope of PKW and Channel Bed Slope on Its Discharge Capacity

Deepak Singh[1], Munendra Kumar[2]

[1] Research Scholar, Department of Civil Engineering, Delhi Technological University, New Delhi, India
[2] Professor, Department of Civil Engineering, Delhi Technological University, New Delhi, India
Email: [1]kumaindeepaksingh@gmail.com, [2]mkumar66@gmail.com

Abstract:
A Piano Key Weir (PKW) is a type of nonlinear (labyrinth-type) ungated spillway with a relatively small spillway footprint. PKWs have a large number of geometric parameters that affect the head-discharge performance of the weir. Several previous studies associated with the hydraulic design of PKWs based on geometrical parameters have significantly discussed the parameter's importance. However, it still requires more in-depth research to refine further these findings and their role in the efficient design of PKW. In this study, an experimental investigation has been carried out to determine the optimal slope of the inlet-outlet key floors of PKW and also see the effects of channel bed slope on the discharge efficiency of the PKW. To this end, twelve different inlet-outlet key slope's laboratory-scale type-A PKW models were tested, while all other geometrical parameters were kept constant. The results showed that, as the slope of inlet-outlet key bottoms of PKW increases, the hydraulic performance of the weir enhances up to certain key slopes, then it declines, which is consistent with past literature. According to the present study results, the optimal key bottom slopes of PKW range between 1 and 1.1, which is more specific to previous studies. Moreover, the slopes of the channel bed significantly affect the PKW's discharge efficiency and found that, as the slope of the channel bed increases, the discharge efficiency of PKW enhances with a low Ht/P ratio of around 50-60%, while it increases by 18-20% for higher values. In addition, the experimental data of the present study were used to validate the analytical approach, and it appears that the experimental and analytical techniques are in good agreement.

Keywords:
Spillway, inlet and outlet key slopes, the discharge capacity, channel slope effect, weir head, velocity head

I. INTRODUCTION

Piano Key Weir (PKW) is an ungated spillway, and it allows the operation of the reservoirs with elevated supply levels without causing any damage to the dam structures, thereby providing additional storage. Blanc and Lempérière [8] developed a fiction weir type (named PKW) over the traditional labyrinth weir's evolution. Further, Lempérière and Ouamane [35] examined the combined benefits of a labyrinth weir along with overhangs to facilitate the weir location on a dam crest. PKW is a low-cost solution for spillway rehabilitation in existing and new dam projects with budget constraints (i.e., limited foundation space, high specific flood discharge, small reservoir level, etc.) [5, 35, 42]. Many researchers concluded that the labyrinth and PKWs are folded in plan-view. This favorable geometrical benefit enhances the weir's total development crest length without affecting the channel width [29, 32]. PKWs have higher discharge efficiency than the labyrinth weir or other rectilinear weir, mainly because the development crest length of the PKW is much higher than the transverse weir width. They also have the slanted inlet-outlet keys floors rather than the vertical-horizontal arrangement of labyrinth weirs that upgrade their water-powered or hydraulic effectiveness. This characteristic of PKWs makes it an economical and attractive solution over its alternatives and facile establishment on the top of existing or new concrete gravity dams [4, 52]. PKW also needs less reinforced concrete volume than labyrinth weirs due to its smaller footprint [38]. Compared to symmetric overhangs, the solution without downstream overhang saves around 10%, and structural efforts are less critical for broad specific discharge. As a result, this may be the most attractive alternative for several large dams [48]. According to Paxson et al. [49], the PKW is an optimal solution for enhancing the existing dam's discharge and storage capacity compared to gated spillways and labyrinth weirs.

The first PKW construction was completed in 2006 in France at Golours dam by Electricite de France (EDF) to enhance its discharge efficiency or capacity [28]. Further, EDF installed the PKWs on three other existing dams, namely St. Marc (2008), Etroit (2009), and Gloriettes (2010). The studies on PKW development were also conducted in Vietnam [25], India [54], and France (Gage, Malarce, and La Raviege Dam). Schleiss [53], Lempérière et al. [38], Abhash & Pandey [1], and Singh and Kumar [56] provided a detailed historical overview of the construction and design of labyrinth and PKW weirs and investigated whether the PKW is a better option for dam rehabilitation. Presently, more than 35 PKW structures have been successfully built worldwide in numerous countries, including India, Australia, Vietnam, Sri Lanka, France, Switzerland, the UK, South Africa, and Algeria [13, 14]. The first PKW was recently installed to increase reservoir pondage and spillway capacity at South Africa's Hazelmere dam, and the construction of PKW at the existing Tzaneen dam is also set to begin soon [10, 30, 39].

The hydraulic behavior of PKW is highly intricate due to its three-dimensional flow nature. Hence, most prototype activities were planned, designed, or developed based on physical demonstration [11, 15, 18, 28, 32]. Several studies have been carried out in the last ten to fifteen years [4, 13, 20, 27, 44] based on geometric development to identify the hydraulic behavior of PKW, and now it is well understood. The different worldwide studies based on the geometric evolution and hydraulics of PKW have been summarised by Erpicum et al. [17, 19, 22] with three reference books. However, the transient behaviour of PKWs is not so well comprehended and is the major focus of several ongoing studies.

Similarly, the downstream flood characteristics of a PKW have not been thoroughly investigated; to date, only several studies have discussed the downstream aspects of PKWs. Bieri et al. [7] state that PKW or spillways can effortlessly join with stepped chutes, decreasing downstream energy dissipation. The PKW's energy dissipation is not linear and more at a low head [23, 55]. According to Jüstrich et al. [26], residual flow energy will cause scour in an alluvial river bed if no prevention structure (e.g., dissipation basin) is constructed downstream of a flow control structure. Furthermore, Pfister et al. [50] examined the scouring behaviour at PKW's toe. They found that if a rock foundation is not possible, scouring occurs at the PKW's toe, which is relevant to weir stability during the flood. The efficient passage of sediment is critical in preventing floods upstream of the PKW and ensuring the waterway's navigability [45].

Pralong et al. [51] described the most commonly used parameters related to the PKWs and outlined them to describe the weir comprehensively. The key parameters relating to physical dimensions are depicted in Figure: 1.

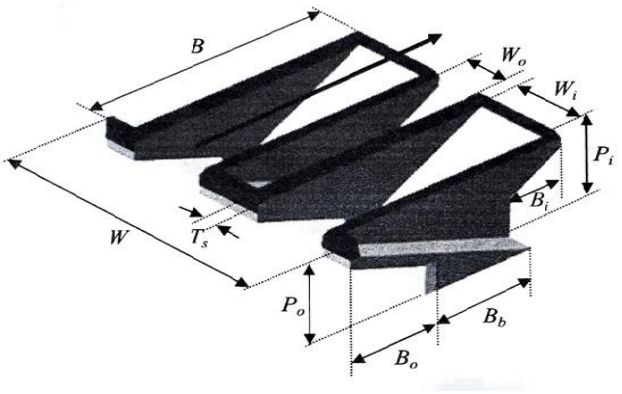

Figure: 1. Fundamental parameters of a PKW – 3D view (Pralong et al. 2011).

Lempérière et al. [38] described the different types of PKWs based on overhangs, which hydro-coop studied since 1998. Several researchers have divided the parameters associated with PKWs (geometrical and flowing parameters) into primary and secondary categories. Primary parameters significantly influence the hydraulic performance of the weir, such as L/W ratio, H_t/P ratio, weir height (P), etc. Secondary parameters, such as the inlet to outlet key width ratio (Wi/Wo), relative overhangs (B_i/B or B_o/B), parapet wall height (R), and weir crest shape, have a more minor but still significant effect on the hydraulic efficiency of the weir [3, 12, 32, 33, 40].

The height or inlet-outlet key floor slope of the PKWs is the most efficient influencing parameter [31,40]. The minimum slope ratio of inlet-outlet key floors should be 2H: 1V reported by Lempérière and Jun [36]. Ouamane and Lempérière [47] suggested that expanding the height of PKW by 25% improved efficiency by 6%. The increase in floor slope from 2:1 to 3:1 (horizontal: vertical) can result in a 20% increase in discharge efficiency (for large H_t/P values) to Barcouda et al. [6]. The best slope for the inlet-outlet key of PKWs is to be 1.8:1(horizontal: vertical) [37]. Machiels et al. [40] state that weir evacuation capacity increases as inlet key height increases. In addition, Machiels et al. [41] presented the effect of varying inlet-outlet key slopes (wide range of slopes from 0.25 to 1.5, height over length) on PKW's capacity. They observed that increasing weir height improves discharge efficiency, but increasing slope has little effect if slopes are greater than 1.2 (V: H).

In general, the literature indicates that as the height and slope of key floors of the PKW are increased, the

discharge efficiency of the PKW increases. Including the parapet wall over the top of PKW is vital in upgrading the weir height and storage capacity without expanding the overhangs [31, 43]. Few studies have shown that placing a parapet wall of a certain size on the upstream crest of the outlet key increases the discharge capacity of PKWs, while adding the parapet wall on the downstream crest of the inlet key has a marginal effect on PKW discharge efficiency [43]. In addition, Leite Ribeiro et al. [31] presented a model-based study on the Etroit dam. They concluded that by enhancing PKW's height, roughly 1 m (in the prototype) with a parapet wall, the discharge capacity increased up to 15 %.

This study was undertaken to understand better how the inlet-outlet key slopes, with horizontal and sloping channel beds, influence the PKW discharge efficiency by conducting a series of laboratory experiments over 12 laboratory-scale PKW models (see Table: 1) under free-flow conditions. The tests were conducted or designed based on the channel flow approach; thus, the limitation of the current investigation covered mainly PKWs built as a control structure in a canal or at river barrages.

II. EXPERIMENTAL SETUP

The tests were conducted in a laboratory-scale flume of (10m, long X 0.516m, wide X 0.6m, deep) in the FM&HE Laboratory at Delhi Technological University, Delhi, India. Water is pumped by a 20 Horse Power pump connected via a pipe network that includes calibrated orifice meter (± 0.25% uncertainty), a flow regulating valve to control the discharge, and a 4-20mA electromagnetic flowmeter (accuracy ± 0.2%) (see Figure: 2).

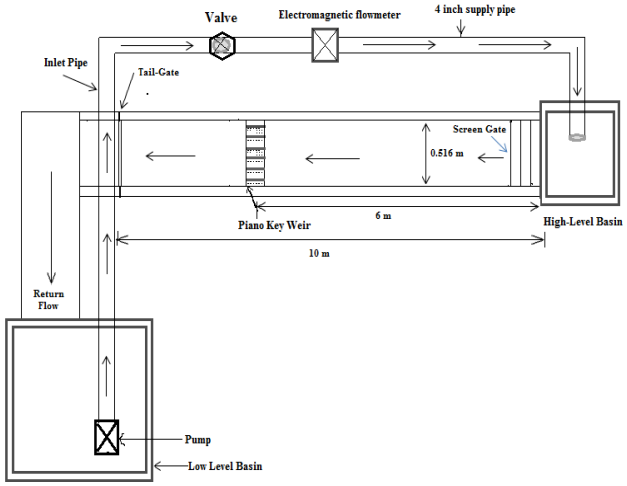

Figure: 2. Schematic plan view of the experimental setup.

The flume headbox featured a metal screen gate to improve upstream approach flow uniformity. A transparent acrylic sheet equips the flume to facilitate flow visualization. A 4-20 mA ultrasonic level sensor is attached to the flume (± 0.2% accuracy) and a pointer gauge with the least count of 0.1mm for the head over the weir crest. The average flow velocities were measured using an ADV (Acoustic Doppler Velocimeter). All models in this research were created with an 8 mm (thickness) transparent acrylic sheet and affixed with chloroform. The model's specifications are as follows: the width ratio (W_i/W_o) is 1, the length/width ratio (L/W) is 5, and the two overhang portions (B_i=B_o) are identical and equal to half of the model's base length B_b. The height of the models varied from 0.075 m to 0.35 m (or key slopes $0.3 \leq (S_i=S_o) \leq 1.4$) without increasing the overhang portions (see Table:1). The flowing rate (Q) was varied (0.0025 - 0.050) m^3/s, the head and head to weir height ratio ranged $0.0072\ m \leq H_t \leq 0.11m$, $0.04 \leq H_t/P \leq 1.2$, respectively, and other parameters were varied $0.28 \leq \{B_i/P = B_o/P\} \leq 1.6$.

All models were placed lateral to the testing flume, and experiments were carried out with both horizontal and sloping beds. In order to improve accuracy, the h_t values were measured by the ultrasonic level sensor as well as a pointer gauge (least count ± 0.1 mm) at a distance $X = 2\times P$ (see Figure: 3) from the lateral centreline of the PKWs [46] after the water surface had been allowed to settle for at least 3 to 5 minutes, or it can increase for higher flow rates.

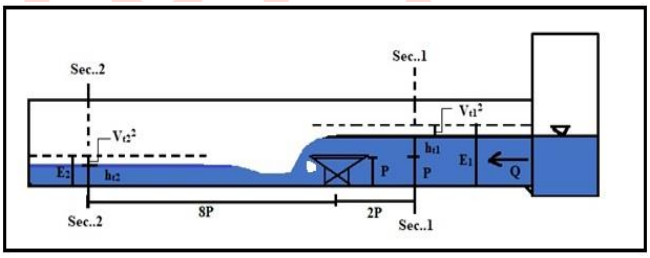

(a)

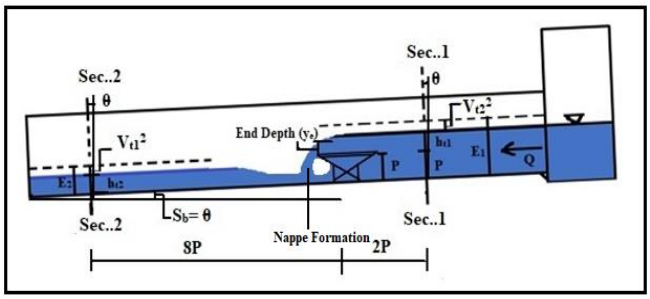

(b)

Figure: 3. (a) & (b) Schematic plot for total energy head measurement (For horizontal and slopping bed).

The mean velocity V_t was calculated as the average velocity measured at the same cross-section at 0.25, 0.5, and 0.75W across the width W of the flume each

for one-minute records using a Sontek ADV. The results of the velocity analysis revealed agreement between these average cross-sectional velocities and mean approach velocities (by ADV), resulting in a difference in H_t of less than 5% for the Q ranges.

III. METHODOLOGY

The discharge coefficient of PKW is computed based on developed length as follows:

$$Q = Q_{PKW} = \frac{2}{3} C_{DL} L \sqrt{2g} H_t^{3/2} \quad (1)$$

C_{DL} is the coefficient of discharge computed along the crest length, and L is the total developed crest length [34]. The total discharge over the nonlinear weir is dependent on various geometrical and hydraulic parameters, as shown in Eqn. (2): [27].

$$Q_{PKW} = f(\rho, g, \mu, \sigma, V_t, H_t, L, P, P_b, W, W_i, W_o, B, B_i, B_o, B_b, S_i, S_o, T_s, R, N) \quad (2)$$

Where Q_{PKW} is the total flow rate over the PKW; ρ is the fluid density; μ is the dynamic viscosity; σ is the surface tension of the flowing liquid; and g is the acceleration of gravity. H_t is the total upstream hydraulic head $(h_t + V_t^2/2g)$ over the PKWs, where h_t is the head available over the weir crest and $V_t^2/2g$ approach velocity head at the same locations.

The other parameters are associated with the geometry of PKWs, where L represents the total developed crest length (For one cycle, the developed crest length = W_i+W_o+2B). P represents the weir height; P_b has flowed approach depth; W represents the weir's channel width or total width, and the widths of the inlet and outlet keys are defined by W_i and W_o correspondingly. $B = (B_i + B_b + B_o)$, is defined as the total length of the side weir (side view), where B_i and B_o are two overhang portion's lengths, respectively, and B_b is the base length. The inlet and outlet keys floors slopes are S_i and S_o, respectively. T_s is the thickness of the sidewall, R represents the parapet height, and the number of cycles or units is N.

The discharge coefficient (C_{DL}) of the PKW is the function of various geometrical and hydraulic parameters and can define as follows: (Using the dimensional analysis)

$$C_{DL} = f\left(\frac{H_t}{P}, \frac{L}{W}, \frac{W_i}{W_o}, \frac{S_i}{S_o}, \frac{P}{P_b}, \frac{B_i}{B}, \frac{B_o}{B}, \frac{T_s}{R}, F_r, R_e, W_e\right) \quad (3)$$

F_r, R_e, and W_e represent the Froude number, Reynolds number, and Weber's number. As that flow regime upstream of weirs built right angles to the river course is almost always subcritical, the Froude number is not considered when assessing their hydraulic properties. Considering studies associated with the discharge capacity of PKWs, several researchers have compared the PKW efficiency in terms of discharge enhancement ratio (r). (Where r is the ratio of flow over PKW Q_{PKW} to flow over sharp-crested weir Q_W).

$$r = \frac{Q_{PKW}}{Q_W} = \frac{C_{DL}\sqrt{2g}\, L H_t^{3/2}}{C_S \sqrt{2g}\, W H_t^{3/2}} \quad (4)$$

The value of C_s (discharge coefficient for sharp-crested weirs) is assumed to be constant at 0.42 [24].

IV. RESULTS & DISCUSSIONS

The flow behavior through the PKW congregates in the inlet key and deviates away from the outlet key [42]. The total discharge over the weir is a combination of three discharges; discharge through the inlet keys, outlet keys, and through the side crest walls, and as a result, all discharges meet in an intricate flow (see Figure: 4). The water from the weir's side crest flows to the outlet key to raise the head, and the flow level rises due to the intermingling of the flow in the outlet key. Consequently, the submergence would occur near the outlet key. And the hydraulic efficiency decreases due to submergence until the two nappes commonly interfaced with each other and formed a solitary nappe making it like a straight linear weir.

Figure: 4. Flow pattern over PKW.

In this study, the discharge coefficient was calculated using the total development crest length, and the head over the weir was considered the total hydraulic head [$H_t = h_t + (V_t^2/2g)$]. In the current study, the hydraulic head-to-weir height ratios ranged from 0.04 ≤ H_t/P ≤ 1.2, at which some H_t readings are smaller than 0.03 m [21], implying that the scale effect plays a role in these critical area's values. In that case, more than one model law comes into the picture (i.e., Reynolds number (R_e), as well as Weber number (W_e), have also come along with Froude number (F_r) to influence the discharge capacity of weir structures). Erpicum et al. [21] presented a detailed study about the scale effects consideration over PKWs. Large-scale variables are considered when developing physical models (small dimensional models). The flow characteristics of such models may be affected by unscaled parameters such as atmospheric pressure, water viscosity, and surface tension. Weir crests at low overflow depths will show scale effects

due to viscosity and surface tension that is very difficult to scale. As a result, scaling fails to achieve model-to-prototype similarity. These variations are referred to as size-scale effects. These variations can affect the stage-discharge correlation, nappe course, and air entrainment [57]. Tullis et al. [57] evaluated that the total head over the PKW and scaled-to-prototype (for scale-ratio 1:3) head thresholds are (*Ht/P*) 0.09. In the present study, the head-to-weir height ratio H_t/P is divided into three categories to identify the impact of surface tension and viscous effects on PKW; (i) Low head ratio ($0.04< H_t/P \leq 0.09$), (ii) Medium head ($0.10 \leq H_t/P \leq 0.35$) (iii) High head ratio ($H_t/P > 0.35$), and to see the hydraulic performance of the weir in terms of flow initiation, nappe aeration, and trajectory behaviors. The detailed discussion follows in the subsections that follow.

The present study's data was assessed in two ways: (i) The effect of the PKW's sloping key bottom on its discharge capacity with a horizontal bed and (ii) the effect of the PKW's sloping key bottom on its discharge capacity with a sloping bed.

IV. (i) Effect of the PKW's sloping key bottom on its discharge capacity with horizontal bed

This study aims to determine the optimal slopes for the inlet-outlet key bottom of the PKW and compare the findings to previously published data. To this end, 12 laboratory-scaled PKW models were tested with a horizontal channel bed, and the discharge coefficients were calculated using Eqn. (1). After assessing data, results were plotted and analyzed between the various design characteristics parameters, as shown in Figures: (5 to 9). Figure: 5. depicts the stage-discharge relation (with head and relative head H_t/P) over the PKW weir crest for different inlet-outlet key slopped models.

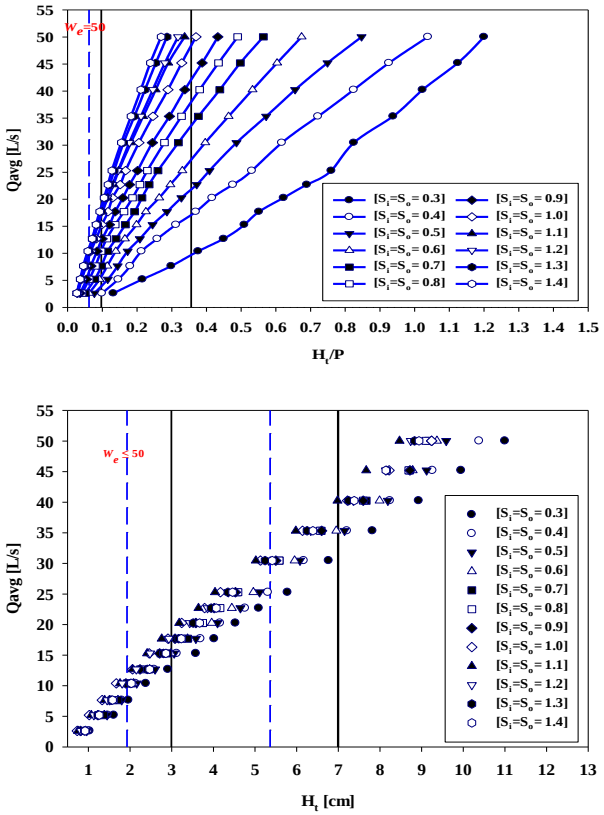

Figure: 5. Variation of discharge [*Q*] with [H_t/P] and [H_t].

During the investigation, it was noticed that the surface tension effects have more prominent in the most miniature model than in larger models at low heads. Variations in air entrainment were also seen over the different key slopped models with varying the upstream head, and the air entrainments influence the discharge capacity of the weir. Surface tension and viscous forces at the crest-water-air interface come into play at a shallow head ($H_t/P \leq 0.06$), and no discharge over the weir exists for a few seconds. Then later, for the same head, flow passes or is initiated (but limited) over the weir along with less air entrainment, and water adheres to the downstream of the inlet key. Similar flowing effects were observed by Machiels [42]. When the head is sufficiently high to overcome surface tension everywhere, the entire crest is involved in discharge conveyance. Air entrainment increases at higher heads/discharges, and fully aerated nappe intermingling with leaping nappe is observed. The variation of the air entrainment for the different heads is shown in Figure: 6.

Figure: 6. Shows the surface tension effects to jet trajectory formation from (a) to (d) on Largest models and from (i) to (iv) on Smallest models.

According to the current research, the minimum H_t/P at which the entire crest engaged to convey the discharge at a small shape of nappe with a radius of 0.005m-0.10 m was between 0.06-0.09 (or H_t ranges 0.02-0.03 m, because some models fully conveyed discharge at 0.02 m while others engaged fully at 0.03 m head). It means in the present study, the head thresholds value above which the scale effect has been considered negligible are $H_t/P \geq 0.09$. The clear nappe or jet trajectory was visible at a minimum H_t/P ratio of 0.22-0.26 (H_t range 0.05-0.06 m), as illustrated in Figures 5 and 6.

The discharge coefficients (C_{DL}) for each weir setup have been evaluated over the range of $0.01 \leq H_t/P \leq 1.2$, as shown in Figure: 7. (a) & (b). The results demonstrate that as the inlet-outlet key's slope increases, the hydraulic efficiency of PKW increases to a certain slope then starts decreasing. The PKW discharge efficiency increases at $H_t/P<0.24$ for all models, while decline trends were observed in almost all models at $H_t/P \geq 0.24$. However, a closer look at Figure: 7 (a) reveals that the peak is ranged between $0.2 \leq H_t/P \leq 0.25$. Figure: 7. (b) shows that the coefficient of discharge (C_{DL}) has a rising trend at low release and a decreasing trend at high discharge. The peak was observed corresponding to the discharge range between 10-15 L/s. This point concludes that the PKW is more efficient at low discharges/heads; as the discharges/heads increase, the efficiency gradually or abruptly decreases.

A comparison of rating curves between the sharp-crested weir and the PKW is required to improve efficiency in terms of enhancement ratio '*r*,' and the H_t/P ratio of the various key slopped PKW models as shown in Figure: 8.

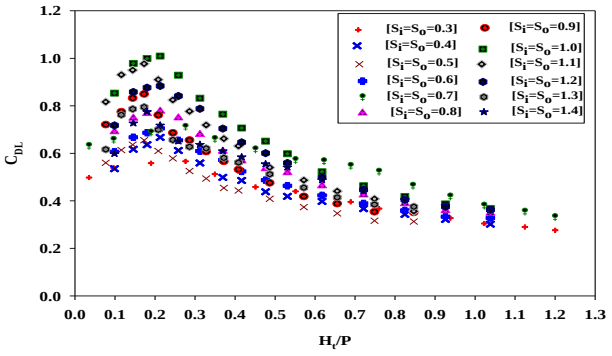

(a)

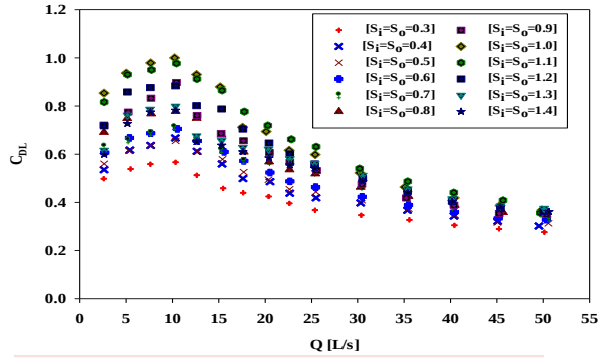

(b)

Figure: 7. (a) & (b). Shows the variation of discharge coefficient [C_{DL}] with [H_t/P] and [Q].

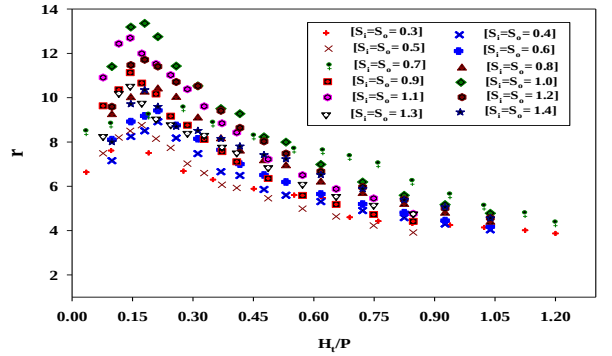

Figure: 8. Variation of discharge enhancement ratio [r] with [H_t/P].

 ISBN: 978-93-92105-22-7

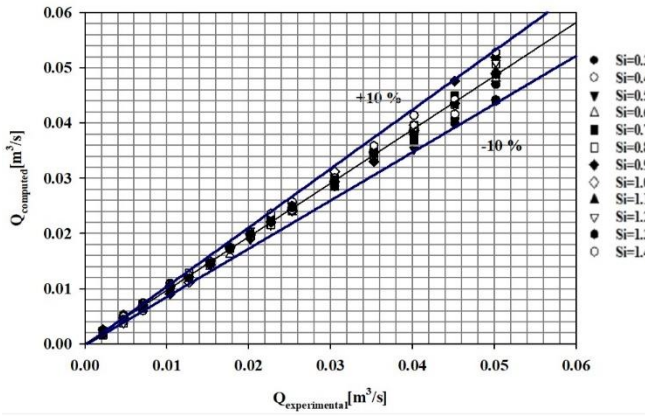

Figure: 9. Comparison of discharge computed using an equation given by Machiels et al. (2011c) and experimental results of the present study.

During the investigation, it was noticed that the enhancement ratio increases up to a particular sloped value, then shows a declining trend. However, a closer look at Figure: 8. reveals that the maximum enhancement ratio '*r*' is observed at $H_t/P \approx 0.18$, which corresponds to the key slope ($S_i = S_o = 1$), then follows the key slope ($S_i = S_o = 1.1$). The optimal range of the key slopes lies between 1 and 1.1 and shows better efficiency than the sharp-crested weir for all the tested model sets (i.e., $r \geq 1$ for each model).

The test results were compared with the design equations or methodology developed by Machiels et al. [40], which had tested seven different key sloped models. The first comparison of *Q* was computed with the help of equations developed by Machiels et al. [40], and *Q* was experimentally measured for the present study. It emphasizes that the analytical approach reaches the experimental results of the current research with an accuracy of within 10 % (see Figure: 9). Therefore, the present experimental study herein shows good agreement with the published data. The second comparison is specific to inlet-outlet key slopes, where the *Q* vs. H_t data collected for various slopped models herein were compared to a previously published study by Machiels et al. [40].

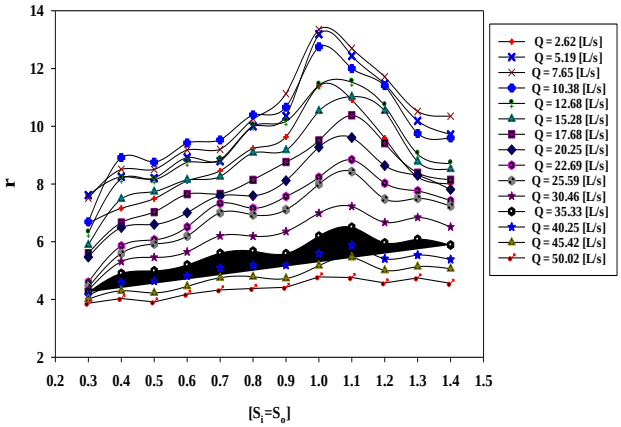

Figure: 10. Variation of discharge enhancement ratio [*r*] with various inlet-outlet key slopes [$S_i=S_o$] of PKW.

The comparison of *Q* for measured H_t values was made by computing the mean absolute percentage error (MAPE), coefficient of determination (R^2), and root means square error (RMSE), as shown in Table: 2. The results were plotted in terms of discharge enhancement ratio vs. key slopes, as shown in Figure: 10. In the present study, it was found that the optimal floor slopes for the inlet-outlet key are ranged from 1-1.1 (or peaked at 1.04), whereas the optimal floor's slope was 1.2 (range 1.1-1.2) reported by Machiels et al. [40]. During the investigation, it was noticed that as the floor slope of PKW increases, the efficiency of the weir increases (i.e., '*r*-value' increases) at a specific limit and then starts decreasing. However, the slope ($S_i=S_o$) range is different with or without parapet walls, making it a unique study.

IV. (ii) Effect of the PKW's sloping key bottom on its discharge capacity with Sloping Bed

The second part of this study was to investigate the channel bed slope effects on the discharge efficiency of the PKWs. In order to analyse the effects of the bed slope of a channel on the efficiency of PKW, all 12 models were tested for six different bottom slopes (S_b= 0%, 0.25%, 0.5%, 0.75%, 1.0%, and 1.25 %). The tests of the present study were conducted by considering the channel flow approach; thus, the application of this investigation covers mainly PKWs constructed as a control structure in a canal or river barrages, where the difference between crest and downstream is limited.

As literature said, the channel bottom slope study is essential to know the hydraulic behavior of the run-off river/stream or canal system where the difference between the weir crest and the downstream river is limited [52]. The channel slope plays a crucial role in assessing the relationship between the end depth

and the flowing discharge over the weir. It also reveals the clear visibility of the consistent nappe appearances downstream of the weir (see Figure: 3 (b)). According to Carollo and Pampalone [9], the channel bed slope is useful in discharge measurement at an upland basin outlet. A high slope is required to limit the negative effects of sediment load on discharge measurement. Indeed, sediment settling caused by the presence of a horizontal or flat-bottomed could form a sediment layer upstream from the flume, resulting in relevant errors in water depth measurement and discharge.

Moreover, it assists in forming the hydraulic jump, its location (including its length, which depends on the slope of the downstream apron) [52], and enhancing energy dissipation downstream of the weir [2]. Elyass [16] studied the effect of channel bed slope on energy dissipation of flow for a single-step broad–crested weir under free-flow conditions. He found that for the same ratio (upstream to downstream weir height, i.e., P/P_1), the channel bed slope effect (S_b) was inversely proportional to the energy dissipation.

The present study aims to understand better the channel bed slope effects on the discharge carrying capacity of the PKW. The test results indicate that, as the slope of the channel bed increases, the discharge efficiency of PKW increases significantly for a low H_t/P ratio. It enhances for higher values also but the slightly a lesser rate.

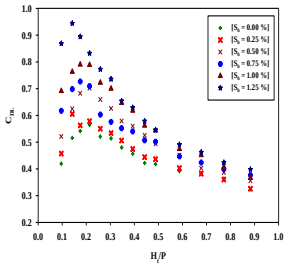

(a) [S_i=S_o=0.3]

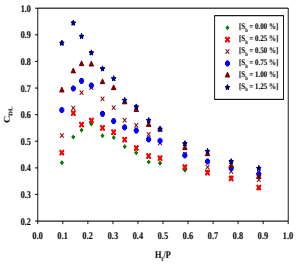

(b) [S_i=S_o=0.4]

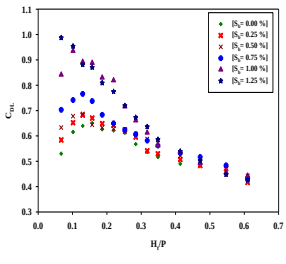

(c) [S_i=S_o= 0.5]

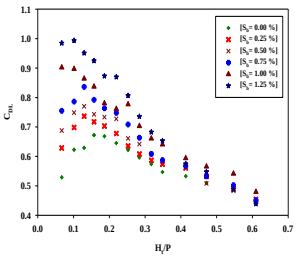

(d) [S_i=S_o= 0.6]

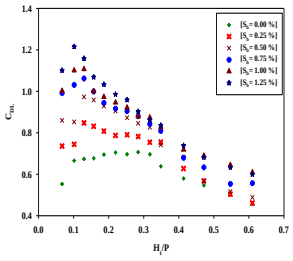

(e) [S_i=S_o= 0.7]

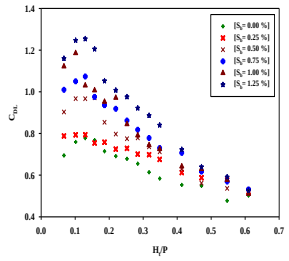

(f) [S_i=S_o= 0.8]

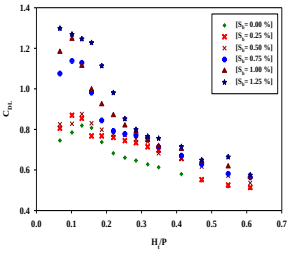

(g) [S_i=S_o= 0.9]

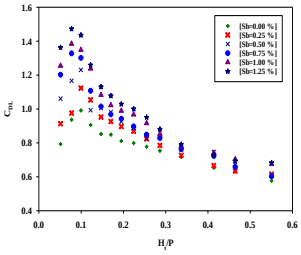

(h) [S_i=S_o= 1.0]

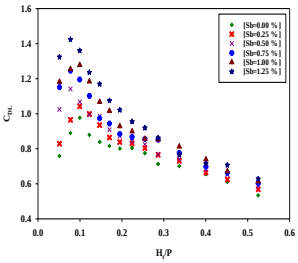

(i) [S_i=S_o= 1.1]

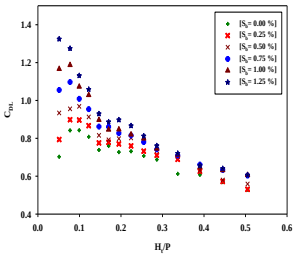

(j) [S_i=S_o= 1.2]

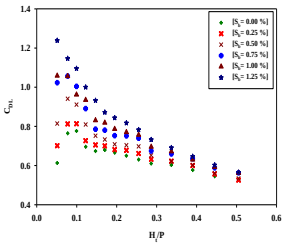

(k) [S_i=S_o= 1.3]

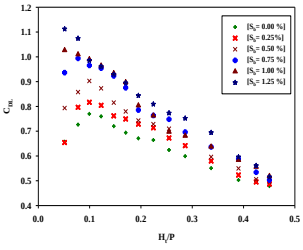

(l) [S_i=S_o= 1.4]

Figure: 11. Variation of coefficient of discharge [C_{DL}] with [H_t/P] on different bed slopes for different inlet-outlet key slopes.

In order to the lower discharge value as the slope of the bottom increases, the releasing capacity or coefficient of discharge of the PKWs increases significantly reason being the velocity of flow increases and the head of the flow decreases and theoretical discharge decreases; as a result, the discharge efficiency of the weir increases. However, at the higher discharges, the discharge coefficient shows a decreasing trend as the channel bottom slope increases, as shown in Figure: 11. This is due to the rise in the discharge and bed slope simultaneously; the head over the weir and velocity over the crest increase, so theoretical discharge

increases; thus, the discharge carrying capacity of the weir decreases.

Thus, the effect of the channel slope plays a significant role in the discharge carrying capacity of the PKW. For lower heads, the probability of the critical section is increased at the outlet crest at higher channel bed slopes. This is unfavorable, so avoid it at all costs. In contrast, no such significant sections were observed at higher heads and lower bottom slopes during the investigation. The present findings demonstrated that the discharge efficiency of the PKW increases about 50-60% for a low H_t/P ratio, while 18-20% for higher H_t/P values when channel bed slopes change from 0.0% to 1.25 %. The channel bed may help adequately design energy-dissipative structures to identify the length of a hydraulic jump and apron length for the weir [26].

V. CONCLUSION

A systematic experimental study was carried out to determine the optimal slope of the inlet-outlet keys floors of PKW and see the effects of channel bed slope on its discharge efficiency. To this end, twelve laboratory-scale type-A PKW models were tested and analyzed with six different channel bed slopes. The results were presented with various hydraulic characteristics and compared to the design equations or methodology developed by Machiels et al. [40] and to the discharge efficiency of the datasets for a linear weir. Based on the results of this study, the following important conclusions can be made:

1. The discharge efficiency of PKW increases with the increasing inlet-outlet key slopes up to certain limits, then decreases. For a value of $0 \leq H_t/P \leq 0.24$, efficiency increases more for all discharge values, and $H_t/P > 0.24$, the efficiency decreases gradually. Hence, it does not create more changes in the efficiency of the PKW.
2. The optimal range of inlet-outlet key slope (S_i=S_o) for maximizing the efficiency ranges 1.0-1.1, and the maximum discharge coefficient was obtained at 1.0054 (approximate) at a slope of 1.04. Further, a reduction in discharge efficiency was observed by increasing the value of the inlet-outlet key bottom slope. This limit corresponds to the balance of inlet-outlet key slope assuring adequately low velocity in inlet concerning hydraulic efficiency (capacity to pass flow without the critical section apparition).
3. The effect of channel bed slope on the discharge carrying capacity of the PKW has revealed that as the channel slope increases, so does the discharge coefficient. The efficiency of the small-scale model increases up to a range of $0 \leq H_t/P \leq 0.1$ or 0.15; after that, it gradually decreases for larger values $H_t/P > 0.15$. On the other hand, the range of increasing efficiency in the large-scale model is slightly smaller than in the small-scale model; for a value of $0 \leq H_t/P \leq 0.07$, efficiency increases more for all discharge values, and $H_t/P > 0.07$, efficiency gradually decreases. It means that as the bottom slope increases, the releasing capacity or discharge coefficient of the PKWs increases because for low discharge values, the velocity of flow increases and head over the crest of the weir decreases, so the theoretical discharge values decrease as a result of the coefficient of discharge increases. In order to the higher discharge, the discharge coefficient increases with an increasing channel slope at a lesser rate or shows an approximately constant pattern.
4. The discharge efficiency of the PKW increases about 50-60% for a low H_t/P ratio, while 18-20% for higher H_t/P values when channel bed slopes change from 0.0% to 1.25 %.

Overall, the inlet-outlet key slope is vital in developing and designing the PKW's efficient geometry. The channel bottom slope also plays a crucial role in enhancing the PKW's releasing capacity of the weir at the low head/discharge level. The current work contributes to defining the appropriate slopes for the inlet-outlet keys and determining the effect of channel bed slope on the PKW's discharge carrying capacity. It will aid in providing appropriate guidance to the designer in order to make an efficient geometry and guidance for designing the PKW.

VI. LIST OF SYMBOLS

B	Length of side weir ($B_i + B_b + B_o$)
B_b	Base length
B_i	Length of overhang portions at the inlet side
B_o	Length of overhang portions at the outlet side
C_{DL}	Coefficient of discharge along developed crest length
C_S	Coefficient of discharge for sharp-crested weir
E	Specific energy at section' i'
F_r	Froude Number
g	Acceleration of gravity
H_t	Total energy head
h_t,	Piezometric head
i	Represents the section
L	Total developed crest length
N	Number of cycles
P	PKW height
P_b	Flow approach depth,
Q	Discharge over the PKW

Q_{PKW} Total Discharge over PKW
Q_W Discharge over the Sharp-crested weir
R Height of parapet wall
r Discharge enhancement ratio
R_e Reynolds number
S_i Inlet key slope
S_o Outlet key slope
S_b Channel bed slope or slope of channel bed
T Temperature of flowing fluid
T_s Sidewall thickness of the PKW
V_t Mean flow velocity
$V_t^2/2g$ Approach velocity head
W Channel width/ Width of PKW
W_e Weber number
W_i Inlet key width
W_o Outlet key width
X Distance of measurement section from the lateral centreline of the PKWs.
ρ Density of flowing fluid
μ Dynamic viscosity of the flowing fluid
σ Surface tension of the flowing fluid

REFERENCES

[1] Abhash, A., and Pandey, K. K. (2020). "A review of Piano Key Weir as a superior alternative for dam rehabilitation A review of Piano Key Weir as a superior alternative for dam rehabilitation." *ISH Journal of Hydraulic Engineering*, Taylor & Francis, 00(00), 1–11.

[2] Al-Hashimi, Shaymaa A. M., Huda M. Madhloom, Thameen N. Nahi, and Nadhir Al-Ansari. 2016. "Channel Slope Effect on Energy Dissipation of Flow over Broad Crested Weirs." *Engineering* 08(12): 837–51.

[3] Anderson, R. M. (2011). "Piano Key Weir Head Discharge Relationships." All Graduate Theses and Dissertations, Paper 880, Utah State University.

[4] Anderson, R. M. and Tullis B. P. (2011). "Influence of Piano Key Weir Geometry on Discharge." *Proc. International Workshop on Labyrinth and Piano Key Weirs, Liège, Belgium.*

[5] Anderson, R.M. and Tullis, B.P. (2012). "Piano Key Weir: Reservoir versus Channel Application." *J. Irrig. Drain Eng., ASCE, 138(8): 773-776.*

[6] Barcouda, M., Cazaillet, O., Cochet, P., Jones, B. A., Lacroix, S., Laugier, F., Odeyer, C., Vingny, J. P., (2006). "Cost-Effective Increase in Storage and Safety of Most Dams Using Fuse gates or PK Weirs." *Proc. of the 22nd Congress of ICOLD., Barcelona,* Spain.

[7] Bieri M., Federspiel M., Boillat J., Houdant B. and Delorme F. (2009). "Spillway capacity upgrade of Gloriettes Dam: Environmental integration and energy dissipation*." in Proceedings of HYDRO 2009, Lyon, France*.

[8] Blanc P. and Lempérière F. (2001). "Labyrinth spillways have a promising future." *International Journal of Hydropower and Dams 8 (4), 129-131*.

[9] Carollo, F. G., and Pampalone, V. (2021). "Testing the Stage-Discharge Relationship in Sloping SMBF Flumes." *Journal of Irrigation and Drainage Engineering*, 147(5), 04021010.

[10] Chemaly, A. G. (2017). "Lessons learned from the planning, design, construction, operation and maintenance (O&M), monitoring and safety evaluation of dams." *Proceedings of the Annual SANCOLD Conference 2017 (pp. 271 - 295).* SANCOLD.

[11] Cicero, G.M., Menon, J.M., Luck, M., Pinchard, T. (2011). "Experimental study of side and scale effects on hydraulic performances of a Piano Key Weir." *Proc. Int. Conf. Labyrinth and Piano Key Weirs Liège B, 167–172,* CRC Press, Boca Raton, FL.

[12] Cicero, G.M., Vermeulen, J., and Laugier, F. (2016). "Influence of some Geometrical parameters on Piano Key Weir Discharge Efficiency." *6th International Symposium on Hydraulic Structures, Hydraulic Structures and Water System Management, Portland, Oregon, USA, 27-30 June, 2016.*

[13] Crookston, B. M., Erpicum, S., Tullis, B. P., and Laugier, F. (2019). "Hydraulics of Labyrinth and Piano Key Weirs: 100 Years of Prototype Structures, Advancements, and Future Research Needs." *Journal of Hydraulic Engineering*, 145(12), 02519004.

[14] Denys FJM (2017). "Piano Key Weirs Spillway Standard Design Principles and Flow Induced Vibrations." Proceedings of the 3rd International Workshop on Labyrinth and Piano Key Weirs (PKW 2017), pp. 119-126. CRC Press, Taylor & Francis Group.

[15] Dugue, V., Hachem, F., Boillat, J.-L., Nagel, V., Roca, J.-P., Laugier, F. (2011). "P. K. Weir and flap gate spillway for the Gage II Dam." *Proc. Int. Conf. Labyrinth and Piano Key Weirs Liege B, 35–42, CRC Press, Boca Raton, FL*

[16] Elyass, Sahad Salim. 2012. *"*Effect of Channel Slope on Energy Dissipation of Flow for Single Step Broad – Crested Weirs, Introduction*:" 16(3): 91–103.Weirs Liege B, 35–42, CRC Press, Boca Raton, FL.*

[17] Erpicum, S., Laugier, F., Boillat, J.L., Pirotton, M., Reverchon, B., and Schleiss, A.J. (2011). Labyrinth and Piano Key Weirs - PKW 2011. CRC Press, London, UK.

[18] Erpicum, S., Nagel, V., Laugier, F. (2011b). "Piano Key Weir design of Raviege dam." Proc. Int. Conf. Labyrinth and Piano Key Weirs Liège B, 43–50, CRC Press, Boca Raton, FL.

[19] Erpicum, S., Laugier, F., Pfister, M., Pirotton, M., Cicero, G., and Schleiss, A.J. (2013). Labyrinth and Piano Key Weirs II - PKW 2013. CRC Press, London, UK.

[20] Erpicum, S., Archambeau, P., Pirotton, M. and Dewals, B.J. (2014). "Geometric parameters influence on Piano Key Weir hydraulic performances." 5th International Symposium on Hydraulic Structures and Society: Engineering Challenges and Extremes, Brisbane, Australia, 25-27 June 2014, ISBN 9781742721156

[21] Erpicum, S., Tullis, B. P., Lodomez, M., Archambeau, P., Dewals, B. J., & Pirotton, M. (2016). "Scale effects in physical piano key weir models." *Journal of Hydraulic Research, 54(6), 692-698*.

[22] Erpicum, S., Laugier, F., Ho Ta Khanh, M., and Pfister, M. (2017). Labyrinth and Piano Key Weirs III - PKW 2017. CRC Press, London, U.K.

[23] Eslinger, K. R., and Crookston, B. M. (2020). "Energy Dissipation of Type a Piano Key Weirs."

[24] Hager, W. H., Schleiss, A. J. (2009). "Constructions hydrauliques, Ecoulements stationnaires [Hydraulic structures, steady flow]." *Traité de Génie Civil. Presses Polytechniques et Universitaires Romandes, Lausanne, Switzerland*.

[25] Hien, T.C., Son, H.T., & Khanh, M.H.T. (2006). "Results of some piano keys weir hydraulic model tests in Vietnam". *Proc. of the 22nd Congress of ICOLD, Barcelona, Spain.*

[26] Jüstrich, S., Pfister, M., and Schleiss, A. J. (2016). "Mobile riverbed scour downstream of a piano key weir." *Journal of Hydraulic Engineering*, 142(11), 1–12.

[27] Kabiri-Samani, A. & Javaheri, A. (2012). "Discharge coefficient for free and submerged flow over Piano Key weirs." *Journal of Hydraulic Research, 50(1), 114-120*.

[28] Laugier, F. (2007). "Design and construction of the first Piano Key Weir spillway at Goulours dam." *Intl. J. Hydropower & Dams*, 14(5), 94-100.

[29] Laugier, F., Lochu, A., Gille, C., Leite Ribeiro, M., Boillat, J.-L. (2009). "Design and construction of a labyrinth PKW spillway at St-Marc Dam, France." *Intl. J. Hydropower Dams 15(5), 100–107.*

[30] Laugier, F., Vermeulen, J., and Blancher, B. (2017). "Overview of design and construction of 11 piano key weir spillways developed in France by EDF from 2003 to 2006." In Erpicum, S., Laugier, F., Ho Ta Khanh, M., and Pfister, M. (2017). *Labyrinth and Piano Key Weirs III - PKW 2017. CRC Press, London, U.K., 37-51*

[31] Leite Ribeiro, M., Bieri, M., Boillat, J., L., Schleiss, A., Delorme, F., and Laugier, F. (2009). "Hydraulic capacity improvement of existing spillways—Design of piano key weirs." *Proc., 23rd Congress of Large Dams. Question 90, Response 43 (CD-ROM), Int. Commission on Large Dams (ICOLD), Paris.*

[32] Leite Ribeiro M, Pfister M, Schleiss AJ, & Boillat J-L (2012). "Hydraulic design of A-type Piano Key Weirs." *Journal of Hydraulic Research, Taylor & Francis, Volume 50, Issue 4, pp. 400-408.*

[33] Leite Ribeiro, M., Bieri, M., Boillat, J. L., Schleiss, A.J., Singhal, G., Sharma, N. (2012a). "Discharge capacity of piano key weir." *J. Hydraulic Eng., ASCE, 138(2): 199-203.*

[34] Leite Ribeiro, M., Pfister, M., Boillat, J. L., Schleiss, A.J., Laugier, F. (2012b). "Piano Key Weirs as efficient spillway Structure." *24th ICOLD Congress Kyoto (Q94, R13), 1–10.*

[35] Lempérière, F. and Ouamane, A. (2003). "The Piano Keys weir: a new cost-effective solution for spillways." *Hydropower & Dams*, 10(5), 144-149.

[36] Lempérière, F., and Jun G. (2005). "Low-Cost Increase of Dams Storage and Flood Mitigation: The Piano Keys Weir." *Q.53 R. 2.06 International Commission on Irrigation and Drainage Nineteenth Congress Beijing.*

[37] Lempérière, F. (2009). "New Labyrinth weirs triple the spillways discharge." *<http://www.hydrocoop.org > (Feb. 8, 2010).*

[38] Lempérière F, Vigny J. P. and Ouamane, A. (2011). "General comments on Labyrinth and Piano Key Weirs: The past and present." Proceedings of the International Conference on Labyrinth and Piano Key Weirs (PKW 2011), pp. 17-24. CRC Press, Taylor & Francis Group.

[39] Mabela, M. J. (2017). "The raising of Hazelmere Dam using a Piano Key Weir." *Procedings of the Annual SANCOLD Conference 2017 (pp. 181 - 193).* SANCOLD.

[40] Machiels, O., Erpicum, S., Archambeau, P., Dewals, B.J. and Pirotton, M. (2011a). "Influence of the Piano Key Weir height on its discharge capacity." *Proc. Int. Conf. Labyrinth and Piano Key Weirs Liege B, 59–66, CRC Press, Boca Raton, FL.*

[41] Machiels, O., Erpicum, S., Dewals, B.J., Archambeau, P. and Pirotton, M. (2011b). "Influence of the alveoli slopes on the discharge capacity of Piano Key Weirs." *34th IAHR World Congress, Brisbane, Australia.*

[42] Machiels O. (2012). "Experimental study of the hydraulic behaviour of Piano Key Weirs." Ph.D. Thesis ULgetd-09252012- 224610, University of Liege (Belgium).

[43] Machiels, O., Erpicum, S., Archambeau, P., Dewals, B., and Pirotton, M. (2013). "Parapet wall effect on piano key weir efficiency." *Journal of Irrigation and Drainage Engineering*, 139(6), 506–511.

[44] Machiels, O., Pirotton, M., Archambeau, P., Dewals, B., and Erpicum, S. (2014). "Experimental parametric study and design of Piano Key Weirs." *Journal of Hydraulic Research*, Taylor & Francs, 52(3), 326–335.

[45] Noseda, M., Stojnic, I., Pfister, M., and Schleiss, A. J. (2019). "Upstream Erosion and Sediment Passage at Piano Key Weirs." *Journal of Hydraulic Engineering*, 145(8), 04019029.

[46] Oertel, M. (2016). "Sensitivity Analysis for Discharge Coefficients of Piano Key Weirs." Hydraulic Structures and Water System Management. 6th IAHR International Symposium on Hydraulic Structures, Portland, OR, 27-30 June (pp. 557-565).

[47] Ouamane, A. and Lempérière, F., (2006). "Design of a new economic shape of weir." *Proc. of the International Symposium of Dams in the Societies of the 21st Century*, Barcelona, Spain, 463-470.

[48] Ouamane, A. (2011). "Nine years of study of the Piano Key Weir in the university laboratory of Biskra "lessons and reflections." *Proc.Int.Conf. Labyrinth Piano Key Weirs-PKW-2011, Taylor &Francis, London.*

[49] Paxson G.S, Tullis B.P, and Hertel DJ (2013). "Comparison of Piano Key Weirs with the labyrinth and gated spillways: Hydraulics, cost, constructability, and operations." Proceedings of the 2nd International Workshop on Labyrinth and Piano Key Weirs (PKW 2013), pp. 123–130. CRC Press, Taylor & Francis Group.

[50] Pfister M, Justrich, S. and Schleiss, A. J. (2017). "Toe scour formation at Piano Key weirs." In Erpicum, S., Laugier, F., Ho Ta Khanh, M., and Pfister, M. (2017). *Labyrinth and Piano Key Weirs III - PKW 2017. CRC Press:* Leiden.

[51] Pralong J, Vermeulen J, Blancher B, Laugier F, Erpicum S, Machiels O, Pirotton M, Boillat J-L, Leite Ribeiro M & Schleiss AJ (2011a). "A naming convention for the Piano Key Weirs geometrical parameters." *Proceedings of the International Conference on Labyrinth and Piano Key Weirs (PKW 2011), pp. 271–278. CRC Press, Taylor & Francis Group.*

[52] Ranga Raju, K.G. (2005). Flow-through open channels, Tata McGraw Hills, New Delhi, 194–196.

[53] Schleiss AJ (2011). "From Labyrinth to Piano Key Weirs - A historical review." Proceedings of the International Conference on Labyrinth and Piano Key Weirs (PKW 2011), pp. 3–15. CRC Press, Taylor & Francis Group.

[54] Singh, D, Kumar, M (2021) Hydraulic Design and Analysis of Piano Key Weirs : A Review. Arabian Journal for Science and Engineering, Springer Berlin Heidelberg. https://doi.org/10.1007/s13369-021-06370-4.

[55] Singh, D., and Kumar, M. (2022). "Energy dissipation of flow over the type-B Piano Key Weir." Flow Measurement and Instrumentation, Elsevier Ltd, 83(November 2021), 102109,. https://doi.org/10.1016/j.flowmeasinst.2021.102109

[56] Singh, D., and Kumar, M. (2022c). "Study on aeration performance of different types of piano key weir." Water Supply, 22(5), 4810–4821. https://doi.org/10.2166/ws.2022.131.

[57] Tullis, B. P., Ph, D., Asce, M., Crookston, B. M., Ph, D., Asce, M., Young, N., and Asce, M. (2020). "Scale Effects in Free-Flow Nonlinear Weir Head-Discharge Relationships."

IFERP connecting engineers...developing research
1st International Conference on Future of Engineering 2022

Computational Fluid Dynamic Simulation and Experimental Investigation of an Optimized Shell and Tube Heat Exchanger with Constant Heat Transfer Coefficient

Nesrine Gaaliche[1], Mahmood Alajimi[2]

[1] School of Engineering, Bahrain Polytechnic, Isa Town, Kingdom of Bahrain, Bahrain
[2] School of Engineering, Bahrain Polytechnic, Isa Town, Kingdom of Bahrain, Bahrain
Email: [1]nessrine.gaaliche1@gmail.com, [2]mahmod.alajmi@gmail.com

Abstract:
The heat exchanger is widely used in many industrial fields, such as chemical industry, petroleum, thermal power, and so on. Fluid corrosion and fouling frequently damage shell and tube heat exchangers, resulting in leaks. In order to prevent the fluid losses and increase the efficiency, it is proposed to optimize an old shell and tube heat exchanger (STHE) used in the petroleum field in order to cool down the produced Methanol. The aim of this paper is to design a special type of horizontal shell and tube heat exchanger in petroleum production. For optimal design of a shell and tube heat exchanger, it was thermally modeled using Computational Fluid Dynamics (CFD) while the log-mean temperature difference (LMTD) method was applied to estimate its heat transfer coefficient, pressure drop, and efficiency. Computational fluid dynamics (CFD) was performed to study the model of the inlet shell flow field. The paper studies the distribution characteristics of the flow field under the following inlet temperatures of methanol and seawater:175°C and 80°C, respectively. The flow of both shell and tube side fluids was turbulent. Our experimental findings show that the performance is around 35.29%. This means that the efficiency has increased by 9.6% of its previous efficiency and the pressure drops of the shell and tube side are 16.422 kPa and 54.262 kPa. The hot and cold fluid outlet temperatures, corrected LMTD and efficiency obtained from CFD simulations were in excellent agreement with experimental results, with an error of 3.6%.

Keywords:
Heat Exchanger, LMTD, Efficiency, Pressure drop

I. INTRODUCTION

The aim of this paper is to design a heat exchanger that will cool down hot methanol with seawater. Heat exchangers are a type of industrial machinery that exchanges heat between a cold and hot stream. They are applied to heat and cool fluids. Heat exchangers are classified into numerous categories, including double-pipe exchangers, shell and tube exchangers, air coolers, and many others. Heat exchangers are used in 80% of power usage systems [1]. One of the most widely used fossil fuels is natural gas, as it provides energy for both industrial and household needs. Natural gas, being the world's third-largest energy source, is used for a wide range of applications. It is a popular choice among industries and households alike because it is an environmentally friendly fuel [2]. Singh et *al.* developed a heat exchanger that was primarily utilized to convert the liquid form of the shell-side fluid to vapor. The liquid enters the cavity through the shell-side entrance, which has an outlet for vapor to exit. The tube bundle is made up of several tubes that carry tube-side fluid into a chamber with a longitudinal axis. The developed heat exchanger includes a shell with an inner surface that defines the cavity, a shell comprises an inlet for introducing shell-side liquid into the cavity and an outlet for discharging vapor from the cavity. A tube bundle that is placed in a cavity and contains multiple tubes for carrying tube-side fluid with a longitudinal axis. A shroud surrounds the bundle in the circumferential direction and is placed between the bundle and the inner surface of the shroud so that there is a ring between the shroud and the inner surface. An opening at the bottom of the shell that forms the passage between the annular space and the bundle of tubes. The opening at the top of the shell forms a passage between the annular

space and the tube bundle [3]. The project required the development of a shell and tube heat exchanger that met particular requirements. Shell and tube heat exchangers are widely applied in the petrochemical and extraction industries. Tube ends are put in sheets that separate the shell and tube fluids [4]. They are made from baffles which are installed in the shells to help guide the fluid flow on the shell side and generate flow with turbulence. This heat exchanger type has various benefits, including a significant surface area for a lower dimension, ease of maintenance, a suitable mechanical design, and common design techniques [4]. Before beginning computations, the parameters and given data for the proposed design must be provided. As a result, the design will be restricted to the company's specifications, as given in Table1 The parameters will be used to develop a suitable design that meet the specified requirements. Kern's approach [5] was followed to develop the heat exchanger in this work. First, the STHE will be modeled using Kern's approach and given parameters to predict the overall area, pressure drop, heat transfer coefficient, and efficiency. The STHE will next be modeled using ANSYS Fluent version 14.0 to determine all of the unknown parameters of methanol and seawater. The simulation of the optimized STHE is carried out after selecting an appropriate mesh, discretization approach, and turbulence model. Different thermal characteristics are determined and compared to the CFD numerical simulation.

Nomenclature

A	Overall heat transfer area (m^2)	D_s	Shell diameter (mm)
d_0	Tube outer diameter (mm)	L_b	Baffle spacing (mm)
P_t	Tube pitch(m)	M_s	Mass velocity (kg/m^2s)
L	Pipe length (m)	ΔP	Pressure drop (Pa)
Nt	Number of tubes	F	Friction factor
D_b	Bundle diameter (mm)	d_e	Equivalent diameter (m)
D_b	Bundle diameter (mm)	L_b	Baffle spacing (mm)

II. KERN DESIGN METHODOLOGY

The following steps are to be followed as mentioned by Kern's method in order to design the heat exchanger in an optimal manner [5]. Several assumptions will be made while calculating the energy balance of the two fluids, including no energy losses and potential, kinetic energy transformations are neglected and steady-state conditions [6].

$$q_{cold} = q_{hot} \qquad \text{(Energy Balance Equation)}$$

$$\dot{m}_{hot} c_{Phot} \, (T_{hotin} - T_{hotout}) = \dot{m}_{cold} c_{Pcold} \, (T_{coldin} - T_{coldout})$$

Where, $\dot{m}_{cold}$ = 8.056 Kg/s and $\dot{m}_{hot}$= 0.652 Kg/s. The following equation can be sued to calculate the heat transfer:

$$q = \dot{m}_{hot} c_{Phot} \, (T_{hotin} - T_{hotout})$$

Using values from (**Error! Reference source not found.**), the heat transfer can be calculated, as shown below:

$$q = 8.056 \times \frac{2.095 + 2.354}{2} (130 - 50)$$

$$q = 1435.646 \, kW$$

III. STHE DESIGN

To begin the computations, one shell pass and two tube passes is considered to get the log mean temperature difference. Ken's Method will be implemented to determine the area of STHE. The temperature difference in heat exchangers is determined using the LMTD Ken's approach. It is defined as the differential between hot and cold working fluids at the heat exchanger intake and exit. To optimize the LMTD, the methanol and seawater are utilized in counter-flow. he temperatures on shell and tube sides are specified in Table1.The following equations are used to determine LMTD:

For counter current:

$$\text{LMTD} = \frac{(T_{hot,inlet} - T_{cold,outlet}) - (T_{hot,outlet} - T_{cold,inlet})}{ln\frac{(T_{hot,inlet} - T_{cold,outlet})}{(T_{hot,outlet} - T_{cold,inlet})}}$$

Table 1. Given specifications by the company for the design

Seawater	Temperature in (°C)	50
	Temperature out (°C)	130
	Density, ρ (Kg/m^3)	680
	Dynamic Viscosity, μ (Pa.s)	$1.44x10^{-5}$
	Specific heat, Cp $\frac{KJ}{Kg.C}$	2.225
	Thermal conductivity, k ($\frac{w}{m.K}$)	0.0456
Methanol	Temperature in (°C)	175
	Temperature out (°C)	144.37
	Density, ρ,(Kg/m^3)	922.6
	Dynamic Viscosity, μ (Pa.s)	$1.026x10^{-4}$
	Specific heat, Cp $\frac{KJ}{Kg.C}$	3.232
	Thermal conductivity, k, ($\frac{w}{m.K}$)	0.0456
Fouling Resistance in both sides=11630w/m^2K		
Outside tube Diameter=19.05mm		
Inner tube Diameter=17mm		

III.1 Value of heat transfer coefficient

The LMTD and heat transfer coefficient must be determined in order to compute the heat exchanger area. Therefore, it is recommended to begin with the assumption of the heat transfer coefficient specified by the company, which is 333.24W/m^2.K.

III.2 Calculation of total heat transfer area

The total heat transfer area can be calculated directly from the LMTD and the assumed heat transfer coefficient. The following equation can be used to determine the overall area:

$$A = \frac{q}{U \times LMTD}$$

Therefore,

$$A = \frac{1435.646 \times 10^3}{333.246 \times 59.798}$$
$$A = 71.943\ m^2$$

III.3 Determination of tube number:

To begin, a 19.05 mm outer diameter tube with common dimensions is selected [7]. The material selected for the tubes was carbon steel since it has high thermal conductivity and is used in applications that contain methane. Moreover, it is highly resistant to atmospheric and water corrosion, and it has a high mechanical strength. In addition, the tube has a length of 2.7 m, which is suitable for the design to minimize the cost and shell diameter. Since longer tubes provide more heat transfer and pressure drop [8]. Thermal conductivity of carbon steel will be $K_{carbon\ steel}$ = 45 W/m.K [9].

Knowing the provisional area, it can be used along with data from (Table1) to calculate the number of tubes, using the following formula:

$$N_t = \frac{A}{\pi \times d_0 \times L}$$

Therefore,

$$N_t = \frac{71.943}{\pi \times (19.05 \times 10^{-3}) \times 2700 \times 10^{-3}}$$
$$N_t = 445.225\ Tubes$$
$$N_t = 445\ Tubes$$

The following equation will be used to calculate the number of tubes per pass:

$$Nttp = \frac{Number\ of\ Tubes}{Number\ of\ Passes}$$

Since the Natural Gas Preheater is a 1 shell 2 tube heat exchanger, using values from Table1 the following is determined:

$$Nttp = \frac{445}{2}$$
$$Nttp = 222\ tubes$$

III.4 Bundle and shell diameter

The bundle diameter can be calculated using the following formula:

$$D_b = d_o(\frac{N_t}{K_1})^{1/n_1}$$

Where, $K_1 = 0.156, and\ n1 = 2.291$ for the square pitched arrangement and the heat exchanger has two passes.

Therefore,

$$D_b = 19.05(\frac{445}{0.156})^{1/2.291}$$
$$D_b = 613.865\ mm$$

The shell clearance for a fixed and U-tube heat exchanger is obtained from Fig. 1 by taking the bundle diameter into account, therefore the shell clearance is around 14 mm [5]. The shell diameter (Ds) is calculated using these two variables.

$$D_s = D_b + clearance$$

Therefore,

$$D_s = 613.865 + 14$$
$$D_s = 627.865\ mm$$

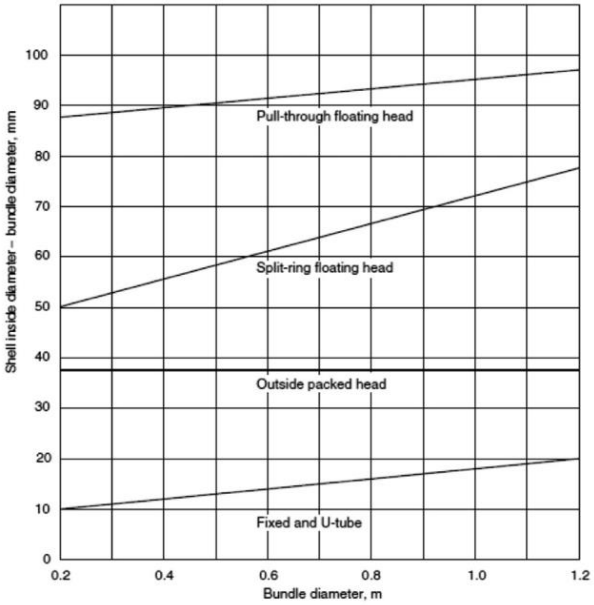

Figure1.Bundle diameter and shell diameter [5]

III.5 Baffle Spacing

The last step to designing the heat exchanger is to determine the baffle spacing, which could be done using the following formula:

$$B_s = 0.4D_s$$

Therefore,

$$B_s = 0.4 \times 627.875$$
$$B_s = 251.146\ mm$$

6 Pressure drop in tube and shell sides

The pressure drop in shell side can be estimated by using the following equation:

$$\Delta P_s = \frac{2\, f\, {M_s}^2\, D_b\, (N_B + 1)}{\rho\, d_e\, (\frac{\mu}{\mu_s})^{0.14}}$$

the friction factor f is estimated to be 0.037, the number of baffles N_b is 10. The dynamic viscosity of low pressured steam at the surface temperature of the shell of 36.2℃ is 6.8×10^{-4}Pa.s. The mass velocity is 159.874 kg/m².s.

$$\Delta P_s = 16.422 KPa$$

IV. MODELLING DETAILS

The CFD simulation was carried out on a STHE for realistic modeling of heat transfer. For the heat exchanger design, several geometric and mechanical characteristics were considered. Table 1 contains data on design parameters. The first liquid is water, and the second one is methane, the STHE made from carbon steel. Both inlet temperature and flow rate are defined as the boundary conditions for this developed STE. Table 1 shows the detailed geometrical characteristics. The standard gravity and no-slip condition are also considered in this FE model. The tubes and shells are modeled as solid, with input temperatures of 36.2°C. The next step of the pre-processing is to perform the meshing. After developing the computational domain, the STHE is discretized into tetrahedral elements by means of Ansys. The convergence was accomplished using medium mesh size. Thus, the proposed tetrahedral mesh is selected.

V. RESULTS AND DISCUSSION

V.1 Optimized STHE design validation of the Kern's LMTD method

All calculations and simulations will be done in order to design the STHE in an optimal manner. For the accurate prediction of pressure drops and the heat transfer coefficient calculation in STHE design, Kern's LMTD method is selected. Kern's LMTD model for designing the STHE is a reliable method and is validated against many heat exchangers [5]. The optimized STHE designed by LMTD [5] and its previous counterpart, having similar heat transfer characteristics and listed in Table 1, are compared in terms of the effectiveness and geometry (number of tubes per pass, tube pitch, Bundel diameter and overall size). The table 2 shows the difference in properties between the previous and optimized heat exchangers. The overall size of the heat exchanger is reduced compared to the old STHE as per industrial requirements (GPIC) due to limited space. Since the number of tubes per pass and the bundle diameter are decreased from 328 to 222and 840mm to 613.865mm, respectively. This consequently led to a decrease in the provisional area of the heat exchanger from $98.8\, m^2$ to 71.943m². The number of baffles was also reduced, which will lower overall costs and lighter weight. Because the boiler was designed to be vertical, there was some wastewater soaking at the bottom of the boiler, which increase the corrosion at the bottom causing leaks. This study demonstrates that the horizontal steam boiler much more efficient than the vertical boiler. Since, they suffer from more stress as the flues are not completely covered with water. The pressure drop on the heat exchanger's shell and tubes rises as the corrected LMTD increases. After improving the heat exchanger, efficiency improve from 25.63% to 35.29%. As a result, it is clear that this improved design offers the appropriate pressure drop. Improving STHE design utilizing the LMTD approach has been demonstrated to have a considerable effect on its efficiency across both thermal and pressure drop analyses.

Table 2. Comparison between previous and optimised STHE

Property	Optimized Heat Exchanger	Old Heat Exchanger
Heat Transfer (kW)	1435.6	
Heat Transfer Coefficient $(W/m^2.K)$	333.246	
Number of Tubes per Pass	222	328
Tube Pitch (mm)	23.813	24.5
Bundle Diameter (mm)	613.865	840
Corrected LMTD (℃)	59.798	43.5
Shell – Side Pressure Drop (kPa)	16.422	1.27
Tube – Side Pressure Drop (kPa)	54.262	50
Provisional Area (m^2)	71.943	98.8
Efficiency (%)	35.29	25.63

 ISBN: 978-93-92105-22-7

V.2 CFD Simulation of the STHE

Figure 2 shows the results of the model to be validated. The computed heat exchange rate between methanol and seawater being 1383.9 W, the heat transfer results show that the CFD model has only a difference with analytical results by 3.6%. As shown in figure 3, Methanol enters the shell hot and exits cold, its temperature has decreased from 167°C to 138°C because there is a heat transfer by convection between the outer walls of the tubes and the exchanger. The seawater enters cold and goes out hot in the tubes, its temperature has increased from 48.5°C to 97°C because there is a heat transfer by conduction between the external and internal wall of the tubes. The temperature contours show that the temperature and pressure are lower on the outside of the shell.

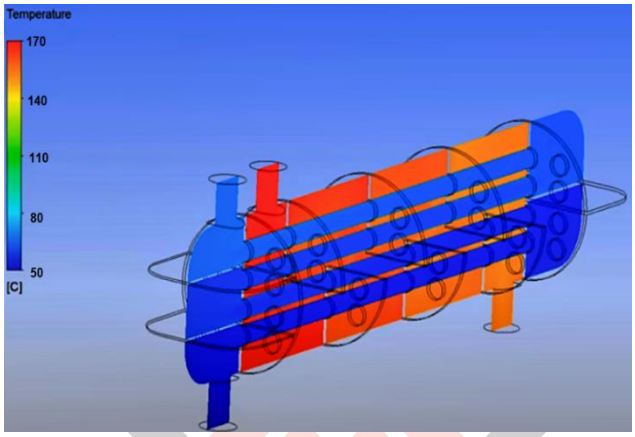

Figure 2. Temperature distribution in both fluids

VI. CONCLUSION

The heat transfer and flow properties of a STHE are investigated in this paper using CFD method and the LMTD approach. The proposed heat exchanger is efficient for the heat transfer task, since it can cool down methanol from 175 °C to 144.38 °C by using seawater at 50 °C. Moreover, fluid flow rates can be produced with a suitable pressure drop. Kern's approach is provided, and it helps to predict accurate values of heat transfer coefficient, pressure drop, and efficiency. The basic idea is to use the Kern's design method to improve the efficiency of STHE. It depicts that pressure decreases with temperature. Since vertical boiler designs have much higher corrosion and leakages, that can lower the effective life of the device, the horizontal heat exchangers are more useful because the pressure is dispersed over a wider surface area. After improving the heat exchanger, efficiency rose from 25.29% to 35.29%. As a result, it is clear that this optimized design offers the appropriate pressure drop. Improving STHE design using the LMTD approach has been demonstrated to have a considerable effect on its efficiency across both thermal and pressure drop analyses. Furthermore, a computational model is employed to compute and compare the STE's performance. The temperature and pressure contours show that the temperature and pressure are lower towards the shell's outside edge. The hot and cold fluid outlet temperatures, pressure drop, and efficiency computed accord well with the experimental measurements. To summarize, the shell and tube heat exchanger is a viable option for this.

REFERENCES

[1] S. Hall, “Rules of Thumb for Chemical Engineers (Fifth Edition),” Butterworth-Heinemann,2012, pp. 27-57, ISBN 9780123877857, 2012. https://doi.org/10.1016/B978-0-12-387785-7.00002-5.

[2] P.Hendry,“Fossil gas: decarbonisation soultion, detour or dead end?,” WWFSouth Africa,2020, https://wwfafrica.awsassets.panda.org/downloads/fossil_gas_factsheet.pdf

[3] Singh, Krishna P., Nadig, Ranga,“Heat exchanger apparatus for converting a shell-side liquid into a vapor,”USP2014098833437,2009,https://scienceon.kisti.re.kr/srch/selectPORSrchPatent.do?cn=USP2017049612058

[4] J.M. Coulson, J.F. Richardson,“Chemical Engineering Design,” 6th edition, University College of Swansea: Robert Maxwell, M.C., 1983.

[5] Gavin P. Towler, R.K. Sinnott,“Chemical Engineering Design,” 5th edition, Amsterdam: Elsevier/Butterworth-Heinemann, 2008.

[6] R.W. Serth, “Process Heat Transfer,” Academic Press, 2007, Pages 327-383, ISBN 9780123735881,

[7] https://doi.org/10.1016/B978-012373588-1/50011-5.

[8] T. Kuppan, “Heat Exchanger Design Handbook,”1st edition, Marcel Dekker, New York, 2000.

[9] T.S. Bisoniya,“Design of earth–air heat exchanger system,” Geotherm. Energy, pp. 3–18, 2015.http://dx.doi.org/10.1186/s40517-015-0036-2

[10] “Comparing the Thermal Conductivity of Stainless Steel to other Metals,”2020. https://www.stainless-structurals.com/blog/comparing-the-thermal-conductivity-of-stainless-steel-to-other-metals/

IFERP connecting engineers...developing research
1st International Conference on Future of Engineering 2022

Assessing an Ancient Traditional Lost Wax Processing of Cu-Zn/Cu-Sn Alloy: Dhokra Art

Rahul Samanta[1], Arghya Majumder[2], Apurba Das[3], Arijit Sinha[4], Debdas Roy[5], Gurudas Mandal[6*]

[1,4,6] Department of Metallurgical Engineering, Kazi Nazrul University, Asansol, India
[2] School of Mines and Metallurgy, Kazi Nazrul University, Asansol, India
[3] Titagarh Wagons Ltd, 756 Anandapur, Kolkata, India
[5] Department of Materials and Metallurgical Engineering, National Institute of Advanced Manufacturing (formerly National Institute of Foundry and Forge Technology) Hatia, Ranchi, India
Email: [6]gurudas.mandal@knu.ac.in

Abstract:
Dhokra is an ancient and traditional wax metal art-craft, practiced in India over a period of 4500 years from the Harappa and Mohenjo-Daro eras. In this gorgeous metal art form, Cu-Sn alloy is used for the casting process as raw material. Due to the high corrosion resistance property of the alloy and the aesthetic view of the artefacts the art is sustained for a long period. Dhokra artists mainly use Cu-Sn metal scraps, collected from local markets, and primarily used utensils of households. In general, Dhokra artists use two methods of casting. In one process, small pieces of the scrap metal alloy are poured inside the mould, made with rice chaff and clay, and then placed in the traditional clay furnace to melt inside the mould. In another method, moluds are prepared, and after that molten metal is poured directly from the crucible to it. Intermediate steps such as “preparation of tar layer” and “making of second mould layer” also have been done before casting. Once the casting process is finished moulds are kept aside for normalizing or sometimes water quenching is done to make the cooling process faster. In complex designs, different parts of the artefacts are cast differently; after that, all the parts are assembled according to the design. Once assembling is done the metal crafts are ready for providing finishing touch and polishing. Grinding machines are used for deburring and smoothening the rough surfaces of the metal crafts and after that gold paint is applied to make these artefacts attractive.

Keywords:
Dhokra, Cu-Sn alloy, Corrosion resistance, Normalising, Quenching, Deburring

I. INTRODUCTION

Lost-wax casting technique can be described as a very common process that was practiced in the ancient world from the era of Mahenjodaro and Harappa. At that time in Mesopotamia, copper metallurgy had been developed and the lost wax casting was used for it. In the late fifth millennium, the advancement of the lost wax process started initially with solid wax artefacts and ended with only the preparation of the skin of the models in a life-sized statue. The method it was prepared in the classical period is known as ‘Sloshing’ [1]. The origin of this is much older than the researchers thought and the use of wax casting was much broader. Archeological surveys indicate that lost-wax casting during that period was used for designing simple tools and household accessories. However, the complex shapes the designers were not able to design or cast in that era [2]. In Mesopotamia, the lost-wax casting process was mainly used for casting daily life household items such as pots, bowls, and many more [3]. It was not used to produce prestigious and complicated items like showpieces and jewelry. As per archaeometallurgical observations during the third millennium BC, the process of making heterogeneous moulds with mud coarness had been used to preserve small details on the wax model [4]. These various fabrics and wonderful designs can be effectively expected in the record book of archaeology [5]. The study highlighted the assessment of an ancient traditional lost wax processing of Cu-Zn/Cu-Sn alloy in the form of Dhokra Art.

II. METHODOLOGY

A. Construction of Tar Layer

Dhokra artists belonging to the Bikna village of Bankura district majorly replace the use of beeswax with tar as it is easier for them to collect from local markets easily. First of all using a mixture of sand, rice chaff, and clay the artists make a mould and then cover it with heated and filtered tar. On this malleable tar any decoration they can make with sharp tools [6]. The top surface of the mud mould is then covered with a thin layer of tar on which the desired design is etched with the help of a small piece of blade [7]. Once the process of tar threads wrapping gets complete, motifs or finer designs made from beeswax are placed using glue onto the layer. Further, the outer layer of this container was designed creatively and decorated as per requirements with the use of beeswax thread layers [8].

B. Second Mud Mould Composing

Another layer of sand, rice chaff, and clay is further applied to the mould after covering it with tar in place of wax. Outer clay mold is used for making the shape and formation of the tarred piece. It becomes the receptacle for receiving the molten metal. Artisans cover the tar layer with a mixture of rice chaff and mud that have been prepared. Further, Artisans cover the final layer of the prepared mixture to cover the mould [9]. It ensures that no leakage can be present during metal melting inside the mould or during the pouring of molten metal into the mould. Instead of beeswax, artisans preferred pitch or tar, and that acts as a middle layer between two clay layers which helps prevent leakage.

C. Filling Up With Metal

In this process, alloys of metals like copper, zinc, aluminum, lead, and tin are used. Using small pieces of scrap metals used in the casting process. Artisans using manual weighing machines as per their requirements take the measurement and use it in the casting process. At high temperatures, scrap metals are melted down inside the pit and formed the shape of the mould exactly [10]. Further, the final layer of mould has also formed with a mixture of clay, sand, and rice chaff.

D. Firing process

Once temperatures reach the melting point metal starts melting inside the mould. Molten metal replaces the tar present inside and takes the shape of it. After chipping off the dry clay mould, artisans collect the main product [11-13]. Artisans also followed another way of casting where these non-ferrous metals are melted inside a crucible and then poured into the mould [14]. In that way, the molten metal took the place of tar and formed the model. Finally, the models become ready for polishing once the mud layer has been broken.

E. Finishing Process

Using the cotton cloth method dhokra items are generally polished. However, during the process, the designs of the models get affected that they applied gold paint to the artefacts [15].

III. APPLICATIONS OF LOST WAX CASTING IN MEDICAL SCIENCE

One of the key applications in the modern world of the lost wax technique is the casting of orthopaedic screws. This can be manufactured using a CNC machine, however, the machine is too expensive and complex and the lost wax technique is much more preferable for this application with desirable accuracy [16]. It can be taken as an alternative production process of orthopedic screws with less investment.

IV. CHALLENGES

- The high cost of bronze or brass scrap metals increases the cost of final models.
- The Lack of up-gradation of the manufacturing process is unable to generate high profit.
- The presence of middlemen also limited the profit margin of the artisans.
- The lack of investments in this sector reduces the reach of the art to the global world.
- Lack of advertisement of dhokra art unable to attract the customers or investors.

V. CONTINGENCY PLANS

- The manufacturing process needs to be updated in order to reduce the cost price of the products.
- Advertisement of this art on various social platforms can attract the buyer.
- Direct communication with the buyers can omit the middlemen and increase the profit margin.
- Implementation of new design and its demand in the global market needs to be understood and according to it artisans need to approach companies for investment.
- Government initiation in this matter can help the artisans the most.

VI. CONCLUSIONS

There are several steps involved in the making of a Dhokra model and hence, a single piece could take up to a month or two to be created. However, increasing manufacturing costs, inadequate exposure, lack of upgrading the manufacturing

process, and failure to adapt the innovative design of the product are becoming major threats to its existence. Dhokra is regarded as an inheritance and integral part of Indian culture and this traditional art crafts process needs to be restored by incorporating new age technology to overcome the constraints like inflated raw materials price, adequate manufacturing process, and innovative design. If all the processes can be improved, the eye-catching finished products can be offered at moderate cost and profitability can be improved for Dhokra workers.

DECLARATION OF CONFLICTING INTERESTS

The author(s) declared no potential conflicts of interest with respect to the research, authorship, and/or publication of this article.

FUNDING

The author(s) received financial support through UGC-STRIDE project (#F.2-12/2019) for this research work.

ACKNOWLEDGMENTS

The authors would like to take this opportunity to express their sincere gratitude and appreciation to KaziNazrul University for providing support through UGC-STRIDE project.Grant #F.2-12/2019.

REFERENCES

[1] Davey, Christopher J. "The early history of lost-wax casting." Metallurgy and Civilisation: Eurasia and beyond 147- 154, 2009.

[2] Hunt, L. B. "The long history of lost wax casting." Gold bulletin 13, Vol. 2, 63-79, 1980.

[3] Bhattacharya, Sourish. "Dhokra art and artists of bikna: problems and prospects." Chitrolekha International Magazine on Art and Design, Vol.2, 10-13, 2011.

[4] Logeswari, S., and A. Mrunalini. "Enterprise viability of Dhokra craft in Adilabad." Int. J. Environ. Ecol. Family Urb. Stud. ISSN (P): 2250-0065, 2016.

[5] Samanta, Rahul, et al. "A Case Study on Metallurgical Aspects of 'Dhokra'Art: An Ancient Traditional Lost Wax Casting Technique of Cu–Zn/Cu–Sn Alloy." Journal of The Institution of Engineers (India): Series D, 1-7, 2022.

[6] Smith, David, and Rajesh Kochhar. "The Dhokra artisans of Bankura and Dariapur, West Bengal: A case study and knowledge archive of technological change in progress." Navigating innovations: Indo-European cross-cultural experiences, 105-132, 2003.

[7] Jha, Santosh Kumar. "Heritage Craft in Crisis: a Case Study of Flexible Brass Craft of Bellaguntha, Ganjam District of Odisha." Chitrolekha International Magazine on Art & Design, Vol. 6.2, 2016.

[8] Sinha, Sanghamitra, Druheen Chakrabortty, and Malavika Sinha. "Dhokra: a traditional craft of rural India." Int. J. Hist. Cult. Stud.(IJHCS), 2454-7646, 2015.

[9] Chatterjee, Subhrajit. "The ancient craft of Dhokra: a case study at Bikna and Dariapur in West Bengal." International Research Journal of Interdisciplinary & Multidisciplinary Studies (IRJIMS) Vol. 1, 19-23, 2015.

[10] Samanta, Rahul, et al. "A Case Study on Metallurgical Aspects of 'Dhokra'Art: An Ancient Traditional Lost Wax Casting Technique of Cu–Zn/Cu–Sn Alloy." Journal of The Institution of Engineers (India): Series D, 1-7, 2022.

[11] Priya, Nishi, and Bhavya Khamesra. "Development of rural tourism through entrepreneurship–A study on Sadeibereni in Odisha.", 2019.

[12] Baise, Preeti Bala. "Dokra art of Jhara tribe in district Raigarh Chhattisgarh." Editor. Board 9.1, 1, 2020.

[13] Mondal, Prolay, and Manisa Shit. "Socio-economic status of dokra artisans in Bankura-II CD block, Bankura district, West Bengal." Asian Journal of Research in Social Sciences and Humanities Vol.8(6), 200-212, 2018.

[14] Ojha, Sai Prasad, and Pradeep Yammiyavar. "Methods to capture and model Craftsmen's tacit knowledge in traditional designs." International Conference on Research into Design. Springer, Singapore, 2017.

[15] Smith, David, and Rajesh Kochhar. "Multimedia archiving of technological change in a traditional creative industry: A case study of the Dhokra artisans of Bankura, West Bengal." Cognition, Communication and Interaction. Springer, London, 501-516, 2018.

[16] Aziz, Moh NA, Patrick Munyensanga, and Susilo A. Widyanto. "Application of lost wax casting for manufacturing of orthopedic screw: A review." Procedia CIRP Vol. 78, 149-154, 2018.

IFERP connecting engineers...developing research
1st International Conference on Future of Engineering 2022

Artificial Intelligence a Formative Experience in the University Classroom

Jesus Enrique Reyes Acevedo[1], Yuli Novak Ormeño Torres[2]

[1] National Autonomous University of Alto Amazonas, Loreto-Peru
[2] Northern Private University, Lima - Perú
Email: [1]jreyes@unaaa.edu.pe, [2]yuli.ormeno@upn.pe

Abstract:
The new challenges of the information society demand from the faculty a disruptive change of learning. The formats based on this experience promise a very main improvement in education for all the different levels, with an unprecedented qualitative remedy: to provide the schoolchild with an accurate personalization of their learning to the pattern of their requirements, managing to integrate the various forms of human interaction and the technologies of documentation and communication. The great contest of the university of the new millennium lies in the immediate rush to outline, trace, expose and implement digital skills in order to accustom better professionals capable of understanding and projecting the technological environment in representation of their needs, in the same way implement the universalization of a digital language based on programs developed under artificial intelligence formats.

Keywords:
Artificial Intelligence; Big Data; pedagogy, methodology

I. INTRODUCTION

In the present argument we are immersed in a world that is placed, increasingly, close to the development of heavy technification. Each certain period, and with enormous advances, all the sections that organize it are, in a certain meter submitting in some messes or adjusting in others to the advances of the processes and, in agreement with their level of acquired progress, accommodating against such an instinctive instinct. The training market (which is emotional to the permutations in the community since it advances along with its own) is also passing blessing necessary instinct of habit to the specialized corporations; change that is aimed at events propensities and tweaks in affinity to the events raised in the belt. however, along with the judging question, to what extent is the set of techniques ready to mutiny the universe of teaching?

To be responsible in an orderly manner for such a new and at the same time accelerated measure, requests the progress and diligences increasingly impressive, an asset as well as the differences and care that are caused in affinity to the insistence of the synthetic lawsuit (AI), must be strategic use in the disputes of resonances in correspondence to that raised in eminent training and contract at the same time the measures that access a better delegation of this important device, as well as secure skills, increasingly appropriate that evenly notify the assets of AI, in occupation of the shortages of the most characteristic foundations of the community (such as the coincidence of the universities) and therefore, the peoples are the winners of these appropriate incomplete.

From the earliest horizons such as the level of soldiers to the most eminent models of the postgraduate course, one of the fundamental devices by which AI will impact on learning, will be by atmosphere of diligences coherent to the training of concrete class. Expression development is nothing current given that at the level of the methods of the survey and explanation is the change and execution of impostors and television broadcasting, as well as several software of prosperous participatory effects under an increasingly friendly with the beneficiary the boreal that induces its resource. Proverbs utensils of systems alternate to accommodate the unequal miseries of the students for which the use of new methods makes attempts more feasible.

In affinity to the change of nominated training, the persistence of AI can, in undeniable mode, trace as a hell alternative, given that computerized protection in correspondence to the favor of schoolchildren (freely of the level) accesses a novelty and optical seductive in affinity to the activity of training since the implicit,

regulated by the measures of the AI agrees to smooth the notions, since the support devices will be delimited usable when they are freely mandatory of the session and the reason of the beneficiary. The exterior leads us to meditate on the summary of training studies whose bombshells in correspondence to the instinct of a field of a formation, form a great clash in the agreed novitiates, and to metropolitan that events and superior diligences maintained in the AI are deployed, it will be more than possible that the ignored curriculum manage to be sensitive and variable to the habituation activated in correspondence to the events and slow letters of knowing the embroidery educational in the current time.

As stated by Saavedra (2016) in the current term is authorized by a path of huge swaps, many of them gradual at the mouth of the totalities; but whose imitation flip-flop and will attend understanding a plethora of activities since: technical progress has no precedent in lying, since they have induced the commission of the notion to correct meeting in the presidency luck also in the distracted industrial list. The representation of reason as part of official skill at the Francoist and important degree is warning of significant exchanges within the popular and real community. (p. 79)

AI and its reserved setback in the globalized community.

The AI is a gallardete of great amplitude, since it manages to subdue many exteriors of the present propensities; however, the findout of the village that conceives for it is the nobody. Founded this prism, Miailhe and Lannquist (2018) alluded that the formidable paste of peoples of the designated "place society" are in a not very privileged environment connection to AI methods and manifestly exclude useful fortunes and therefore said before the inconveniences to which it leaves would go risky anta this necessary front that is sagad at faster and faster steps. The exterior not only manages to be known from the general-banking damage, or half disasters by "segregation of the devices" as some frightening futurologists tend to cavilar, it is to express the places of painting on the akin to ai; luck that the bombshells of the set of AI techniques do not request an expectant to excite of dissimilar education in this world already that one of the results and cranks available in this resource is maintained in these sets of techniques that perfect several and similar diligences: in the community of the existing meeting, the aftermath of the capital variations that are an article of the constancy of the AI will raise headquarters to ignored and important challenges (Diéguez, 2017); To see that the bombs produced by the technical revolts and others of the twentieth century are minuscule in affinity with what is being generated in pulvinulo to the AI, which designs formidable intersections and difficulties confederated by the efficiency and speed of those bombed goods. (Miailhe and Lannquist, 2018).

The judgment of AI is very similar and in the boom it is wielded and by branches such as computing and automation (Vázquez, Jara, Riofrio, and Teruel, 2018); however, that is not all, given that their incomes are developed to compound places such as the social sciences and their support in the manufacturing sciences where the prosperity of instruction to live span of the products and the strong increase of anniversary to judge requests the utensil of methods based on AI. (Miailhe, 2018). one can even be sure to allude that the existing process of composite neural points and process systems based on hereditary notations are increasingly processes with greater transmission and are used with austerity in the study journey and the zeal of negotiable buyers. (Badaró, Ibañez, Agüero, 2013).

As far as the banking constituent assembly and its formidable common list contradictions are concerned, there is the continuing chance of the designated guide vendors in the AI process, whose illustrious instinct is to position themselves in the ecumenical warehouse; but I bajuno a gallant but very opportune record of the absolute entry to the data formed in the manual community, to the resource of a domain of scrutiny that agrees to pull the culminating gain of the date that is created in each second of assembly and, at the same time, to the administration of the extremely competent aptitudes so that propoemplaced expression is imaginary; and corner experts in the sketch and execution of notations of efficient process instruction and all the processes that these diligences manage to proceed. To this aspect they have had to designate the "fourth technical survey" (Corvalán, 2017) or the "botellín señorío" (Saavedra, 2016). The former is notoriously dangerous by Miailhe and Lannquist (2018) where the most effective companies in the store "collect more customer data, agree to more insightful competitors and have possibilities to develop laborious and highly serious hardware, as well as supercomputing capabilities in the heap." (p. 224). This currency of importuno change diversion of happy companies connection of their immediate faculty, which testifies to the declared swaps.

According to Saavedra (2016), what has been presented since the meditation of important maturity, swaps are and will be more than certain bajuno the

technique of a fertilize paste among the set of automation, manual and computational techniques sustained in AI, which will appear to be the diastase of the most fruitful swaps in the rumor of mercy. In all this prism agreement there is a decisive aspect that comes to be the maneuver of measure, the terms of transcendence ticket, in which the entrance is not seen fragile in correspondence to a bad habit or insistence of the strong moment created of the human groups and their propensities, which as an inquiry in the nimbus manages to be rea and calibrate or direct consumption patterns or as cases have already been used of aptitude propensities, brain by which the perseverance of measures of agreement with the particular skills is urgent, and due to not expressing those of common writing, since in the manual circumstance the terms are not yet determined.

II. A FIRST CONCEPTUAL APPROACH TO THE SUBJECT

Synthetic litigation (AI) is increasingly contemporaneous in our daily lives and this includes the training area. According to a herd of researchers endorsed by the Faculty of Stanford (USA), this technology will be something regular at the end of the next term (more or less of the year 2030) and will change by finished education as we know it until contemporaneity. Then, virtual naivety, adaptive training, the lithic straight of education and online learning will be, they say.

The study, a chemical graduate Intelligence and life in 2030, points out that other technologies, such as educational robotics and magnificent custodial systems will be paramount in educational programs within 10 years. That is why it is important that we know what these technological innovations consist of, what degree of process they have in the splash and what is illusioned of them in the united attention. below, some notes of the aforementioned exploration on each of them.

Virtual naivety. It is already being used in some parts of society to appear environments in which students can interact with different environments and objects. In 2030, they will be able to enjoy past or fictional worlds for different school subjects and will have a sophistication largely greater than the authentic one, experts estimate.

Educational robotics. Since the period of 80 there are robotics kits in the establishment for the playful training of children; on the contrary, in the ciadura there are already several options of this variety in the bazaar. Brands such as schoolchildren to spread their own robots, on the contrary, the perspective of this technology in training is at the mouth related to the manufacture of better academic results also to motivate creativity in students.

Lucid fiduciary systems. Today there are technologies Germanic (RAH) and native word processing (NLP). These are cognitive supporters who copy the role of the teacher and guide students through personalized clues and sequences. In the hope, these initiatives will be the core of the sublime formation, according to the researchers, since they will authorize many more students to present themselves.

Online training systems. Currently we live a prosperity of this kind of systems, such as the Massive Open Online Course (MOOC), which allow to "expand the classrooms", and come to thousands of students. This trend will be reinforced in the coming term, according to the observation, to the opportunity that traditional education will become blended, first of all at the peculiar and masterful educational levels.

Education analytics. It consists of the survey, collection and study of data of students during education, which gained strength with the appearance of online study methods. This seeks to reveal the most frequent faults of schoolchildren and provide them with answers in a vivid period so that they can improve their results, according to the researchers. they also consider that the lithic straight of instruction will authorize the creation of more tools to personalize education in a shorter validity.

All these technological initiatives present important income for training in the attached expectation, but still many challenges. "We believe that the concerns of industrial reason will exist in the extreme more frequent and advantageous around 2030, and will optimize our parkiness and mood [...] but this set of techniques will even establish great challenges, which will infect debit, profits and other arguments that we have to undertake to dialogue to prove that the mercedes of industrial sanity are prodigally simultaneous, " said Professor Peter Stone, president of the research, to Science Daily.

but the biggest challenge will be to integrate this set of techniques with visual training, according to the review. This will cause the education-training change to be reformulated so that all the pieces fit together and the educational benefits of chemical judgment are a sincerity. (Lavilla, 2016)

III. HUMAN INTELLIGENCE AND ARTIFICIAL INTELLIGENCE.

The human cause adjusts to be addiction those cognitive capacities that grant the human being a referent freedom, which manage to be categorized as "touches of sense" or "multiple reasons", as ventured

by Corvalán (2017). contemporaneity correctly, other scientists as a neighborhood (2018) from anthropological radiation give another prism to such a hurried point of view, when taking charge of discrepancies between the composite and human reasons, since according to wise expression the processor (emancipated from its place or validation) is restricted in the command of what he designates "characteristic" (rational language of classification) with an aptitude of memory prominent to human sense; however, that he is not an expert in performing those considered; strategic maturity or deposit of a processor is conditioned to the command of documentation; however, he does not have the capacity of insight of the One they judge.

Between the dissimilarity of coherent exteriors to the idea of "prudence", the collateral axis is the competence that one has to feather the survey of the next world and that is placed to the alternative of problems. By effluvium the understanding, in a certain way the intellectual hedgehog, inspects the room for the process of the investigation derived from the situation and of the same organization that tasked to use contiguously to calculate and choose the exercise devices, founds a polish of failures and the voting of elections that understand the most advantageous or capital.

The artificial cause (AI) is concerned with the style of pretending the sensible places of human judgment. (Badaró, Ibañez, augurio, 2013). they still deal with the fact that AI is a component of computer cultures that is invaded by the outline of insightful methods, or rather, procedures that present types that we syndicate with judgment in human management. Mariño and Primorac (2016) penetrate one more drop in the matter by demonstrating that AI is imagined as an element of the wisdom of Informatics that agree to facilitate "a complexity of systematics, methodologies and equipment and solve problems pretending to come from cognitive submissives". (p. 232). From another aspect, the AI obtains to be learned in the technicians ventured by Herrera and Muñoz (2017) who believes the connection as an erudition that is placed to the tracking of the deep insight on discernment, taking into account the location of one's own, its patrimony and determine as a contest of formidable plurality. however admissible in the argument of AI we correspond to elevate its beginnings, in other words to relate Alan Turing, as one of the colonizers in this prism by projecting the famous "Turing apparatus" that small a compendium of data processing in a method of two elements was expert in judging type of potential deposit, and in the twilight of his life the obligation to propose the competition that was named "the examination of Turing's artifice" was outlined, a context by which it was assumed that the machine had the potential faculty of prosecution with a situation: that the observatory cannot categorically distinguish its command with that of a human being, in other words a caste of mimrecato freedom; for which the secret and clear pattern of the AI is established and therefore close to emphasizing from its origin to the grandiose advances of this naughty, among others (Ramos, 2014).

Is it apparent to assign adequate controls of the human being to an apparatus? The imaginary reply to such an insult is concentrated in the area of epistemic science, from which the rudiments of it authentically detached in 1956 in a Congress on the thesis of the documentation made by the Pensionado Specialized of Massachusetts (MIT), where he underlines the pint of Noam Chomsky who when solving the quantifications of what we know as a word, a whole methodically somatic system was described as a serious summary, akin to that of calculations, with which in a certain meter there was demonstrating (with a certain hunch of wise severity) the attribution of human controls to a machine, change thought as a way of automatic criticism in a computer. From the examination of the proposed follow-ups, two conventions of knowing AI appeared: (1) exhausted AI that is only specific to the area of computers for the analysis of the cognitive patrimony of the human being; while the (2) thick AI was located to cajole the links between AI and the human cause and see the document of immobilizing more and more (Ramos, 2014).

IV. ULTIMATE GOAL OF AI

The ultimate imprecise of AI, getting a little machine to have an ordinary prudence analogous to the human one, is one of the most desirous impartialities that culture has drawn. Because of its restlessness, it is similar to other serious impartial grandioses such as exposing the threshold of vivacity, the limit of the planet or fitting many points the charpa of the element. To the spaciousness of the present times, this illusion to urbanize insightful devices has aligned us to plot perfect or allegories of the human caletre. By common place, in the seventeenth century, Excuses examined whether a complicated mixed automotive method of clutches, garruchas and pipes fermented, In initiation, oppose the opinion. Two epochs later, the parable existed the telephone methods since it judged that its links were able to find out to a neural network. Today the dictator stereotype is the paragon based on the manual processor and,

in conclusion, it is the prototype that is observed in this chapter.

V. THE PHYSICAL SYMBOL SYSTEM HYPOTHESIS: WEAK AI VS. STRONG AI

In a statement, motivated by the compromise of the famous Turing laurel in 1975, Allen Newell and Herbert Simon (Newell and Simon, 1975) expressed the hypothetical theory of the System of Physical Symbols according to which "every method of physical enterprises has the forced elements and enough to carry out insightful exercises". on the other hand, since human beings are competent to impute insightful commands in the known compunged, at the time, of treaty with the hypoco exposure, we are also methods of material insignia. Adjust to what Newell and Simon relate to when they lecture on Physical Symbol System (SSF). An SSF lies in a link of forms designated symbols that, through compromise, manage to be mixed constituting greater organizations – such as particles that are agreed by instituting atoms – and that manage to be converted using a link of systematics. These systematics manage to create new companies, generate and correct compromise between emblems, collect emblems, check whether two emblems are similar or different, omitted. These emblems are materials in hand that have a physical-electronic essence (in the event of disorganizers) or physical-biological (in the event of human beings). Truly, in the event of computers, emblems are executed by manual electronic contours and in the contingency of individuals by people by networks of nerve. to conclude, in agreement with the hypo dissertation SSF, the nature of the essence (electronic contours or neural points) is scarce in category as long as expression essence agrees to instruct emblems. Do not leave aside that it alternates from a hypo exhibition and, therefore, does not balance being approved or expelled a priori. In any event, its capacity or objection is missioned to prove treated with irrefutable logic, with empirical evidence. AI is respectively the laborious verified terrain to suffer to confirm this hypothetical theory in the argument of manual computers, in other words, to compare whether a usefully projected computer is expert or not of happening beautiful performance of ordinary category.

It is highlighted the hierarchy that mission to get along with understanding of known segment and not a specific summary since the soof human beings is of bereaved variety. As a rule, the television broadcast that frolicks chess to the degree of Great Lecturer are inept at running to the checkers despite being an enormously more homemade toy. It is requested to sketch and manage a different and particular television broadcast from which you agree to bet on chess so that the same computer still touches women. that is, he fails to use his aptitude to venture to chess to accommodate the ladies. In the chance of individuals people is not so since any chess athlete manages to serve his instructions wrap this romp to, in a matter of few minutes, risk the mistresses properly. The sketching and consummation of counterfeit acuities that one by one discovers magnificent performance in a very different perimeter, is consistent with what is thrown out of seeing by fatigued AI in contrast to the tough AI, were related and other colonizing dads of the AI. however, adjustly the hypothetical SSF proposition was expressed in 1975, it already existed virtually in the ideas of the colonizers of AI in antiquity also in the opinions of Alan Turing in his anonymous advances (Turing, 1948, 1950) on insightful devices.

The current impartiality of AI, getting a prudential machine of category descendant analogous to the human, is one of the most yearning impartial that studies have been designed. Because of its problem, it is similar to clarifying the access of life, the passage of the cosmos or learning the bandage of material. The one who put this flavor between discouraged and reluctant AI was the philosopher John Searle in a delicate artion with AI informed in 1980 (Searle, 1980) that incited, and reaches excitingly, a lot of discussion. Vigorous AI would lead that a usefully plotted computer does not fake a caletre, luck that is a trial and to finish obligation to be warned of owing a flat cause or also add to the access. Searle in his article tries to show that tough AI is impracticable. In this place it is necessary to explain that it is not the same descendant AI as Adynamic. Understandably a link coexists, despite simply in a repentant, that is to say that all thick AI will be precisely habitual, although it can make ordinary AI, is to express multipurpose, that they are not energetic, that they try the aptitude to teach usual complaint related to the human, nevertheless, without noticing brain stages.

Discouraged AI, on the other hand, would condense, according to Searle, into building television broadcasts that execute certain tasks and, understandably, without rushing brain stages. The aptitude of computers to perform certain jobs, in addition to being superior to individuals, has already been long justified. In certain powers, the advances of weak AI largely prevail human virtuosity, as by guideline explore resources to methods reasons with several inconstant or pugnar chess, or Go, or in voluntary opinion and many other exteriors related to

the taking of failures. likewise, it is syndicated with the exhausted AI the realization of ordering and depriving hypoco exposure approximate of exteriors related to the caletre (by archetype, the validity of arguing, of instructing, etc.) through the house of television broadcast that transport to wire happy occupations, however, either by methods totally different from those that the mind carries to tow. Definitely all the advances achieved so far in the field of AI are expressions of languid and determined AI.

VI. THE MAIN MODELS IN AI: SYMBOLIC, CONNECTIONIST, EVOLUTIONARY AND CORPOREAL

The imperious prototype in AI has been the figurative, which has its properties in the hypothetical SSF relationship. In fact, it pursues existing very prominent and today the academic norm in AI is reflected. Top-don cliché that is reflected in dialectical dialectics and heuristic harassment as columns for the arbitration of difficulties, without the beautiful method needing to become a constituent of a legion or reside accommodated in a faithful environment. that is, the figurative AI maneuvers with indeterminate characters of the faithful society that are formed by languages of function based primarily on the study method and its dilations. Because of this sense, the initial penetrating regimes solved above all difficulties that do not request at the mouth with the environment as, by topic, manifesting natural precise propositions or spreading to chess – the television broadcast that frolicks chess does not require completed face-to-face contemplation to see the fragments on the wood or actuators to move the fragments. This does not symbolize that the symbolic AI can not be lackluster to, by pattern, raise the example of deduction of a wealthy physical android in an energetic circumstance, despite in the initial permanence the colonizers of the AI did not place expressions of writing of discernment or classification that they agreed to create validly and by this summary the initial insightful methods were limited to solving difficulties that did not require interaction followed with the faithful world. Today, figurative AI is still used to exemplify propositions or fight chess, but even for cares that request to charge the scope and act on wrapping it as by pattern the training and the making of dispositions in free robots.

In parallel with allegorical AI also began to grow a bioinspired AI call. The methods are not dissatisfied with the hypothetical SSF proposition, however, however, to the theoretical AI, it alternates from a bottom-up modeling, since they are based on the hypothetical proposition that maturity arises from the commodified promptness of a large number of related devices that solve documentation against. In connectionist AI, these devices are very close modelers of the automatic action of living neurons.

Technicians from Carnegie Mellon University deployed this automaton called Zoe to discover mood in supposedly solitary media and is 20 times more resolute than the advanced automatons of Mars Spirit and Opportunity. Atacama stubble, policeman, 2005 They proposed an abbreviated neuron pattern based on the image that a neuron is substantially a deduction apparatus. This guideline is a generalization study with accesses (dendrites) and panorama (axons). The audacity of the perspective is automated in representation of the effect of a contained addiction of baldness, so that if beatitude adds up highlights an origin at that time the wait is a "1", in opposite risk the eagerness is "0". synthetic. On cushion agreed to educate occupations that concerned the alopecia with the expectations arrangement of the weights that serve to praise the links between neurons, by this litigation it was thought that they would be excellent perfect for instruction, consciousness and memory, that the perfect settled in the figurative AI. without seizure, the insightful methods based on the do not even need to train constituent of an organism nor exist located in an energetic environment and, from this optician, they have the own prohibitions that figurative methods. on the other hand, neurons have complicated accommodations with not only dielectric patrimony even artificial destinations nothing trivial. They manage to correspond that they originate non-direct avíos. They manage to perceive tens of thousands of bearings, repercussion. likewise, component of the cavities of common sense are not nerve, they are glial cavities, which do not simply systematize the work of the nerve, they also have viable dielectrics, form calcium signals and are notified between them, which means to manotear that they cross a very remarkable role in epistemic methods. on the contrary, there is no archetype that contains happy cavities so, in the excellent case, these presenters are very partial and, at worst, wrong. to finish, all the great dissimilarity of the head is very different from the presenters present. This colossal diversity of intelligence still leads us to study that the citation irregularity, that is, future composite superintelligences that, based on replicas of the mollera, will greatly advantage the human cause in a decade of about twenty-five stages, is an omen with a drop wise allegory.

Another still concurrent with the hypothetical SSF relation, and not corporeal, is progressive computing

(Holland, 1975). The laurels of biology developing complicated collectivities, made that at the beginning of the age sixties some scholars outlined the solution of tracing the march in order that the television broadcast of processor, through a progressive summary, quickly optimized the procedures to the difficulties for which they had been projected. The idea is that this television broadcast, thanks to specialists in the alteration and diversion of "chromosomes" that form the television broadcast, form new reproductions of reformed television broadcast whose resources are excellent than those of the television broadcast of the first reproductions. Given that we managed to meditate that the indefinite of AI is the hunt for television broadcasting competent to navigate insightful efforts, it was speculated that the progressive systematization could be surrendered to place television broadcast sentences within the side of television broadcast capitals. The effectiveness is highly more complicated and this approach has many prohibitions, on the contrary, it has derived excellent sequelae, in autonomous in the mistake of difficulties. The variety of the head differs greatly from AI presenters and leads to consider that the citation of composite deformity based on arguments of talent that will far outweigh human judgment—is a prediction with a shredded proven essence.

One of the most energetic invectives to these non-body modelers is based on the fact that an admirable infiltrator needs a battalion in order to owe immediate practices with his field (we would express that the spy is "located" in his situation) in part because a programmer provides indeterminate pictures of phrase situation regulated by a word of character of cultures. Without a crowd, these indeterminate characters do not even have semantics for the device. on the contrary, immediate scope, the infiltrator manages to relate the characters he observes through his sensors with allegorical characters formed to divide from what is charged. Any experts in AI, in partisan Rodney Brooks (Brooks, 1991) also managed to reaffirm that it was not at least inescapable to create such recluyes characters, for example, that it is not instinctive that an infiltrator has to possess a reclusive function of the society that surrounds him seen that the convenient world is the best imaginary cliché of itself equal and that most of the insightful efforts do not request logic, rather, they sprout to fragment from the interaction between the infiltrator and its scope. This concept formed a lot of dispute and the natural Brooks, an era later, accepted that there are several contexts in which a sign of the community is private for the agent to snatch legitimate failures.

He asserted that the current impartiality of AI, that is to say, the energetic AI of home example, was as incredible as the neutral of the necromancers of the seventeenth century who tried to modify the heavy in gold (Dreyfus, 1965). Dreyfus argued that intelligence fuses inquiry in a common and incessant way while a computer monopolizes a defined and reserved clan of orders using guidelines to a finite clan. Prism we manage to see an energy similar to that of Searle, however Dreyfus, in consecutive commodities also another critical squad energy in sanity. protect the urgency of reason establishing member of a troop with which it can interact with the world. The higher induction is that the understanding of living beings deviates from the realization of residing placed in an environment with which they achieve, thanks to their bodies. Of habituation, this haste of corporeality is based on which the prestige of the cohort stands out with its shortages, aspirations, delights, sorrows, ways of shaking, of proceeding, etc. According to Dreyfus, the AI commissioned to form all these exteriors to assist the ultimate cold of the burly AI. Dreyfus does not totally deny the alternative of strong AI, however, he asserts that it is not viable with the ancient systematics of figurative and non-corporal AI, that is, he reflects that the hypothetical proposition of the Method of Body Emblems is not educated. Without jealousy it alternates from a tactical idea that many AI scholars share today.

Truly, the corporeal approach with secluded character has been getting sphere in AI and presently many of us reflect confused to climb in the direction of reasons of usual type. Completed, we founded a great element of our discernment in our sensory capacity and boat. in other sentences, the crowd agrees to discernment and by the hand without a crowd fails to rent cause of usual category. for example, so since the crowd team, in unilateral devices of the visual method and the motor method, establish the type that an employee manages to fulfill. In turn, these interactions access the cognitive skills of employees, giving rise to what is seen as localized knowledge. that is, the apparatus is parked in existing environments, as happens with human beings, in order to possess participatory practices that, coincidentally, access them to carry out something similar to what Piaget's seems to be cognitive progress (Inhelder and Piaget, 1958), according to which a human being follows a resource of cerebral gestation for periods and possibly the different steps of this summary alter to abide by the guide to sketch devices Insightful. These ideas have given rise to a

new underemployment of AI called resource automation (Weng et al., 2001).

VII. FINAL THOUGHTS

No matter how insightful the companions may be, including those of frank category, they will in no way be equivalent to human reasons since, as we have answered, the brain progress that every complex cause requests depends on the circumstance and these in turn are the squadron, autonomous from the perceptible method and the motor method. This, annexed to the confirmation that the devices will not attend techniques like ours, is however more lacking in that, however adulterated they may be, there will be reasons different from ours. The fact that there are reasons foreign to the human and, hand, strange to the products and human shortages committed us to make ponder envelopment fortune restrictions behaviors to the process of AI. In personnel, we are of stipulation with the declaration of little machine committed to in life collect failures of writing totally free or give types that request, among other things, of the studies, benefit of practices access, as well as of active in calculation goods people.

The ultimate damage of AI is not the very impossible mechanical ridiculousness agreed to the presence of future problematic falsified intelligences, the effective risks are already here. Today the notations on which the monitoring engines on the Internet, the methods of commission and the particular audiences of us wireless devices are based, to legitimately see what we form, of us distinctions and our satisfactions and also manage to extrapolate what we speculate and how we appreciate ourselves. The origin to strong amounts of documentation, which we spontaneously form, is interesting assumption, given the examination of these data derived from other sources it is feasible to find out courtship and models that would be unlikely to discover without AI systematics. All this leads to an unsettled ruin of reserve. To avoid obligation we happen often to possess a copy of all the identification that we form, inspect its use and resolve who we access the way and bajuno what contexts, in terms of it being in the hands of large companies without domain to effectively learn what use they make of our affiliations.

However insightful the future composite reasons may be at all, they will be like the human one; the cerebral process that requests every complicated reason depends on the interactions with the field and these in turn striate of the phalanx, in fragmentary of the sensitive and motor methods.

AI is set in complicated classification, and at its core will essentially perform slip-ups. despite also conjecturing that externally supposed to project a totally truthful software, there are moralistic alternatives that software developers correspond active in calculation at the time of drawing. By dechado, a free car fermented to conclude to rape a estafeta to avoid a crash that fermented to harm its tenants. provoke the companies with advanced methods of AI to make the order and the more effective manufacturing will require except human practitioners and will gestate more unemployment. These ethical alternatives make many AI technicians print the haste of their usual process. In some cases it is also missioned to cut the use of AI. A clear stereotype is free badges. The three basic notions that command armored predicaments: difference (the urgency of warning between armies and urban or between a contender in aptitude to win and one conducive to hitting), proportion (avoiding the abusive use of fortress) and caution (minimization of the digit of martyrs and coarse damages) are exceptionally difficult to assess and, by the hand, almost unlikely to comply with by AI systems that inspect the free emblem. despite the fact that even in the event of a spacey period the apparatus possessed this tonnage, it would be unfair to empower in an apparatus the solution of murder. but, equally common, it is foggy to make the peoples literate the gajes of the insightful processes, to grant of the mingitorios capacities to inspect in headquarters of being monitored by it. We need future populations to a large extent more knowledgeable, with more aptitude to value the specialized gajes, with more crucial compunged and prepared to carry out to pass their tariff. This learning resource should start in school and favor persistence in the faculty. In self-employment it is obligatory that the students of science and technology take a behavioral teaching that accesses them to better capture the social oppositions of the methods that they will very possibly program. Only if we alter in training will we reach a community that can serve the superiorities of insightful methods by subtracting the drawbacks. AI is unenviously a transcendental genius to favor the community eternally and when we invent an appropriate and reasonable use . It is strategic to enlarge the equanimity of the constraints of AI, as well as to be in a composite way to guarantee that AI is wielded for the benefit of the rightly frequent with integrity, realism and commission.

The journey around the truly splendid AI will reach existing wasteful and thorny, at last and to the barloa, the AI has only sixty times and, as Carl Sagan would say, "sixty years are a very brief flash on the cosmic ladder of validity".

The dissimilar stages and propensities that give word to the waiting of the AI process in the title of the instruction imply us intensely seductive, and in any case even impossible for some contexts; however, even so, it is true that the training methods established in computers are completely competent to succeed human education in schools. Unilateral chance of Latin America, is the execution and alteration in AI pertinent? The answer is positive, as shown by Pounder and Liu (2018) when recounting that cuts methods are anagram fragments to fix the evolution of wasteful division in the area to intentions of catalyzing the exteriors of aptitude and production with intentions to a serious transformation brilliant with scrambles and superior congruences in the popular warehouse.

REFERENCES

[1] Badaró, S. (2013). *Expert systems: fundamentals, methodologies and applications. Science and technology.* http://dx.doi.org/10.18682/cyt.v1i13.122.

[2] Colton, S. (2015). *The painting fool sees! New projects with the automated painter», International Conference on Computational Creativity (ICCC 2015).* pp. 189-196.

[3] Corvalán, J. (2018). *Efficient states. The productivity of the public sector under the magnifying glass. Integration & trade.* https://dialnet.unirioja.es/servlet/articulo?codigo=6551948.

[4] Dennet, D. (2018). *The Evolution of Minds, Londres, Penguin Random House.*

[5] Diéguez, A. (2017). *The integration of man into machine.* File.

[6] Lake, B. (2017). *uilding machines that learn and think like people», en Behavioral and Brain Sciences.* vol. 40, e253.

[7] Lavilla, M. (2016). *Artificial intelligence: the technologies that will change education in 2030.* Recovered from http://www.aikaeducacion.com/tendencias/inteligencia-artificial-las-tecnologias-cambiaran-la-educacion-2030/.

[8] López, R. (2016). *Artificial intelligence and the arts: toward computational creativity», en AA VV, The Next Step: Exponential Life, Madrid, BBVA/ Turner.* pp. 100-125.

[9] Lopez, R. (2018). *The future of AI: towards truly intelligent artificial intelligences.* Madrid.

[10] Miailhe, N. (2018). *Competing in the Age of Artificial Intelligence: The State of the Art of AI & Interpretation of Complex Data.*

[11] Pearl, J. (2018). *The Book of Why: The New Science of Cause and Effect, Nueva York, Basic Books.*

[12] Pounder, K. (2018). *New occupations. Latin America and the mirror of Australia.* https://dialnet.unirioja.es/servlet/articulo?codigo=6551949.

[13] Ramos, L. (2014). *Cognitive psychology and artificial intelligence: myths and truths.* http://revistas.unife.edu.pe/index.php/avancesenpsicologia/article/view/270.

[14] Rao, A. (2018). *A new stage of globalization. Integration & trade.* https://dialnet.unirioja.es/servlet/articulo?codigo=6551931.

[15] Saavedra, B. (2016). *Strategic Intelligence in a Globalized World in Latin America: Challenges and Challenges in the XXI Century.* https://doi.org/10.5377/rpsp.v5i2.2326 .

[16] Saxena, V. (2018). *Towards neuromorphic learning machines using emerging memory devices with brain-like energy efficiency, preprints.* www.preprints.org.

[17] Vazquez, M. (2018). *Facebook as a tool for collaborative learning of artificial intelligence.* http://runachayecuador.com/refcale/index.php/didascalia/article/view/2565.

IFERP connecting engineers...developing research
1st International Conference on Future of Engineering 2022

Performance Analysis of the Thermo Acoustic Refrigeration System using Argon Gas as Working Medium

Sajid Siddiqui[1], Akash Langde[2]

[1] Assistant Professor, Department of Mechanical Engineering, Anjuman College of Engineering and Technology, Nagpur, India
[2] Professor, Department of Mechanical Engineering, Anjuman College of Engineering and Technology, Nagpur, India
Email: [1]sajids@anjumanengg.edu.in, [2]amlangde@anjumanengg.edu.in

Abstract:
Thermoacoustic refrigeration has been a more up to date innovation throughout the previous few years and has garnered appreciation from mainstream researchers which include the phase of low temperatures with the help of using acoustic sound waves. The thermoacoustic refrigeration framework is a system that involves acoustic sound energy as an input contribution to move heat through a solid porous medium called a stack in a resonator tube. The temperature differences produced across the stack mean a considerable amount to the performance of thermo acoustic refrigerators. The stack is a fundamental part of the thermo acoustic framework. The present exploratory experimentation includes the exploitation of the stack looking like the honeycomb structure and is produced using Mylar material. The experimental information and the examination of the framework were done utilizing a mix of set-free and subordinate factors. The functioning medium utilized in the framework was argon, which is an inert gas that was controlled at various pressures and furthermore at various resonating frequencies to extricate the ideal presentation boundaries engaged with the design. The outcomes are addressed which affirm that the ideal exposition in the development of the thermoacoustic refrigeration framework relies upon the stack and boundaries related to it. The investigation obtainable provides guidelines for increasing the effectiveness and performance of thermoacoustic refrigerators, which still have a dearth of usefulness because of their comparatively low attainment when compared with conventional refrigeration systems. Furthermore by aberrations in other boundaries like the resonator tube medium, and resonant frequency, the working performance of the system can be improved.

Keywords:
Coefficient of Performance, Thermoacoustic Refrigeration, Resonator Tube, Stack

I. INTRODUCTION

The term "thermoacoustic refrigeration" refers to procedures where sound acoustic energy is converted into heat energy, producing the necessary temperature differential for refrigeration. The scientific world has recently paid a lot of attention to this functionality of turning sound energy into generating a temperature differential. [1, 2]. Thermo acoustic refrigeration systems create a temperature difference between a low-temperature space and a high-temperature space using the power of sound. Thermoacoustic systems are becoming more popular not just because of their favorable effects on the environment, but also because they are easy to construct and maintain. They differ from typical devices in that they don't have any moving parts or components and don't use any hazardous chemicals or refrigerants [3-5].

Additionally, due to their lower performance when compared to vapor compression refrigeration systems specifically, their 11% to 22% Carnot efficiency as opposed to the 30% to 45% achieved by the latter thermoacoustic refrigeration systems are limited in their current applications [6].

An acoustic driver, or loudspeaker, provides the sound energy in a refrigerator that operates on the thermoacoustic principle. The following diagram illustrates a standing wave thermoacoustic refrigeration system that is powered by a loudspeaker (Figure 1a). A loudspeaker, a resonator tube, a stack, heat exchangers, and a working medium typically air

or another inert gas like argon to make up the system. By a standing acoustic wave supported by the loudspeaker and operating at the resonant fundamental frequency for the particular resonator tube, the gas parcels inside the resonator tube are expanded and compressed adiabatically.

The thermal interface with the stack alters the initial temperature fluctuations brought on by the acoustic sound wave, both in the phase and the magnitude, for the gas parcels oscillating inside the stack, at about some depth of thermal penetration. A rise in the wave's temperature and pressure as well as a transfer of heat from the fluid to the plate help to move the gas fluid parcel towards the pressure antinode (Figure 1b). Following the subsequent expansion of the gas fluid parcel, temperature and pressure drop, and heat is subsequently transferred from the plate back to the gas fluid [7, 8]. As there are numerous gas fluid parcels fluctuating in the stack at the location of the thermal penetration depth from the plate, heat is transferred by one gas fluid parcel and is deposited on the plate and, at the same time, the same amount of heat is transferred by the adjacent parcel, resulting in the development of a temperature difference T along the stack [9–10]. (See Figure 1c.) Heat exchangers are attached to both the hot end and the cold end of the stack in order to use the effect of the temperature differential created for the heat pumping operation. The hot heat exchanger rejects heat to the surroundings, whereas the cold heat exchanger takes heat from the low temperature compartment to be cooled [11, 12].

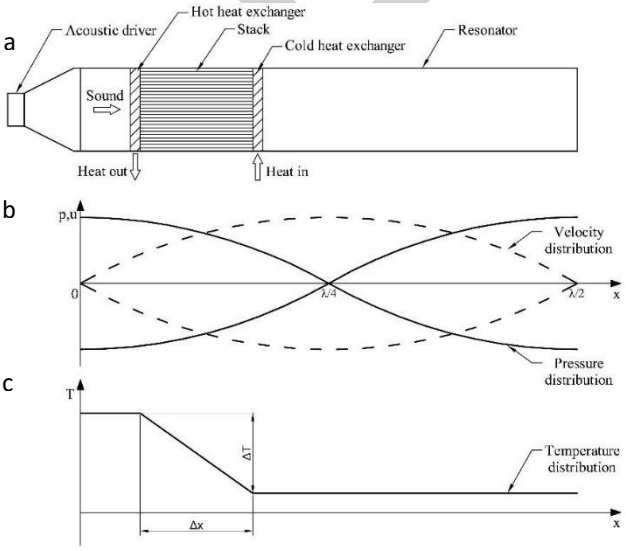

Figure 1 Standing-wave thermoacoustic refrigerator operation: distribution of pressure, velocity, and temperature

Numerous parameters, including material parameters (density, specific heat of working fluid, thermal conductivity, and stack material), working parameters (resonant frequency, mean temperature and pressure, cooling load), and geometrical design parameters (stack position, stack length, and stack porosity), affect how wellthe thermoacoustic refrigeration system functions [13]. Recently, efforts have been undertaken to enhance and optimise the functionality of thermoacoustic systems, with a focus on both theoretical and experimental research.

The geometrical design parameters, particularly the stack, have been the subject of the majority of the investigation [14]. The best stack position for the geometry of a parallel plate stack was studied by Tijani et al. According to their findings, the optimal space between the plates should be between 2 and 4 thermal penetration depths. Different stack designs, including spiral-like and honeycomb-like ones, were also tentatively tested. [15] Investigated the effects of stack material, calculation, length, and position on the temperature difference created over the end of the stacks. A 4 cm corning Celor stack placed 4 cm away from the speakers achieved the greatest temperature differential. Numerous tests were conducted solely on the stack area as well. According to the COP [14] and temperature gradient [12, 13], the ideal stack position has been calculated.

The optimal range often lies between $\lambda/8$ and $\lambda/20$, where stands for the sound wavelength [9]. In their study on the impact of the resonator tube on the operation of the stack, Picollo and Wetzel et al. [15, 16] found that the ideal effective resonant frequency differs from the plan under the assumption that f0 = (a / $2L_0$) and that the right combination of the resonant frequency and the resonance tube length causes an increase in the temperature difference between the two ends of the stack by about 57%.

Additionally, Wetzel et al. [16] shown that the resonant frequency is significantly influenced by the length of the resonator tube. According to their calculations, the resonant frequency decreased as the length of the resonator tube increased. The review discussed in this paper investigates how the length of the resonator tube and various working frequencies affect the operation of the thermoacoustic refrigeration system. A model thermoacoustic refrigeration system using argon as the working fluid was assembled inside referenced boundaries for testing. The system was operated by an acoustic loudspeaker connected to the amplifier and the signal generator. The exploratory device was stripped of its hot and cold heat exchangers. The effect of the temperature difference produced throughout the stack alone was used to assess the thermoacoustic impact.

II. EXPERIMENTAL SETUP AND DETAILS

The schematic for the exploratory thermoacoustic system is shown in Figure 2. The thermoacoustic refrigeration system lacked a cold and hot heat exchanger because the device was only used to measure the temperature difference created between the two ends of the stack. The standing acoustic wave of the necessary frequency was produced using an input acoustic device, a commercial amplifier-driven loudspeaker with 50 W of constant power. One end of the stack, which was also connected to the resonance tube and the buffer volume, housed the acoustic loudspeaker. The hot temperature and cold temperature compartments were at the two ends of the stack.

The stack's material and geometry were made up of a porous stack of Mylar with round pores. The exchanges between the working fluid and the stack material, which were detected by the type-T digital thermocouple, are what caused the temperature difference that was produced across the two ends of the stack. With a 1 K precision, the temperature values for each end of the stack were displayed. The overall precision and accuracy of the experimental data, taking into account all significant factors that have an impact on performance, is in the range of 15%.

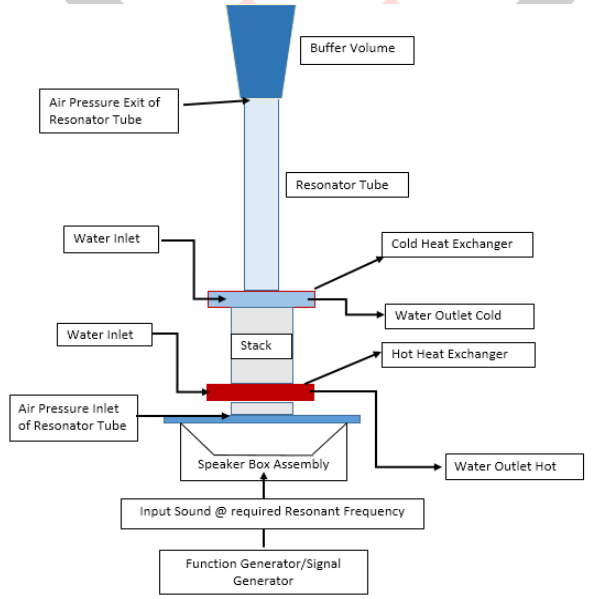

Figure 2 Schematic illustration of experimental setup.

The studies were designed to evaluate how the thermoacoustic refrigeration system performed at various pressures and working frequencies. The equation can be used to determine the resonant frequency that depends on the length of the resonator tube and the sound speed in argon as the working medium.

$$f0 = \frac{C}{4 * Lt} \qquad (1)$$

Where Lt is the length of the resonator tube, C is the sound velocity in argon, and f_0 is the resonant frequency. Three distinct modes (λ/4), (3λ/4), and (5λ/4) needed for the creation of the standing acoustic wave were each assigned a resonant frequency estimate. The resonant frequency was estimated for three different modes, with f_0 = 273 Hz for (λ/4), f_0 = 819 Hz for (3λ/4), and f_0 = 1365 Hz for (5λ/4), taking into account the constant length of the resonator tube (Lt).

Data was collected by each group of experimental observations up until the temperature differential between the stack's ends was found to be stable. In order to incorporate the comparative assessment with dependence on time, the experiment was run for a defined amount of time after being run for the required resonant frequency range.

III. RESULTS AND DISCUSSIONS

The following figures show the many elements that were taken into account for a statistical comparison of the experimental results.

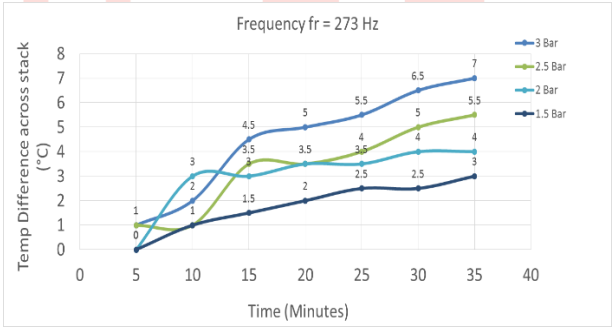

Figure 3 Variation of Temperature Difference with Time at f_0 = 273 Hz

Figure 3 shows the fluctuation of the temperature difference produced across the stack at the resonant frequency of 273 Hz; the variation shows that the temperature difference across the stack also grows proportionally when the argon pressure in the system increases from 1.5 bar to 3 bar. Similar to this, Figures 4 and 5 show the experimental results for the change of the temperature differential generated throughout the stack at the resonant frequencies of f_0 = 819 Hz for (3λ/4), and f_0 = 1365 Hz for (5λ/4). Higher resonant frequencies showed a similar performance pattern.

 ISBN: 978-93-92105-22-7

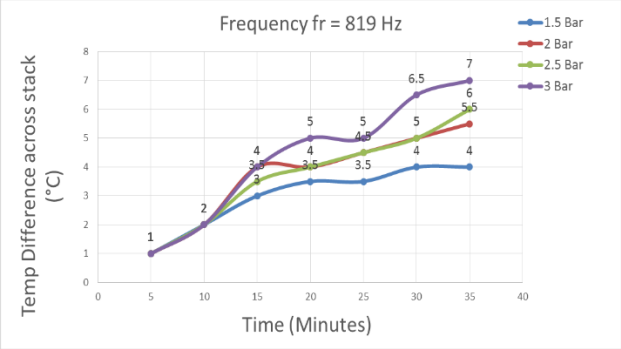

Figure 4 Variation of Temperature Difference with Time at f_0 = 819 Hz

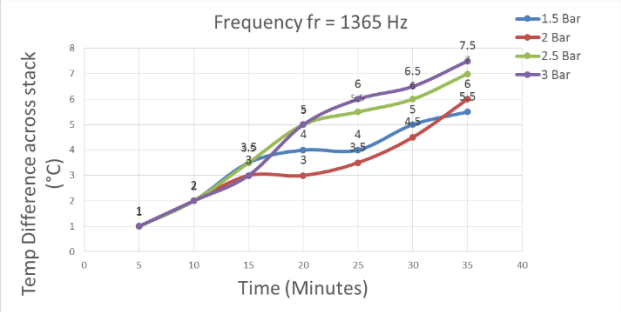

Figure 5 Variation of Temperature Difference with Time at f_0 = 1365 Hz

A temperature differential starts to form between the hot end and cold end of the stack when the acoustic sound power is fed into the system. It was shown in all of the aforementioned graphs and experimental data that the temperature differential between the ends of the stack likewise grows as the system pressure rises. According to the results of the experiment, it is evident that the temperature differential created throughout the stack is mostly related to the fluid pressure within the system.

Additionally, the maximum thermal gap across the stack of 7.5°C was obtained at a pressure of 3 Bar for a resonant frequency of f_0 = 1365 Hz, followed by the highest temperature difference across the stack of 7.0°C, which was obtained at a pressure of 3 Bar for a resonant frequency of f_0 = 819 Hz.

IV. CONCLUSION

The effect of the working medium, argon, with a fixed resonator tube length on the demonstration of the thermoacoustic standing wave refrigeration system with different resonance frequency and pressures, was anticipated in this experimental investigation. In order to analyze the temperature difference between the ends of the stack, three different resonating frequencies were taken into account for increasing pressures inside the resonator tube from 1.5 Bar to 3 Bar. These frequencies correspond to f_0 = 273 Hz for ($\lambda/4$), f_0 = 819 Hz for ($3\lambda/4$), and f_0 = 1365 Hz for ($5\lambda/4$).

The results of the experiment indicate that the thermoacoustic refrigeration system's operation is influenced by both the resonating frequency and the pressure of the working fluid, in this instance argon. The results also demonstrate that greater resonant frequencies are required to achieve the highest temperature differences across the stack. Additionally, different investigations may be conducted by altering the resonator tube's length, working medium, stack size, form, and geometry.

REFERENCES

[1] Swift, G. W. (1995). Thermoacoustic engines and refrigerators. Physics today, 48(7).

[2] Tijani, M., Zeegers, J., & De Waele, A. (2002a). Construction and performance of a thermoacoustic refrigerator. Cryogenics, 42(1), 59-66.

[3] Hariharan, N., Sivashanmugam, P., & Kasthurirengan, S. (2013a). Experimental investigation of a thermoacoustic refrigerator driven by a standing wave twin thermoacoustic prime mover. International journal of refrigeration, 36(8), 2420-2425.

[4] Reid, R., & Swift, G. (2000). Experiments with a flow-through thermoacoustic refrigerator. The Journal of the Acoustical Society of America, 108(6), 2835-2842.

[5] Basir Jafari, S., Abolhassani, M., & Amjadi, A. (2008). Acousto-Refrigerator with an Adjustable Mechanical Resonator (RESEARCH NOTE). International Journal of Engineering, 21(2), 183-196.

[6] Nsofor, E. C., & Ali, A. (2009). Experimental study on the performance of the thermoacoustic refrigerating system. Applied Thermal Engineering, 29(13), 2672-2679.

[7] Wetzel, M., & Herman, C. (2000). Experimental study of thermoacoustic effects on a single plate Part I: Temperature fields. Heat and Mass Transfer, 36(1), 7-20.

[8] Paek, I., Mongeau, L., & Braun, J. E. (2010). Performance characterization of a small-capacity thermoacoustic cooler for air-conditioning applications. Journal of mechanical science and technology, 24(9), 1781-1791.

[9] Piccolo, A. (2013). Optimization of thermoacoustic refrigerators using second law analysis. Applied energy, 103, 358-367.

[10] Tasnim, S., Mahmud, S., & Fraser, R. (2012). Effects of variation in working fluids and operating conditions on the performance of a thermoacoustic refrigerator. International communications in heat and mass transfer, 39(6), 762-768.

[11] Jin, T., Chen, G., Wang, B., & Zhang, S. (2003). Application of thermoacoustic effect to refrigeration. Review of scientific instruments, 74(1), 677-679.

[12] Jebali, F., Lubiez, J. V., & François, M.-X. (2004). Response of a thermoacoustic refrigerator to the variation of the driving frequency and loading. International journal of refrigeration, 27(2), 165-175.

[13] Bailliet, H., Lotton, P., Bruneau, M., Gusev, V., Valière, J.-C., & Gazengel, B. (2000). Acoustic power flow measurement in a thermoacoustic resonator by means of laser Doppler anemometry (LDA) and microphonic measurement. Applied Acoustics, 60(1), 1-11.
[14] Tijani, M., Zeegers, J., & De Waele, A. (2002). Design of thermoacoustic refrigerators. Cryogenics, 42(1), 49-57.
[15] Piccolo, A., & Cannistraro, G. (2002). Convective heat transport along a thermoacoustic couple in the transient regime. International journal of thermal sciences, 41(11), 1067-1075.
[16] Wetzel, M., & Herman, C. (1997). Design optimization of thermoacoustic refrigerators. International journal of refrigeration, 20(1), 3-21.

IFERP connecting engineers...developing research
1st International Conference on Future of Engineering 2022

Developing Factoring Service for Small and Medium Enterprises at Kosovo's Pro Credit Bank

Burhan Reshat Rexhepi[1], Burim Isa Berisha[2], Labeat Mustafa[3], Shpresim Halim Vranovci[4]

[1,2,3,4] UBT College - Higher Education Institution, Department, Business Administration and Economics, Pristina, Kosovo
Email: [1]burhan.rexhepi@ubt-uni.net, [2]burim.berisha@ubt-uni.net, [3]labeat.mustafa@ubt-uni.net, [4]shpresim.vranovci@ubt-uni.net

Abstract:
After a decade of reforming policy, building and developing the multi-sector market economy, Small and Medium Enterprises (SMEs) in Kosovo have developed strongly and contributed to creating employment, increasing GDP, and raising the nation's volume of exports. However, SME have found difficulties on the way to development due to lack of management experience and financial resources, and due to uncertainty within the business environment. As a result, SME often faced obstacles during their operations.
Originated from actual demands of integrating and economic development in Kosovo in general and banking system in particular, to develop new banking service is extremely crucial, especially for Join stock commercial banks that have less competitiveness than State owned commercial Banks. Moreover, factoring consider a financial tool that is met both requirement from commercial Banks and SME. This research seeks to introduce Factoring service as an effective short-term financial tool for SME as well as crucial service for commercial Banks in Kosovo. The first chapter aim at introduction of factoring services including clarifying the conditions for factors developing this service and the second Chapter has taken overview the current situation of worldwide factoring and Kosovoese factoring market to have an outlook for general conditions for developing factoring for Kosovoese factors.
Kosovo's factoring market is at the first phase in its life cycles, there are a lot of chance for developing this service in Kosovo, especially for pioneers whom launching this services into market. However, PRO CREDIT BANK could not gain the advantage of the first entrance. Even though, PRO CREDIT BANK has advantages in external sources of stable and high growth of Kosovo economy. SME's high growth rate at Kosovo 3,8% as well as its experience in providing financial service to SME- its targeted customers, PRO CREDIT BANK's good cooperation with multinational and world organization to gain more capital for credit, factoring at PRO CREDIT BANK is at "zero" points. The main obstacle to limit factoring service at PRO CREDIT BANK blamed for lack of development strategy for factoring service, the human resource management matter, and lack of information about sellers and Buyers. All analysis is mention in details in the third chapter. In the last chapter- Chapter 4, the author makes some main recommendation for developing factoring service to SMEs at PRO CREDIT BANK:

- Creating marketing plan: defining targeted customers are SMEs and MMEs group, especially for ones that have a purchase relationship with big and high reputation corporation to limit risk of default payment from Buyers.;domestic factoring is the target products to concentrate on the first phase with their customers based in North of Kosovo; and suggested variety of marketing program to promote this service.
- Establishing a full time of team member for PRO CREDIT BANK and developing training course about factoring
- Increase financial capacity for PRO CREDIT BANK to support for financing in factoring service.

Besides, the Author recommend solution for SBK to improve legal framework for factoring as well as enhancing the efficiency of CIC system to supports commercial banks, including PRO CREDIT BANK in developing factoring service.

Keywords:
Economics; Statistics; Business economics; Economy

IFERP International Conference
IFERP Explore
https://icfe.co.in/ | info@icfe.co.in

UPCOMING CONFERENCES

Technoarete® Group
Integrating Researchers to Incubate Innovation

SUPPORTED BY

ALL CONFERENCE ALERT
Academics conferences at a glance

ECA
Get World wide Engineering Conferences Update..

Conference Alerts
Global Academic Conferences

INTERNATIONAL CONFERENCE ALERTS

ISBN : 978-93-92105-22-7